New Strategies to Improve the Expression of Recombinant Mammalian Proteins in Engineered Animal Cell Lines

Von der Fakultät für Lebenswissenschaften

der Technischen Universität Carolo-Wilhelmina

zu Braunschweig

zur Erlangung des Grades

einer Doktorin der Naturwissenschaften

(Dr. rer. nat.)

genehmigte

D i s s e r t a t i o n

von Bahar Baser

aus Gießen

1. Referent: Prof. Dr. Wulf Blankenfeld

2. Referent: Prof. Dr. Stefan Dübel

eingereicht am: 02.03.2015

mündliche Prüfung (Disputation) am: 21.07.2015

Druckjahr 2015

Vorveröffentlichungen der Dissertation

Teilergebnisse aus dieser Arbeit wurden mit Genehmigung der Fakultät für Lebenswissenschaften, vertreten durch den Mentor der Arbeit, in folgenden Beiträgen vorab veröffentlicht:

Publikationen

Steffen Meyer, Carmen Lorenz, Bahar Baser, Mona Wördehoff, Volker Jäger, Joop van den Heuvel (2013). Multi-Host Expression System for Recombinant Production of Challenging Proteins. PLoS ONE 8(7): e68674.

Tagungsbeiträge und Seminarvorträge

Bahar Baser, Steffen Meyer, Sonja Wilke, Konrad Büssow and Joop van den Heuvel. New Strategies to Improve the Expression of Recombinant Mammalian Proteins in Engineered Animal Cell Lines, Progress Seminar, Braunschweig, Germany (2014)

Bahar Baser, Steffen Meyer, Sonja Wilke, Konrad Büssow and Joop van den Heuvel. New Strategies to Improve the Expression of Recombinant Mammalian Proteins in Engineered Animal Cell Lines, 4th Annual Retreat HZI Grad School, Goslar-Hahnenklee, Germany (2013)

Bahar Baser, Steffen Meyer, Sonja Wilke, Konrad Büssow and Joop van den Heuvel. New Strategies to Improve the Expression of Recombinant Mammalian Proteins in Engineered Animal Cell Lines, 3ed Annual Retreat HZI Grad School, GSI Bad Bevensen, Germany (2012)

Bahar Baser, Steffen Meyer, Sonja Wilke, Konrad Büssow and Joop van den Heuvel. New Strategies to Improve the Expression of Recombinant Mammalian Proteins in Engineered Animal Cell Lines, Progress Seminar, Braunschweig, Germany (2012)

Posterbeiträge

Bahar Baser, Steffen Meyer, Sonja Wilke, Konrad Büssow and Joop van den Heuvel. New Strategies to Improve the Expression of Recombinant Mammalian Proteins in Engineered Animal Cell Lines, PEGS Europe 2013: Protein & Antibody Engineering Summit, Lisbon, Portugal (2013)

Bahar Baser, Steffen Meyer, Sonja Wilke, Konrad Büssow and Joop van den Heuvel. New Strategies to Improve the Expression of Recombinant Mammalian Proteins in Engineered Animal Cell Lines, RPP7 – Laupheim , 7th Conference on Recombinant Protein Production, Laupheim, Germany (2013) **(1st Poster Award)**

Bahar Baser, Steffen Meyer, Sonja Wilke, Konrad Büssow and Joop van den Heuvel. New Strategies to Improve the Expression of Recombinant Mammalian Proteins in Engineered Animal Cell Lines, 6th International PhD Symposium, Braunschweig, Germany (2013)

Bahar Baser, Steffen Meyer, Sonja Wilke, Konrad Büssow and Joop van den Heuvel. New Strategies to Improve the Expression of Recombinant Mammalian Proteins in Engineered Animal Cell Lines, 5th International PhD Symposium, Braunschweig, Germany (2011)

Bahar Baser, Steffen Meyer, Sonja Wilke, Konrad Büssow and Joop van den Heuvel. Multi-Gene Expression of Recombinant Proteins in Engineered Cell Lines, 2nd Annual Retreat HZI Grad School, Goslar-Hahnenklee, Germany (2011)

Bahar Baser, Steffen Meyer, Sonja Wilke, Konrad Büssow and Joop van den Heuvel. New Strategies to Improve the Expression of Recombinant Mammalian Proteins in Engineered Animal Cell Lines, 4th International PhD Symposium, Braunschweig, Germany (2010)

Content

Abbreviations

ADP	Adenosine diphosphate
Amp	Ampicillin
AMPPNP	Adenylyl-imidodiphosphate
ANOVA	Analysis of variance
AP	Alkaline phosphatase
Asn	Asparagine
ATG	Translation start codon
ATP	Adenosintriphosphat
BCIP	5-Bromo-4-chloro-3-indoxyl phosphate
BD	Becton Dickinson
BEVS	Baculovirus expression vector system
BFP	Blue fluorecent protein
BHK	Baby hamster kidney
bp	Base pair
BSA	Bovine serum albumin
CaPi	Calcium phosphate
CBD	Client binding domain
CDG	Congenital disorders of glycosylation
CFP	Cyan fluorecent protein
CHO	Chinese hamster ovary
CNPY3	Canopy FGF signalling regulator 3
CMV	Cytomegalovirus
CpG	C-phosphate-G
Cre	Causes recombination
CRISPR/Cas	Clustered, regulatory interspaced, short palindromic repeats-associated
C-terminal	Carboxy-terminal

CV-1	Monkey kidney cell line from *Cercopithecus aethiops*
DAMP	Damage-associated molecular pattern
DC	Dendritic cell
DD	Death domain
ddH2O	H_2O bidest
DHFR	Dihydrofolate reductase
DMSO	Dimethyl sulfoxide
DNA	Deoxyribonucleic acid
dNTP	Deoxy ribonucleosid-triphosphate
DS	Dyad symmetry
DSB	DNA double-strand break
dTomato	Dimer Tomato
ε	Extinctions coefficient [$l \times g^{-1} \times cm^{-1}$]
EBNA-1	Epstein-Barr nuclear antigen 1
EBV	Epstein-Barr virus
ECD	Ectodomain
E. coli	*Escherichia coli*
EDTA	Ethylen diamine tetra acetic acid
eGFP	Enhanced green fluorescent protein
Endo	Endoglycosidase
ER	Endoplasmic reticulum
ES	Embryonic stem cells
EXIM	Research group experimental immunology
fAβ	β-amyloid plaques
FACS	Fluorescence-activated cell sorting
FBS	Foetal bovine serum
FCS	Foetal calf serum
Flp	Flippase
for	Forward (-primer)

FR	Family of repeats
FRT	Flp recognition target
Fuc	Fucose
G418	Geneticin
Gal	Galactose
GalNAc	N-Acetylgalactosamine
GFP	Green fluorecent protein
Glc	Glucose
GlcNAc	N-Acetylglucoseamine
GNTI	N-acetylglucosaminyltransferase I
GOI	Gene of interest
gp96	Glycoprotein 96
GPCR	G-protein-coupled receptor
GRP94	Glucose-regulated protein 94
GS	Glutamine synthase
HDR	Homology-directed repair
HEK	Human embryonic kidney
HEPES	4-(2-hydroxyethyl)-1-piperazineethanesulfonic acid
His_n	n consecutive Histidin residues as affinity tag
HJ	Holiday junction
HPLC	High performance liquid chromatography
hpt	Hours post transfection
HR	Homologous recombination
HSP	Heat shock protein
HTP	High-throughput
HZI	Helmholtz Centre for Infection Research
IFN	Interferon
IKK	IκB kinase
IL-1	Interleukin-1

IMAC	Immobilised metal ion affinity chromatography
IPTG	Isopropyl-β-D-thiogalactopyranoside
IRES	Internal ribosomal entry site
IRF3	IFN-regulatory factor-3
Kan	Kanamycin
kDa	Kilodalton
LB	Luria-Bertani
*lox*P	Locus of crossing over (x), P1
LPS	Lipopolysaccharide
LRR	Leucin rich repeat
LTA	Lipoteichoic acid
MAL	MyD88-adaptor-like protein
MALDI	Matrix assisted laser desorption ionisation
Man	Mannose
MCS	Multiple cloning site
MilliQ water	Ultrapure (type 1) water
mRFP1	Monomeric red fluorecent protein-1
MS	Mass spectrometry
MSX	Methionine sulfoximine
MTX	Methotrexate
MW	Molecular weight
MWCO	Molecular weight cut off
MyD88	Myeloid differentiation primary-response protein
N/A	Not applicable
NB-DNJ	N-butyl-deoxynojirimycin
NBT	Nitro blue tetrazolium chloride
NEB	New England Biolabs
Neo	Neomycin phosphotransferase
NeuAc	N-Acetylneuraminic acid

NF-κB	Nuclear factor kappa-light-chain-enhancer of activated B cells
NHEJ	Non-homologous end joining
Ni-NTA	Complex of nickel ions and nitriloacetic acid
NRCC	National Research Council of Canada
N-terminal	Amino-terminal
OD	Optical density
OH	hydroxyl group
oriP	Origin of replication
pA	Polyadenylation signal
PAGE	Polyacrylamide gel electrophoresis
PAMP	Pathogen associated molecular pattern
PBS	Phosphate buffered saline
PCR	Polymerase chain reaction
PDB	Protein Data Bank
PE-DTPA	1,2-dimyristoyl-sn-glycero-3-phosphoethanolamine-N-diethylenetriaminepentaacetic acid
PEI	Polyethylenimine
PES	Polyethersulfon
pFlpBtM	pFlp-Bac-to-Mam
PGK	Phosphoglycerate kinase
PGN	Peptidoglycan
PNGase F	Peptide-N-glycosidase F
PRAT4A	Protein associated with toll-like receptor 4A
PRR	Pattern recognition receptor
PTM	Posttranslational modification
Puro	Puromycin N-acetyl transferase
PVDF	Polyvinylidene difluorid
rcf	Relative centrifugal force

RDIF	Research group gen regulation and differentiation
rev	Reverse (-primer)
RMCE	Recombinase-mediated cassette exchange
rpm	Revolutions per minute
SAA	Serum amyloid A
SD	Standard deviation
SDS	Sodium dodecyl sulphate
Ser	Serine
Sf	*Spodoptera frugiperda*
SM	Selection marker
S/MAR	scaffold/matrix attachment regions
SSR	Site-specific recombinase
S. Typhimurium	*Salmonella enterica* serotype Typhimurium
SV40	Simian virus 40
TAE	Tris-acetate-EDTA
TALEN	Transcription activator-like effector nuclease
TBS-T	Tris buffered saline with Tween-20
TCA	Trichloroacetic acid
tdTomato	Tandem dimer Tomato
TE	Tris-EDTA
TEMED	N,N,N´,N´-Tetramethylethylendiamin
T_H cell	T-helper cell
Thr	Threonine
TIL	Toll/Interleukin-1-receptor-Like
TIR	Toll/interleukin-1 (IL-I) receptor
TIRAP	TIR-domain-containing adaptor protein
TLR	Toll-like receptor
T_m	Melting temperature
TN1	Tryptone

Tn7	Bacterial transposon Tn7
TNF	Tumor-necrosis factor
TOF	Time of flight
TRAM	TRIF-related adaptor molecule
TRIF	TIR-domain containing adaptor protein inducing IFN-β
Tris	2-Amino-2-hydroxymethyl-propane-1,3-diol
U	Catalytical units
UPR	Unfolded protein responses
UV	Ultraviolet
VLR	Variable lymphocyte receptor
v/v	Volume fraction (volume per volume)
w/v	Mass concentration (weight per volume)
×g	Gravitational acceleration
ZNF	Zinc-finger nuclease

Synopsis

Die Aufklärung von Proteinstrukturen liefert wertolle Einblicke in die vielfältigen Funktionen zellularer Prozesse. Jedoch müssen bestimmten Herausforderungen gemeistert werden um Proteine Struckturbiologisch analysieren zu können. Die Produktion von adequaten Mengen an kristallisierbarem Protein stellt sich vor allem für komplexe Zielproteine aus Säugetieren als mühsam dar. In solchen Fällen ist die Verwendung von Säugetierzelllinien von Vorteil. Mechanismen für die korrekte Faltung von Proteinen und die Fähigkeit posttranslationale Modifikationen durchzuführen sind in Säugetierzelllinien gegeben. Die Herstellung von stabilen Zelllinien für die rekombinante Proteinproduktion ermöglicht die robuste Expression in einer Reihe von Set-ups: vom kleinen Maßstab in Batch-Kultur bis hin zu größeren Maßstäben in Bioreaktoren. Stabile Zellliniengenerierung ist jedoch ein sehr zeitaufwendiger Prozess. Sie erfordert eine extensive Analyse und Charakterisierung von hochproduzierenden Zellklonen nach der zufälligen Integartion eines Transgenes in die Wirtszelllinie. Darüber hinaus stellen komplexe heterogene Glycanstrukturen auf der Proteinoberfläche die nächste Herausforderung dar. Diese beeinträchtigen Proteinkristallisation und Diffraktion. Mutante Zelllinien wie z.B. CHO Lec3.2.8.1 ermöglichen die Expression von Proteinen mit einer homogene $GlcNAc_2Man_5$ Glycanstruktur. Um die lösliche Expression von rekombinanten Proteinen zu fördern können verschiedene Strategien angewandt werden. Beispielsweise die Expression verkürzter oder chimerer Konstrukte alswohl die Co-expression von Multiproteinkomplexen oder molekularer Chaperone.

In dieser Arbeit wurde die glykosylierungsdefizente Zelllinie CHO Lec3.2.8.1 genutzt um ein schnelles und flexibles System für die Herstellung von stabilen Zelllinien zu etablieren, welche die Co-expression von Zielproteinen in bereits charakterisierten chromosomalen Loci ermöglicht. Dieses binäre System enthält stabil integrierte Austauschkassetten welche die zielgerichtete Integration von Transgenen ermöglichen. Hiermit wird die zügige Herstellung von Produktionszelllinen mit vorhersehbaren Expressionseigenschaften gewährleistet.

Dieses binäre System wurde genutzt um Produktionszelllinien für die Co-expression von Toll-like Rezeptor Ectodomainen in Kombination mit Chaperonen zu generieren.

Synopsis

The elucidation of protein structures provides a valuable insight into the diverse functions of cellular processes. However the field of structural biology faces some major bottlenecks. The production of adequate amounts of high quality protein, particularly for complex mammalian targets can be a demanding process. In such cases the use of mammalian expression hosts is favourable to the widely used prokaryotic systems due to their capability to process the most genuine post-translational modifications and employ proper protein folding mechanisms. The generation of stable mammalian cell lines for recombinant protein production enables the robust expression in various settings from small scale batch cultures to large scale bioreactors. Stable cell line development however is a very time-intensive process that requires extensive screening for high producer clones after random integration of the gene of interest into the host genome. Another challenge structural biologists are confronted with are complex heterogeneous glycosylation pattern on the protein surface. These interfere in proper crystal formation and thus diffraction analysis. The use of glycosylation mutant cell lines such as CHO Lec3.2.8.1, that express a uniform glycosylation profile of the high mannose type ($GlcNAc_2Man_5$), address this problem. To improve the soluble expression of recombinant proteins various strategies can be pursuit. This includes the expression of truncated and chimeric constructs as well as the co-expression of multi-protein complexes and molecular chaperones.

In this work the glycosylation deficient cell line CHO Lec3.2.8.1 was used to create a fast method to generate stable producer cell lines that co-express target genes at pre-characterized chromosomal loci. Binary CHO Lec3.2.8.1 master cell lines, stably tagged with two different exchange cassettes comprising fluorescent marker genes, were established during this work. Targeted integration of recombinant genes into these pre-defined genomic loci using recombinase mediated cassette exchange (RMCE), based on the Flp/*FRT* system, enables the fast generation of stable producer cell lines with predictable expression properties.

This binary system was used to generate producer cell lines for the expression of Toll-like receptor ectodomains in combination with molecular chaperones.

1 Introduction

1.1 Recombinant protein expression

The importance of protein function in biological systems is evident by their diverse roles in all cellular processes. Proteins do not only provide a structural matrix but are also directly or indirectly involved in catalytic processes, cellular signalling, transport and storage as well as the immune defence and cell-cell interactions (Alberts, 2008). Protein aberrations due to genetic mutations can lead to malfunctioning of one or more cellular processes resulting in a multitude of phenotypes with different levels of severity e.g. haemoglobin disorders (Weatherall, 2004), neurodegenerative diseases (Chiti *et al.*, 2006) and cancer (Frank, 2004). Therefore, the elucidation of protein structure and function is essential for the understanding of biological processes which will aid in the development of therapeutical coping strategies.

The historically important protein insulin was not only the first protein to be sequenced (Sanger, 1949) but also the first recombinant drug brought onto the market after its successful recombinant expression in *Escherichia coli* (Goeddel *et al.*, 1979). This eliminated the need for cumbersome extraction from natural sources and met the increasing demands with a qualitatively superior product. Since its initial use (Cohen *et al.*, 1973) recombinant deoxyribonucleic acid (DNA) technology evolved to a diverse tool for researchers as well as for the life science industry. Recombinant proteins can now be manipulated to display specific properties such as improved solubility, expressibility and affinity to chromatographic resins using fusion-tags (Malhotra, 2009). Single domains, truncated and chimeric proteins can be generated (Hudson *et al.*, 2003, Jin *et al.*, 2008) as well as completely engineered proteins which do not occur naturally such as bispecific antibodies (Hudson *et al.*, 2003). Codon optimisation can be used to aid expressibility in different hosts (Angov *et al.*, 2008) and posttranslational modifications (PTM) can be optimized to influence a variety of functions including plasma-half life, system clearance and protection from immunogenic reactions (Walsh *et al.*, 2006).

As specified before, the elucidation of protein structures is important. Since the first protein structures were obtained for myoglobin (Kendrew *et al.*, 1958) and haemoglobin (Muirhead

et al., 1963), over 100,000 more entries were deposited in the Protein Data Bank (PDB) to date. The continued development of new and improved expression systems, recombinant engineering and technical tools results in the constant release of new structures that contribute to a more holistic picture of cellular mechanisms. Nonetheless, recombinant protein expression for structural biology applications is confronted with major bottlenecks. For one, the soluble expressibility of protein is limited particularly for complex protein structures. Moreover, heterogeneity resulting from complex glycosylation patterns makes it difficult to obtain well diffracting crystals. Properties that influence protein expression and crystallization are strongly impacted by the choice of expression system used for heterologous protein production. So far bacterial expression hosts like *E. coli* are most commonly used due to their inexpensive and uncomplicated technical and cultivation requirements which makes them easy to handle. However, prokaryotes lack the secretory pathway present in eukaryotes and thus the machinery necessary for PTMs. This results often in incorrectly folded non-functional protein that accumulates in inclusion bodies. Even though refolding procedures can be attempted, these are not always successful. Thus the limit of bacterial expression systems is reached at this point for many protein targets. Therefore the use of eukaryotic expression systems becomes more and more widespread. While heterologous expression in yeast is still considered as relatively inexpensive the costs of insect and mammalian systems are elevated due to complex media requirements. In comparison to bacterial systems insect and mammalian systems are time-consuming particularly when generating stable cell lines (Villaverde *et al.*, 2003, Aricescu *et al.*, 2006, Nettleship *et al.*, 2010, Aricescu *et al.*, 2013).

1.2 Glycosylation – friend or foe

In this work the focus lies on the production of difficult to express protein targets for structural biology. The importance and drawbacks of glycosylation for structural biology as well as approaches that deal with protein glycosylation are described in this chapter. Roughly 50 % of proteins found in humans are glycosylated which highlights the central role of glycosylation for biological function. Deficiencies in the glycosylation pathway are associated with medical condition such as congenital disorders of glycosylation (CDG) including mucolipidosis II or Walker-Warburg syndrome (Freeze, 2006). However, at the same time glycoform variations can be used as disease markers for the diagnostic determination of medical conditions (Walsh *et al.*, 2006). Protein glycosylation regulates

structural stability, proper folding, endosomal trafficking, proteolytic processing and protein solubility. Glycan patterns also influence protein-protein interactions and *in vivo* protein functions such as signal transduction, functional activity, immunogenicity, bioavailability, biodistribution and pharmacokinetics. Glycosylation patterns are divided into N-linked and O-linked glycans which are either connected to nitrogen atoms of asparagine residues comprising an Asn-X-Ser/Thr motif or hydroxyl groups of serine or threonine residues respectively. N-linked glycosylation is initiated through the attachment of branched glycan precursors in the endoplasmic reticulum (ER) which are further modified when passing the Golgi apparatus whereas O-linked glycosylation takes place through the sequential attachment of single N-Acetylgalactosamine (GalNAc) monosaccharaides. While O-linked glycosylation sites are less problematic for structural biology applications as they are mostly found in extended, unfolded serine-, threonine- and proline-rich regions of proteins. N-linked glycosylation poses a problem as it interferes with protein crystallization and diffraction. However, N-linked glycosylation sites are known to be relevant for glycan-protein interactions and the protection of hydrophobic regions and thus cannot be dismissed as easily (Walsh *et al.*, 2006, Chang *et al.*, 2007, Croset *et al.*, 2012). Therefore glycosylation deficient cell lines such as CHO Lec3.2.8.1 or HEK293-*GNTI*$^-$ cells which only express truncated glycan patterns (Stanley, 1989, Reeves *et al.*, 2002) as well as glycosylation inhibitors are employed. N-glycosylation can be inhibited by the presence of kifunensine which inhibits mannosidase I (Elbein *et al.*, 1990) or swainsonine which inhibits lysosomal α-mannosidase (Elbein *et al.*, 1981) or *N*-butyl-deoxynojirimycin (NB-DNJ) which inhibits α-glucosidase during expression. The truncated glycan chains attain a sensitivity for enzymes including endoglycosidase (endo) H or endo F1 leaving a single N-Acetylglucosamine (GlcNAc) residue. Butters *et al.*, (1999) demonstrated that the combined use of CHO Lec3.2.8.1 cells with ND-DNJ improved the deglycosylation efficiency of glycoproteins with endoH from 12 % to almost 100 %. Finally, if all N-linked glycans shall be removed peptide-N-glycosidase F (PNGase F) will do so. However PNGase F will also convert the asparagine side chain-residue to aspartate which might negatively affect protein interactions and thus often results in the aggregation of the protein (Chang *et al.*, 2007, Aricescu *et al.*, 2013). An overview of glycosylation profiles is given in Table 1-1.

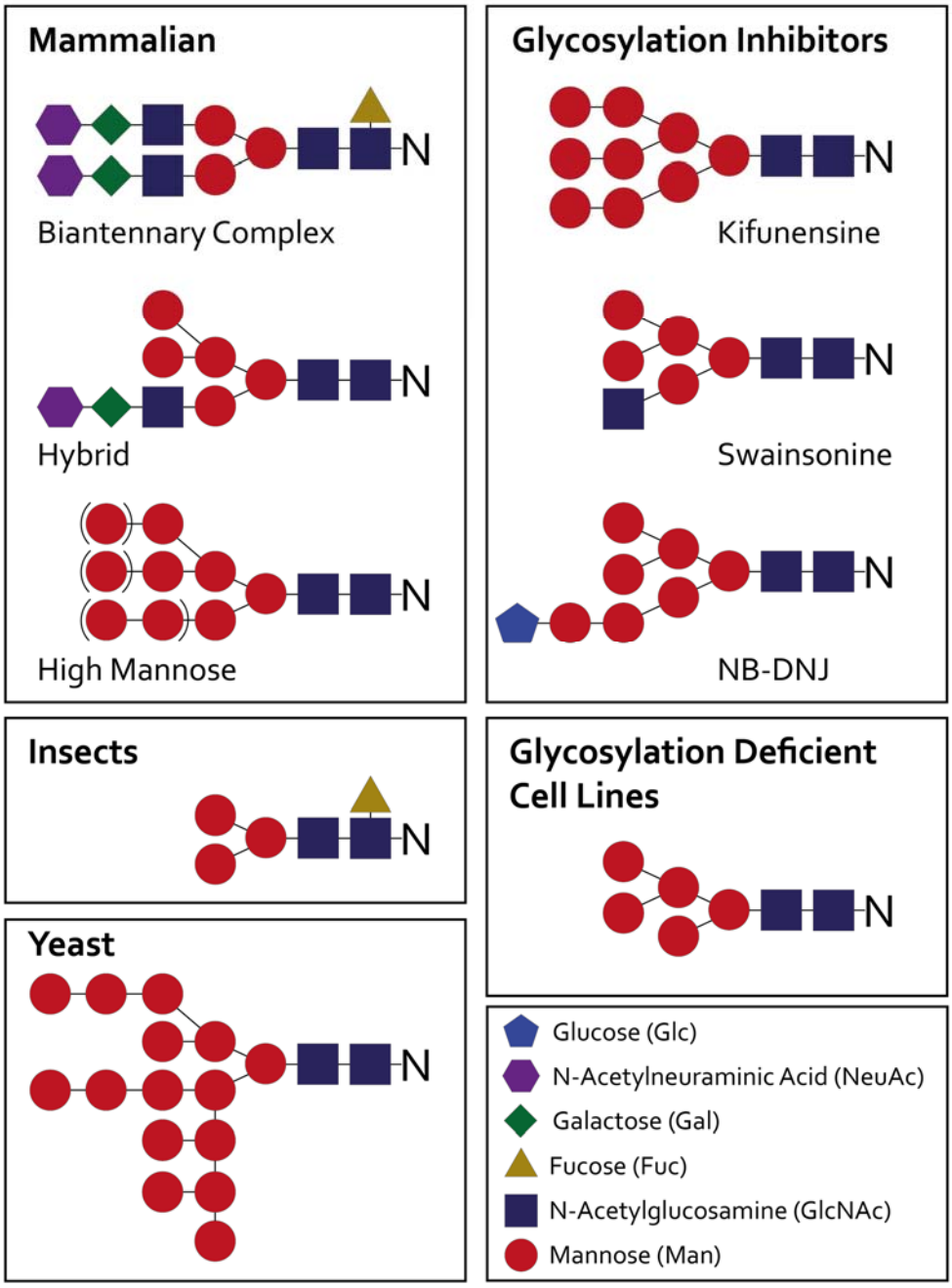

Figure 1-1: Control of N-glycosylation. (Left) N-glycosylation patterns are exemplified for mammalian cells including examples for complex (can be fucosylated), hybrid and high mannose type glycan structures as well as fucosylated insect cells of the paucimannose type and hyper-mannosylated yeast cells. **(Right)** Truncated N-glycosylation profiles are shown for glycosylation inhibitors kifunensine, swainsonine and ND-DNJ as well as glycosylation deficient cell lines CHO Lec3.2.8.1 and HEK293-*GNTI*$^{-}$. Adapted from (Gomord *et al.*, 2004, Chang *et al.*, 2007, Lee *et al.*, 2009, Nettleship *et al.*, 2010, Johnson *et al.*, 2013).

1.3 Mammalian expression systems

Mammalian expression systems become more popular as an alternative to bacterial expression hosts as well as other eukaryotic systems including insect and yeast platforms. This is due to their ability to process the most genuine glycosylation pattern and the

availability of the cellular folding machinery necessary for complex human target proteins. Those advantages ease the approval of biopharmaceuticals by regulatory agencies as well as the soluble expression and proper folding of proteins for structural biology applications. However, complex glycan structures need to be removed before crystallization. Alternatively, mutant cell lines with truncated glycosylation profiles for structural biology can be employed. Therefore, the glycosylation mutant cell line CHO Lec3.2.8.1 was used to generate stable master and producer cell lines for the co-expression of demanding target proteins during this work. For the transient screening of constructs and small scale test expressions HEK293-6E cells were utilized.

Transient and stable protein expression in mammalian cell lines was optimized in the last years as described in the following chapters (Durocher *et al.*, 2002, Aricescu *et al.*, 2006, Nettleship *et al.*, 2010). Transient expression in Human embryonic kidney (HEK) cells is commonly used for construct screening in small scale formats. Chinese hamster ovary (CHO) cells on the other hand are generally used for the generation of stable producer cell lines which enables rapid scale-up in bioreactors and repeatable protein production. Detailed information on HEK and CHO cells used for transient and stable protein expression are given in the following chapters.

1.3.1 Transient protein expression in HEK293 cell lines

HEK293 cell lines are most commonly used for the transient expression of proteins. In our lab the transient expression in HEK293-6E cells, described below, is established and routinely used. HEK293 cells were originally derived from HEK cells transformed with sheared adenovirus type 5 DNA (Graham *et al.*, 1977). HEK293 derivative cell lines followed, including HEK293T cells expressing the simian virus 40 (SV40) large T-antigen (Lebkowski *et al.*, 1985) and HEK293-EBNA cells expressing the Epstein-Barr virus (EBV) Epstein-Barr nuclear antigen 1 (EBNA-1) (Young *et al.*, 1988). These allow episomal amplification of plasmids containing the viral SV40 or EBV origins of replication *SV40 ori* and *oriP* respectively. As a result, a larger copy number of plasmid is retained within the cell during expression which improves protein yields (Schlaeger *et al.*, 1999, Aricescu *et al.*, 2006). Yates *et al.*, (2000) demonstrated more specifically that the components DS (dyad symmetry) and FR (family of repeats) within *oriP* comprise several EBNA-1 binding sites which function as replicator and retain plasmids during cell division respectively after binding of EBNA-1. Furthermore it was shown that the replicator DS only requires two

EBNA-1 binding sites for proper functioning (Yates *et al.*, 2000). HEK293-6E is a HEK293-EBNA cell line which expresses a truncated version of the EBNA-1 protein (Durocher *et al.*, 2002). HEK293-6E cells were used in this work for the transient expression and screening of protein targets before the generation of stable glycosylation mutant CHO Lec3.2.8.1 cell lines since HEK293-6E cells are already routinely used in our laboratory. However, glycosylation mutant HEK293-*GnTI*$^-$ cells unable to synthesise complex N-linked glycans due to the lack of N-acetylglucosaminyltransferase are also available and only express homogenous $Man_5GlcNAc_2$ residues on the glycoprotein surface (Reeves *et al.*, 2002, Chaudhary *et al.*, 2012).

Transient expression protocols for HEK293 cell lines were optimized over the years as an alternative to laborious stable cell line generation. The improvement of protein yields, downstream processing and transient scalability as well as the reduction of cultivation related costs for adherent culture methods and the setup of high-throughput (HTP) applications were addressed. The use of inexpensive transfection reagents such as calcium phosphate (CaPi) or polycationic linear and branched polyethylenimine (PEI) were explored and improved over the years. In this work suspension adapted HEK293-6E cells were used for transient test expressions in batch culture before the generation of stable CHO Lec3.2.8.1 production cell lines. The HEK293-6E cells were cultivated under serum free conditions (Meissner *et al.*, 2001) and transfected with 25 kDa liner PEI with prior DNA:PEI complex formation (Schlaeger *et al.*, 1999, Durocher *et al.*, 2002). Nonetheless, it was demonstrated that the use of high cell densities ($20x10^6$ cells/mL) during transfection without prior complex formation (Backliwal *et al.*, 2008) can yield equally high results. Even though CaPi co-precipitation is an equally efficient method for the transient transfection of HEK cells compared to PEI, the presence of foetal calf serum (FCS) during transfection is a major drawback for large scale applications as it requires the removal of serum through complete medium exchange (Baldi *et al.*, 2005). Furthermore, the supplementation with valproic acid five days after transfection was used to improve transient protein expression during this work. It was shown that supplementation with valproic acid a histone deacetylase inhibitor was used to obtain volumetric yields up to 1 g/L of recombinant antibody (Backliwal *et al.*, 2008). The inhibition of histone deacetylases increases the level of histone acetylation and thus endorses a relaxed conformation in the chromatin structure. This results in higher transcription levels and thus increased protein yields (Kazantsev *et al.*, 2008).

Transient transfection in various suspension adapted HEK293 cell lines is now used for HTP screening of protein constructs in small scale multiwell formats with subsequent purification (Davies *et al.*, 2005) and crystallisation (Lee *et al.*, 2009) as well as large scale expression in Wave™ bioreactors (Geisse *et al.*, 2005, Chaudhary *et al.*, 2012). Nevertheless the use of adherent HEK293T and HEK293-*GNTI*$^-$ cells for transient transfection was also optimized for economic construct screening in T-flasks and consequent expansion into roller-bottles for protein production. Through the adaption to affordable culture media (Dulbecco's Modified Eagle's Medium, Sigma), costs were reduced significantly and are extensively used until today for medium scale applications (Aricescu *et al.*, 2006). Moreover, automated sterile systems, such as the CompacT SelecT cell culture robot, enable the transient transfection in adherent HEK293T and HEK293-*GnTI*$^-$. Thus, user-specific variations during the time-consuming manual handling and transfection steps are eliminated and allow the continuous cultivation of backup cells and transient protein production (Zhao *et al.*, 2011).

1.3.2 Stable protein expression in CHO cell lines

Since the first clinical approval of a recombinant biopharmaceutical produced in CHO, namely human tissue-type plasminogen activator (Kaufman *et al.*, 1985), CHO cells became the most commonly used cell line for stable protein production in the biopharmaceutical industry in which 70 % of protein targets are expressed. Cellular processes in CHO cells were genetically engineered over the years to exhibit specific properties such as improved glycosylation pattern, proper gene amplification, reduced lactate production, resistance against apoptosis and the adaptation to suspension culture. Methodological developments including expression vector design, advanced cloning procedures, codon optimization, superior transfection protocols, improvement of stable integration and clonal selection methods as well as process improvements such as the optimization of media formulations, feeds, additives, pH, temperature and bioreactor design were brought forward to enhance growth and expression properties (Datta *et al.*, 2013). Recent advances in the deciphering of the CHO and CHO-K1 genomic sequence (Wurm *et al.*, 2011, Xu *et al.*, 2011, Lewis *et al.*, 2013) as well as proteome, secretome (Baycin-Hizal *et al.*, 2012), transcriptome (Becker *et al.*, 2011), glycome (North *et al.*, 2010, Tep *et al.*, 2012) and metabolome (Dietmair *et al.*, 2012) open new doors for metabolic and proteomic engineering.

CHO cells were originally isolated by Puck *et al.*, (1958) as an alternative to the malignant tissues derived cell lines available at that time. The low chromosome number of Chinese hamsters 2n=22 made them an attractive choice for genetic studies (Puck *et al.*, 1958). Several CHO derived cell lines are currently employed for protein production. For example subclone CHO-K1 (Kao *et al.*, 1968) and CHO DHFR-deficient cells (*dhfr*$^-$) that lack dihydrofolate reductase (DHFR) activity that usually converts dihydrofolate to tetrahydrofolate which is required for the *de novo* synthesis of purines (Urlaub *et al.*, 1980). CHO-*dhfr*$^-$ cells are used in combination with methotrexate (MTX) a DHFR antagonist which blocks residual DHFR activity to select cells that regain DHFR activity through co-amplification of the *dhfr* gene supplied on the expression vector (Kim *et al.*, 1998).

To produce demanding protein targets for structural biology applications CHO Lec3.2.8.1 cells were used for the generation of stable master and producer cell lines in this work. Glycosylation deficient CHO Lec3.2.8.1 cells are used when glycoproteins are desired with a minimum of heterogeneity in there glycosylation pattern. Stanley, (1989) isolated the CHO Lec3.2.8.1 cell line through sequential screening against several plant lectins from the Pro$^-$Lec3.6B mutant cell line derived from the CHO cell line Pro$^-$5. Resistance against a number of plant lectins, which were the consequence of reduced cell surface binding of those lectins, accounted for several glycosylation deficient phenotypes with a cumulative effect thus resulting in highly truncated and uniform glycosylation patterns. The lectin resistant mutation Lec1 accounts for a lack in N-acetylglucosaminyltransferase-1 activity, whereas the Lec2 and Lec3 phenotypes exhibit reduced transport of CMP-sialic acid into the Golgi lumen. Similarly the Lec8 phenotype shows reduced transport of UDP-galactose into the Golgi lumen (Stanley, 1989).

The generation of stable cell lines (Figure 1-2) follows a specific order; random integration of the gene of interest (GOI) into the host chromosome is followed by a selection method of choice. Popular selection methods include the use of the DHFR system described previously which is based on the rescue of a defective nucleotide metabolism through the over-expression of the enzyme DHFR (Urlaub *et al.*, 1980, Kim *et al.*, 1998) or the glutamine synthase (GS) system which similarly compensates for the lack of glutamine in culture media through the over-expression of GS thus strengthening the glutamine synthase pathway. Methionine sulfoximine (MSX) a GS inhibitor is used to increase selection stringency (Cockett *et al.*, 1990). Alternatively resistance against antibiotics can be prompted

through the integration of bacterial genes such as *neo* or *puro*. The *puro* gene is a codon optimized version of *Pac* with reduced CpG (C-phosphate-G) motives and thus is less affected by epigenetic silencing in mammalian cells. These encode neomycin phosphotransferase and puromycin N-acetyl transferase respectively rendering the cell line resistant to G418 or puromycin (Southern *et al.*, 1982, Vara *et al.*, 1986, InvivoGen, 2014). After random chromosomal integration, of a recombinant gene and initial selection procedures, several time-consuming rounds of extensive labour-intensive screening are required to isolate stable isogenic high producer cell lines. To reduce development costs and time in a pipeline that result from clonal screening and isolation, HTP automated platforms were established in industrial setups (Shi *et al.*, 2011). This HTP platform combines fluorescence-activated cell sorting (FACS) as well as imaging and liquid handling systems and thus allows screening of up to 10,000 clones in one run (Shi *et al.*, 2011). In this PhD thesis fluorescent marker genes were used for the isolation of stable CHO Lec3.2.8.1 master cell lines via FACS whereas the resistance genes *neo* or *puro* were used for the isolation of stable producer cell lines.

Following random genomic integration within a transfected population of cells, expression level between distinct cells of this population can vary strongly depending on the number of transgene integrations and chromosomal integration sites (position effect). While chromosomal integration into the loosely packed euchromatin favours protein expression, integration into dense inactive heterochromatin does not (Wurm, 2004). Therefore clonal isolation of single cell derived or phenotypically homogenous high producer cell lines from the initially obtained pool of transfected cells is necessary to obtain isogenic clones with constant expression level. However, even after the isolation of producer cell lines, inter-clonal variation can be observed within these clonal isolates (Kim *et al.*, 1998, Liu *et al.*, 2006, Kaufman *et al.*, 2008, Pilbrough *et al.*, 2009). These differences are attributed to genetic mosaicism that results from specific cell intrinsic variations as well as gradual termination of gene expression due to silencing effects that result from epigenetic downregulation of exogenous DNA. To circumvent epigenetic silencing *cis*-regulatory elements such as scaffold/matrix attachment regions (S/MARs) or ubiquitous chromatin opening elements can be used to flank the GOI (Wurm, 2004). Furthermore additives such as butyrate (Davie, 2003) or valproic acid (Backliwal *et al.*, 2008) which block histone deacetylase activity can be employed to boost protein expression. Moreover, it was shown that the methodology used for the isolation of isogenic clones does play a role in the constancy of homogenous

expression. For example Liu *et al.*, (2006) demonstrated that the removal of selective pressure after clonal isolation can result in epigenetic silencing which was further confirmed by Kaufman *et al.*, (2008) who compared the use of drug-based selection pressure to FACS. Thus clonal isolates obtained through cell sorting were shown to exhibit a higher degree of uniformity (Kaufman *et al.*, 2008). Nevertheless, the use of FACS for the isolation of producer cell lines with a high level of fluorescence can also result in heterogeneity due to non-genetic random stochastic fluctuations in expression during clonal isolation. Thus a population of isolated high producers may also contain cells with lower expression profiles that were temporary present within the isolated gate. This results in the co-isolation of cells with a lower production yield. These low producer subpopulations may outgrow the high producers over time. *Vice versa* when isolating producer cell lines with a low level of fluorescence these might be outgrown from high producers (Pilbrough *et al.*, 2009). To ease the generation of homogenous high producer cell lines and cut down development times, targeted integration approaches for stable cell line development are being pursuit (described in Section 1.4).

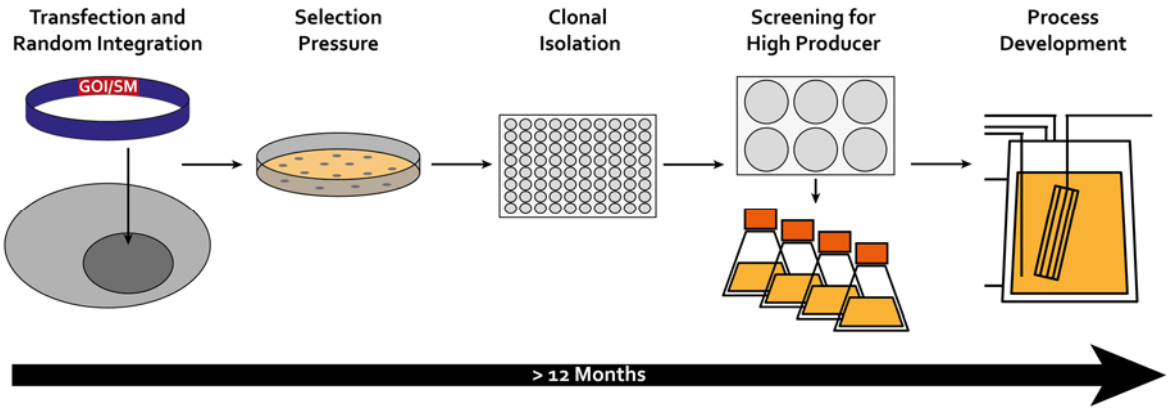

Figure 1-2: Conventional method for stable cell line development. A vector comprising the GOI and a selection marker (SM) of choice are randomly integrated into the genome. Application of selective pressure is followed by clonal isolation and extensive screening for high producers before large scale production and process optimization. Adapted from Wurm, (2004).

1.4 Stable cell line development through targeted integration

In this work the generation of stable CHO Lec3.2.8.1 producer cell lines is based on targeted integration with site-specific recombinases (SSR). Site-specific recombination as well as alternative approaches towards targeted integration are described below.

Site-specific targeted integration methods including nuclease based methods such as the zinc-finger nuclease (ZFN) system, the transcription activator-like effector nucleases

(TALEN) system and the clustered, regulatory interspaced, short palindromic repeats associated (CRISPR/Cas) system were developed to enable efficient genomic alterations as an alternative to homologous recombination (HR). While ZFNs and TALENs employ linked arrays of proteomic DNA-binding domains which each recognize specific bases of a desired DNA sequence to guide their chimeric nuclease to a specific chromosomal location, DNA targeting of one or more loci with the CRISPR/Cas system is mediated by RNA using base-pairing. Sequence-specific targeting is followed by the introduction of DNA double-strand breaks (DSBs) which are repaired by the cellular machinery using either non-homologous end joining (NHEJ) or homology-directed repair (HDR) which either leads to the insertion or deletion of DNA sequences. Particularly ZFNs have been used for *in vivo* gene-knockouts, replacements or repair in gene therapy as an alternative to gene silencing (Gaj *et al.*, 2013, Sander *et al.*, 2014). However, neither ZFNs, TALENs nor CRISPR are ideal for stable cell line development with the aim of high yield recombinant protein production as this would require specific knowledge of genomic loci within an expression host which is not yet available. Transposon based methods such as *Sleeping Beauty* (*SB*) or *piggybac* similarly to nuclease based methods are used for *in vivo* modifications of animal models and cell culture applications. Chromosomal integration is targeted to naturally occurring sites with specific insertion pattern for each transposon. However, even though integration is directed it may occur in several transcriptionally active or inactive sites (Ivics *et al.*, 2010). Nevertheless the use of *piggyBac* for protein expression was demonstrated for mixed stable populations (Li *et al.*, 2013). To target a GOI at a pre-characterised genomic locus with predictable protein expression level, site specific recombinases (SSR) are the method of choice for stable cell line development as they do not require previous knowledge of a genomic locus but still enable the generation of isogenic cell lines.

Site-specific recombination systems are commonly found in bacteria, bacteriophages and yeast but not in higher eukaryotes. They catalyse DNA integration, excision/resolution or inversion through site specific recombination between specific DNA sequences. Depending on the residue which catalyses the recombination, SSRs are divided into tyrosine-type or serine-type recombinases. While the mechanism of tyrosine-type recombinases includes the formation of a holiday junction (HJ) intermediate (Figure 1-3), serine-type recombinases cause a 180 ° rotation of the substrate DNAs during recombination. According to the directionality of their recombination tyrosine-type recombinases are further subdivided into unidirectional tyrosine-type recombinases like λ and HK022 integrases which require

non-identical recognition sites (*attP* and *attB*) or bidirectional tyrosine-type recombinases like Cre and Flp recombinase which require identical recognition sites i.e. *loxP* or *FRT* respectively. Serine-type integrases on the other hand are subdivided according to their protein size into small serine-type recombinases which may act in a unidirectional or bidirectional manner (e.g. γδ and Tn3 resolvases or Hin and Gin invertases respectively) or large serine-type recombinases like ΦC31 and R4 integrases which act in an unidirectional way (Hirano *et al.*, 2011).

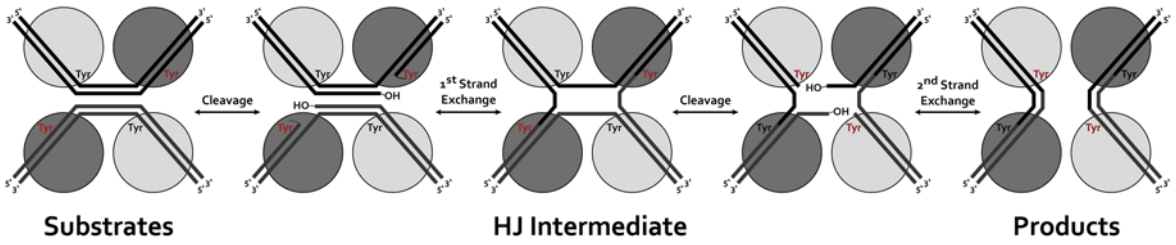

Figure 1-3: Mechanism of tyrosine-type recombinases. Four tyrosine-type recombinase monomers (e.g. Cre or Flp) attach to their corresponding recombinase binding sites (*lox*P or *FRT* respectively) to catalyse a step-wise strand exchange between two recombining DNA strands. First the nucleophilic tyrosine residue in the active catalytic centre (red) of one recombinase monomer on each DNA strand (dark grey) mediates cleavage of the first DNA strand between the linker and the recombinase binding site. This results in the formation of a covalent 3'-phophotyrosine intermediate and free 5'-OH (hydroxyl) groups. The 5'-OH groups subsequently attack the covalent DNA-Protein bond to exchange the first pair of DNA strands through the formation of a HJ intermediate. The exchange of the second pair of DNA strands is mediated by the remaining pair of recombinases (light grey) after isomerization of the HJ intermediate (not shown). Successful recombination does not destroy the recombination site and thus further exchanges are possible. Adapted from (Ghosh *et al.*, 2002, Chen *et al.*, 2003).

Since the early 90's the tyrosine-type recombinases Flp and Cre were employed in mammalian cells (O'Gorman *et al.*, 1991, Fukushige *et al.*, 1992). These were further optimized (Buchholz *et al.*, 1998, Raymond *et al.*, 2007) and used for tag-and-target (targeted integration) and tag-and-exchange (targeted replacement) strategies in *in vitro* and *in vivo* applications to tailor mammalian genomes. In this work the tyrosine type recombinase Flp is used for a tag-and-exchange approach in CHO Lec3.2.8.1 cells via recombinase mediated cassette exchange (described in Section 1.4.2).

1.4.1 Flp recombinase

The eukaryotic flippase (Flp) recombinase originates from the 2μM plasmid of *Saccharomyces cerevisiae*. Flp binds to Flp recognition target sites (*FRT*) comprising two 13 bp inverted repeats separated by an 8 bp spacer region. A third 13 bp symmetry element was shown to be non-essential (Andrews *et al.*, 1985, McLeod *et al.*, 1986) (Figure 1-4). However as a yeast protein Flp is active at 30 °C, to adapt it for use in mammalian systems the thermodynamic properties of Flp were improved through directed evolution strategies to

be active at 37 °C resulting in the mutant Flpe (Buchholz *et al.*, 1998). Flpe was further enhanced by *de novo* synthesis of the mouse-codon optimised Flpo variant (Raymond *et al.*, 2007) which was shown to be 5x more active than Flpe in *murine* embryonic stem cells (Kranz *et al.*, 2010). This optimised Flp variant, Flpo, is used in this work.

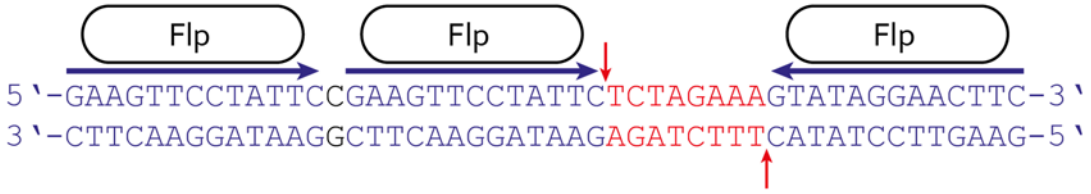

Figure 1-4: Flp recognition target site. *FRT* sites consist of two or three 13 bp symmetry elements (blue arrows, blue script) which flank an 8 bp asymmetric spacer region (red script) as inverted repeats. Flp mediates cleavage at the 5' ends of the 8 bp asymmetric spacer region (red arrows). Adapted from (Andrews *et al.*, 1985, Zhu *et al.*, 1995).

In 1994 the engineering of mutant *FRT* sites (FRT_{mut}) for use in tag-and-exchange applications began to further expand the Flp/*FRT* toolbox. Using PCR based mutagenesis the 8 bp spacer region was modified to obtain 5 different *FRT* mutants (FRT_{1-5}) (Schlake *et al.*, 1994). This list of *FRT* mutants was later expanded by Turan *et al.*, (2010) and examined for cross-interaction and self-recognition potential (Table 1-1). The *FRT* sites FRT_{wt}, FRT_3, FRT_{13}, and FRT_{14} are employed in this work.

Table 1-1: Overview of Flp recognition target sites (Schlake *et al.*, 1994, Turan *et al.*, 2010)

FRT	8 bp Spacer Sequence
FRT_{wt}	TCTAGAAA
FRT_1	TCTAGATA
FRT_2	TCTACTTA
FRT_3	TTCAAATA
FRT_4	TCTAGAAG
FRT_5	TTCAAAAG
FRT_{10}	ACTAGAAT
FRT_{11}	TGAACTAA
FRT_{12}	TTTCTGAA
FRT_{13}	TCATATAA
FRT_{14}	TATCAGAA
FRT_{15}	TTATAGGA
FRT_{16}	TCCGGGCA

1.4.2 Recombinase mediated cassette exchange (RMCE)

RMCE based targeted integration was used for the generation of stable producer cell lines during this work. Approaches towards targeted integration and its advantages are described below.

Random integration of gene targets into chromosomal loci can result in unpredictable gene expression as the genomic environment as well as the co-introduction of prokaryotic vector sequences may cause epigenetic silencing. The use of SSRs in tag-and-target and tag-and-exchange systems enabled the targeted integration into a previously characterized genomic locus to obtain suitable expression profiles. Tag-and-target systems based on the Flp/*FRT* system employ one *FRT* site to integrate a GOI into a tagged locus (Flp-in) (O'Gorman *et al.*, 1991). The Flp-in system was also commercialised by Invitrogen which now offers an array of cell lines for targeted exchange projects (Invitrogen, 2010). A variation of the Flp-in system, the Flp-mediated DNA integration and rearrangement at prearranged genomic targets (FLIRT) system was introduced by Huang *et al.*, (1997). The FLIRT system employs two tandemly oriented homospecifc *FRT* sites which can be used to flank a marker gene, tag a cell line and remove the marker gene again using a Flp-out reaction leaving only one *FRT* site in the genome. This single *FRT* site in turn can be used for the Flp-in reactions of a transgene into this specific chromosomal locus. However, during Flp-in reactions prokaryotic elements are still co-introduced which potentially induces epigenetic silencing. As a Flp-in reaction results in the GOI being flanked with two unidirectional homospecifc *FRT* sites, the reverse reaction (Flp-out) will be catalysed if recombinase activity should be persistent i.e. through random integration of the flippase-vector (Oumard *et al.*, 2006, Turan *et al.*, 2011). Therefore Schlake *et al.*, (1994) introduced a tag-and-exchange strategy, RMCE, which utilises a combination of wild type *FRT* and mutant *FRT* sites flanking a selection marker. The use of heterospecific *FRT* sites enabled the double-reciprocal crossover between a donor vector containing the GOI and a genomic exchange cassette with a compatible set of heterospecific *FRT* sites. Thus a single copy of a GOI without any prokaryotic elements could be integrated into a predefined genomic locus. RMCE has been used by several groups for the generation of master cell lines in embryonic stem (ES) cells (Seibler *et al.*, 1998), CHO-K1, HEK293 (Nehlsen *et al.*, 2009), CHO (DUXX-B11) (Mayrhofer *et al.*, 2014), CHO Lec3.2.8.1 (Wilke *et al.*, 2011) and *Spodoptera frugiperda* 9 (*Sf*9) cells (Fernandes *et al.*, 2012). Industrial applications of the Flp/*FRT* based RMCE system in CHO cells were described (Rehberger *et al.*, 2013). Similarly *loxP* and *FRT* sites can be used in combination (Froxing) if a non-reversible approach is desired (Lauth *et al.*, 2002). A strategy which combines the use of different *FRT* variants in an inverse oriented homospecifc fashion as well as *loxP* variants is the flip-excision (FlEx) system. FlExing introduces an inversely oriented GOI together with a

correctly oriented marker gene in the first round of recombination. In the second round of recombination the GOI and the marker gene are turned around thus reversing their expressible status (Schnütgen *et al.*, 2003, Schnütgen *et al.*, 2005). The Flp/*FRT* system was further brought forward by Turan *et al.*, (2010) which generated additional *FRT* mutants and evaluated their capability for self-recognition and level of cross-interaction to enable their simultaneous use to the classic FRT_3/FRT_{wt} combination. The identification of compatible sets of heterospecific *FRT* sites enabled the use of multiplexing which targets two distinct chromosomal exchange cassettes in parallel. To obtain functional *FRT* mutants the three rules listed in Table 1-2 needed to be considered when mutating the 8 bp spacer region of a *FRT* site. Alternative approaches for the integration of two transgenes in distinct loci using a combination of the Flp/*FRT* and the ΦC31/*attP* system were demonstrate in HEK293 cells (Waldner *et al.*, 2011). An overview of Flp/*FRT* based methods is shown in Figure 1-5.

Table 1-2: Traditional rules determining *FRT* interaction potential (Turan *et al.*, 2010)

		Sequence	AT content
Rule 1	No major interruptions of the **5'-polypyrimidine-tracts** may occur	5'-TCTAGAAA-3' 3'-AGATCTTT-5'	75 %
Rule 2	**Bordering base pairs** of the spacer sequence must be unchanged	5'-TCTAGAAA-3' 3'-AGATCTTT-5'	75 %
Rule 3	The **AT content** of the spacer sequence must be over 75 %	5'-TCTAGAAA-3' 3'-AGATCTTT-5'	75 %

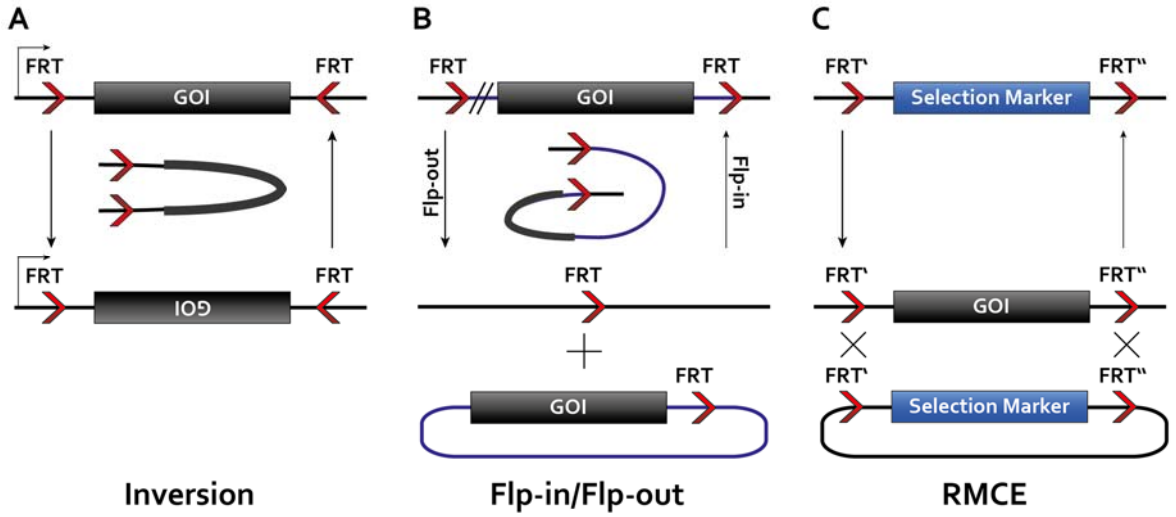

Figure 1-5: Flp mediated exchange reactions. (A) Flp recombinase can catalyse inversions between inversely oriented homospecific *FRT* sites which for example are utilized in the FlEx system (described in the text). **(B)** Equi-oriented homospecific *FRT* sites on the other hand catalyse integration or excision reactions. Insertion is prompted against thermodynamic and kinetic hindrances (Flp-in) whereas entropy driven excision (Flp-out) reactions are favoured if recombinase activity persists. The FLIRT system (described in the text) is based on the Flp-in/Flp-out system. One drawback however is the integration of prokaryotic segments which may trigger heterochromatization and thus epigenetic silencing. **(C)** RMCE circumvents this problem through the use of heterospecific *FRT* sites which enable the integration of a GOI without co-introducing prokaryotic vector elements. Adapted from Turan *et al.*, (2011).

1.4.3 The use of FACS for stable cell line development

In this work RMCE is used for the targeted integration of transgenes. No matter which method is chosen for targeted integration, the appropriate isolation of master cell lines needs to be put into consideration. The importance of proper master cell line selection and isolation was highlighted by Liu *et al.*, (2006). Not only should cell lines be screened for locus integration but also for homogenous unenforced expression to ensure long-term stability if selective pressure was used for clonal isolation which may otherwise result in heterogeneous expression level as well as epigenetic silencing. Qiao *et al.*, (2009) even suggested two rounds of RMCE following FACS. The first after genomic tagging of the master cell lines and one after a successful round of RMCE to isolate master cell lines with the desired phenotype and reusable high expressible loci. Thus FACS based methods are the most suitable for the isolation of master cell lines when avoiding drug selection marker. The use of fluorescent marker genes for the FACS based isolation of cell lines was demonstrated by several groups. For example Mancia *et al.*, (2004) separated a *eGFP* marker gene with an internal ribosomal entry site (IRES) element from the GOI to avoid direct proteomic linkage which would otherwise require eGFP removal after purification. Likewise the direct connection of a fluorescent marker gene to the GOI can be circumvented when using a modified version of the FLIRT system. If a fluorescent marker gene flanked with homospecifc FRT_3 sites is followed by the GOI during genomic tagging, the fluorescent marker gene can be removed after clonal isolation of a high producer cell line through Flp-mediated excision (Kaufman *et al.*, 2008, Wilke *et al.*, 2010). Renschler relies entirely on FACS for the isolation of RMCE master cell lines (Master TurboCells™) that contain an *eGFP* marker flanked with heterospecific *FRT* sites as well as on the isolation of producer cell line (Producer TurboCells™) pools that are 90-99% eGFP negative (Rehberger *et al.*, 2013). However many groups successfully employ selection traps for the isolation of producer cell lines (Nehlsen *et al.*, 2009, Wilke *et al.*, 2011, Fernandes *et al.*, 2012). In this work fluorescent marker genes are used for the isolation of CHO Lec3.2.8.1 master cell lines after genomic tagging. An introduced selection trap than is used for the isolation of producer cell lines after successful RMCE to isolate stable producer cell lines.

1.4.4 pFlp-Bac-to-Mam exchange vectors

The multi-host vector pFlp-Bac-to-Mam (pFlpBtM) and its derivative pFlpBtM-II were developed in our group to enable the fast screening of protein constructs in several

expression hosts (Meyer, 2012, Meyer *et al.*, 2013). In this work pFlpBtM vectors were used as exchange vectors for the generation of stable CHO Lec3.2.8.1 producer cell lines and as expression vectors in HEK293-6E cells. For the RMCE based generation of stable CHO Lec3.2.8.1 producer cell lines pFlpBtM vectors comprise heterospecific *FRT* sites flanking a GOI as well as a phosphoglycerate kinase (PGK) promoter and a start codon which activates a selection trap in the previously tagged chromosomal locus upon successful integration (Wilke *et al.*, 2011). For the transient expression in HEK293-6E (Durocher *et al.*, 2002) pFlpBtM vectors comprise the EBV origin of replication as well as a cytomegalovirus (CMV) promoter. All pFlpBtM based vectors can also serve as donor vectors for the generation of recombinant bacmids using the MultiBac system. Those bacmids can be utilised for baculovirus expression vector system (BEVS) based protein production in insect hosts (Berger *et al.*, 2004, Fitzgerald *et al.*, 2007). Detailed information on the generation and evaluation of pFlpBtM vectors was described previously (Meyer, 2012, Meyer *et al.*, 2013). A schematic overview of pFlpBtM-II is given in Figure 1-6.

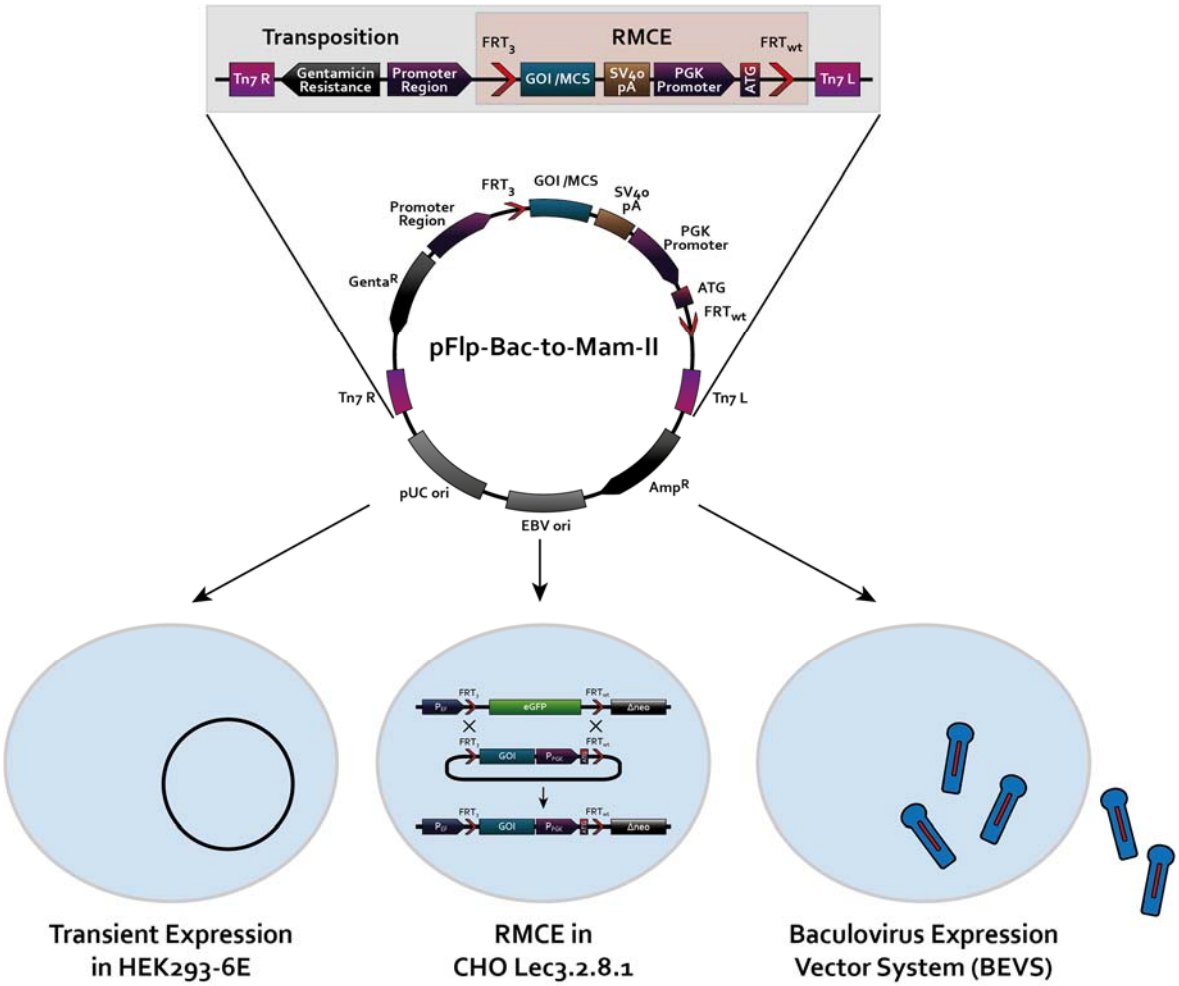

Figure 1-6: pFlpBtM-II. The multi-host vector pFlpBtM-II can be used for transient protein expression in HEK293-6E cells as it comprises the EBV origin of replication in its vector backbone and a CMV promoter in its promoter region. Protein production in insect cells is done through the generation of recombinant bacmids using Tn7-based transposition for use in the BEVS (relevant vector region highlighted in grey). Finally, the pFlpBtM-II vector can be used for stable cell line generation in CHO Lec3.2.8.1 cells using RMCE (relevant vector region highlighted in red) as it comprises heterospecific *FRT* sites flanking the GOI as well as a PGK promoter and a start codon for the activation of a selection trap. Adapted from Meyer *et al.*, (2013).

1.5 Protein targets

1.5.1 Fluorescent proteins

In this work eGFP (enhanced green fluorescent protein) and tdTomato (tandem dimer Tomato) were used as fluorescent markers in the establishment of a binary RMCE system in CHO Lec3.2.8.1 cells. Their presence within the stably integrated exchange cassettes for one allowed the FACS based isolation of master cell lines. On the other hand successful exchange of fluorescent marker genes against target genes enabled the identification of producer cell lines using flowcytometry and fluorescence microscopy. As shown in Figure 1-7 the emission spectra of eGFP and tdTomato can be distinguished accurately

which is important for their differentiation when used in parallel in the same system. Moreover, tdTomato was used as a model protein to evaluate the newly established binary RMCE system. tdTomato was integrated into "single" RMCE master cell lines (contain only exchange locus 1 with eGFP) and binary RMCE master cell lines (contain both loci) using RMCE. The specific expression capabilities of each locus were determined and correlated to the binary RMCE system.

Fluorescent proteins are extensively used in the life sciences community for an array of applications in living cells, tissues and imaging. Information about the cellular localization, movement and thus function of proteins as well as cell, tissue and nucleic acid labelling can be gathered. Green fluorescent protein (GFP) family proteins are approximately 25 kDa in size with a length of 220-240 amino acid. They comprise a β-barrel structure and have a tendency to oligomerize which prompted the development of monomeric forms (Chudakov *et al.*, 2010). The existence of GFP was first reported by Shimomura *et al.*, (1962) in the jelly fish *Aequorea aequorea*. 30 years later Prasher *et al.*, (1992) cloned and determined the first sequence of a *Aequorea victoria* derived *gfp* gene which laid the basis for its use as a fluorescent marker in prokaryotic and eukaryotic cells as shown by Chalfie *et al.*, (1994). Mutations within the *gfp* gene gave rise to GFP variants with increased sensitivity level as for enhanced GFP (eGFP) (Cormack *et al.*, 1996) or fluorescent shifts as for cyan and blue fluorescent protein (CFP/BFP) (Heim *et al.*, 1994, Heim *et al.*, 1996). Later on the red fluorescent GFP homologue from the mushroom coral *Discosoma* sp. DsRed was isolated (Matz *et al.*, 1999) and served as basis for directed evolution to obtain monomeric red fluorescent protein-1 (mRFP1) (Campbell *et al.*, 2002). Further directed evolution efforts of mRFP1 gave rise to an array of fluorescent proteins including mCherry, mHoneydew, mBanana, mOrange, mTangerine and mStrawberry (Shaner *et al.*, 2004), whereas directed evolution of the faster maturing DsRed.T1 variant (Bevis *et al.*, 2002) gave rise to dimer (d)Tomato which was further modified to avoid aggregation by fusing two copies together to obtain tandem dimer (td)Tomato (Shaner *et al.*, 2004).

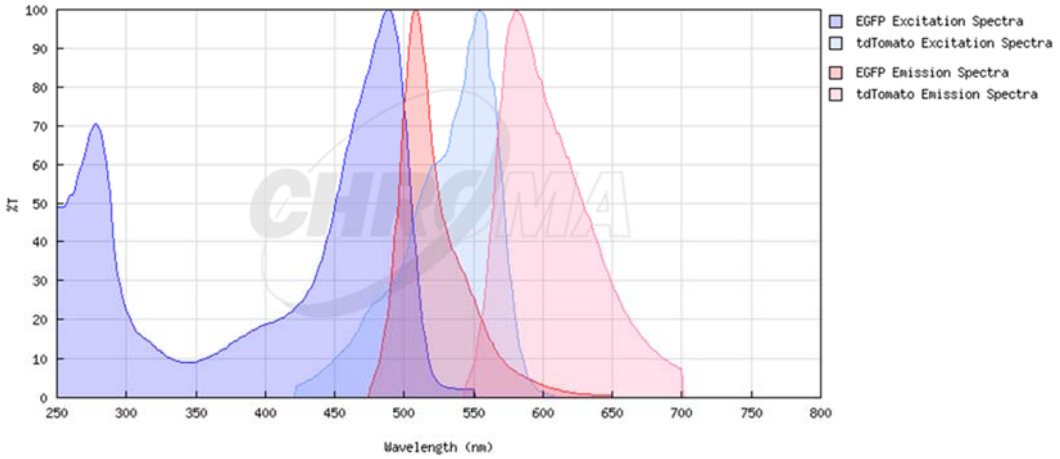

Figure 1-7: Excitation and emission spectra for eGFP and tdTomato. Overlay of eGFP and tdTomato excitation (blue) and emission (red) spectra. Wavelength (nm) plotted against the percentage of transmittance (%T). Spectrum obtained from http://www.chroma.com (08Sep14).

1.5.2 Toll-like receptor (TLR) function

The binary RMCE system in CHO Lec3.2.8.1 cells, established during this work, enables the co-expression of integrated transgenes at pre-characterized genomic loci. It is expected that the co-expression of difficult to express proteins with their molecular chaperones will improve the expression of demanding targets. The difficult to express target proteins chosen for this work are TLR1, TLR2 and TLR5 (detailed description in Section 1.5.4 and Section 1.5.5).

TLRs received their name due to their conserved homology to the *Drosophila melanogaster* receptor Toll. They are type-I integral membrane glycoproteins and belong to the Toll/interleukin-1 (IL-I) receptor (TIR) superfamily. TLRs are usually found in sentinel cells including B-cells, macrophages, monocytes, neutrophils or dendritic cells but also in non-immune cells like epithelial and endothelial cells. As patter recognition receptors (PRRs) TLRs respond to pathogen associated molecular pattern (PAMP) such as pathogen derived carbohydrate, peptide and nucleic acid structures and therefore play an important role within the innate immune response in the defence against bacterial, fungal, protozoal and viral pathogens. Nonetheless, it becomes evident that TLRs also have a purpose in the initiation of the adaptive immune response as they regulate T-helper (T_H) cell profiles through differential binding of their ligands. Furthermore TLRs also recognize damage-associated molecular pattern (DAMP), cell-derived non-microbial components which are released upon non-programmed cell death. So far 13 TLRs were identified in mammals, 10 of those are present in humans. Depending on their ligand specificity TLRs are either located on the cell membrane (TLR1, 2, 4, 5, 6 and 10) or within endosomal

compartments (TLR3, 7, 8, 9, 11, 12 and 13). Malfunctioning of the TLR system is associated with several clinical pictures; including allergies, cancer and inflammatory diseases as well as neurodegenerative and autoimmune disorders. This makes the elucidation of TLR signalling pathways, mechanisms and consequently their specific role in innate and adaptive immunity essential for translational medical applications (Agrawal *et al.*, 2003, Ishii *et al.*, 2005, Barton *et al.*, 2009, Hidmark *et al.*, 2012, Tang *et al.*, 2012, Raetz *et al.*, 2013).

TLRs are divided into three domains an N-terminal ectodomain (ECD), a single spanning transmembrane domain and an intracellular TIR domain responsible for downstream signal transduction. The N-terminal ECD adapts a horseshoe-like structure involved in ligand recognition. It is composed of 16-28 leucine rich repeat (LRR) modules each comprising 24 amino acid residues with conserved "LxxLxLxxN" motives (Figure 1-8). The hydrophobic LRR domain is capped with C- and N-terminal disulphide-bonded caps (LRR-CT and LRR-NT) which do not comprise any LRR motives and thus protect the hydrophobic core from solvent and aid domain stabilisation (Jin *et al.*, 2008).

TLR signalling follows two different paths; either the myeloid differentiation primary-response protein 88 (MyD88)-dependent pathway triggering a nuclear factor kappa-light-chain-enhancer of activated B cells (NF-κB) response followed by the transcription of inflammatory cytokines or the MyD88-independent pathway triggering either a NF-κB response as well as an interferon (IFN) regulatory factor (IRF3) response followed by the transcription of IFN-β. Ligand binding initiates the dimerization of TLRs accompanied by conformational changes which activate a downstream cascade. In the MyD88-dependent pathway the adaptor molecule MyD88 is directly recruited to the TIR domains of TLR5, 7, 8, 9 and 11 upon receptor dimerization through homodimerization of its own C-terminal TIR domain. The association of MyD88 with TLR2 and TLR4 is bridged through the adaptor molecule TIRAP (TIR-domain-containing adaptor protein also known as MyD88-adaptor-like protein, MAL). In addition to the MyD88-dependent pathway TLR4 also employs the MyD88-independent pathway through the adaptor molecules TRIF (TIR-domain containing adaptor protein inducing IFN-β) and TRAM (TRIF related adaptor molecule). In contrast TLR3 employs only the adaptor molecule TRIF (Akira *et al.*, 2004, Liew *et al.*, 2005, O'Neill *et al.*, 2007, Trinchieri *et al.*, 2007). A schematic overview of TLR structure and signalling is given in Figure 1-8.

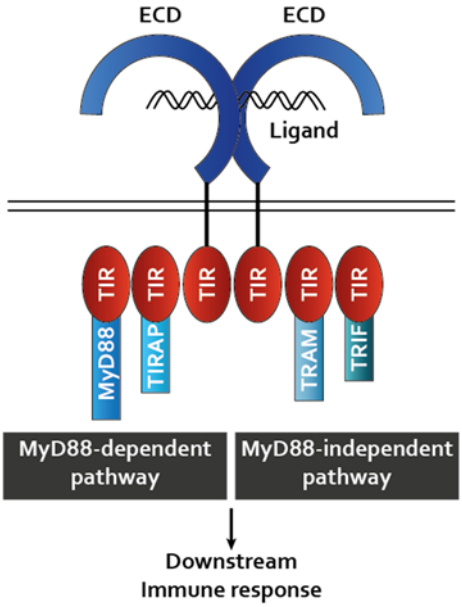

Figure 1-8: Schematic representation of Toll-like receptor dimer in interaction with intracellular adaptor molecules. TLRs are comprised of an N-terminal ECD containing 16-28 LRR modules, a single transmembrane spanning domain and an intracellular TIR domain which recruits different adaptor molecules to activate a downstream immune response over the MyD88-dependent or MyD88-independent pathway. Adapted from Akira *et al.*, (2004).

1.5.3 The hybrid LRR technique in TLR structural biology

To improve the expression of demanding protein targets for structural biology applications a binary RMCE system was established in glycosylation deficient CHO Lec3.2.8.1 cells. The co-expression of molecular chaperones shall improve the expression of TLR targets. To further improve the soluble expression and crystallization properties of TLRs the "hybrid LRR technique", described below, was used in this work.

To date crystal structqures for TLR ECDs alone or in complex with agonistic or antagonistic ligands were solved for TLR1, TLR2, TLR3, TLR4, TLR5, TLR6 and TLR8 (References listed in Table 1-3). The soluble expression and crystallization of TLRs however is a major hurdle. To tackle this problem Kim *et al.*, (2007) developed the "hybrid LRR technique" to improve the soluble expression of TLRs and their protein crystallization properties. The hybrid LRR technique uses variable lymphocyte receptor (VLR) fragments attached to one or both termini of a TLR ECD construct at conserved "LxxLxLxxN" motives (Figure 1-9).

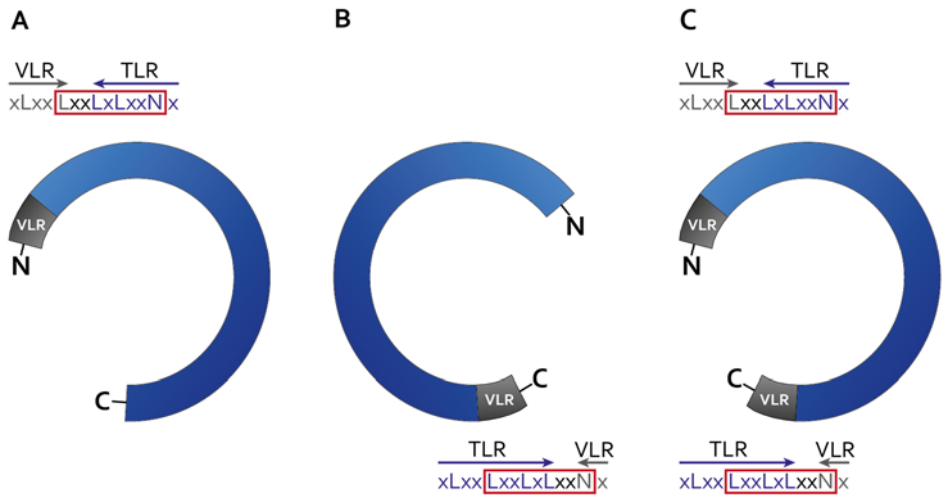

Figure 1-9: Hybrid LRR technique. TLR-VLR hybrids can be obtained by fusion of truncated TLR constructs (blue) with VLR fragments (gray) at conserved LxxLxLxxN motives (red box) using (A) N-terminal fusion (B) C-terminal fusion or (C) fusion at both termini. Non-native amino acids (black) result from the cloning site (Jin *et al.*, 2008).

VLRs belong to the LRR family of proteins. They are found in jawless fish (Pancer *et al.*, 2004) where an abundant array of VLR variants derived from germline genes *VLR-A*, *VLR-B* (Pancer *et al.*, 2005) and *VLR-C* (Kasamatsu *et al.*, 2010) regulate adaptive immune responses. Crystal structures for inshore hagfish *Eptatretus burger* VLR-A and VLR-B variants were described by Kim *et al.*, (2007). VLRs are "typical" LRR family proteins displaying a horseshoe-like structure. Their shape results from conserved asparagine ladder and phenylalanine spine structures of the LRR module backbone. This hydrophobic core is flanked by protective caps (LRR-NT and LRR-CT respectively). Sequence variations are limited to the concave surface where ligand binding occurs (Kim *et al.*, 2007). The hybrid LRR technique employs the conserved "LxxLxLxxNxL" motive common to all LRR family proteins. Residues annotated with "x" are exchangeable hydrophilic amino acids which are exposed at the concave surface of the horseshoe-like structure whereas conserved residues are responsible for the structural network (Jin *et al.*, 2008). The hybrid LRR technique was shown to maintain the structural integrity of fusion partners and thus enabled the truncation of TLR constructs without loss of their protective LRR-NT or LRR-CT caps as those were replaced by matching hybrid VLR fragments (Kim *et al.*, 2007).

The hybrid LRR technique was used to solve crystal structures for TLR4 (Kim *et al.*, 2007), TLR1, TLR2, TLR6 (Jin *et al.*, 2007, Kang *et al.*, 2009) and TLR5 (Yoon *et al.*, 2012). TLRs interact with protein and non-protein ligands using their concave, lateral or convex surface which induces the dimerization of TLR homo- or heterodimers forming a typical "m"-shape demonstrated by several crystallographic studies (Jin *et al.*, 2007, Liu *et al.*, 2008, Kang *et al.*,

2009, Park *et al.*, 2009, Yoon *et al.*, 2012, Tanji *et al.*, 2013) (Figure 1-10). A list of currently available TLR ECD structures with or without bound agonistic or antagonistic ligands is summarized in Table 1-3.

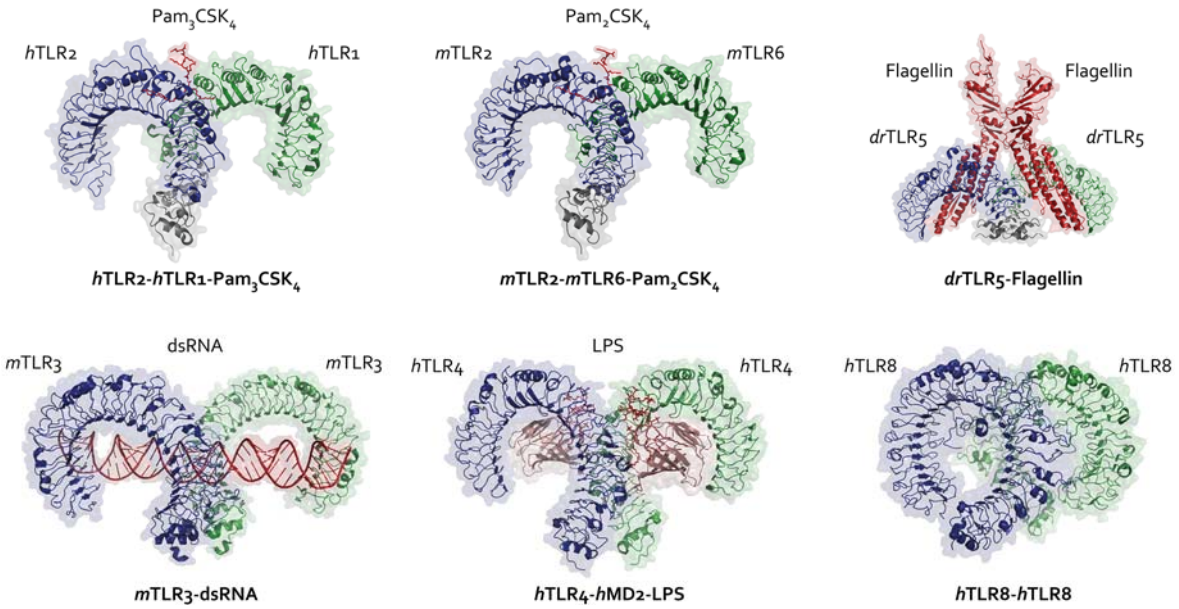

Figure 1-10: TLR homo-and heterodimers. TLR homo-and heterodimer structures in complex with their ligands are shown for *h*TLR2-*h*TLR1-Pam_3CSK_4 (PDB 2Z7X), *m*TLR2-*m*TLR6-Pam_2CSK_4 (PDB 3A79), *dr*TLR5-Flagellin (PDB 3V47), mTLR3-dsRNA (PDB 3CIY) and *h*TLR4-*h*MD2-LPS (PDB 3FXI). A homodimer structure without bound ligand is shown for *h*TLR8 (PDB 3W3G). References are listed in Table 1-3.

Table 1-3: Overview of TLR ECD crystals structures with or without bound ligand.

Organism	TLR/Complex	PBD ID	VLR Hybrid	Reference
Human	TLR1-TLR2-Pam3CSK4	2Z7X	Yes	(Jin *et al.*, 2007)
Mouse	TLR2-mTLR6-Pam2CSK4	3A79	Yes	(Kang *et al.*, 2009)
Mouse	TLR2-lipoteichoic acid	3A7B	Yes	(Kang *et al.*, 2009)
Mouse	TLR2-PE-DTPA	3A7C	Yes	(Kang *et al.*, 2009)
Human	TLR3	2A0Z	No	(Bell *et al.*, 2005)
Human	TLR3	1ZIW	No	(Choe *et al.*, 2005)
Mouse	TLR3/dsRNA	3CIY	No	(Liu *et al.*, 2008)
Human	TLR3/mAB1068/mAB12/mAb15	3ULV, 3ULU	No	(Luo *et al.*, 2012)
Mouse	TLR4/MD-2 complex	2Z64	No	(Kim *et al.*, 2007)
Human	TLR4	2Z63, 2Z62, 2Z66	Yes	(Kim *et al.*, 2007)
Human	TLR4/MD-2/Eritoran	2Z65	Yes	(Kim *et al.*, 2007)
Human	TLR4-MD-2-LPS dimer	3FXI	No	(Park *et al.*, 2009)
Mouse	TLR4/MD-2/Re-LPS	3VQ2	No	(Ohto *et al.*, 2012)
Mouse	TLR4/MD-2/lipid IVa	3VQ1	No	(Ohto *et al.*, 2012)
Human	TLR4 (D299G/T399I)-MD-2-LPS	4G84	No	(Ohto *et al.*, 2012)
Zebrafish	TLR5	3V44	Yes	(Yoon *et al.*, 2012)
Zebrafish	TLR5/FliC	3V47	Yes	(Yoon *et al.*, 2012)
Human	TLR8/TLR8	3W3G	No	(Tanji *et al.*, 2013)
Human	TLR8/TLR8/CL097	3W3J, 3W3N	No	(Tanji *et al.*, 2013)
Human	TLR8/TLR8/CL075	3W3K	No	(Tanji *et al.*, 2013)
Human	TLR8/TLR8/R848	3W3L, 3W3M	No	(Tanji *et al.*, 2013)
Human	TLR8/Ds-877	3WN4	No	(Kokatla *et al.*, 2014)

1.5.4 TLR1 and TLR2

For the co-expression in the binary RMCE system established during this work ECD constructs for mTLR1 and mTLR2 were selected. The co-expression with their molecular chaperones (described in Section 1.5.6) was predicted to improve the soluble expression for both. While crystal structures for TLR1 and TLR2 are already available in complex with di- or tri-acylated lipopeptides (Jin *et al.*, 2007, Kang *et al.*, 2009) no structure for TLR1 or TLR2 is yet available in complex with a protein ligand. The elucidation of TLR1 and TLR2 structures in complex with curli fibrils was of interest for collaboration partners and thus was selected for the expression in the binary RMCE system.

TLR1 was first identified by Nomura *et al.*, (1994) as KIAA0012, later on by Taguchi *et al.*, (1996) as Toll/Interleukin-1-receptor-Like (TIL) and finally by Rock *et al.*, (1998) as TLR1. TLR2 was first identified by Chaudhary *et al.*, (1998) as Toll/Interleukin-1-receptor-Like-4 (TIL-4) when searching for human Toll homologues and rediscovered together with other TLRs by Rock *et al.*, (1998). TLR1 and TLR2 are located on the cell surface of leukocytes, dendritic cells (DCs), lymphatic endothelial cells and epithelial cells (Muzio *et al.*, 2000, Furrie *et al.*, 2005, Pegu *et al.*, 2008). TLR2, with TLR1 or TLR6 as co-receptor, recognizes non-protein ligands including tri-acylated or di-acylated lipopeptides, LPS, lipoteichoic acids and zymosan (Jin *et al.*, 2007, Kang *et al.*, 2009). Nonetheless a protein-ligand, CsgA, the main component of amyloid-like curli fibrils expressed in a small subset of *Enterobacteriaceae* including *Salmonella enterica* serotype Typhimurium (*S.* Typhimurium) and *E.coli* was shown to be a TLR2 agonist (Tükel *et al.*, 2005, Tükel *et al.*, 2009, Oppong *et al.*, 2013). In cooperation with TLR1, TLR2 mediates a ligand induced immune response upon CsgA recognition (Tükel *et al.*, 2010). A stronger NF-κB response was observed when CD14, serving as an accessory protein, binds to curli fibres before TLR2-TLR1 activation (Rapsinski *et al.*, 2013). Amyloid formation in bacteria is of biological importance as part of the extracellular biofilm matrix. In humans however amyloid formation can cause neurodegenerative disorders including Alzheimer's and Huntington's disease. These phenotypes result from inflammation-mediated tissue damage from amyloid formation and deposition (Tükel *et al.*, 2009, Tükel *et al.*, 2010). Interactions of TLR2 with fibrillar β-amyloid plaques (fAβ) a component of plaques in Alzheimer's disease (Jana *et al.*, 2008, Udan *et al.*, 2008, Reed-Geaghan *et al.*, 2009, Liu *et al.*, 2012) and serum amyloid A (SAA) (Cheng *et al.*, 2008, He *et al.*, 2009) were demonstrated.

1.5.5 TLR5

To begin of this work no crystal structure for TLR5 was yet available. Thus the hTLR5 ECD was chosen as a target for the expression in the binary RMCE system. Meanwhile the crystal structure for *ds*TLR5 became available (Yoon *et al.*, 2012). However the expression of human TLR5 ECDs was shown to be a real challenge (Hong *et al.*, 2012, Yoon *et al.*, 2012) and thus remained a worthwhile target.

TLR5 was first identified by Chaudhary *et al.*, (1998) as Toll/Interleukin-1-receptor-Like-3 (TIL-3) when searching for human Toll homologues and rediscovered together with other TLRs by (Rock *et al.*, 1998). TLR5 is located on the cell surface of leukocytes, DCs, lymphatic endothelial cells and epithelial cells (Chaudhary *et al.*, 1998, Muzio *et al.*, 2000, Miller *et al.*, 2005, Pegu *et al.*, 2008). So far TLR5 is unique compared to other TLRs as it was shown to recognize protein-ligands only, namely bacterial flagellin (Hayashi *et al.*, 2001). However only flagellin monomers are recognized by TLR5 as the 13 amino acid binding site of flagellin is located within the flagellar filament. Each flagellin monomer comprises 4 domains (D0, D1, D2 and D3). D1, one of the most conserved domains interacts with TLR5 (Smith *et al.*, 2003). This was further confirmed through mutation studies within the D1 domain which eliminated flagellin-TLR5 interactions (Andersen-Nissen *et al.*, 2005) as well as the flagellin-*ds*TLR5 crystal structure (Yoon *et al.*, 2012). The flagellin binding site on TLR5 was studied by several groups using truncation, mutation as well as *in silico* studies (Jacchieri *et al.*, 2003, Mizel *et al.*, 2003, Andersen-Nissen *et al.*, 2007). An *in silico* prediction which postulated residues 552-561 as potential TLR5 binding site (Jacchieri *et al.*, 2003) could not be confirmed by *in vivo* studies which narrowed the TLR5 binding site down to residues 386-407 including an accessory function of residues 408-425 (Mizel *et al.*, 2003) and residues 174-401 (Andersen-Nissen *et al.*, 2007) respectively. The flagellin-*ds*TLR5 crystal structure revealed two primary binding interfaces of *ds*TLR5 (Yoon *et al.*, 2012) one within the experimentally postulated binding sites as well as one located downstream. Moreover it was revealed that TLR5 binding affinities within different species vary and thus each species recognises and binds a certain set of bacterial flagellins more or less efficiently (Andersen-Nissen *et al.*, 2007, Keestra *et al.*, 2008, Metcalfe *et al.*, 2014). Besides its role in innate and adaptive immunity in which TLR5 supports MHC class-II presentation of flagellin fragments to CD4 T cells (Letran *et al.*, 2011), the therapeutic relevance of TLR5 is indicated by its increased presence on breast cancer carcinoma which are highly receptive

to TLR5 mediated signal-transduction. Cai *et al.*, (2011) demonstrated that flagellin can induce anti-carcinogenic effects as a TLR5 agonist by inhibiting proliferation of carcinogenic cells. Nonetheless TLR and cell-type specific differences have been observed in tumorigenesis (Cai *et al.*, 2011).

1.5.6 Accessory proteins – GRP94 and PRAT4A

The eukaryotic ER chaperone glucose-regulated protein 94 (GRP94) (alias: heat shock protein 90b1 (HSP90b1), HSPC4, glycoprotein 96 (gp96), endoplasmin and ERp99) an ER paralogue to the cytosolic HSP90 and the chaperone-like ER resident protein, protein associated with toll-like receptor 4A (PRAT4A) (alias: canopy FGF signalling regulator 3 (CNPY3)) were shown to chaperone serval TLRs as described below. In this work mGRP94 and mPRAT4A were used for the co-expression of mTLR1, mTLR2 and hTLR5 ECDs in the binary CHO Lec3.2.8.1 RMCE system. It was anticipated that the co-expression of TLRs with molecular chaperones will improve their soluble expression.

GRP94 is divided into three domains. An N-terminal adenosintriphosphate (ATP)ase domain with intrinsic ATPase activity which binds and hydrolyses ATP is separated by a non-conserved highly charged intermediate domain from a C-terminal homodimerization domain which influences enzymatic activity of the ATPase domain. GRP94 is expressed in most cell types and is induced under stress conditions following the accumulation of misfolded proteins. (Randow *et al.*, 2001, Liu *et al.*, 2010). The structural basis of GRP94 was elucidated by Dollins *et al.*, (2007) for *canine* (*cl*)GRP94 (73-754Δ287-327) in complex with adenosine diphosphate (ADP) and the non-hydrolysable ATP analogue adenylyl-imidodiphosphate (AMPPNP). GRP94 shows a left handed helical twist (twisted V) conformation which allows C-terminal domain homodimerization but prevents N-terminal homodimerization. A C-terminal client binding site was suggested and later confirmed by Wu *et al.*, (2012) which identified a C-terminal loop structure formed by amino acid residues 652-678 (Figure 1-11). In contrary to GRP94, PRAT4A shows no intrinsic ATPase activity nor does it influence ATPase activity of GRP94 as co-chaperone (Liu *et al.*, 2010). Mutation studies demonstrated that PRAT4A interacts differently with different TLR clients (Kiyokawa *et al.*, 2008).

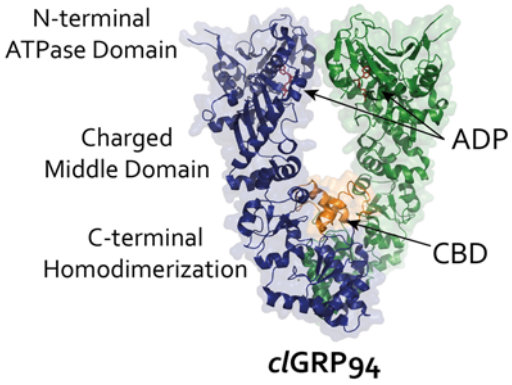

Figure 1-11: Crystal structure of *canine* GRP94 dimer (PDB 2O1U). *cl*GRP94 adapts an homodimeric twisted V structure. Each monomer (blue, green) is composed of 3 domains, an N-terminal ATPase domain (bound ADP shown in red), a charged middle domain and a C-terminal homodimerization domain. The client binding domain (CBD, yellow) ranges from amino acid residues 652-678. Adapted from (Dollins *et al.*, 2007, Wu *et al.*, 2012)

The use of immune co-precipitation and knockdown studies typically in HEK cells, B-cells or macrophages demonstrated that the conformational maturation of TLRs is dependent on the ER chaperones GRP94 and PRAT4A which regulate TLR cell surface display or trafficking to lysosomes. Randow *et al.*, (2001) demonstrated that GRP94 is not required for cell survival even though it represents one of the most abundant ER proteins in a cell. However GRP94 was shown to be essential for the regulation of innate immunity as it controls cell surface trafficking of TLR1, TLR2 and TLR4. It was observed that the GRP94 deficient mutant cell line E4.126 derived from *murine* pre-B-cells (70Z/3) retained expressed TLRs within the ER and thus inhibited the response to bacterial toxins including LPS (lipopolysaccharide), LTA (lipoteichoic acid) and PGN (peptidoglycan). A few years later Yang *et al.*, (2006) demonstrated that the response to TLR ligands is dependent on GRP94 expression for cell surface TLRs (TLR2, TLR4, TLR5) as well as endosomal TLRs (TLR7 and TLR9) using macrophage-specific GRP94-deficient mice.

The same year Wakabayashi *et al.*, (2006) described another protein which regulates cell surface expression of TLRs. PRAT4A associates with the immature hypoglycosylated form of TLR4, but not MD-2 or TLR2, thus regulating trafficking of TLR4 in HEK293, B-cells and/or DCs. A similar protein which also associates with TLR4, PRAT4B, was identified through database analysis as it shares 54 % amino acid sequence with PRAT4A (Konno *et al.*, 2006). In contrary to PRAT4A, PRAT4B was shown to be a negative regulator for TLR trafficking (Hart *et al.*, 2012). The importance of PRAT4A for innate and adaptive immunity was demonstrated by the same group as gene-silencing of PRAT4A inhibits not only the trafficking of TLR4 but also TLR1 to the cell surface as well as TLR9 trafficking to the

lysosome. In contrary to their previous results cell surface trafficking of TLR2 trafficking is also down-regulated but not inhibited (Takahashi *et al.*, 2007). Functional loss of TLR4 and TLR9 was confirmed by Liu *et al.*, (2010) after PRAT4A knockdown. Furthermore, knock down studies of PRAT4A added TLR2 and TLR7 to the list of PRAT4A clients (Liu *et al.*, 2010) as well as TLR5 (Shibata *et al.*, 2012).

It was suggested that GRP94, in contrary to common expectations, does require PRAT4A as a co-chaperone for TLR trafficking. This was supported by co-localization studies of PRAT4A and GRP94 in the ER as well as the demonstration of adenosine nucleotide sensitive chaperone interactions between both. Moreover, it was shown that TLR9 requires both PRAT4A and GRP94 in a tri-molecular complex for maturation (Liu *et al.*, 2010).

To improve the soluble expression of TLR ECDs in this work the molecular chaperones mPRAT4A or mGRP94 are stably co-expressed in a binary CHO Lec3.2.8.1 RMCE system.

2 Aim of this work

Stable cell line development is a time-consuming process. The generation of homogenous high producer cell lines does require extensive screening and needs to be repeated for each individual target (Wurm, 2004). Targeted integration via RMCE however does cut the timelines for stable cell line development significantly as the integrated gene is incorporated into a previously tagged chromosomal locus (Wilke *et al.*, 2011). The use of stable cell lines for protein production does enable the convenient scale up into bioreactors which is particularly useful for difficult to express protein targets with low volumetric yields. Nevertheless, the expression of demanding protein targets can also be aided through the co-expression of protein subunits or accessory molecules (Neuhaus *et al.*, 2006, Bieniossek *et al.*, 2008). The level of protein production however is not the only bottleneck that needs to be faced for structural biology applications. Heterogeneous glycosylation patterns do interfere during crystal formation and thus need to be removed *a priori* or glycosylation deficient cell lines such as CHO Lec3.2.8.1 need to be employed (Stanley, 1989, Aricescu *et al.*, 2006).

The aim of this work focuses on the stable co-expression of difficult to express protein targets with accessory molecules for structural biology applications. This requires the establishment of a binary master cell line in glycosylation deficient CHO Lec3.2.8.1 which will enable the targeted integration of genes at two pre-defined genomic loci via RMCE. RMCE will ease the generation of homogenous high producer cell lines by reducing development times for their generation.

The binary RMCE system will be evaluated with the model protein tdTomato. Targeted integration via RMCE of tdTomato into "single" RMCE master cell lines (with only one exchange locus) and binary RMCE master cell lines (with both exchange loci) will enable the determination of specific expression capabilities for each locus and its correlation to the binary RMCE system. Moreover, the reproducibility of tdTomato expression for each locus will be determined.

Producer cell lines co-expressing Toll-like receptors in combination with their chaperones GRP94 or PRAT4A will be generated to improve volumetric yields of soluble protein production.

3 Materials and Methods

3.1 Instruments

Instruments used for this work are listed in Table A.1-1 in the appendix.

3.2 Chemicals, kits and reagents

If not specified otherwise, all chemicals were obtained from Bayer, Becton Dickinson (BD), GE Healthcare, InvivoGen, Invitrogen, Life Technologies, Lonza, Macherey-Nagel, Merck, Millipore, New England Biolabs (NEB), Novagen, Qiagen, Promega, Roche, Roth, Sigma-Aldrich or Thermo Scientific.

3.2.1 Enzymes and molecular weight standards

Restriction endonucleases, enzymes and molecular weight standards commonly used in this work are listed in Table 3-1, Table 3-2 and Table 3-3.

Table 3-1: Restriction endonucleases

Restriction Endonucleases	Cat#	Supplier
*Avr*II (5.000 U/mL)	R0174L	NEB
*BamH*I-HF (20.000 U/mL)	R3136L	NEB
*Bbs*I (5.000 U/mL)	R0539L	NEB
*BsaB*I (10.000 U/mL)	R0537L	NEB
*BstB*I (20.000 U/mL)	R0519L	NEB
*Cla*I (5.000 U/mL)	R0197L	NEB
*EcoR*I (20.000 U/mL)	R0101L	NEB
*EcoR*I-HF (20.000 U/mL)	R3101L	NEB
*Hin*dIII (20.000 U/mL)	R0104L	NEB
*Hin*dIII-HF (20.000 U/mL)	R3104L	NEB
*Kpn*I (10.000 U/mL)	R0142L	NEB
*Kpn*I-HF (20.000 U/mL)	R3142L	NEB
*Mlu*I (10.000 U/mL)	R0198L	NEB
*Nco*I (10.000 U/mL)	R0193L	NEB
*Nco*I-HF (20.000 U/mL)	R3193L	NEB
*Nhe*I-HF (20.000 U/mL)	R3131L	NEB
*Sal*I (20.000 U/mL)	R0138L	NEB
*Sal*I-HF (20.000 U/mL)	R3138L	NEB
*SnaB*I (5.000 U/mL)	R0130L	NEB
*Xho*I (20.000 U/mL)	R0146L	NEB

Table 3-2: Enzymes

Enzyme	Cat#	Supplier
T4 DNA Ligase (1.000 U/ mL)	11000324/ 14395420	Roche
Antarctic Phosphatase (5.000 U/mL)	M0289S	NEB
Phusion® Hot Start II DNA Polymerase (2.000 U/mL)	F-549L/ M0530S/ B0515A	Finnzymes/ Thermo Scientific/ NEB
KOD Hot Start DNA Polymerase (1.000 U/mL)	71086-3	Novagen/Millipore
DNase I (1ng/µL)	N/A	MOSB, HZI
Trypsin/ EDTA (1x)	L11-004	PAA Laboratories GmbH
Trypsin/ EDTA (10x)	L11-003	PAA Laboratories GmbH

Table 3-3: Molecular weight standards

Molecular weight standard	Usage	Cat#	Supplier
Smart Ladder	Agarose gel electrophoresis	MW-1700-10 MW-1700-02	Eurogentech
PageRuler Plus prestained	SDS-PAGE	SM1811/ 26620	Fermentas / Thermo Scientific
PageRuler unstained	SDS-PAGE	SM0661/ 26614	Fermentas / Thermo Scientific
Precision Plus Protein unstained	SDS-PAGE	161-0363	Bio-Rad
Precision Plus Protein All blue	SDS-PAGE	161-0373	Bio-Rad
Precision Plus Protein Dual Color	SDS-PAGE	161-0374	Bio-Rad

3.2.2 Culture media and supplements

Culture media for bacteria (Table 3-4) were prepared in purified water (MilliQ) and autoclaved at 121 °C before additional compounds were added after being sterile filtered (0.2 µm). Antibiotics are listed in Table 3-5. Cell culture media and supplements for mammalian cells are listed in Table 3-6 and Table 3-7; those were either obtained as ready-to-use solutions or prepared from powdered formulations in MilliQ. Prepared media were sterilized by a custom made filtration line containing the component Sealkleen (ZLK702G23LHKH4, Pall) in which the medium is run through two nylon filters with decreasing pore size (1 µm and 0.2 µm).

Table 3-4: Media for bacterial cultures

Medium	Composition	Final concentration	Cat#	Supplier
LB-medium	Bacto™ Tryptone	10 g/L	211705	BD
(Luria-Bertani)	Bacto™ Yeast Extract	5 g/L	212750	BD
(Bertani, 1951)	NaCl	5 g/L	3957.2	Roth
LB-agar	LB-medium	-	-	-
	Bacto™-Agar	16 g/L	214010	BD
Medium		**Antibiotics**	**Cat#**	**Supplier**
E. coli FAST-Media TB Liquid Blas		100 µg/ mL blasticidin	fas-bl-l	InvivoGen
E. coli FastMedia BLAS AGAR		100 µg/ mL blasticidin	fas-bl-s	InvivoGen

Table 3-5: Antibiotics and reagents for bacterial cultures

Medium	Final concentration	Cat#	Supplier
Ampicillin (Amp)	100 µg/mL	A9518-100G	Sigma-Aldrich
Kanamycin (Kan)	50 µg/mL	T832.3	Roth

Table 3-6: Cell culture media

Medium	Used for cell line	Cat#	Supplier	Supplements
ProCHO5	CHO Lec3.2.8.1	BE12-766Q	Lonza	7.5 mM L-glutamine (and 11 mg/mL phenol red)
CD Hybridoma	CHO Lec3.2.8.1	11279-023	Invitrogen	8 mM L-glutamine, 5 % FBS
F17	HEK293-6E	05-0092DK	Invitrogen	7.5 mM L-glutamine, 0.1 % pluronic, 25 µg/mL G418
ProCHO5 +ZKT-I [1:2]	CHO Lec3.2.8.1	-	Lonza/ Biochrome	9.2 g/L ProCHO5 powder, 8.1 g/L Hybridomed DIF 1000, 3.1 g/L $NaHCO_3$, 3.6 mM L-glutamine, 1.9 mM NaOH, 0.06 % (v/v) human insulin, 0.02 % (v/v) 2x CHO7 lipids supplement

Table 3-7: Cell culture supplements

Supplement	Cat#	Supplier
2x CHO7 lipids supplements	BE13-668C	Lonza
DMSO	D2650	Sigma-Aldrich
Fetal Bovine Serum	S0115	BIOCHROM AG
Foetal Bovine Serum	A11-043	PAA Laboratories GmbH
G418 solution	P11-012	PAA Laboratories GmbH
Geneticin (G418)	10131-027	Gibco
Geneticindisulfat (G418)	CP11.3	Roth
Gentamicin	1510-049	Invitrogen
Heparin	H3149-50KU	Sigma-Aldrich
Human insulin	BE02-033E	Lonza
Hybridomed DIF 1000	TZ999-E	Biochrom
Hygromycin B	P02-015	PAA Laboratories GmbH
L-Glutamine	HN08.3	Roth
Methylcellulose	M7027	Sigma
$NaHCO_3$	6885.1	Roth
NaOH	6771.2	Roth
Penicillin/Streptomycin	P11-010	PAA Laboratories GmbH
Phenol red	P3532-5G	Sigma-Aldrich
Phleomycin	P9564-5MG	Sigma-Aldrich
Pluronic F-68	P1300-500G	Sigma
ProCHO5 Powder	VPW-045F	Lonza
Puromycin	P-7255	Sigma
Puromycin	Ant-pr-1	InvivoGen
Trypton-N1	19553	Organotechnie S.A.S.
Valproic acid	P6273	Sigma-Aldrich
Zeocin	Ant-zn-5p	Invivo-Gen

3.2.3 Transfection reagents

Transfection of recombinant plasmid DNA into CHO cell lines was done using electroporation based nucleofection (Lonza). A cationic lipofection technique on the other hand was used for transfection in HEK cells (Table 3-8).

Table 3-8: Transfection reagents

Reagent	Used for cell line	Cat#	Supplier
Polyethylenimine (linear, MW ~25 kDa)	HEK293-6E	23966	Polysciences
Nucleofection solution	CHO Lec3.2.8.1	VCV-1003	Lonza

3.3 Oligonucleotides and plasmids

Plasmids used in this work are listed and explained in Table 3-9. Oligonucleotides are listed in Table 3-10; these were purchased from MWG Eurofines Operon in HPLC purified quality and used for cloning and sequencing.

Table 3-9: Plasmids

pFlpBtM variants
pFlpBtM-I (Steffen Meyer, HZI) Vector used as exchange vector for stable genomic integration via RMCE into CHO Lec3.2.8.1 master cell lines employing FRT_3 and FRT_{wt} sites. Also used as donor vector for the creation of bacmids via TN7 transposition sites and transient expression in insect cells.
pFlpBtM-II (Steffen Meyer,HZI) Versatile multi-host expression and donor vector for stable genomic integration via RMCE into CHO Lec3.2.8.1 master cell lines employing FRT_3 and FRT_{wt} sites, transient expression in HEK293-6E and TN7 based transposition for the creation of bacmids. It also contains an inducible T7 promoter for the expression in *E.coli*. The version pFlpBtM-II(beta) lacks a Shine-Dalgarno sequence and differs in the design of the MCS and included tags.
pFlpBtM-II_F13/F14 Versatile multi host expression and donor vector derived from pFlpBtM-II. *FRT* sites FRT_3 and FRT_{wt} were replaced against *FRT* sites FRT_{13} and FRT_{14} to enable stable genomic integration via RMCE into binary CHO Lec3.2.8.1 master cell lines. Cloning of pFlpBtM-II_F13/F14 exchange vector is described in this work.
Tagging vectors
pEF-FS-eGFP-dneo (Sonja Wilke, HZI) Tagging vector originally used for genomic integration of an eGFP expressing exchange locus (FRT_3-*eGFP*-FRT_{wt}-Δ*neo*) into CHO Lec3.2.8.1 cells resulting in the RMCE master cell lines SWI3_26 and SMT_dneo(2)_24 used in this work.
pEF-FS-eGFP-dpuro (Sonja Wilke, HZI) Tagging vector derived from tagging vector pEF-FS-eGFP-dneo containing a puromycin selection trap instead of a neomycin selection trap. Tagging vector pEF-FS-eGFP-dpuro was used for cloning of the tagging vector pEF-FS-tdTomato-dpuro described in this work.

pEF-FS-tdTomato-dpuro

Tagging vector used for genomic integration of an tdTomato expressing exchange locus (*FRT$_{13}$-tdTomato-FRT$_{14}$-Δpuro*) into CHO Lec3.2.8.1 RMCE master cell lines SWI3_26 and SMT_dneo(2)_24. Construction of tagging vector and genomic integration are described in this work.

Vectors used for construction

11AAYGEC_F13-F14_dpuro_pMA-RQ

Vector containing synthesized *FRT$_{13}$* and *FRT$_{14}$* sites for cloning of tagging vector pEF-FS-tdTomato-dpuro (Life Sciences).

11AAYGFC_F13-F14_pFlpBtM_II_pMK-RQ

Vector containing synthesized *FRT$_{13}$* and *FRT$_{14}$* sites for cloning of exchange vector pFlpBtM-II_F13/F14 (Life Sciences).

11AAYGFC_F13-F14_pFlpBtM_II_pMK-RQ_(No_Insect_Promoter)

Intermediate vector used for cloning of exchange vector pFlpBtM-II_F13/F14.

11AAYGFC_F13-MCS_PGK-F14_pFlpBtM_II_pMK-RQ

Intermediate vector used for cloning of exchange vector pFlpBtM-II_F13/F14.

11AAYGEC_F13-tdTomato_SV40pA-F14_dpuro-pMA-RQ

Intermediate vector used for cloning of tagging vector pEF-FS-tdTomato-dpuro.

Parental vectors for inserts

pUNO1-mGRP94 (HSP90B1)

Commercial vector purchased from InvivoGen (Cat No. puno1-mgrp94). Vector was used as PCR template for the cloning of C- and N-terminally FLAG-tagged mGRP94 constructs cloned into pFlpBtM-II_F13/F14.

pUNO1-mPRAT4A

Commercial vector purchased from InvivoGen (Cat No. puno1-mprat4a). Vector was used as template for the cloning of C- and N-terminally FLAG-tagged mPRAT4A constructs cloned into pFlpBtM-II_F13/F14.

pDUO-mTLR1/mTLR2

Commercial vector purchased from InvivoGen (Cat No. pduo-mtlr1tlr2). Vector was used as template for the cloning of mTLR2 and mTLR1 constructs cloned into vector pFlpBtM-II(beta).

Exchange vectors

pFlpBtM-II(beta)-tdTomato (Steffen Meyer,HZI)

Exchange vector comprising the full length tdTomato sequence with a C-terminal His-tag derived from vector ptdTomato (Clontech). Vector was used for integration of tdTomato into RMCE master cell line SWI3_26, binary RMCE master cell line TE3-B4-L1.1 and cloning of tagging vector pEF-FS-tdTomato-dpuro.

pFlpBtM-ssmTLR2H8 (Steffen Meyer,HZI)

Exchange vector comprising a C-terminally His-tagged murine TLR2 ectodomain sequence (amino acids 1-587) with its genuine signal peptide, derived from vector pFBDM-mTLR2 (N. Kuklik, HZI) (uniprot accession no. Q9QUN7, kindly provided by C. Kirschner, Univ. Essen). Vector was used for integration of the ssmTLR2 ECD into RMCE master cell lines SWI3_26, SMT_dneo(2)_24 and binary RMCE cell line TE3-B4-H1.

pFlpBtM-II(beta)-sshTLR5-1-391-VLR-TEV-STrEP-H8

Exchange vector comprising a human TLR5 ectodomain sequence (amino acids 1-391) with its genuine signal peptide, derived from vector pFlpBtM-II-sshTLR5 wt-c-QC_R387Q_(Klon3) (Steffen Meyer,HZI). The sshTLR5 construct is C-terminally fused to a VLR fragment (amino acids 133-200). The C-terminal twin-Strep-tag and His-tag are separated through a TEV cleavage site. Vector was used for integration of the sshTLR5 ECD into RMCE master cell lines SMT_dneo(2)_24 and binary RMCE cell line TE3-B4-H1.

pFlpBtM-II-sshTLR5 wt-c-QC_R387Q_(Klon3) (Steffen Meyer,HZI)

Exchange vector comprising a human TLR5 ectodomain sequence (amino acids 1-639) with its genuine signal peptide. Exchange vector was used as parental vector for the amplification of sshTLR5-1-391 and thus cloning of pFlpBtM-II(beta)-sshTLR5-1-391-VLR-TEV-STrEP-H8.

pFlpBtM-IIbeta-mTLR1_1-408-VLR-TEV-Strep-H8

Exchange vector comprising a murine TLR1 ectodomain sequence (amino acids 1-408) with its genuine signal peptide, derived from vector pDUO-mTLR1/mTLR2 (InvivoGen). The mTLR1 construct is C-terminally fused to a VLR fragment (amino acids 133-200). The C-terminal twin-Strep-tag and His-tag are separated through a TEV cleavage site. Cloning of the vector is described in this work. Vector was used for transient expression of the mTLR1 ECD in HEK293-6E.

pFlpBtM-IIbeta-mTLR1_1-455-VLR-TEV-Strep-H8

Exchange vector comprising a murine TLR1 ectodomain sequence (amino acids 1-455) with its genuine signal peptide, derived from vector pDUO-mTLR1/mTLR2 (InvivoGen). The mTLR1 construct is C-terminally fused to a VLR fragment (amino acids 133-200). The C-terminal twin-Strep-tag and His-tag are separated through a TEV cleavage site. Cloning of the vector is described in this work. Vector was used for transient expression of the mTLR1 ECD in HEK293-6E and stable integration into the binary RMCE master cell line TE3-B4-H1.

pFlpBtM-IIbeta-mTLR1_1-500-VLR-TEV-Strep-H8

Exchange vector comprising a murine TLR1 ectodomain sequence (amino acids 1-500) with its genuine signal peptide, derived from vector pDUO-mTLR1/mTLR2 (InvivoGen). The mTLR1 construct is C-terminally fused to a VLR fragment (amino acids 133-200). The C-terminal twin-Strep-tag and His-tag are separated through a TEV cleavage site. Cloning of the vector is described in this work. Vector was used for transient expression of the mTLR1 ECD in HEK293-6E.

pFlpBtM II F13_FLAG_mGRP94_F14

Exchange vector comprising the full length murine GRP94 sequence with a N-terminal FLAG-tag, derived from vector pUNO1-mGRP94 (InvivoGen). Vector was used for transient expression of mGRP94 in HEK293-6E.

pFlpBtM_II_F13_FLAG_mPRAT4A_F14

Exchange vector comprising the full length murine PRAT4A sequence with a N-terminal FLAG-tag, derived from vector pUNO1-mPRAT4A (InvivoGen). Vector was used for transient expression of mPRAT4A in HEK293-6E.

pFlpBtM_II_F13_mGRP94_F14

Exchange vector comprising the full length murine GRP94 sequence with a C-terminal FLAG-tag, derived from vector pUNO1-mGRP94 (InvivoGen). Vector was used for transient expression of mGRP94 in HEK293-6E and stable integration into the binary RMCE cell line TE3-B4-H1.

pFlpBtM_II_F13_mPRAT4A_F14

Exchange vector comprising the full length murine PRAT4A sequence with a C-terminal FLAG-tag, derived from vector pUNO1-mPRAT4A (InvivoGen). Vector was used for transient expression of mPRAT4A in HEK293-6E and stable integration into the binary RMCE cell line TE3-B4-H1.

Flp helper vectors

Pflpopuro (Turan *et al.*, 2010)

Helper vector expressing the mouse codon optimised recombinase FlpO (Raymond *et al.*, 2007). Upon co-transfection with an exchange vector in CHO Lec3.2.8.1 RMCE master cell lines FlpO mediates exchange between compatible *FRT* sites in the genome.

pPGKFLPobpA (O54715) (Adgene plasmid 13793)

Helper vector expressing the mouse codon optimised recombinase FlpO (Raymond *et al.*, 2007). Upon co-transfection with an exchange vector in CHO Lec3.2.8.1 RMCE master cell lines FlpO mediates exchange between compatible *FRT* sites in the genome.

Other vectors

pUC19 (Invitrogen)

Control vector supplied with OneShot® Top10 electrocompetent cells. pUC19 was used to determine transformation efficiencies in Top10 electrocompetent cells.

pTTo/GFPq (NRCC)

This vector is used as a control vector to determine transfection efficiency in HEK293-6E cells using flowcytometric measurements upon co-transfection with the target vector. It encompasses GFPq a red shifted green fluorescent protein.

Table 3-10: Oligonucleotides – restriction sites are underlined

Name	Sequence 5' to 3'	Comment
TLR1_FWD_NcoI	AGGAAG**CCATG**GGCACTAAACCAAATTCCCTCATCTTCTACTG	Sense primer for all mTLR1 ECD constructs which are amplified from pDUO_mTLR1_mTLR2 vector and cloned into pFlpBtM-II or pFlpBtM-II(beta) vector (1 Glycine codon (red) was added after the start codon to introduce a *Nco*I restriction site).
TLR1_408_NheI_r	AGGAAG**GCTAGC**AATGTCTAGTTTTTGTAGGGATGTCAT	Antisense primer for a mTLR1_1-408 amino acid ECD construct which was amplified from pDUO_mTLR1_mTLR2 vector and cloned into pFlpBtM-II(beta) (introduces *Nhe*I restriction site).
TLR1_455_NheI_r	AGGAAG**GCTAGC**AAGGTCAAGGACCTTGACTTTGGGAGG	Antisense primer for a mTLR1_1-455 amino acid ECD construct which was amplified from pDUO_mTLR1_mTLR2 vector and cloned into pFlpBtM-II(beta) (introduces *Nhe*I restriction site).
TLR1_500_NheI_r	AGGAAG**GCTAGC**GATGACCAGCACAGAAAGGCT	Antisense primer for a mTLR1_1-500 amino acid ECD construct which was amplified from pDUO_mTLR1_mTLR2 vector and cloned into pFlpBtM-II(beta) (introduces *Nhe*I restriction site).
TLR1_seq_mid_f	GGTTCTCGGGTACAAAGTTCAAGTG	Sense sequencing primer for middle section of mTLR1 ECD.
TLR1_seq_mid_re	GGAAGCTGAAGACATCAGTGACAAC	Antisense sequencing primer for middle section of mTLR1 ECD.

TLR5_1-391NheRev	AGGA**GCTAGC**GAGATCCAAGGTC TGTAATTTTTCCAG	Antisense primer for a sshTLR5_1-391 amino acid ECD construct which was amplified from pFlpBtM-II-sshTLR5 wt-c-QC_R387Q_(Klon3) (introduces *Nhe*I restriction site).
BamHI-Nco-For	AGGA**GGATCC**AA**CCATGG**GAGA**T** CA**T**CT**TC**ACCTTCTCCTAGGAGTG GTGC	Sense primer for a sshTLR5_1-391 amino acid ECD construct which was amplified from pFlpBtM-II-sshTLR5 wt-c-QC_R387Q_(Klon3) (introduces *BamH*I and *Nco*I restriction sites). Primer also introduces 4 silent mutations.
PRAT_Nco_F_FLAG	AGGAAG**CCATGG**ACTACAAGGAC GACGACGACAAGGAGTCCATGTC TGAGCTCGCG	Sense primer for mPRAT4A construct with N-terminal FLAG tag (red). For amplification from pUNO1-mPRAT4A vector. Introducing a N-terminal FLAG-tag between start codon and mPRAT4A and an *Nco*I restriction site. Cloned into pFlpBtM-II_F13/F14.
mPRAT4A_NcoI_F	AGGAAG**CCATGG**AGTCCATGTCT GAGCTCGCG	Sense primer for mPRAT4A construct with C-terminal FLAG tag. For amplification from pUNO1-mPRAT4A vector. Introducing a *Nco*I restriction site. Cloned into pFlpBtM-II_F13/F14.
PRAT_MluI_R_FLAG	CTTCCT**ACGCGT**TACTTGTCGTCG TCGTCCTTGTAGTCCAGCTCATCA GGGGGGCTGTGTGGGA	Antisense primer mPRAT4A construct with C-terminal FLAG tag. For amplification from pUNO1-mPRAT4A vector. Cloned into pFlpBtM-II_F13/F14, this primer removes the Strep-tag, His-tag and the original stop codon from pFlpBtM-II_F13/F14 vector. Instead, a FLAG-tag (red) is introduced followed by a stop codon as part of the *Mlu*I site.
mPRAT4A_MluI_R	CTTCCT**ACGCGT**TACAGCTCATCA GGGGGGCTG	Antisense primer for mPRAT4A construct with N-terminal FLAG tag. For amplification from pUNO1-mPRAT4A vector. Includes a *Mlu*I restriction site. When cloned into pFlpBtM-II_F13/F14 it removes the Strep-tag, His-tag and the original stop codon from pFlpBtM-II_F13/F14 vector. Instead a stop codon is introduced as part of the *Mlu*I site.
GRP_MluI_R_FLAG	CTTCCT**ACGCGT**TACTTGTCGTCG TCGTCCTTGTAGTCCAATTCATCC TTCTCTGTAGATTCC	Antisense primer for mGRP94 with C-terminal FLAG tag (red). For amplification from pUNO1-mGRP94 vector. Introduces a *Mlu*I restriction site for cloning into pFlpBtM-II_F13/F14 which removes the Strep-tag, His-tag and the original Stop codon from pFlpBtM-II_F13/F14 vector. Instead a FLAG-tag is introduced followed by a stop codon as part of the *Mlu*I site.
mGRP94_MluI_R	CTTCCT**ACGCGT**TACAATTCATCC TTCTCTGTAGATTCC	Antisense primer for mGRP94 with C-terminal FLAG tag. For amplification from pUNO1-mGRP94 vector. Introduces *Mlu*I restriction site for cloning into pFlpBtM-II_F13/F14 which removes the Strep-tag, His-tag and the original Stop codon from

		pFlpBtM-II_F13/F14 vector. Therefore a stop codon is introduced as part of the *Mlu*I site.
GRP_ClaI_F_FLAG	AGGAAG**ATCGAT**TTAAAGGAGAT ATACCATGGACTACAAGGACGAC GACGACAAGAGGGTCCTGTGGGT GTTGG	Sense primer for mGRP94 with N-terminal FLAG tag. For amplification from pUNO1-mGRP94 vector. Primer contains a *Cla*I site as the *Nco*I site cannot be used for cloning as it is present within mGRP94. Instead the *BstB*I site within pFlpBtM-II_F13/F14 will be used for cloning, however as the PCR fragment cannot be cut with *BstB*I either, the compatible *Cla*I site will be introduced which will destroy the *BstB*I site after cloning into pFlpBtM-II_F13/F14. Furthermore the Shine Dalgarno sequence (orange) needs to be reintroduced as it will be cut out using the *BstB*I cloning site in pFlpBtM-II. Furthermore a N-terminal FLAG-tag (red) is introduced between the start codon and mGRP94.
mGRP94_ClaI_F	AGGAAG**ATCGAT**TTAAAGGAGAT ATACCATGAGGGTCCTGTGGGTG TT	Sense primer for mGRP94 with C-terminal FLAG tag. For amplification from pUNO1-mGRP94 vector. Primer contains a *Cla*I site as the *Nco*I site cannot be used for cloning as it is present within mGRP94. Instead the *BstB*I site within pFlpBtM-II_F13/F14 will be used for cloning, however as the PCR Fragment cannot be cut with *BstB*I either, the compatible *Cla*I site will be introduced which will destroy the *BstB*I site after cloning into pFlpBtM-II_F13/F14. Furthermore the Shine Dalgarno sequence (orange) needs to be reintroduced as it will be cut out using the *BstB*I cloning site in pFlpBtM-II.
pFlpBtN13_seq	GGATCCGAAGTTCCTATTCCG	Sense sequencing primer for pFlpBtM-II_13/14 vector.
pFlpBtM_seq_for	CGGATCGGGAGATCAGCTTGAAG	Sense sequencing primer for pFlpBtM vector.
pFlpBtM_Seq_rev	CAGCCATACCACATTTGTAGAGG	Antisense sequencing primer for pFlpBtM vector.
TLR1_seq_mid_f	GGTTCTCGGGTACAAAGTTCAAG TG	Sense sequencing primer for internal section of mTLR1.
TLR1_seq_mid_re	GGAAGCTGAAGACATCAGTGACA AC	Antisense sequencing primer for internal section of mTLR1.
Cassette-neo-AS	TCAGAAGAACTCGTCAAGAAGGC GATAG	Antisense primer for genomic PCR annealing at the end of the Δ*neo* selection trap.
Cassett-puro-AS	TCAGGCACCGGGCTTGCGGGTCA TGC	Antisense primer for genomic PCR annealing at the end Δ*puro* selection trap.
Cassette-pEF-S	GCTCCGGTGCCCGTCAGTGGGCA GAGCG	Sense primer for genomic PCR annealing at the beginning of the pEF promoter.

Insert-dneo-AS	CAGTTCATTCAGGGCACCGGACAG	Antisense primer for genomic PCR annealing at the beginning of Δ*neo* selection trap.
Insert-dpuro-AS	CGCACCGTGGGCTTGTACTCG	Antisense primer for genomic PCR annealing at the beginning of Δ*puro* selection trap.
Insert-pEF-S	GTGTCGTGAGGAATTAGCTTGACCAAGC	Sense primer for genomic PCR annealing at the end of the pEF promoter.

3.4 Bacterial strains and cell lines

3.4.1 Bacterial strains

The electrocompetent *E.coli* strains One Shot® TOP10 or XL1 blue were used for cloning and plasmid amplification (Table 3-11).

Table 3-11: *E.coli* strains

Strain	Genotype	Cat#	Supplier
One Shot® TOP10	F⁻ *mcr*A Δ(*mrr-hsd*RMS-*mcr*BC) ϕ80 (*lac*Z) ΔM15 Δ*lac*X74 *rec*A1 *ara*D139 Δ(*ara, leu*) 7697 *gal*U *gal*K *rps*L (Str^R) *end*A1 nupG λ-	C4040-50	Invitrogen
XL1-Blue	*rec*A1 *end*A1 *gyr*A96 thi-1 *hsd*R17 *sup*E44 *rel*A1 *lac* [F′ proAB *lac*I^{q}ZΔM15 Tn*10*(Tet^r)	200249	Stratagene

3.4.2 Cell lines

The mammalian cell lines used in this work are listed and explained in Table 3-12.

Table 3-12: Cell lines

CHO Lec3.2.8.1 derived cell lines SWI3_26 and SMT_dneo(2)_24
The glycosylation deficient cell line CHO Lec3.2.8.1 was isolated by Stanley, (1989) through sequential screening for the resistance against the cytotoxicity of plant lectins. The cell lines SWI3_26 (Wilke *et al.*, 2011) and SMT_dneo(2)_24 established in our group are CHO Lec3.2.8.1 cells tagged with an exchange cassette (*FRT$_3$-eGFP-FRT$_{wt}$-Δneo*). This enables the integration of a GOI via RMCE (Section 3.6.8).
HEK293-6E
HEK293 cells were established by Graham *et al.*, (1977) by transformation of a primary culture with an adenovirus. Later on the subclone HEK293-6E (NRC Canada) was generated by Durocher *et al.*, (2002) which comprised a truncated version of the Epstein-Barr nuclear antigen 1 (EBNA 1).

3.5 Molecular biological methods

Protocols used for molecular biological methods were adapted from standard collections such as Sambrook *et al.*, (2001) or established in our laboratory. Sequence analysis of plasmid DNA was done by the genome analysis department at the HZI.

3.5.1 Polymerase chain reaction (PCR)

PCR kits and reagents used in his work are listed in Table 3-13. PCR was used to amplify fragments for molecular cloning or analyse the genetic background of chromosomal DNA via genomic PCR. PCR for molecular cloning was used to amplify full length or truncated constructs from template vectors and insert restriction sites for cloning or affinity-tags for purification. PCR reactions were set up in volumes from 25 µL - 50 µL (Table 3-14) and amplified using either a thermocycler or a gradient thermocycler). Correct amplification was analysed by agarose gel electrophoresis (Section 3.5.2). If required PCR amplifications were extracted from a preparative agarose gel (Section 3.5.3) before further use. For genomic PCR amplification PCR reactions were set up in 50 µL volumes according to Table 3-15. Amplification was analysed via agarose gels (Section 3.5.3).

Table 3-13: PCR kits and reagents

Kit / Reagent	Cat#	Supplier
Phusion® Hot Start II DNA Polymerase (2.000 U/mL)	F-549L/ M0530S/ B0515A	Finnzymes/ Thermo Scientific/ NEB
KOD Hot Start DNA Polymerase (1.000 U/mL)	71086-3	Novagene/Millipore
dNTP (10 mM)	F-5602/ N0447S	Finnzymes/ NEB

Table 3-14: PCR Reaction for molecular cloning

Components	Phusion®Hot Start II
Forward primer	0.5 µM
Reverse primer	0.5 µM
Template DNA	16 ng/100µL
5x Phusion® HF Reaction Buffer (contains 7.5 mM MgCl2)	1x → 1.5 mM $MgCl_2$
dNTPs	0.2 mM
Polymerase	0.02 U/µL
MilliQ water	Total volume 25 µL -50 µL

Table 3-15: PCR Reaction for genomic amplification

Components	KOD Polymerase
Forward primer	0.5 µM
Reverse primer	0.5 µM
Template DNA	200 ng/50µL
10x PCR Reaction Buffer for KOD Hot Start DNA Polymerase	1x
$MgSO_4$	1 mM
dNTPs	0.2 mM
Polymerase	0.02 U/µL
MilliQ water	Total volume 50 µL

Table 3-16: (Gradient) Thermocycler conditions for molecular cloning

Program Steps	Temperature	Time	Cycles
Initial denaturation	98 °C	1 min	
Denaturation	98 °C	30 sec	
Annealing (adjusted using gradient PCR in a range suitable for the primers T_m)	49 °C – 72°C	30 sec	x 30 cycles
Extension	72 °C	1 min	
Final extension	72 °C	10 min	
Pause	10 °C	For ever	

Table 3-17: (Gradient) Thermocycler conditions for genomic PCR

Program Steps	Temperature	Time	Cycles
Initial denaturation	94 °C	5 min	
Denaturation	94 °C	1 sec	
Annealing	72 °C	1 min	x 35 cycles
Extension	68 °C	4 min	
Final extension	68 °C	10 min	
Pause	10 °C	For ever	

3.5.2 Agarose gel electrophoresis

DNA samples obtained from PCR amplifications (Section 3.5.1) or restriction digests (Section 3.5.4) were analysed using agarose gel electrophoresis. 0.8 % (w/v) agarose in TAE buffer was boiled in a microwave and cooled down to approximately 60 °C before the addition of 5-10 µL ethidium bromide. Well number and sizes were adjusted with the appropriate combs. DNA samples were mixed with 6x DNA loading buffer, applied to the wells and run at 70 V - 100 V. The gels were documented under UV illumination at 254 nm. Consumables for agarose gel electrophoresis are listed in Table 3-18.

Table 3-18: Consumables for agarose gel electrophoresis

Reagent		**Cat#**	**Supplier**
LE Agarose		840004	Biozymes
LE GP Agarose		850074	Biozymes
LE Agarose		500042	Lonza
Ethidium bromide (10 mg/mL)		E1510-10ML	Sigma
Buffer	**Composition**	**Cat#**	**Supplier**
TAE buffer	35.4 mM Trizma® base	T1503-1KG	Sigma
	0.1 % acetic acid	3738.5	Roth
	1 mM EDTA	A1103.1000	AppliChem
	pH 8.5		
6 x DNA loading buffer	0.4 % (w/v) glycerol p.A.	1.04092.1000	Merck
	10 % (v/v) 100x bromphenol blue	A512.1	Roth
	0.03 M EDTA	A1103.1000	AppliChem

3.5.3 DNA extraction

The NucleoSpin® Extract II kit (MN, Cat# 740609.150) was used for the extraction of linearized plasmids, DNA fragments and PCR products. The DNA extraction was done according to the manufacturer's protocol.

3.5.4 Digestion of DNA with restriction endonuclease

Restriction digests were generally set up in a 40 µL reaction volume with 5 µg – 10 µg plasmid DNA in an appropriate NEBuffer, 0.5 U/µL – 1.0 U/µL of the required restriction endonucleases and 1x BSA (bovine serum albumin) if required. The reaction mixtures were incubated for 2 h – 3.5 h at the temperature instructed from the manufacturer and heat-inactivated afterwards if possible. If required the digests were done sequentially with either adding a second enzyme after the first digest directly to the reaction mixture and adjusting the temperature or isolating the required fragment from an preparative 0.8 % agarose gel (Sections 3.5.2) and setting up a new restriction digest. Plasmid backbones were dephosphorylated to avoid religation by adding 10 U antarctic phosphatase (NEB, Cat# M0289S) and NEBuffer for antarctic phosphatase to the restriction digest and incubating it for 20 min at 37 °C. All digests were stored at -20 °C for storage. Restriction digests made for testing plasmid construct integrity were typically made with 500 ng plasmid DNA in a 30 µL reaction volume.

3.5.5 Ligation of DNA fragments

To prepare a ligation as well as controls for re-ligation and no ligation, a ligation master mix was prepared containing the ligation buffer (Roche, Cat# 14028100), 20 ng/µL linearized vector DNA. For the ligation the insert DNA in a 1:3 molar ration and 1 U T4 DNA ligase (Roche, Cat# 14295420) were added to 20 µL ligation master mix, only 1 U T4 DNA ligase into the re-ligation control and neither T4 DNA ligase nor insert DNA into the negative control. The samples were ligated for 16 h at 12 °C in a Thermocycler.

3.5.6 Preparation of electrocompetent cells

For the preparation of electrocompetent cells glycerol stocks of *E.coli* One Shot® TOP10 or XL1 blue were stroke out on non-selective LB-agar plates and incubated overnight at 37 °C. An isolated colony was used to inoculate a 40 mL pre-culture at 37 °C overnight shaking at 130-160 rpm. The pre-culture was used in a 1:100 or 1:50 dilution to inoculate the main

culture (500 mL – 2 L of bacterial culture) and grown at 37 °C and 130-160 rpm until an optical density $(OD)_{600}$ between 0.5-1.0 was reached. Sterile centrifuge tubes were used to chill the cell suspension on ice for at least 30 min and mixed occasionally to avoid a temperature gradient. Centrifugation of the chilled bacterial suspension for 10 min at 4 °C and 3000 rpm was followed by a washing step with sterile ice-cold HEPES-glycerol wash buffer (1 mM HEPES, 10 % (v/v) glycerol, pH 7.0). For each pellet obtained from 1 L of bacterial culture 500 mL of sterile ice-cold HEPES-glycerol wash buffer were used. The centrifugation and washing step was repeated after pooling the cell pellets if required in 250 mL HEPES-glycerol wash buffer. The newly obtained pellet was resuspended in 20 mL ice-cold 10 % glycerol and transferred to sterile Oak Ridge SS34 centrifuge tubes and centrifuged again at 3000 rpm for 10 min. The harvested pellet was take up in 1 mL – 3 mL ice-cold sterile 10 % glycerol and aliquoted in sterile Eppendorf tubes, shock frozen in liquid nitrogen and stored at -80 °C.

3.5.7 Transformation of competent bacteria

Before electroporation the Gene Pulser® Cuvette (Cat# 165-2086, Bio-Rad) was chilled on ice. 2 µL (~4 ng) of plasmid DNA were mixed with 50 µL – 60 µL of electrocompetent cells and incubated on ice for 1 min. The Bio-Rad Gene Pulse™ was set to a capacitance of 25 µFD and 2.5 kV. The Bio-Rad Controller was set to 200 Ω and the Bio-Rad capacity extender to 126 µFD. The dried cuvette was placed in the chamber slide and a pulse applied once. After addition of 1 mL LB-medium the cells were incubated between 30 min – 60 min at 37 °C and 300 rpm. 20 µL – 200 µL of bacterial suspension were plated on selective LB-agar plates and incubated overnight at 37 °C.

3.5.8 Bacterial pre-cultures

Bacterial pre-cultures were prepare by inoculation of 3 mL – 4 mL LB medium containing the appropriate antibiotics with a colony picked from an LB agar plate or a 1:1000 dilution of an existing bacterial culture. The pre-cultures were grown at 37 °C and 130 rpm overnight and can be used for the inoculation of larger volumes of LB medium for the preparation of glycerol stocks or plasmid preparations.

3.5.9 Glycerol stock

To enable the quick preparation of new plasmids, 8 % glycerol stocks were prepared and stored at -80 °C. To do so 50 mL LB medium with the appropriate antibiotics were

inoculated 1:1000 or 1:500 with a pre-culture and grown at 37 °C and 130 rpm until an OD_{600} between 0.5 – 0.8 was reached. 900 µL of cell suspension were mixed together with 100 µL sterile 80 % glycerol (8 % glycerol end-concentration) in cryogenic vials and stored at -80 °C.

3.5.10 Plasmid preparation

Pre-cultures were used to inoculate appropriate volumes of LB medium containing the appropriate amount of antibiotics. Plasmid preparations were done according to the manufacturer's guidelines (Table 3-19).

Table 3-19: Plasmid DNA preparation Kits

Kit	Cat#	Supplier
PureYield™ Plasmid Mini Prep System	A1223	Promega
PureYield™ Plasmid Midi Prep System	A2495	Promega
PureYield™ Plasmid Maxi Prep System	A2393	Promega
NucleoSpin® Plasmid	740588.250	MN
EndoFree Plasmid Maxi kit	12362	Qiagen
EndoFree Plasmid Giga kit	12391	Qiagen

3.5.11 Genomic DNA preparation

AquaGenomic™ Solution [MoBiTec, Cat# 2030MT] was used for the isolation of genomic DNA. 1-2 $x10^6$ CHO cells were harvested at 12.000 xg and stored at -20 °C. To lyse the cells 100 µL AquaGenomic™ Solution were added to the frozen pellet and vortexed for 1 min (or until the pellet was thoroughly resuspended). Following an incubation time of 4 min the lysate was pelleted at 13.000 xg for 2 min. The clear lysate was transferred to a new reaction tube and the DNA precipitated with 90 µL isopropanol. The precipitated DNA was pelleted at 13.000 xg for 2 min, the supernatant removed and the DNA pellet washed twice with 70 % ethanol. The air dried DNA pellet was dissolved in autoclaved MilliQ water or in Nuclease-Free Water (Promega, Cat# P119C). Insoluble material was pelleted at 13.000 xg for 1 min and the supernatant transferred to a new Eppendorf. Genomic DNA was stored at -20 °C.

3.5.12 Photometric quantification of DNA and protein concentrations

NanoDrop ND-1000 and NanoDrop ND-2000 spectrophotometer were used to quantify DNA concentrations at 260 nm and protein concentrations at 280 nm. The measurements were carried out with 2 µL sample volume after calibration with a corresponding buffer. In DNA read outs the A_{260nm}/A_{280nm} ratio was used to determine protein contaminations.

Ratios of 1.8 -2.0 were considered pure. In protein read outs the Beer-Lambert law (equation below) had to be considered and the acquired absorbance values needed to be divided through the molar extension coefficient (ε) of each target protein to obtain the correct protein concentration. The molar extinction coefficients for each protein target were calculated by VectorNTI.

$$c\frac{mg}{mL} = \frac{A_{280}}{\varepsilon x l}$$

c	Protein concentration [mg/mL]
A_{280}	Absorbance at 280 nm
ε	Molar extinction coefficient [mL mg^{-1} cm^{-1}]
l	Length [cm]

3.6 Cell culture

3.6.1 Cell culture consumables

Cell culture consumables are listed in Table A.1-2 in the appendix.

3.6.2 Maintaining cells in culture

Cell lines were maintained as suspension cultures in flat bottom shake flasks on orbital shakers. Media and supplements were used according to Table 3-6 and Table 3-7. CHO Lec3.2.8.1 cells were cultivated at 37 °C and 110 rpm in a humidified atmosphere with 5 % CO_2. Adherent CHO Lec3.2.8.1 cells were incubated at 37 °C at 8 % CO_2. Cells were routinely split every 3-4 days with a seeding cell density of 2-3 x10^5 cells/mL to maintain an exponential growth phase. Adherent cells were expanded to larger multi-well plates or transferred to suspension culture when reaching a confluency of approximately 80 %. Expansion of adherent cells was done as follows; the culture medium was removed and the cell layer trypsinized with 50 µL – 1 mL 1x trypsin/EDTA. The cells were pelleted at 180 xg for 4 min and resuspended in culture medium.

HEK293-6E were cultivated at 37 °C and 110 rpm in a humidified atmosphere with 5 % CO_2. Cells were routinely split every 3-4 days with a seeding cell density of 3 x10^5 cells/mL to maintain an exponential growth phase.

3.6.3 Determination of cell number and viability

Determination of cell number and cell viability was done by the trypan blue dye exclusion method with a Neubauer hemocytometer or flowcytometry after propidium iodide staining. If cells contained mCherry or tdTomato cassettes no propidium iodide staining was used and thus only a measure of cell density but no measure of cell viability was performed in such cases. Both dyes can only permeate the cell membranes of dead cells and thus cause staining (blue and red respectively).

Using the trypan blue exclusion method cell suspensions were mixed 1:1 with 0.5 % trypan blue, transferred to one chamber of the Neubauer hemocytometer and viable (white) and non-viable (blue) cells were counted in 2 or 4 big squares under the light microscope. Cell density and viability were calculated according to the equations below.

$$\frac{cells}{mL} = \frac{cells \times 10^4 \times dillution\ factor}{no.of\ squares} \qquad viability\ [\%] = \frac{viable\ cells\ \times\ 100}{total\ cells}$$

Using the flow cytometer (Guava EasyCyte™) cell suspensions were mixed 1:10 with 1x PBS (phosphate buffer saline) if cell viability was also determined a final concentration of 50 µg/mL propidium iodide was added. (Section 3.6.10).

3.6.4 Cryopreservation

For long term storage cell banks were kept in vapour phase over liquid nitrogen. Cells were harvested from suspension culture by centrifugation at 180 xg for 4 min. The pellets were resuspended in freezing medium (80 % culture medium, 10 % dimethylsulfoxid (DMSO, Sigma, Cat# D2650) and 0.01 % methylcellulose) at a cell density of 0.5 x10^7 cells/mL. Cryogenic vials were filled with 1.8 mL cell suspension and transferred to a special freezing container in isopropanol which constantly decreases the temperature for -1 °C/min. Freezing container were stored at -70 °C for 24 h before transferring the cryogenic vials to the nitrogen tank.

3.6.5 Revitalisation

Cells were thawed and washed with 10 mL of culture medium, mixed and centrifuged again at 180 xg for 4 min. The pellet was resuspended in 30 mL culture medium.

3.6.6 Transfection of eukaryotic cells

An electroporation based method was used to deliver substrates into the cytoplasm and the nucleus of mammalian cells for either protein production or genomic tagging. Since it is a direct transfer this technique is independent of cell division for the transport of DNA into the nucleus.

Table 3-20: Cell lines

CHO Lec3.2.8.1 – Nucleofection
To transfer plasmid DNA for the generation of RMCE producer cell lines or genomic tagging the Amaxa nucleofector kit V (Lonza, Cat# VCV-1003) was used. 1x10^6 cells in an exponential growth phase were pelleted at 180 xg for 4 min and resuspended in 100 µL cell line nucleofector solution V mixed with 1 µg exchange vector containing the GOI and 4 µg of a Flp helper plasmid (Table 3-9) for recombinase mediated cassette exchange or 3 µg of linearized tagging vector (Table 3-9) for genomic tagging. The suspension was transferred to an electroporation cuvette of the Amaxa kit and transfected using program U-24 of the Amaxa nucleofector. 500 µL ProCHO5 medium were added immediately to the cuvette and the content was transferred to 12-well plates with pre-warmed ProCHO5 medium. The 12-well plate was cultivated at 37 °C and 5 % CO_2 on a shaker.
HEK293-6E – PEI transfection
HEK293-6E cells at a cell density of 1.5-2.0x10^6 cells/mL were transfected in their exponential growth phase using a 1:2.5 DNA to PEI ration. 0.5 µg - 0.75 µg DNA were used to transfect 1x10^6 cells. The DNA 95 % expression vector and 5 % pTTO/GFP which was required to monitor the transfection efficiency were mixed in supplemented F17 medium. PEI was diluted in a separate tube with supplemented F17 medium before it was added to the DNA mixture. The DNA:PEI mixture was given 15 min at RT to allow complex formation before addition the HEK293-6E cells.

3.6.7 Genomic tagging of CHO Lec3.2.8.1 cell lines for the generation of binary RMCE cell lines

To generate binary CHO Lec3.2.8.1 RMCE cell lines which allow the integration of gene targets at two defined loci the introduction of a second exchange cassette into the RMCE cell lines SWI3_26 and SMT_dneo(2)_24 was required. To do so the tagging vector pEF-FS-tdTomato-dpuro was linearized with the restriction endonuclease *Sal*I and the RMCE master cell lines SWI3_26 and SMT_dneo(2)_24 were transfected with the linearized tagging vector using the Amaxa Nucleofector system (Section 3.6.6). The cells were cultivated in suspension culture and ~ 1x10^7 cells were sorted as a pool for double positive clones (containing eGFP and tdTomato) with the highest 4 % tdTomato fluorescence using FACS (Section 3.6.10). The sorted cells were plated adherently in 96-well plates and expanded stepwise (Section 3.6.2). If required the sorted cells were serially diluted (Section 3.6.9) or send for a second round of FACS sorting to obtain binary RMCE master cell lines. The stability of the binary RMCE master cell lines was observed for at least 11 weeks using flowcytometry (Section 3.6.10)

3.6.8 Generation of producer cell lines by RMCE

RMCE master cell lines were cultivated in ProCHO5 medium. Three days before transfection the cells were split to 2x10^5 cells/mL to ensure an exponential growth phase. Transfection of the RMCE master cell lines was done with the Amaxa nucleofector kit V (Section 3.6.6). The next day the cells were pelleted at 180 xg for 4 min, resuspended in 10 mL CD Hybridoma medium and transferred to a 100 mm cell culture dish to grow adherently. The Corning dish was cultivated at 37 °C and 8 % CO_2. The CD Hybridoma medium was exchanged every 2-3 days. From day 5 after transfection antibiotic pressure was applied through the addition of 2 mg/mL G418 to the CD Hybridoma medium during medium exchange. 1-2 weeks after application of antibiotic pressure the colonies were picked from the Corning dish and transferred to 96-well plates containing CD Hybridoma medium with G418 and left to grow at 37 °C and 8 % CO_2 . At a cell density of approximately 50 % - 80 % positive cell clones were isolated using serial dilutions (Section 3.6.9) in 96-well plates with CD Hybridoma medium. To obtain clonal isolates this step was repeated as often as required. Alternatively cells were directly picked semi-sterile under the microscope and transferred to 96-well plates after florescence analysis. After clonal isolation the cells were stepwise expanded to 6-well plates. To transfer the cells to suspension culture the cells were trypsinized, pelleted at 180 xg for 4 min and resuspended in ProCHO5 medium with 0.01 U/mL heparin to avoid clumping but antibiotic pressure was removed. Flowcytometry was used to confirm the successful cassette exchange as this resulted in the loss of the stably integrated fluorescent marker gene.

Binary RMCE cell lines (Section 3.6.7) were produced similarly. However, the cassettes were exchanged sequentially as the simultaneous exchange of both loci against a GOI did not yield enough positive clones to enable their isolation (data not shown). Thus locus 2 (*FRT_{13}-tdTomato-FRT_{14}-Δpuro*) was generally exchanged first as the puromycin selection trap is more selective than the neomycin selection trap. Thus the isolation of positive clones was completed quicker. For the same reason selective pressure with 150 µg/mL puromycin was applied 7 days after transfection instead of 5 days. The isolated cell lines were than used for a second round of RMCE to exchange the other locus.

3.6.9 Single cell cloning by serial dilution

To obtain isolated clones serial dilutions in 96-well plates were used. To do so 100 µL CD Hybridoma medium with the required antibiotics was aliquoted into a 96-well plate

and incubated at 37 °C and 8 % CO_2 for 15 min. The 100 µL medium from well A1 was removed again. The cells from a 96-well plate grown to approximately 50 % - 80 % confluency were transferred to well A1 (~ 200 µL) and diluted 1:2 down the column from well A1 to well H1. With a multichannel pipette 100 µL CD Hybridoma medium with antibiotics was added to the wells A1 – H1 and diluted 1:2 across the rows of the plate. 100 µL CD Hybridoma medium was added to the wells to obtain a total volume of 200 µL in each well. The 96-well plates were incubated for about a week at 37 °C at 8 % CO_2 before the next round of clonal isolation or expansion.

3.6.10 Flow cytometry and preparative cell sorting

The Guava EasyCyte™ Mini System is a flowcytometer which uses a 488 nm diode laser for the excitation of samples and 3 fluorescence detectors (525 nm (green), 583 nm (yellow) and 680 nm (red)) to measure emission signals. The Guava EasyCyte™ was used to analyse the fluorescent level of eukaryotic cells after transient transfection or stable integration of gene targets. Cells were diluted 1:10 with 1x PBS; non-florescent cells could also be stained with 50 µg/mL propidumiodid to determine cell viability and exclude dead cells from the analysis.

Preparative cell sorting was done with the MoFlo XDP, Aria-II or Vantage SE by Lothar Gröbe research group experimental immunology (EXIM) at the HZI or Maria Höxter research group gen regulation and differentiation (RDIF) at the HZI. To obtain binary RMCE cell lines $1x10^7$ tdTomato tagged cells (Section 3.6.7) were sorted for tdTomato positive cells and/or the highest 4 % fluorescence for tdTomato as a pool in 1-2 mL ProCHO5 medium using a 100 µm tip.

3.6.11 Resistance of SWI3_26 (CHO Lec3.2.8.1) cell line to antibiotics

Objective was to determine the antibiotic concentration which causes total cell death of the CHO Lec3.2.8.1 RMCE master cell line SWI3_26. To determine the resistance of the CHO Lec3.2.8.1 RMCE master cell line SWI3_26 against antibiotics; $2x10^4$ cells were seeded in 24-well plates (BD Falcon) and cultivated at 37 °C at 8 % CO_2. After one day antibiotic pressure was applied according to Table 3-21. Every 3-4 days the antibiotic containing CD-Hybridoma medium (Lonza) was exchanged. The change in cell density was observed under the light microscope (Olympus CKX41) over 17 days and estimated visually as the percentage of density.

Table 3-21: Antibiotic pressure applied to SWI3_26 (CHO Lec3.2.8.1)

G418 [µg/µL]	Hygromycin B [µg/µL]	Zeocin [µg/µL]	Phleomycin [µg/µL]	Puromycin [µg/µL]
0	0	0	0	0
150	50	50	2.5	1
300	100	100	5	2
450	150	150	7.5	3
600	200	200	10	4
900	300	300	15	5
1200	400	400	20	6
1500	500	500	25	8
1800	600	600	30	10
2100	700	700	40	12
2400	800	800	50	15
2700	900	900	100	20

3.7 Protein production and purification

3.7.1 Transient protein expression in HEK293-6E

Transient expression in HEK293-6E cells was used for the screening of constructs as well as for test expressions in batch culture. Transfections of HEK293-6E cells were carried out according to Section 3.6.6. The transfection efficiency was monitored daily using flowcytometry (Section 3.6.10) as well as cell number and viability (Section 3.6.3). The starting culture volume used during transfection was expanded 48 h post transfection by adding the same amount of fresh F17 medium to the culture. Furthermore the culture was supplemented with tryptone (TN1) to a final concentration of 0.5 %. Supplementations with a final concentration of 4.5 g/L glucose at 72 hpt to avoid nutrient depletion and 3.75 mmol/L valproic acid at 96 hpt to boost expression rates in the stationary phase (Backliwal *et al.*, 2008). Cells were typically harvested at 4.000 rpm in a bench top centrifuge using 50 mL Falcon tubes, if necessary the culture supernatants were pooled and supplemented with 0.1 % sodium acid for storage at 4 °C. If the cell pellets were needed those were washed with 1x PBS pooled in one Falcon tube and centrifuged again. The supernatant was removed and stored at -20 °C.

3.7.2 Protein production in stable CHO Lec3.2.8.1 cell lines

For small scale protein production producer cell lines generated in Section 3.6.8 were expanded to a volume of 150 mL - 1.5 L and cultivated for 3-5 days in shaker flasks. Culture supernatants or cell pellets were typically harvested at 7330 rcf for 30 min or at 4.000 rpm in a bench top centrifuge using 50 mL Falcon tubes. Cell pellets were further washed with

1x PBS transferred to a 50 mL Falcon tube and centrifuged again at 4.000 rpm. Culture supernatants were supplemented with 0.1 % sodium acid and stored at 4 °C. Cell Pellets were stored at -20 °C.

For large scale protein production, in a 2.5 L – 40 L scale, producer cell lines were cultivated in an autoclavable stirred tank bioreactor by Nadine Konisch in batch (2.5 L) or perfusion mode (> 2.5 L). A double membrane stirrer within the 2.5 L bioreactor was equipped with two types of membrane tubing (Accurel® S6/2, Membrana); one for bubble-free aeration via 8 meters of hydrophobic polypropylene membrane tubing and one that enables perfusion with internal cell retention via 8 meters of hydrophilized, micropourous membrane tubing (Lehmann *et al.*, 1987, Blasey *et al.*, 1991). Figure 3-1 shows a flow diagram for the process. Producer cell lines were cultivated in a 1:1 blend of ProCHO5 and ZKT-I medium at 37 °C with a stirring speed of 45 rpm and a dissolved oxygen concentration of 40 % air saturation at pH 7.4. If cell densities exceeded 10^7 cells/mL during the production phase the temperature was reduced to 32 °C. Perfusion rates were adjusted according to the metabolic consumption of glucose preventing a drop below 2.5 g/L. Samples of 2 mL were drawn daily for in-process control. Harvested culture supernatants were concentrated and diafiltrated against an exchange buffer (50 mM Tris-HCl, 500 mM NaCl, pH 8.0) with the ProFlux® tangential flow system (Millipore) equipped with two Pellicon 2 cassettes (MWCO 10kD, Cat# P2C010C05, Millipore). The diafiltrated sample was supplemented with 0.1 % sodium acid and stored at 4 °C until purification.

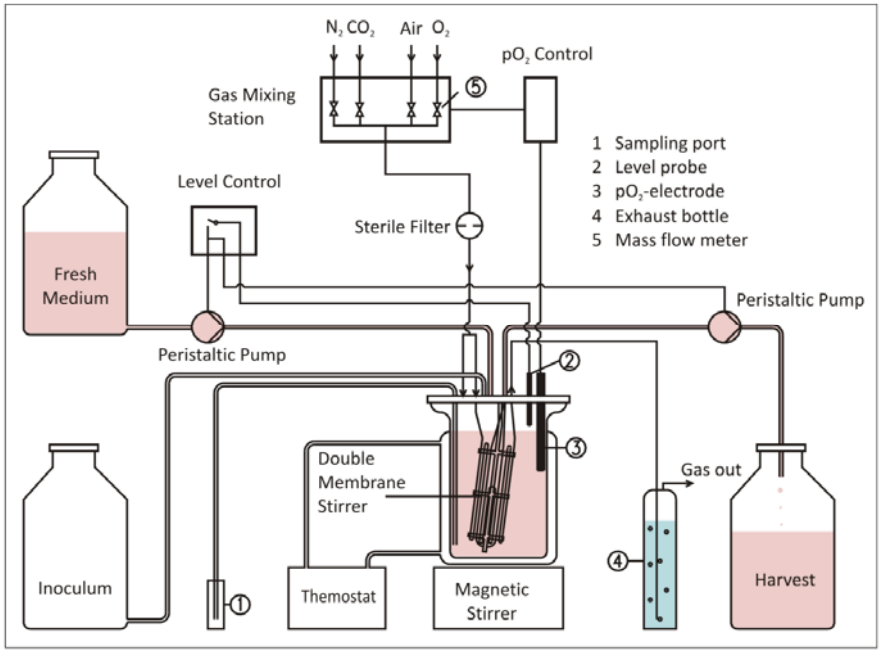

Figure 3-1: Flow diagram for a stirred tank perfusion reactor (source: V. Jäger, HZI).

3.7.3 Trichloroacetic acid (TCA) precipitation

To preliminary test protein expression using small volumes of culture supernatant or total cell lysate, TCA precipitation is used to concentrate the protein for Western blot analysis. To do so 1 mL of culture supernatant or total cell lysate are mixed with 100 µL 100 % TCA and incubated on ice for 30 min. The precipitated protein is centrifuged down at 13.000 rpm for 15 min. the protein pellet is washed with 1 mL ice-cold 70 % ethanol and pelleted again for 5 min at 13.000 rpm. The protein pellet is dissolved in 50 µL water and 50 µL 2x Laemmli buffer.

3.7.4 Cell lysis

To lyse mammalian cell pellets 10 mL - 50 mL lysis buffer together with one Roche complete EDTA-free protease inhibitor cocktail tablet and 2 µg – 5 µg DNase I (Table 3-22) were added to a frozen cell pellet in a Falcon tube and vortexed. The tube was left on ice for approximately 40 min – 60 min and the content centrifuged at 30.000 xg for 20 min - 60 min and eventually filtered with a 0.45 µm syringe filter. Small cell pellets in Eppendorf tubes were lysed with 50 µL – 700 µL lysis buffer, kept on ice for 15 min and centrifuged at 12.000 rpm for 10 min.

Table 3-22: Lysis buffers

Buffer	Composition
Lysis buffer, pH 8.0	50 mM $Na_xH_yPO_4$, 300 mM NaCl, 5 mM– 20 mM imidazole, 0.5 % IGEPAL CA-630 (Cat# 13021-100mL, Sigma), 3 mM 3-β-mercaptoethanol
FLAG-Lysis buffer, pH 8.0 (magnetic beads)	50 mM $Na_xH_yPO_4$, 300 mM NaCl, 0.1% IGEPAL CA-630
FLAG-Lysis buffer, pH 7.4 (affinity resin)	50 mM Tris-HCl, 150 mM NaCl, 1 mM EDTA, 1 % Triton X-100 (Cat# 1.08605.0050, Merck)
Ni-NTA Lysis buffer, pH 8.0	50 mM Na_2HPO4, pH 8.0, 300 mM NaCl, 10 mM imidazole, 0.1 % IGEPAL CA-630, 1 mM KH_2HPO4, 1.35 mM KCl

* 1 Roche complete EDTA-free protease inhibitor cocktail tablet and 2 µg – 5 µg DNase I were added either directly to the sample or to 50 mL lysis buffer and aliquoted.

3.7.5 Dialysis and diafiltration

The VIVAflow 200 system or the KrosFlow® research IIi TFF system were set up according Figure 3-2 or Figure 3-3 respectively. The 10 % storage ethanol was removed from the VIVAflow 200 cartridge or MidiKros column and the system cleaned with at least 500 mL MilliQ water to remove residual ethanol. The MilliQ water was drained from the system and approximately 200 mL of the cell culture supernatant were placed into the concentrate reservoir. The remaining cell culture supernatant was connected as feed reservoir to the

concentrate reservoir. The sample was concentrated down to approximately 50 mL - 100 mL by re-circulation through the system. After concentration of the sample the exchange buffer (50 mM Tris-HCl, 500 mM NaCl, pH 8.0) was connected to the feed reservoir and the concentrated sample was diafiltrated through re-circulation through the system with at least 500 mL exchange buffer. The concentrated and diafiltrated sample was recovered, the system cleaned according to the manufacturers guidelines and stored in 10 % ethanol.

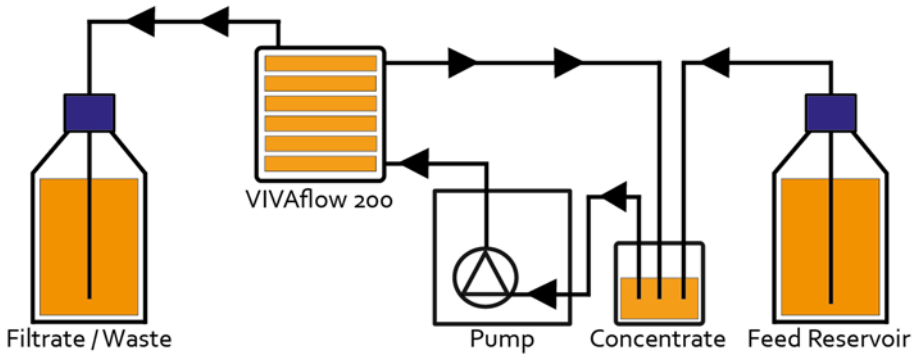

Figure 3-2: System set up for diafiltration with VIVAflow 200.

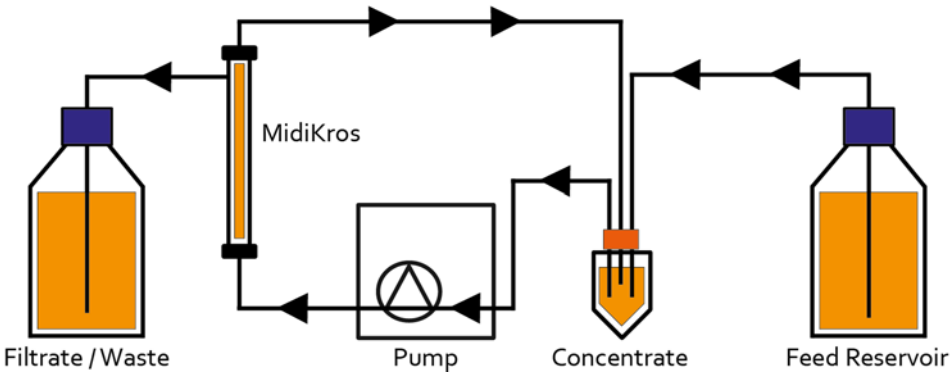

Figure 3-3: System set up for diafiltration with MidiKros column.

3.7.6 Concentration of protein solutions with Vivaspin concentrators

Vivaspin concentrators with a polyethersulfon (PES) membranes (Table 3-23) were used to concentrate smaller volumes of protein solutions and/or use them for buffer exchange. Protein solutions were centrifuged at up to 5000 xg in Vivaspin 20 concentrators or up to 4000 xg in Vivaspin 6 concentrators until the desired volume was reached. If the buffer should be exchanged after concentration this was added and centrifuged again as necessary.

Table 3-23: Vivaspin concentrators

Concentrator	MWCO (kDa)	Cat#	Supplier
Vivaspin 20	30.000	VS2022	Vivascience /Satorius
Vivaspin 20	10.000	VS2002	Vivascience /Satorius
Vivaspin 20	5.000	VS2012	Vivascience /Satorius
Vivaspin 20	3.000	VS2092	Vivascience /Satorius
Vivaspin 6	30.000	VS0622	Vivascience /Satorius
Vivaspin 6	10.000	VS0602	Vivascience /Satorius
Vivaspin 6	5.000	VS0612	Vivascience /Satorius
Vivaspin 6	3.000	VS0692	Vivascience /Satorius

3.7.7 Small scale purification of tagged proteins with magnetic beads

Small scale purifications of cell extracts or cell culture supernatants were done using magnetic beads. All fractions were collected and analysed by SDS-PAGE and Western blot (Sections 3.8.1 and 3.8.2).

Table 3-24: Small scale purification methods

MagneHis™ Ni-Particles (Promega, Cat# V8560)
An appropriate amount of MagneHis ™ beads were added to dialysed culture supernatant and incubated. The magnetic beads were captured with a magnetic rack and washed 3x with MagneHis™ Binding/Wash buffer containing 500 mM NaCl. MagneHis™ elution buffer was used for elution in volumes from 50-100 µL.
MagStrep "type2" beads (IBA, Cat# 2-1611-002)
An appropriate amount of MagStrep beads were equilibrated with 200 µL Buffer W and added directly to the culture supernatant. After incubation beads were captured with a magnetic rack and washed 3x with 100 µL buffer W before elution with buffer BE in 50-100 µL volume.
ANTI-FLAG® M2 Magnetic beads (Sigma, Cat# M8823-1ML)
100 µL suspended beads (= 50 µL beads with a binding capacity of ~ 30 µg protein) were transferred to a 2 mL Eppendorf. The beads were separated from the suspension using a magnetic stand and the beads equilibrated twice with TBS buffer (50 mM Tris-Cl, 150 mM NaCl, pH 7.5). The beads were recovered with the magnetic stand 2 mL cell lysate (Section 3.7.4) were added to the magnetic beads and incubated for 2 h on a shaker. The magnetic beads were washed 3x with TBS buffer and the protein eluted with 200 µL elution buffer (0.1 M glycine/HCl pH 3.0) and the eluate transferred to 60 µL 1 M Tris pH 8.0. The elution step was repeated with 150 µL elution buffer.

3.7.8 Affinity chromatography of tagged proteins

Purifications of cell extracts or cell culture supernatants were done using commercially available or stacked columns. Fractions were collected and analysed by SDS-PAGE and Western blot (Sections 3.8.1 and 3.8.2).

Table 3-25: Small scale purification methods

Ni-NTA His-Bind® Superflow™ Resin (Novagen, Cat# 70691)
A 5 mL columns (MoBiTec, Cat# S1013) with 35 µm filter were stacked 500 µL Ni-NTA His-Bind® Superflow™ resin and a 20 mL syringe was screwed on top of the column as a reservoir. The resin was equilibrated with 10 CV binding buffer (50 mM Na_2HPO_4, 300 mM NaCl, 10 mM imidazole, pH 8.0) before loading the cell extract via gravity flow. The resin was washed with 10 CV of binding buffer followed by 10 CV of wash buffer (50 mM Na_2HPO_4, 300 mM NaCl, 20 mM imidazole, pH 8.0) to remove unspecifically bound protein. Protein was eluted with 10 CV of elution buffer (50 mM Na_2HPO_4, 300 mM NaCl, 250 mM imidazole, pH 8.0). As the column was overloaded a second round of purification was necessary, so the resin was equilibrated again with 10 CV of binding buffer and the flowthrough loaded 3x consecutively to the column to assure complete protein binding. The resin was washed with 10 CV of binding buffer followed by 10 CV of wash buffer to remove unspecifically bound protein and the protein eluted with 8 CV of elution buffer.
Ni-IMAC with Profinia™ Protein Purification System
For the purification of His-tagged proteins with the Profinia protein purification system Bio-Scale™ Mini Profinity™ IMAC Cartridges with 1 mL (Cat# 732-4610, Bio-Rad) or 5 mL (Cat# 732-4614, Bio-Rad) bed volume were used. The purification step was followed by desalting of the eluate with Bio-Scale™ Mini Bio-Gel® P-6 Desalting Cartridge with 10 mL (Cat# 732-5304, Bio-Rad) or 50 mL (Cat# 732-5314, Bio-Rad) bed volume. Pre-programmed methods were used for the purification and desalting of target proteins. Buffers for purification are listed in Table 3-26.
Ni-NTA with ÄKTApilot
Ni-NTA His-Bind® Superflow™ resin was used to purify larger volumes of His-tagged protein. After application of the diafiltrated and concentrated sample to the column a wash with 200 mL binding buffer (50 mM Tris-HCl, 500 mM NaCl, pH 8.0) was used to remove unspecifically bound protein. The target protein was eluted with a step gradient mixing binding buffer with elution buffer (50 mM Tris-HCl, 500 mM NaCl, 500 mM imidazole, pH 8.0).
StrepTactin Superflow Cartridge H-PR (IBA, Cat# 2-1231-001)
Concentrated dialysed culture supernatant is loaded to the column washed with washing buffer (100 mM Tris-Cl, 150 mM NaCl, 1 mM EDTA, pH 8.0), and eluted with 4 mL elution buffer (100 mM Tris-Cl, 150 mM NaCl, 1 mM EDTA, 2.5 mM desthiobiotin, pH 8.0).
Anti-FLAG® M2 Affinity Gel (Sigma, Cat# A2220)
A 1 mL column (Mobicol classic, MoBiTec, Cat# M1002) with a 35 µm filter was stacked with 300 µL Anti-FLAG® M2 affinity gel resin. The resin was washed 3x with 1 CV of regeneration buffer (0.1 M glycine HCl, pH 3.5) followed by equilibration with 5 CV of TBS (50 mM Tris-HCl, 150 mM NaCl, pH7.4). Proper equilibration was tested with pH strips and the cell extract was slowly applied with a syringe passing it consecutively 3x over the column. The column was washed with 20 CV of TBS to remove unspecifically bound protein. Protein was eluted in six 1 mL aliquots of elution buffer (0.1 M glycine HCl, pH 3.5) into 25 µL 1 M Tris, pH 8.0 for neutralization. These steps were repeated a second time using the flowthrough from the first round of purification to assure that all present protein was purified.

Table 3-26: Buffers used for Ni-IMAC with the Profinia Protein Purification system

Buffer	Working formulation
Native IMAC wash buffer 1	300 mM KCl, 50 mM KH_2PO_4, 5 mM imidazole, pH 8.0
Native IMAC wash buffer 2	300 mM KCl, 50 mM KH_2PO_4, 10 mM imidazole, pH 8.0
Native IMAC elution buffer	300 mM KCl, 500 mM KH_2PO_4, 250 mM imidazole, pH 8.0
Cleaning solution 1	500 mM NaCl, 50 mM Tris, pH 8.0
Cleaning solution 2	500 mM NaCl, 100 mM sodium acetate, pH 4.5
Storage solution	2% $C_6H_5CH_2OH$ (benzyl alcohol)
Desalting buffer	50 mM Tris-HCl, 500 mM NaCl, pH 8.0

Table 3-27: Buffer for Ni-IMAC with the ÄKTApilot

Buffer	Working formulation
Binding buffer	50 mM Tris-HCl, 500 mM NaCl, pH 8.0
Elution buffer	50 mM Tris-HCl, 500 mM NaCl, 500 mM imidazole, pH 8.0

3.8 Protein analytical methods

3.8.1 SDS-PAGE

To analyse protein purity and yield as well as expression kinetics SDS-PAGE (sodium dodecyl sulphate polyacrylamide gel electrophoresis) was used under denaturing conditions (Laemmli *et al.,* 1970). 12 % or 10 % gels were either made according to Table 3-28 or precast gels from Bio-Rad were used. Samples were mixed with 8x SDS loading buffer and boiled for 5 min at 90 °C before applying them to a SDS-gel. Typically 10 µL - 15 µL of sample were loaded to 15-well SDS-gels and 15 µL - 20 µL to 10-well SDS-gels. Mini-Protean® TGX™ were loaded with 15 µL or 30 µL sample (15-well and 10-well respectively). The gels were pre-focused under constant voltage of 120 V for 5 min and run at 160 V until the dye front reached the end of the gel. To remove the SDS the gel was washed in water and then stained with either Instant blue or coomassie staining solution. The buffers used for SDS-PAGE are listed in Table 3-29. The molecular weight standards used are listed in Table 3-3.

Enzyme	Cat#	Supplier
T4 DNA Ligase (1.000 U/ mL)	11000324/ 14395420	Roche
Antarctic Phosphatase (5.000 U/mL)	M0289S	NEB
Phusion® Hot Start II DNA Polymerase (2.000 U/mL)	F-549L/ M0530S/ B0515A	Finnzymes/ Thermo Scientific/ NEB
KOD Hot Start DNA Polymerase (1.000 U/mL)	71086-3	Novagen/Millipore
DNase I (1ng/µL)	N/A	MOSB, HZI
Trypsin/ EDTA (1x)	L11-004	PAA Laboratories GmbH
Trypsin/ EDTA (10x)	L11-003	PAA Laboratories GmbH

Table 3-28: SDS-Gel composition (for 8 gels)

Solution	Resolving gel		Stacking gel	
	12 %	**10 %**	**5 %**	**3 %**
Acrylamide/bisacrylamide 30 % (v/v)	12 mL	10 mL	1.5 mL	1 mL
4x lower buffer	7.5 mL	7.5 mL	-	-
4x upper buffer	-	-	2.5 mL	2.5 mL
10 % SDS	0.3 mL	0.3 mL	-	-
H_2O	10.1 mL	12.4 mL	5.9 mL	6.4 mL
TEMED	40 µL	40 µL	30 µL	30 µL
40 % APS	60 µL	60 µL	30 µL	30 µL

Table 3-29: Buffers and commercial products for SDS-PAGE

Solution	Composition	
4x upper buffer	0.5 M Tris-base pH 6.8, 0.4 % SDS (v/v)	
4x lower buffer	1.5 M Tris-base, pH 8.8	
SDS running buffer	3 g/L Tris-base, 14.4 g/L glycine, 1 g/L SDS, pH 8.3	
Coomassie staining solution	50 % methanol, 10 % acetic acid, 0.1 % coomassie brilliant blue R250 (Serva, Cat# 17525)	
Coomassie destaining solution	50 % methanol, 10 % acetic acid	
8x SDS loading buffer	7.0 % SDS (v/v), 0.22 % glycerol (v/v), 9.6 mM Tris-HCl pH 6.8, 2.4 mM β-mercaptoethanol, 0.22 mg/mL bromphenol blue	
Product		**Cat#** **Supplier**
InstantBlue™		ISB01L Biozol/ expedeon
Mini-Protean® TGX™		Bio-Rad
12 %, 10-well		456-1043
12 %, 15-well		456-1046
10 %, 15-well		456-1036
10 %, 10-well		456-1033

3.8.2 Native PAGE

Native PAGE was used to analyse proteins in there non-denatured globular state. Pre-cast NativePAGE Novex 4-1 % Bis-Tris gels (Invitrogen, Cat# BN1004BOX) were used according to the manufacturer's protocol in combination with the XCell *Sure*Lock® system. Gels were run for 105 min at 150 V and stained with coomassie staining solution (Section 3.8.1). Samples were mixed with 4x sample buffer before loading 10 µL of the non-boiled mixture to the well. Buffers used for native PAGE are listed in Table 3-30.

Table 3-30: Buffers for Native-PAGE

Solution	Composition
4x sample buffer	200 mM BisTris, 6N HCl, 40 % (w/v) glycerol, 200 mM NaCl, 0.001 % Ponceau S (Sigma, Cat# P-3504), pH 7.2
20x running buffer	1 M BisTris, 1 M Tricine, pH 6.8
20x cathode buffer additive	0.4 % Coomassie® Brilliant Blue G250 (Serva, Cat# 17524)
Sample buffer additive	5 % Coomassie® Brilliant Blue G250 (Serva, Cat# 17524)
Anode buffer	1x running buffer
Cathode buffer	1x running buffer, 1x cathode buffer

3.8.3 Western blot

Western blots were made for the specific detection of proteins. Protein samples were separated using SDS-PAGE (Section 3.8.1) and then transferred to a polyvinylidene fluoride (PVDF) membrane with the Trans-blot SH semi-dry transfer cell (Bio-Rad) or the Trans-blot Turbo Transfer System (Bio-Rad) by a semi-dry blotting procedure (Kyhse-Andersen, 1984) before immunostaining. The SDS-gels as well as two pieces of blotting paper were equilibrated in transfer buffer. The PVDF membrane was first activated shortly in 100 % methanol before equilibration in transfer buffer. For the protein transfer the PVDF-membrane was placed bubble-free below the SDS-gel and sandwiched between two pieces of blotting paper on the anode of a blotting apparatus. The blot was run for 30 min - 35 min at 12 V when using the Trans-blot SH semi-dry transfer cell (Bio-Rad) or for 7 min – 10 min when using the Trans-blot Turbo Transfer System (Bio-Rad). After the transfer the PVDF-membrane was blocked in 5 % skim milk powder in 1x PBS or Tris buffered saline with Tween-20 (TBS-T). The membrane was washed 3x for 5 min in TBS-T and the primary antibody diluted in TBS-T (+ 3 % milk for FLAG antibody) applied to the membrane. The primary antibody was incubated overnight on a shaking platform and then removed by washing the membrane again 3x for 5 min with TBS-T. The secondary antibody (if required) was applied to the membrane diluted in TBS-T and incubated for at least 2 hours. The membrane was washed again as described before and 1x for 5 min in alkaline phosphatase (AP) buffer. AP-conjugated antibodies bound to the protein of interest were detected with a 5-Bromo-4-chloro-3-indoxyl phosphate (BCIP) / nitro blue tetrazolium chloride (NBT) colour development substrate mixture diluted in AP buffer. The Materials, antibodies and reagents used for Western blotting are listed in Table 3-31.

Table 3-31: Materials, antibodies and reagents for Western blotting

Materials	**Model**	**Cat#**	**Supplier**
PVDF membrane	Immobilon^{TM}-P, PVDF, pore size 0.45	IPVH00010	Millipore
Blotting paper	GB 004 Gel-Blotting Paper	426994	Schleicher und schuller
Antibodies	**Type and Dilution**	**Cat#**	**Supplier**
His-Tag®Monoclonal Antibody (mouse)	Primary 1:2000 or 1:1000	70796-3	Novagen
StrepMAB-Classic (mouse), 1 mg/mL	Primary 1:1000	2-1507-001	IBA
Anti-mouse TLR1 (N-term) antibody (rabbit)	Primary 1:500	SAB1300197-100UG	Sigma-Aldrich
Monoclonal ANTI-FLAG® M2 (mouse), 3.8 mg/mL or 4.2 mg/mL	Primary 1:4000	F3165-.2MG	Sigma
Goat-anti mouse IgG (H+L) –AP, 1 mg/µL	Secondary 1:7000	S3721	Promega
Anti-rabbit IgG (Fc) AP Conjugate, 1 mg/mL	Secondary 1:7500	S3731	Promega
Reagents	**Concentration**	**Cat#**	**Supplier**
BCIP	50 mg/mL in 100 % dimethylformamide	S381C	Promega
NBT	50 mg/mL in 70 % dimethylformamide	S3801C	Promega
Buffers	**Composition**		
Transfer buffer	25 mM Tris-base, 192 mM glycine, 15 % methanol, pH 8.0		
1x PBS	140 mM NaCl, 3 mM KCl, 12 mM Na_2HPO_4, 2 mM KH_2PO_4, pH 7.4		
TBS-T	20 mM Tris-base, 150 mM NaCl, 0.05 % (v/v) Tween, pH 8.0		
AP-buffer	100 mM Tris-base, 100 mM NaCl, 5 mM $MgCl_2$, pH 9.5		

3.8.4 Fluorescent measurements with the Tecan MD 1000 plate reader

Cell extracts or purified protein eluates obtained from cell lines expressing the fluorescent protein tdTomato were analysed with the Tecan MD 1000 plate reader on Nuncleon Delta Surface plates (Thermo Scientific/Nunc, Cat# 137101). Purified tdTomato was used to generate a suitable standard curve diluted in either cell extract obtained from cell lines not expressing tdTomato or buffer corresponding to the one present in purified eluates. Samples and standards were analysed in two sets of triplicates on two separate plates using 100 µL volume. Settings used during the measurements are listed in Table 3-32. Concentrations for tdTomato expression were calculated according to the calibration curve obtained during the same measurement.

Table 3-32: Settings of Tecan MD 1000 plate reader

Parameter	Setting
Mode	Fluorescence top reading
Excitation Wavelength	554 nm
Emission Wavelength	581 nm
Excitation Bandwidth	5 nm
Emission Bandwidth	5 nm
Gain	100
Number of Flashes	50
Flash Frequency	400 Hz
Integration Time	20 µs
Lag Time	0 µs
Settle Time	0 ms
Z-Position:	19276 µm

3.8.5 MALDI-TOF

To identify protein samples after separation with SDS-PAGE MALDI-TOF (Matrix Assisted Laser Desorption Ionisation – Time-of-Flight) mass spectrometry (MS) was used. Tryptic digestion of the isolated protein sample was followed by the co-crystallization with organic acids. A UV laser mediated the desorption of protein fragments and was than ionized by protonation of the peptide fragments. Thus the mass-to-charge ratios were derived from the TOF measurements. This data was compared with the MASCOT database to identify the analysed proteins. The analyses were done by the research group Cellular Proteome Research at the HZI.

3.9 Statistical methods

3.9.1 Standard deviation

The standard deviation (SD) for repeated measurements or values of one population were calculated according to the formula below which corresponds to the STDEV.P function in Microsoft Excel.

$$\sigma = \sqrt{\frac{\sum(x - \bar{x})^2}{n}}$$

- σ Standard deviation
- x Value of sample
- $\bar{x}$ Mean value of sample
- n Number of samples

3.9.2 Analysis of variance – ANOVA

To determine if there is a significant difference between mean protein yields obtained from triplicate batch cultures or different harvesting timepoints, a two-factor ANOVA without replication was used.

First null-hypothesis (H_{0A}): No significant difference in expression between batch cultures (μ = average yield, r = number of batch).

$$H_{0A} = \mu_1 = \mu_2 = \cdots = \mu_r$$

Second null-hypothesis (H_{0B}): No significant difference in expression between different harvesting time points. (μ = average yield, c = number of harvesting time point).

$$H_{0B} = \lambda_1 = \lambda_2 = \cdots = \lambda_c$$

To confirm these null-hypothesises the F-ratio needed to be calculated for each by dividing the mean sum of squares (MS) of an analysed group through the MS of the within group variation. A and B refer to the analysed groups (batch and harvesting time point) and E to the within group variation or random error.

$$F_A = \frac{MS_A}{MS_E} \qquad F_B = \frac{MS_B}{MS_E}$$

If an observed F-ratios was lower than the critical F value ($F<F_{crit}$) and the p-value (probability) was larger than the set significance level α ($p > \alpha$) the null-hypothesis could be accepted. All calculations were done using the two-factor ANOVA without replication function in Microsoft Excel. The significance level α was set to 0.05 to obtain a 95% confidence level. The formulas below show the different components required for the calculation of the F-ratio (SS = Sum of squares, df = degrees of freedom, x = measured values, $\bar{x}$ = total average of all measured values).

$$SS_A = c\sum_j (x_i - \bar{x})^2 \qquad df_A = r - 1 \qquad MS_A = \frac{SS_A}{df_A}$$

$$SS_B = r\sum_j (x_j - \bar{x})^2 \qquad df_A = c - 1 \qquad MS_B = \frac{SS_B}{df_B}$$

$$SS_E = \sum_i \sum_j (\bar{x}_{ij} - \bar{x}_i - \bar{x}_j - \bar{x})^2 \qquad df_E = (r-1)(c-1) \qquad MS_E = \frac{SS_E}{df_E}$$

4 Results

4.1 Establishment of binary RMCE master cell lines

To enable the stable co-expression of difficult to express proteins with accessory molecules at pre-defined genomic loci a binary RMCE system was established during this work. The RMCE master cell lines SWI3_26 (Wilke *et al.*, 2011) and SMT_dneo(2)_24 (Konrad Büssow, HZI) previously created in our group already contain the first exchange locus (P_{EF}-FRT_3-*eGFP*-FRT_{wt}-Δ*neo*) and were used for the stable integration of a second exchange cassette. In this section the steps for the generation of binary CHO Lec3.2.8.1 RMCE master cell lines for the targeted integration of transgenes at two distinct genomic loci are described.

The groundwork required for the preparation of a second exchange cassette included the screening for antibiotic sensitivity in SWI3_26 cells to determine a suitable resistance marker for its selection trap (Section 4.1.1). Furthermore, the analysis of the fluorescent marker tdTomato (Section 4.1.2) ensured the compatibility with the existing eGFP marker in a binary system. To enable the site-specific integration into different loci heterospecific *FRT* sites (FRT_{13} and FRT_{14}) which do not cross-interact with the existing ones (FRT_3 and FRT_{wt}) (Turan *et al.*, 2010) were chosen for the second exchange locus. The chosen components were cloned into a tagging vector (Section 4.1.3) and used for genomic tagging of the SWI3_26 and SMT_dneo(2)_24 RMCE master cell lines followed by FACS and clonal isolation to obtain a new set of binary RMCE master cell lines (Section 4.1.4). To confirm the full integration of the exchange cassettes genomic PCR (Section 4.1.5) was used to determine RMCE master cell line integrity. Finally, to enable the integration of target genes into the second exchange locus a new donor vector was cloned (Section 4.1.6) comprising the new set of heterospecific *FRT* sites (FRT_{13} and FRT_{14}). The binary RMCE system was used for the co-expression of TLRs with molecular chaperones as described in Section 4.4.

4.1.1 Resistance of the CHO Lec3.2.8.1 cell line SWI3_26 to antibiotics

To isolate cells that successfully integrated a GOI during RMCE, the second exchange locus in the binary RMCE system requires a different selection marker in its selection trap than exchange locus one. To select a resistance marker the resistance of the CHO Lec3.2.8.1 RMCE master cell line SWI3_26 (Wilke *et al.*, 2011) against the antibiotics geneticin (G418),

puromycin, phleomycin, zeocin and hygromycin B was tested according to Section 3.6.11. The decrease in cell density stagnated at a confluency of 20-30 % (visual observation) with all tested antibiotics. At this point no cell proliferation took place anymore indicating total cell death. Total cell death was observed at a concentration of 2100 µg/mL for G418, 15 µg/mL for puromycin and phleomycin, 400 µg/mL for zeocin and 500 µg/mL for hygromycin B (Figure 4-1). The highest sensitivity was observed for puromycin and phleomycin which were equally suitable as potential selection traps for the second exchange locus. As a Δ*puro* selection trap was already available in our group, on the vector pEF-FS-eGFP-dpuro (Konrad Büssow, HZI), puromycin was used as antibiotic marker for the second selection trap in the binary RMCE system.

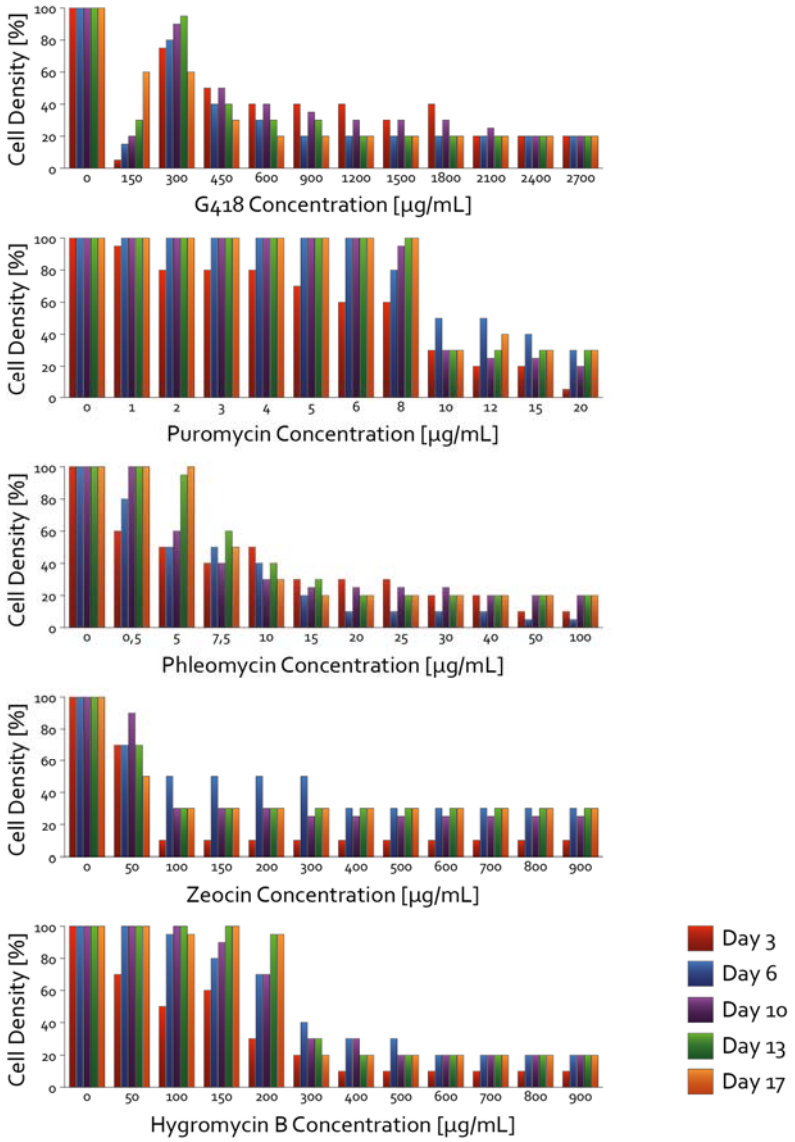

Figure 4-1: Resistance of SWI3_26 (CHO Lec3.2.8.1) against antibiotics. Antibiotic pressure was applied to SWI3_26 cells and observed over 17 days to determine their resistance against different antibiotics. Stagnation in the decrease of cell density at a confluency of 20-30 % was defined as total cell death. Stagnation can be observed at a concentration of 2100 µg/mL for G418, 15 µg/mL for puromycin and phleomycin, 400 µg/mL for zeocin and 500 µg/mL for hygromycin B.

4.1.2 Suitability of tdTomato as fluorescent marker

For the generation of binary RMCE cell lines a second fluorescent marker was required for simultaneous use with the eGFP marker already present in the first integration site of the RMCE master cell lines SWI3_26 and SMT_dneo(2)_24. To determine the suitability of tdTomato as a fluorescent marker in this setup a tdTomato producer cell line was derived from the master cell line SWI3_26 using the pFlpBtM-II_(beta)_tdTomato exchange vector for RMCE (Section 3.6.8).

Flowcytometric analysis of this tdTomato producer cell line BBA10-tdTomato-C1 with the Guava easyCyte showed that tdTomato does not interfere with the green channel (BP 525/30 nm) which is used to determine the efficient exchange of the eGFP locus. However, the yellow channel (BP 583/26 nm) in which tdTomato is detected most efficiently as it is close to its emission maximum at 581 nm also detects eGFP (emission maximum 510 nm) and thus is not suitable for the detection of neither in a binary RMCE setup. Nonetheless, as tdTomato is also detected in the red channel (BP 680/ 30 nm) in which eGFP does not interfere significantly this one can be used for the analysis of tdTomato in a binary RMCE cell line (Figure 4-2). Similar testing was done to exclude any cross-interference with the Axiovert 100 fluorescence microscope using filter set 43 (BP 605/70 nm), filter set 9 (LP 515 nm), filter set 44 (BP 530/50 nm) and filter set 25 (TBP 460 + 530 + 625 nm). The most suitable combination was filter set 44 for eGFP with filter set 43 for tdTomato (data not shown). In conclusion, tdTomato is a suitable second fluorescent marker and can be used in simultaneously to the eGFP fluorescent marker in a binary RMCE system.

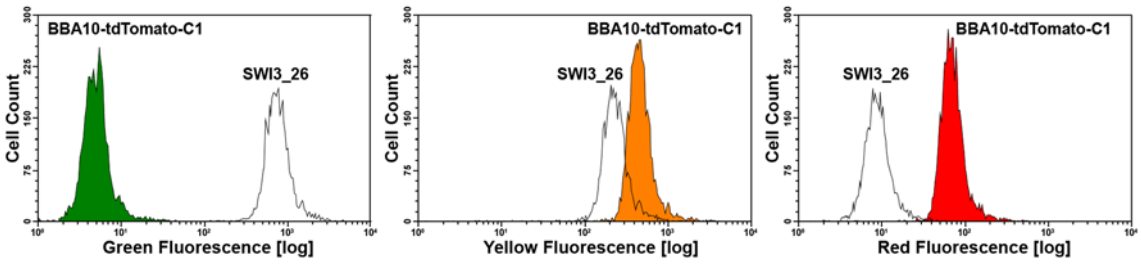

Figure 4-2: Flowcytometric analysis of the BBA10-tdTomato-C1 producer cell line and SWI3_26 RMCE master cell line. Histogram overlays of the red fluorescent cell line BBA10-tdTomato (solid green, orange or red) and the green fluorescent cell line SWI3_26 (black line) are shown (left to right) in the green (BP 525/30 nm), yellow (BP 583/26 nm) and red (BP 680/30 nm) channel of the Guava easyCyte flowcytometer.

4.1.3 Cloning of tagging vector pEF-FS-tdTomato-dpuro

For the integration of an additional exchange cassette into the RMCE master cell lines SMT_dneo(2)_24 and SWI3_26 (Section 4.1.4) it was necessary to prepare a new tagging vector. This new tagging vector required a different set of heterospecific *FRT* sites (FRT_{13} and FRT_{14}) which does not cross-interact with the existing set of *FRT* sites (FRT_3 and FRT_{wt}) (Turan *et al.*, 2010). Furthermore, a second fluorescent selection marker (tdTomato) which emits at a distinct wavelength to the already introduced eGFP marker in the first exchange cassette was needed for analytic purposes (Section 4.1.2). Lastly, a Δ*puro* selection trap (Section 4.1.1) was chosen as an additional selection system to the existing Δ*neo* selection trap.

The vector pEF-FS-eGFP-dpuro (Konrad Büssow, HZI) a variant of the vector pEF-FS-eGFP-dneo (Wilke *et al.*, 2011), which was used for genomic tagging of CHO Lec3.2.8.1 cells to integrated the first exchange locus of the RMCE master cell lines SMT_dneo(2)_24 and SWI3_26, already contains a Δ*puro* selection trap. To introduce the new set of heterospecific *FRT* sites (FRT_{13} and FRT_{14}) into the tagging vector pEF-FS-eGFP-dpuro a fragment containing the new set of *FRT* sites and the required restriction sites for cloning was synthesised by Life Technologies (Figure 4-3) and delivered in the vector 11AAYGEC_F13-F14_dpuro_pMA-RQ.

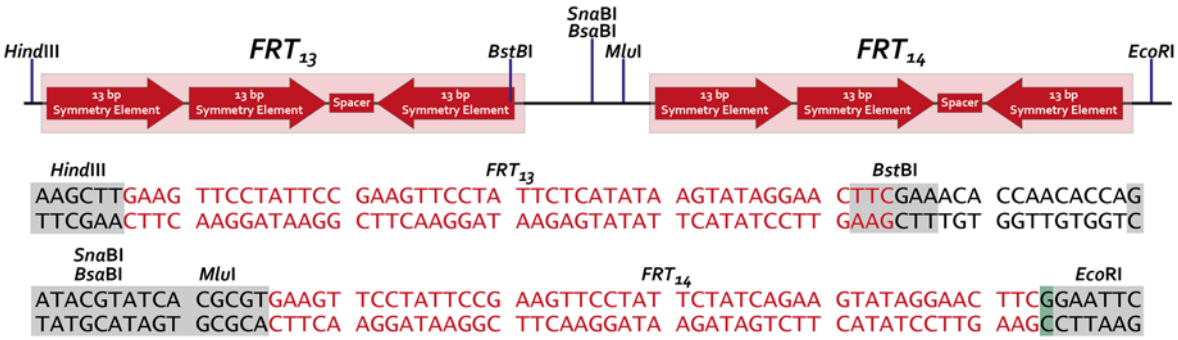

Figure 4-3: Design of synthesised FRT_{13}/FRT_{14} and restriction endonuclease sites for cloning of tagging vector pEF-FS-tdTomato-dpuro. The heterospecific *FRT* sites FRT_{13} and FRT_{14} (red) were synthesised separated by a linker with the required restriction endonuclease sites for molecular cloning (grey) by Life Technologies and delivered in the vector 11AAYGEC_F13-F14_dpuro_pMA-RQ. An additional nucleotide (green) was introduced upstream of the *Eco*RI restriction site to assure that upon RMCE the inserted start codon for the selection trap is in frame with the downstream Δ*puro* selection trap (not shown).

Cloning of the pEF-FS-tdTomato-dpuro tagging vector was done in two steps. First the tdTomato fluorescent marker together with its SV40pA signal were retrieved from the vector pFlpBtM-II(beta)_tdTomato (Steffen Meyer, HZI) with the restriction endonucleases

*Bst*BI and *Bsa*BI. The 1718 bp tdTomato_SV40pA fragment was ligated into the 2478 bp 11AAYGEC_F13-F14_dpuro_pMA-RQ vector backbone (cut with *Bst*BI and *Sna*BI) in between the *FRT* sites FRT_{13} and FRT_{14} thus destroying the *Sna*BI site. The resulting intermediate vector 11AAYGEC_F13-tdTomato_SV40pA-F14_dpuro-pMA-RQ containing the tdTomato selection marker with its SV40pA signal flanked by the heterospecific *FRT* sites FRT_{13} and FRT_{14} was used in the second cloning step. From this intermediate vector the FRT_{13}-tdTomato_SV40pA-FRT_{14} fragment (1831 bp) was recovered through digestion with the endonucleases HF-*Hin*dIII and HF-*Eco*RI. The vector pEF-FS-eGFP-dpuro was also digested with the endonucleases HF-*Hin*dIII and HF-*Eco*RI to remove the eGFP marker gene and the old *FRT* sites FRT_3 and FRT_{wt} to obtain a backbone (4253 bp) for the new tagging vector which still contains the Δ*puro* selection trap. Thus the pEF-FS-dpuro backbone was ligated with the FRT_{13}-tdTomato_SV40pA-FRT_{14} fragment to obtain the final tagging vector pEF-FS-tdTomato-dpuro (Figure 4-4). All plasmids used in this work are described in Table 3-9.

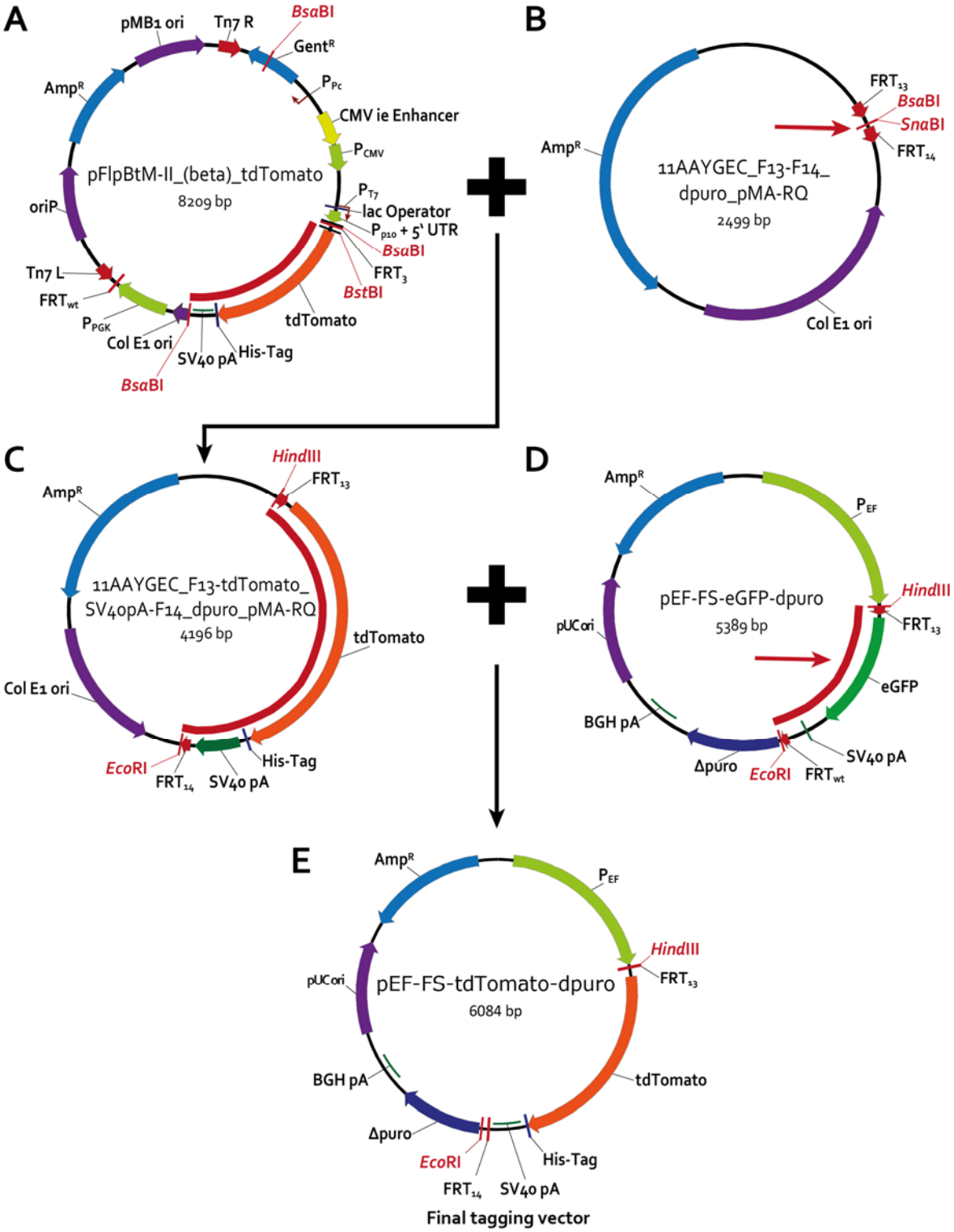

Figure 4-4: Cloning of tagging vector pEF-FS-tdTomato-dpuro. (A) The "tdTomato_SV40pA" fragment (red line) was retrieved from vector pFlpBtM-II(beta)_tdTomato with *Bst*BI and *Bsa*BI endonucleases. **(B)** The "tdTomato_SV40pA" fragment was then ligated into the 11AAYGEC_F13-F14_dpuro_pMA-RQ vector backbone (cut with *Bst*BI and *Sna*BI) between the FRT_{13} and FRT_{14} sites (red arrow) thus destroying the *Sna*BI site. **(C)** From the resulting intermediate vector 11AAYGEC_F13-tdTomato_SV40pA-F14_dpuro-pMA-RQ the "FRT_{13}-tdTomato_SV40pA-FRT_{14}" fragment (red line) was recovered (with HF-*Hin*dIII and HF-*Eco*RI). **(D)** The "FRT_{13}-tdTomato_SV40pA-FRT_{14}" fragment was used to replace the "FRT_3-eGFP-FRT_{wt}" cassette (red line) in the vector pEF-FS-eGFP-dpuro. **(E)** New tagging vector pEF-FS-tdTomato-dpuro.

4.1.4 Generation of binary RMCE master cell lines

The tagging vector pEF-FS-tdTomato-dpuro (Section 4.1.3) was used for genomic integration of a second exchange cassette (P_{EF}-FRT_{13}-*tdTomato*-FRT_{14}-Δ*puro*) into the RMCE master cell lines SWI3_26 and SMT_dneo(2)_24 already comprising the first exchange cassette (P_{EF}-FRT_3-*eGFP*-FRT_{wt}-Δ*neo*). These two cell lines differ in their level of eGFP fluorescence as shown in Figure 4-5. SMT_dneo(2)_2 shows a higher level of fluorescence for eGFP indicating that the P_{EF}-FRT_3-*eGFP*-FRT_{wt}-Δ*neo* exchange cassette was integrated at a locus with better expression capabilities. The tagged cell lines were subjected to 1 or 2 rounds of FACS followed by clonal isolation as required to isolate binary RMCE master cell lines.

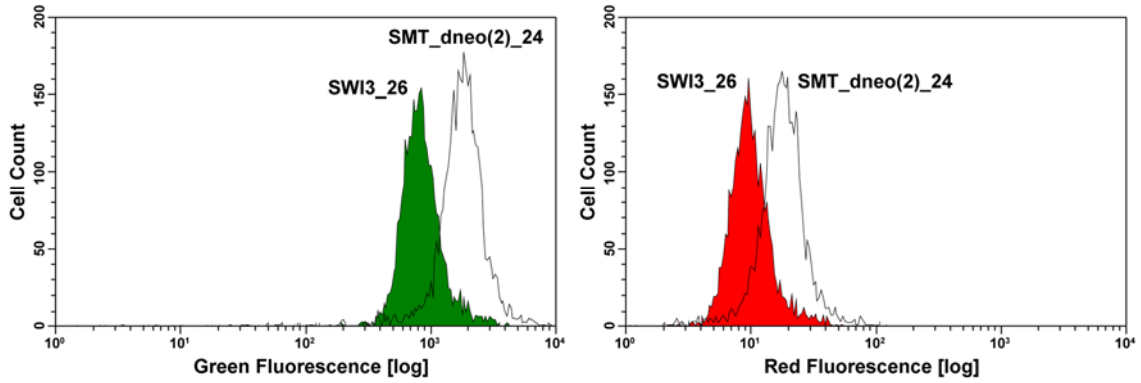

Figure 4-5: Flowcytometric analysis of RMCE master cell lines SWI3_26 and SMT_dneo(2)_24 before genomic tagging with pEF-FS-tdTomato_dpuro. Histogram overlays obtained with the Guava easyCyte flowcytometer show the level of green fluorescence (left) and the level of red fluorescence (right) for the RMCE master cell lines SWI3_26 (solid green or red) and SMT_dneo(2)_24 (black line) containing an eGFP exchange cassette. **(Left)** As shown SMT_dneo(2)_24 demonstrates a higher level in eGFP fluorescence than SWI3_26. **(Right)** Furthermore it can be noted that the higher level of eGFP fluorescence also causes a shift within the red channel even though neither of both cell lines exhibits red fluorescence.

Terminology of the cell lines changed after sorting of the tagged cells and was further distinguished after clonal isolation. The first part of the name refers to a transfection experiment (TE) with a specific cell line designated with the number 1 for SWI3_26 derived cell lines and number 3 for SMT_dneo(2) derived cell lines during which the cells were genomically tagged. The second part of the name refers to the batch (B) of this transfection experiment that was done and send for the first round of FACS. Thus the SWI3_26 derived binary RMCE cell lines were named TE1-B1 (transfection experiment 1 batch 1) after the first round of FACS followed by a suffix after clonal isolation TE1-B1-[Clone ID]. The SMT_dneo(2)_24 derived binary RMCE cell lines were named TE3-B4 (transfection experiment 3 batch 4) after the first round of FACS followed by a suffix referring to the

method of sorting in the second round of FACS (high or low tdTomato fluorescence) and a clonal number TE3-B4-[Clone ID].

As seen in Figure 4-6 one round of FACS alone was not sufficient to isolate uniform tdTomato positive clones for neither TE1-B1 nor TE3-B4. Clonal isolation of TE1-B1 cells was done manually using limiting dilution according to Section 3.6.9 resulting in the isolation of 18 uniform tdTomato positive clones. Stable integration of the tdTomato exchange cassette was verified for four TE1-B1 clones by tracking their flowcytometry profiles over 11 weeks with the Guava easyCyte. Figure 4-7 shows flowcytometric data obtained for the binary RMCE master cell line TE1-B1-C2. In contrast, TE3-B4 cells were subjected to a second round of FACS which sorted the cells for "high" and "low" fluorescent tdTomato positive cells which resulted in the "high" tdTomato fluorescent clone TE3-B4-H1 as well as the "low" tdTomato fluorescent clones TE3-B4-L1.1 and TE3-B4-L1.2 which were derived from the same pool (Figure 4-8). Stable genomic integration of the tdTomato exchange cassette was verified for the binary RMCE master cell lines TE3-B4-H1 and TE3-B4-L1.1 by tracking their flowcytometry profiles over 11 weeks (Figure 4-9).

The binary RMCE master cell lines TE3-B4-H1 and TE3-B4-L1.1 were further used to generate several producer cell lines as higher yields for locus 1 (P_{EF}-FRT_3-*eGFP*-FRT_{wt}-Δ*neo*) were anticipated compared to the SWI3_26 derived TE1-B1 clones (Figure 4-5).

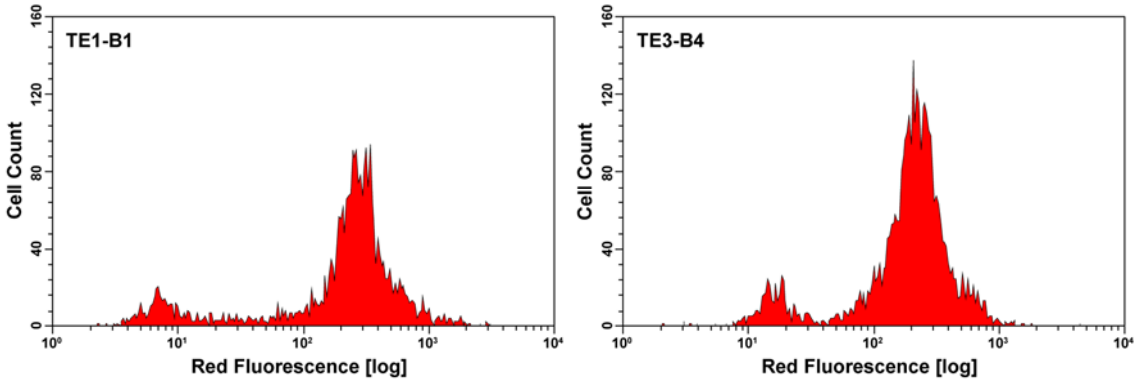

Figure 4-6: Flowcytometric analysis after 1st round of FACS for tdTomato positive clones following genomic tagging of RMCE master cell lines SWI3_26 and SMT_dneo(2)_24 with pEF-FS-tdTomato_dpuro. Histograms obtained with the Guava easyCyte flowcytometer show the level and divergence of red fluorescence for TE1-B1 cells derived from the tdTomato tagged RMCE master cell line SWI3_26 (left) and for TE3-B4 cells derived from the tdTomato tagged RMCE master cell line SMT_dneo(2)_24 (right) after one round of FACS for tdTomato positive cells 3 and 5 weeks after sorting respectively.

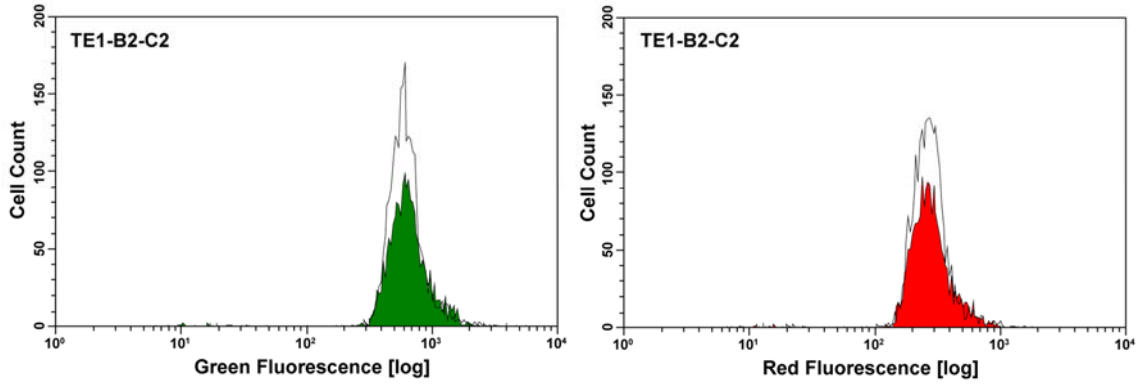

Figure 4-7: Long term stability test in the binary RMCE master cell line TE1-B1-C2. Histogram overlays obtained with the Guava easyCyte flowcytometer show the level of green fluorescence (left) and the level of red fluorescence (right) of the binary RMCE cell line TE1-B1-C2 after clonal isolation (solid red or green) and its consistency after 11 weeks in suspension culture (black line).

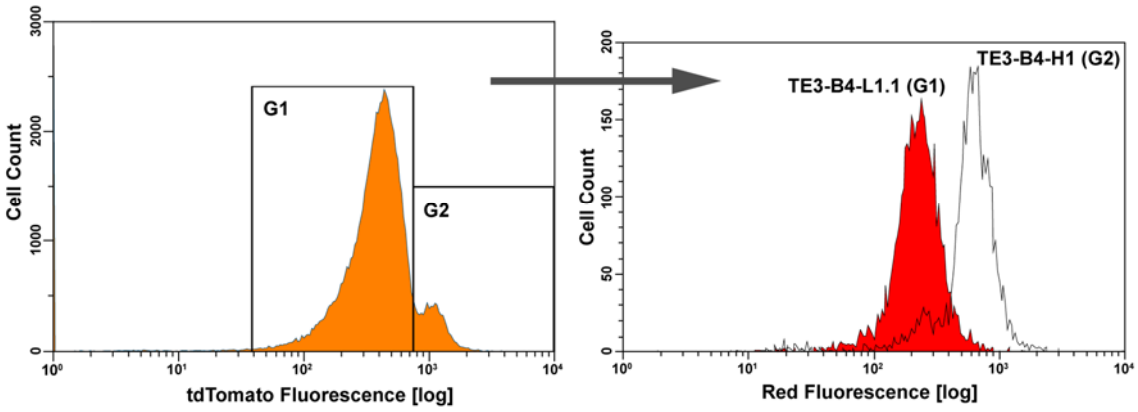

Figure 4-8: Isolation of high and low fluorescent TE3-B4 clones via FACS. (Left) Clone TE3-B4 before second round of FACS (shown are only tdTomato positive cells). **(Right)** Histogram overlay of isolated binary RMCE master cell lines TE3-B4-L1.1 (solid red) and TE3-B4-H1 (black line) showing the distinct level in red fluorescence.

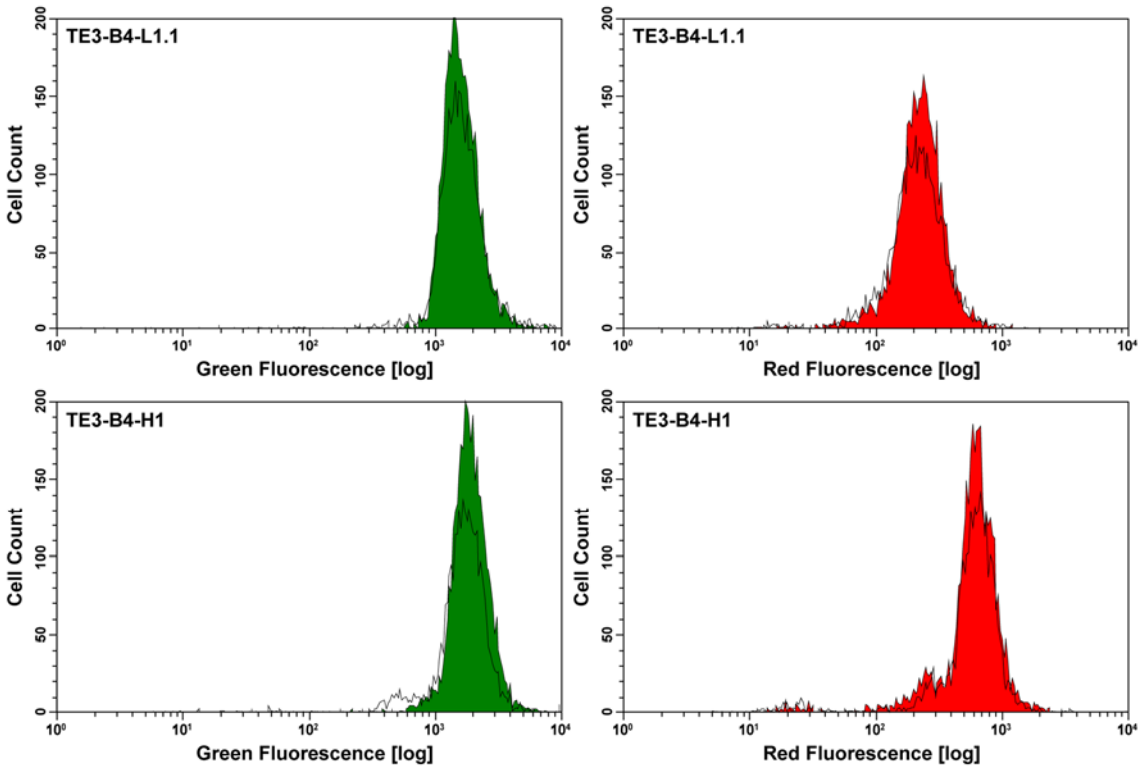

Figure 4-9: Long term stability tests in the binary RMCE master cell lines TE3-B4-H1 and TE3-B4-L1.1. Histogram overlays obtained with the Guava easyCyte flowcytometer show the level of green fluorescence (left) and the level of red fluorescence (right) of the binary RMCE cell line TE3-B4-L1.1 and TE3-B4-H1 (solid red or green) and its consistency after 11 weeks in suspension culture (black line).

4.1.5 Determination of exchange cassette integrity in binary RMCE master cell lines via genomic PCR

To confirm the full integration of the exchange cassettes P_{EF}-FRT_3-*eGFP*-FRT_{wt}-Δ*neo* and P_{EF}-FRT_{13}-*tdTomato*-FRT_{14}-Δ*puro* genomic DNA was extracted from the binary RMCE master cell lines TE3-B4-H1 and TE3-B4-L1.1 as described in Section 3.5.3. Forward oligonucleotide Cassette-pEF-S was combined with the reverse oligonucleotides Cassette-neo-AS or Cassette-puro-AS to amplify the entire exchange cassettes for both loci (Figure 4-10). PCR amplifications of the size 3130 bp for locus 1 (P_{EF}-FRT_3-*eGFP*-FRT_{wt}-Δ*neo*) and 3651 bp for locus 2 (P_{EF}-FRT_{13}-*tdTomato*-FRT_{14}-Δ*puro*) confirmed the full integration of both loci as show in Figure 4-12.

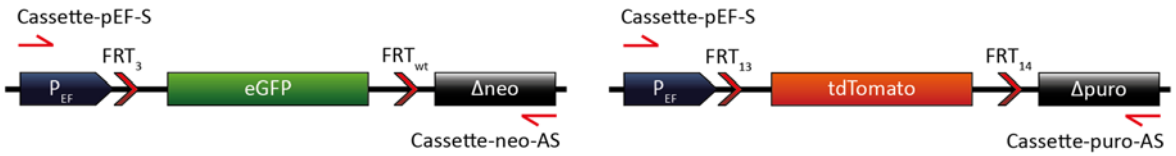

Figure 4-10: Genomic PCR amplification of both exchange loci in binary RMCE master cell lines.(Left) Genomic PCR amplification of locus 1 (P_{EF}-FRT_3-*eGFP*-FRT_{wt}-Δ*neo*) with the oligonucleotides Cassette-pEF-S and Cassette-neo-AS will result in an 3130 bp amplicon. **(Right)** Genomic PCR amplification of locus 2 (P_{EF}-FRT_{13}-*tdTomato*-FRT_{14}-Δ*puro*) with the oligonucleotides Cassette-pEF-S and Cassette-puro-AS will result in an 3651 bp amplicon.

In addition to the expected 3651 bp band during the genomic amplification of exchange locus 2 (P_{EF}-FRT_{13}-*tdTomato*-FRT_{14}-Δ*puro*) with the oligonucleotide pair Cassette-pEF-S/Cassette-puro-AS a strong 900 bp band was observed. To determine its origin the producer cell line BBA10-tdTomato-C1 (Section 4.2) which only contains locus 1 with an integrated tdTomato gene (P_{EF}-FRT_3-*tdTomato*-P_{PGK}-*ATG*-FRT_{wt}-Δ*neo*) was analysed (Figure 4-11). Even though the forward oligonucleotide Cassette-pEF-S also binds to the P_{EF} promoter of this locus the reverse oligonucleotide Cassette-puro-AS has no binding site in locus 1. While no amplification was expected for this oligonucleotide combination, the 900 bp amplicon was detected (Figure 4-12) which demonstrates that amplification is not dependent on the presence of the Δ*puro* binding site for oligonucleotide Cassette-puro-AS. The cell line TE3-B4-L1.1-tdTomato/tdTomato-C1 (Section 4.2) was used as positive control as it contains both loci with a tdTomato gene (Figure 4-11). As expected this cell line also displayed the 900 bp background band (Figure 4-12). The use of individual oligonucleotides, either Cassette-pEF-S or Cassette-puro-AS, in the binary master cell line TE3-B4-H1 demonstrated that both oligonucleotides are required for the amplification of the 900 bp band (Figure 4-12). All FRT sites as well as tdTomato do contain repetitive sequences which theoretically might result in artefacts, however none would result in the observed 900 bp amplicon. Potential binding sites of the Cassette-puro-AS oligonuclotide within the tdTomato gene which would explain the observed background band could not be detected through alignment (similarity down to 55%). Thus this strong background band at 900 bp appears to result from a chromosomal binding site not associated with either exchange locus.

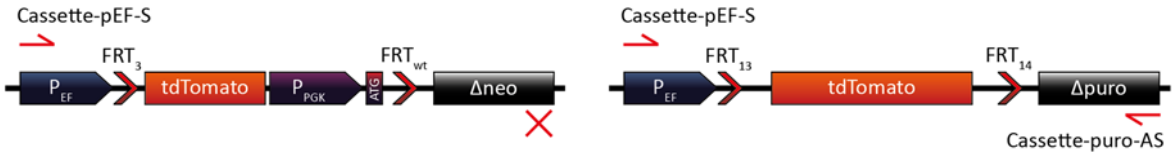

Figure 4-11: Genomic PCR amplification of producer cell lines BBA10-tdTomato-C1 and TE3-B4-L1.1-tdTomato/tdTomato-C1. (Left) Genomic PCR amplification of locus 1 (P_{EF}-FRT_3-*tdTomato*-P_{PGK}-*ATG*-FRT_{wt}-Δ*neo*) with the oligonucleotides Cassette-pEF-S and Cassette-puro-AS present in both cell lines serves only one binding site in the exchange cassette. Therefore no amplicon is expected. **(Right)** Genomic PCR amplification of locus 2 (P_{EF}-FRT_{13}-*tdTomato*-FRT_{14}-Δ*puro*), present only in cell line TE3-B4-L1.1-tdTomato/tdTomato-C1, with the oligonucleotides Cassette-pEF-S and Cassette-puro-AS will result in an 3651 bp amplicon.

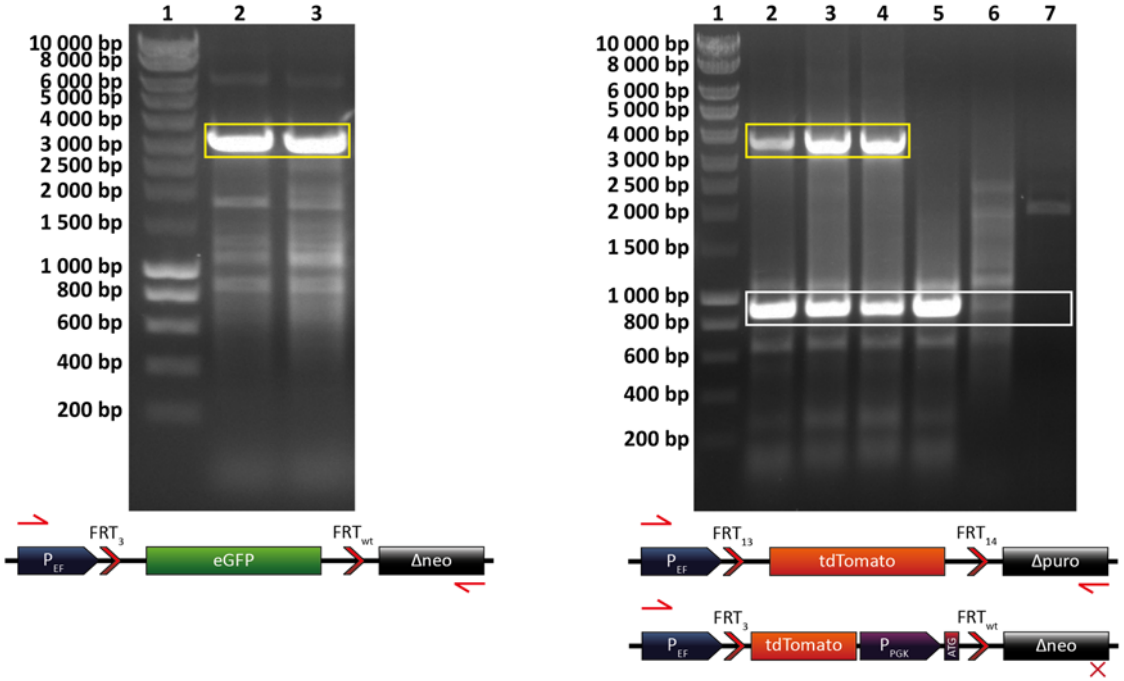

Lane	Locus 1 (P_{EF}-FRT_3-*eGFP*-FRT_{wt}-Δ*neo*)	Locus 2 (P_{EF}-FRT_{13}-*tdTomato* FRT_{14}-Δ*puro*)
1	Smart Ladder (Eurogentech)	Smart Ladder (Eurogentech)
2	TE3-B4-H1 – Locus 1, size 3130 bp	TE3-B4-H1 – Locus 2, size 3651 bp
3	TE3-B4-L1.1 – Locus 1, size 3130 bp	TE3-B4-L1.1 – Locus 2, size 3651 bp
4	-	TE3-B4-L1.1-tdTomato/tdTomato – Locus 2, size 3651 bp
5	-	BBA10-tdTomato-C1 – **No** Locus 2 → No Fragment Expected
6	-	TE3-B4-H1 – (Locus 2) – Cassette-pEF-S
7	-	TE3-B4-H1 – (Locus 2) – Cassette-puro-AS

Figure 4-12: 0.8 % analytic agarose gel showing genomic PCR amplifications of the binary RMCE master cell lines TE3-B4-H1 and TE3-B4-L1.1 and two tdTomato producer cell lines: Full integration of exchange locus 1 (P_{EF}-FRT_3-*eGFP*-FRT_{wt}-Δ*neo*) at 3130 bp (left) and exchange locus 2 (P_{EF}-FRT_{13}-*tdTomato*-FRT_{14}-Δ*puro*) at 3651 bp (right) were demonstrated for both binary RMCE master cell lines (Lane 2 and 3 - yellow box). Moreover it was shown that the oligonucleotide pair Cassette-pEF-S /Cassette-puro-AS used for the amplification of locus 2 (right) shows a strong background band at approximately 900 bp (Lanes 2-5 - white box). However, the amplification of this fragment is not dependent on the presence of the second exchange cassette as shown in lane 5 (white box) were the background band is still amplified even though this cell line (BBA10-tdTomato-C1) does not contain a second locus. The control cell line BBA10-tdTomato-C1 only contains locus 1 with an integrated tdTomato gene (P_{EF}-FRT_3-*tdTomato*-P_{PGK}-*ATG*-FRT_{wt}-Δ*neo*). Thus only the forward oligonucleotide which anneals to the P_{EF} promoter binds. The producer cell line TE3-B4-L1.1-tdTomato/tdTomato-C1 which does contain both loci, does also show the 900 bp band as expected. Furthermore, the use of individual oligonucleotides showed that both oligonucleotides are required for the amplification of the strong 900 bp background fragment (lane 6 and 7, white box, right).

4.1.6 Cloning of exchange vector pFlpBtM-II_F13-F14

To enable the integration of a GOI into the P_{EF}-FRT_{13}-*tdTomato*-FRT_{14}-Δ*puro* locus of a binary RMCE cell line the new set of *FRT* sites (FRT_{13} and FRT_{14}) needed to be introduced into the exchange vector pFlpBtM-II. To do so a fragment containing FRT_{13} and FRT_{14} sites as well as the required restriction endonuclease sites for cloning were synthesised by Life Technologies (Figure 4-13) and delivered in the vector 11AAGFC_F13-F14_pFlBtM-II_pMK-RQ.

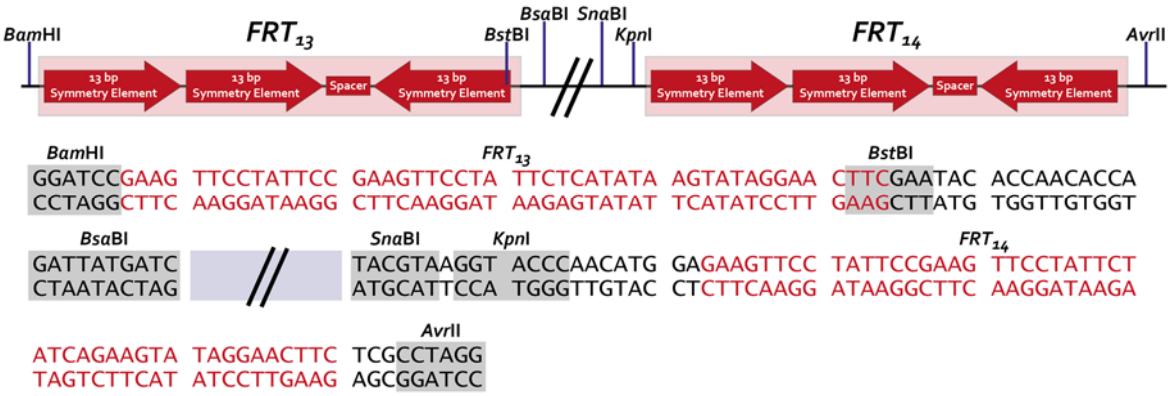

Figure 4-13: Design of synthesised FRT_{13}/FRT_{14} and restriction endonuclease sites for cloning of exchange vector pFlpBtM-II_F13-F14. The heterospecific *FRT* sites FRT_{13} and FRT_{14} (red) were synthesised separated by non-relevant vector sequences (indicated as **//**) and the required restriction endonuclease sites for molecular cloning (grey) by Life Technologies and delivered in the vector 11AAGFC_F13-F14_pFlBtM-II_pMK-RQ.

Besides the FRT_{13} and FRT_{14} sites the vector 11AAGFC_F13-F14_pFlBtM-II_pMK-RQ also comprised an insect promoter, an enhancer and a TMV leader sequence not required for this work. These non-relevant vector elements needed to be removed. To remove these elements the plasmid was first partially digested with *Bsa*BI. The linearized vector (3537 bp) was isolated from an preparative agarose gel and digested in a second step with *Sna*BI to obtain a 2429 bp backbone without the non-relevant sequences which than was religated, thus destroying the *Bsa*BI and *Sna*BI sites. The intermediate vector 11AAGFC_F13-F14_pFlpBtM-II_pMK-RQ_(no_Insect_Promoter) was than digested with the endonucleases HF-*Kpn*I and *Bst*BI to obtain a backbone (2396 bp) for the insertion of the "Shine-Dalgarno_MCS_PGK" fragment (1141 bp) extracted from pFlpBtM-II with the endonucleases *Bst*BI and *Kpn*I. This ligation results in the next intermediate vector 11AAYGFC_F13-MCS_PGK-F14_pFlpBtM-II_pMK-RQ containing the "Shine-Dalgarno_MCS_PGK" fragment of the pFlpBtM-II vector flanked with the new set of heterospecific *FRT* sites. This fragment "FRT_{13}-Shine-Dalgarno_MCS_PGK-FRT_{14}" (1255 bp) was than retrieved with the endonucleases HF-*Bam*HI and *Avr*II and cloned into a pFlpBtM-II vector backbone (5592 bp) which was obtained through the digestion with HF-*Bam*HI and *Avr*II restriction endonucleases, resulting in the new vector pFlpBtM-II_F13/F14 (Figure 4-14).

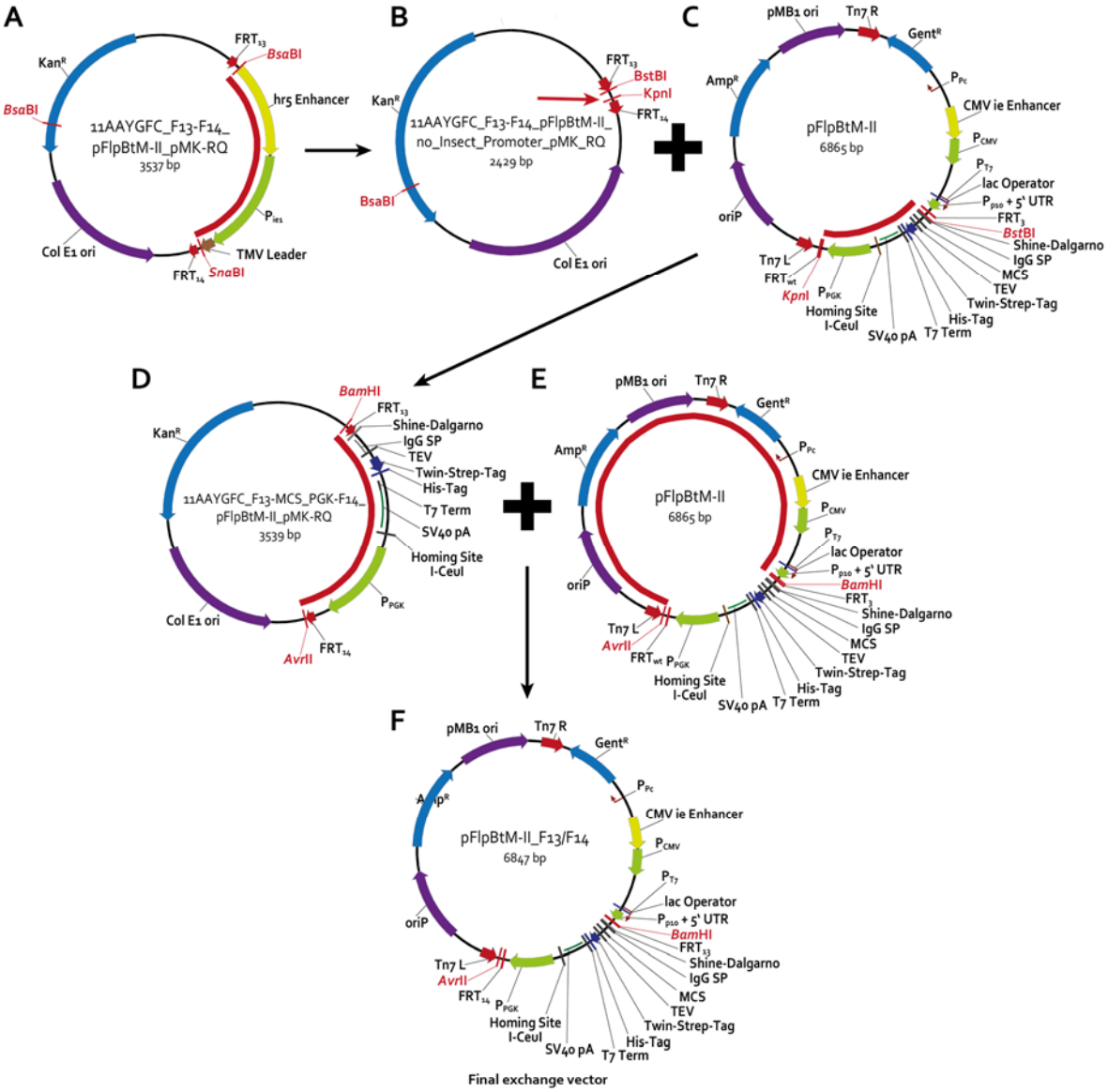

Figure 4-14: Cloning of exchange vector pFlpBtM-II_F13/F14. (A) Non-relevant vector sequences (red line) were removed stepwise from the synthesised vector 11AAGFC_F13-F14_pFlBtM-II_pMK-RQ using *Bsa*BI and *Sna*BI endonucleases. **(B)** The backbone was religated thus destroying the *Bsa*BI and *Sna*BI sites before digestion with *Bst*BI and HF-*Kpn*I to obtain a vector backbone. **(C)** The "Shine-Dalgarno_MCS_PGK" fragment (red line) was retrieved from pFlpBtM-II with *Bst*BI and HF-*Kpn*I. **(D)** The fragment "Shine-Dalgarno_MCS_PGK" was inserted into the 11AAGFC_F13-F14_pFlpBtM-II_pMK-RQ_(no_Insect_Promoter) backbone to subsequently retrieve the fragment "FRT_{13}-Shine-Dalgarno_MCS_PGK-FRT_{14}" (red line). **(E)** A pFlpBtM-II vector backbone (red line) obtained with HF-*Bam*HI and *Avr*II **(F)** was ligated with the "FRT_{13}-Shine-Dalgarno_MCS_PGK-FRT_{14}" fragment to obtain the new exchange vector pFlpBtM-II_F13/F14.

4.2 Evaluation of (binary) RMCE master and producer cell lines expressing tdTomato

As described in Section 4.1 the RMCE master cell lines SWI3_36 and SMT_dneo(2)_24 comprise one exchange locus (P_{EF}-FRT_3-*eGFP*-FRT_{wt}-Δ*neo*) at different chromosomal locations. The binary RMCE master cell lines TE3-B4-H1 and TE3-B4-L1.1, that were derived from SMT_dneo(2)_24, additionally comprise a second exchange locus (P_{EF}-FRT_{13}-*tdTomato*-FRT_{14}-Δ*puro*). The first exchange locus (P_{EF}-FRT_3-*eGFP*-FRT_{wt}-Δ*neo*) of the binary RMCE cell lines is located at the same chromosomal position for both; whereas the second exchange locus (P_{EF}-FRT_{13}-*tdTomato*-FRT_{14}-Δ*puro*) is located at different chromosomal positions. To evaluate position and gene dose effects for these cell lines, tdTomato was integrated into the cell lines SWI3_26 and SMT_dneo(2)_24 using RMCE thus replacing eGFP in locus 1. Likewise tdTomato was integrated into the first locus of the binary RMCE cell lines TE3-B4-H1 and TE3-B4-L1.1, which than expressed tdTomato in both exchange loci (Section 4.2.4). Figure 4-15 gives an overview of the analysed cell lines and their heritage.

Genomic PCR (Section 4.2.1) and flowcytometry (Section 4.2.4) were used to demonstrate the successful exchange of genomic loci. The binary master cell lines TE3-B4-H1 and TE3-B4-L1.1 described in Section 4.1.4 as well as the producer cell lines BBA10-tdTomato-C1 and TE3-B4-L1.1-tdTomato/tdTomato-C1 described in Section 4.2.4 were analysed as follows: Fluorescence based methods including flowcytometry (Section 4.2.4) and the quantification with a fluorescent plate reader (Section 4.2.2) were used to visualize and quantify the expression level of tdTomato and thus complement and support results obtained from protein purification (Section 4.2.3). The producer cell lines TE3-B4-H1-tdTomato/tdTomato-C1 and SMT_dneo(2)_24-tdTomato-C1 that were generated at a later timepoint were analysed using flowcytometry alone (Section 4.2.4).

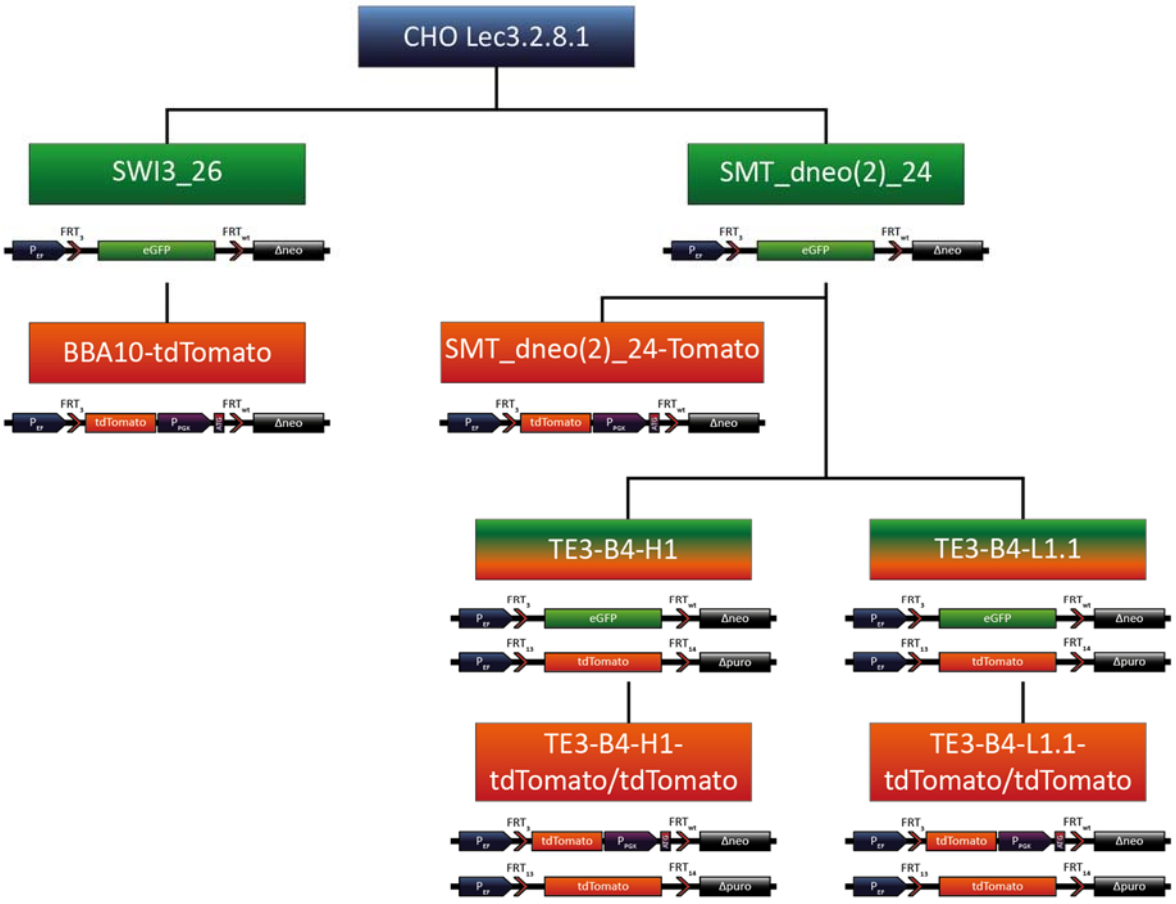

Figure 4-15: Overview of tdTomato expressing RMCE master and producer cell lines and their heritage. CHO Lec3.2.8.1 cells were genomically tagged with exchange locus 1 (P_{EF}-FRT_3-*eGFP*-FRT_{wt}-Δ*neo*) from which the master cell lines SWI3_26 (Wilke *et al.*, 2011) and later on a higher fluorescent version SMT_dneo(2)_24 were derived. The producer cell line BBA10-tdTomato-C1 was derived from master cell line SWI3_26 through exchange of eGFP against tdTomato. Likewise the producer cell line SMT_dneo(2)_24-tdTomato was derived from the master cell line SMT_dneo(2)_24.The master cell line SMT_dneo(2)_24 was used for the integration of a second exchange locus (P_{EF}-FRT_{13}-*tdTomato*-FRT_{14}-Δ*puro*) to create the binary RMCE master cell lines TE3-B4-H1 (higher level of fluorescence for locus 2) and TE3-B4-L1.1 (lower level of fluorescence for locus 2) which therefore expressed tdTomato in their second exchange locus. The binary producer cell lines TE3-B4-H1-tdTomato/tdTomato-C1 and TE3-B4-L1.1-tdTomato/tdTomato-C1 were derived from the binary master cell line TE3-B4-H1 and TE3-B4-L1.1 respectively through exchange of eGFP against tdTomato in locus 1 thus expressing tdTomato in two loci.

4.2.1 Genomic PCR of tdTomato expressing RMCE master and producer cell lines

The tdTomato expressing RMCE master and producer cell lines were analysed using genomic PCR to address several questions. Firstly, as already described in Section 4.1.5, genomic PCR was used to determine full integration of the exchange cassettes P_{EF}-FRT_3-*eGFP*-FRT_{wt}-Δ*neo* and P_{EF}-FRT_{13}-*tdTomato*-FRT_{14}-Δ*puro* in the binary RMCE master cell lines TE3-B4-H1 and TE3-B4-L1.1.

Secondly, genomic PCR was used to control the successful exchange of eGFP against tdTomato for the producer cell lines TE3-B4-L1.1-tdTomato/tdTomato-C1 and

BBA10-tdTomato-C1. The eGFP and/or tdTomato inserts in both loci were amplified using the forward oligonucleotide Insert-pEF-S with the reverse oligonucleotide Insert-dneo-AS or Insert-dpuro-AS (Figure 4-16). The amplified sequences showed the presence of either eGFP (1334 bp band), tdTomato (1896 bp band) or tdTomato with a downstream PGK promoter (2795 bp band), if eGFP was replaced against tdTomato using RMCE, in a given locus. The successful exchange of eGFP against tdTomato in exchange locus 1 of the tested producer cell lines TE3-B4-L1.1-tdTomato/tdTomato-C1 and BBA10-tdTomato-C1 was demonstrated as seen in Figure 4-17. Both producer cell lines amplified the 2795 bp band specific for the integrated tdTomato gene with a downstream PGK promoter. As expected the binary master cell lines, which served as a control, amplified the 2795 bp band for eGFP in exchange locus 1 and the 1334 bp band for tdTomato (without downstream PGK promoter) in exchange locus 2. Moreover it was shown that no detectable cross-interaction between the two exchange loci occurred as this would have resulted in the larger 1896 bp tdTomato band in both loci of the binary tdTomato producer cell line TE3-B4-L1.1-tdTomato/tdTomato-C1.

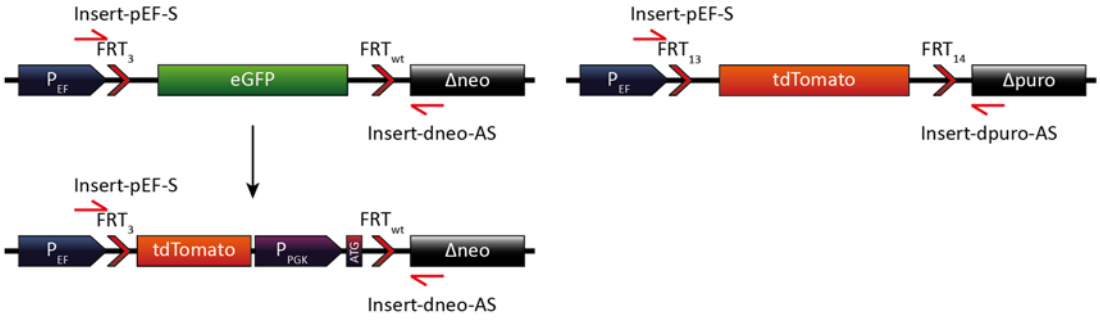

Figure 4-16: Genomic PCR amplification of tdTomato producing master and producer cell lines. (Left) Genomic PCR amplification of locus 1 before and after exchange of eGFP against tdTomato via RMCE. Amplification of the eGFP containing locus 1 (*P_{EF}-FRT_3-eGFP-FRT_{wt}-Δneo*) with the oligonucleotide pair Insert-pEF-S/Insert-dneo-AS will result in an 1334 bp amplicon for all master cell lines. The same locus after integration of tdTomato (*P_{EF}-FRT_3-tdTomato-P_{PGK}-ATG-FRT_{wt}-Δneo*) will yield an 2795 bp amplicon for producer cell lines TE3-B4-L1.1-tdTomato/tdTomato-C1 and BBA10-tdTomato-C1. **(Right)** Genomic PCR amplification of locus 2 (*P_{EF}-FRT_{13}-tdTomato-FRT_{14}-Δpuro*) with the oligonucleotide pair Insert-pEF-S/Insert-dpuro-AS will result in an 1896 bp amplicon.

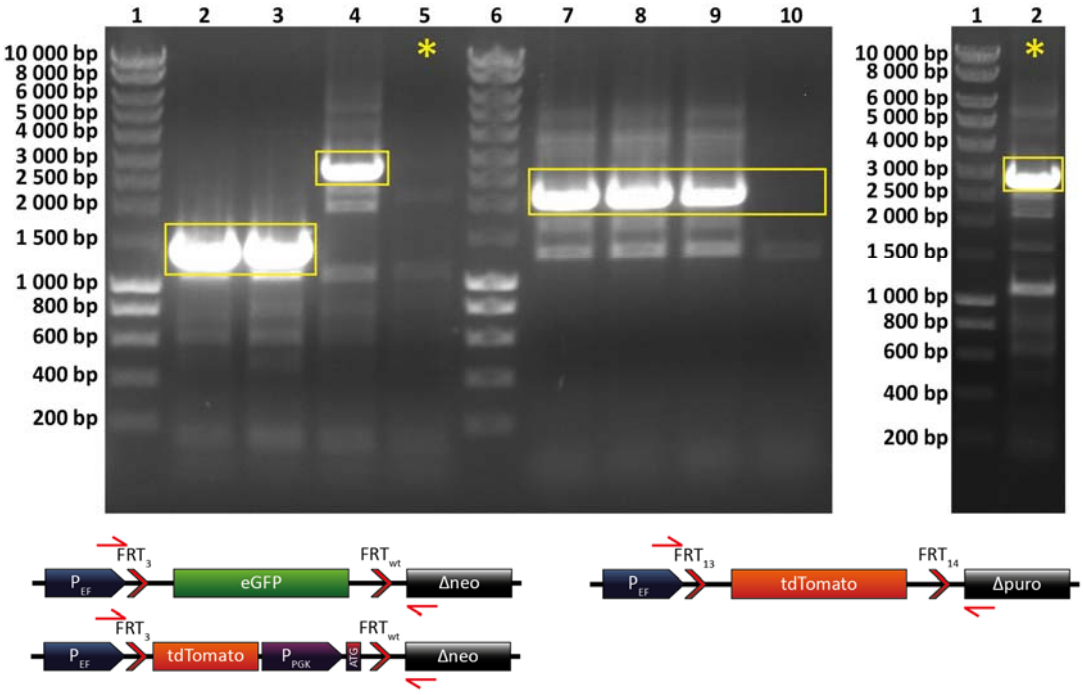

Lane	Left agarose gel	Right agarose gel
1	Smart Ladder (Eurogentech)	Smart Ladder (Eurogentech)
2	TE3-B4-H1 – Locus 1, size 1334 bp (eGFP)	*BBA10-tdTomato-C1 – Locus 1, size 2795 bp (tdTomato + PGK promoter)
3	TE3-B4-L1.1 – Locus 1, size 1334 bp (eGFP)	
4	TE3-B4-L1.1-tdTomato/tdTomato-C1 – Locus 1, size 2795 bp (tdTomato + PGK promoter)	
5	*BBA10-tdTomato-C1 – Locus 1, size 2795 bp (Did not Amplified → see gel on the right)	
6	Smart Ladder (Eurogentech)	
7	TE3-B4-H1 – Locus 2, size 1896 bp (tdTomato)	
8	TE3-B4-L1.1 – Locus 2, size 1896 bp (tdTomato)	
9	TE3-B4-L1.1-tdTomato/tdTomato-C1 – Locus 2, size 1896 bp (tdTomato)	
10	BBA10-tdTomato-C1 – No Locus 2 → No Fragment Expected	

Figure 4-17: 0.8 % analytic agarose gel showing genomic PCR amplifications of the binary RMCE master cell lines TE3-B4-H1 and TE3-B4-L1.1 as well as producer cell lines TE3-B4-L1.1-tdTomato/tdTomato-C1 and BBA10-tdTomato-C1: The genomic amplification of either eGFP or tdTomato in locus 1 or locus 2 demonstrated the successful exchange of eGFP against tdTomato in the cell lines TE3-B4-L1.1-tdTomato/tdTomato-C1 and BBA10-tdTomato-C1. The amplification marked with a wildcard (*,left gel) did not work and was repeated (*,right gel).

4.2.2 Quantification of tdTomato expressing RMCE master and producer cell lines by fluorescence with the Tecan MD 1000 plate reader

To quantify the expression of tdTomato and determine eventual batch to batch variations that might occur; the tdTomato expressing cell lines TE3-B4-H1, TE3-B4-L1.1,

TE3-B4-L1.1-tdTomato/tdTomato-C1 and BBA10-tdTomato-C1 were cultured in triplicates using parallel batch cultures. To evaluate the kinetics of tdTomato expression at different timepoints, a specific cell number ($3x10^6$ cells) was withdrawn from the cultures 24 h (timepoint 1), 48 h (timepoint 2) and 72 h (timepoint 3) after expansion. Cell extracts were analysed with the Tecan MD 1000 plate reader as described in Section 3.8.4. The acquired values were compared with a tdTomato calibration curve (Figure A.2-1 in appendix) and subjected to statistical analysis. Figure 4-18 shows the average tdTomato protein concentrations obtained for cell extracts measured with the Tecan MD 1000 plate reader for each cell line including the standard deviation (SD). As expected the binary cell line TE3-B4-L1.1-tdTomato-tdTomato shows the highest level of tdTomato expression. The cell lines TE3-B4-H1, TE3-B4-L1.1 and BBA10-tdTomato, which express tdTomato in only one but different chromosomal locus for each cell line, show lower expression yields. While the cell line TE3-B4-L1.1 clearly shows the lowest level of tdTomato expression the cell lines TE3-B4-H1 and BBA10-tdTomato-C1 exhibit a similar level of expression which becomes clear when comparing the standard deviations. In conclusion chromosomal position of each locus exhibits specific, reproducible expression properties for each cell line.

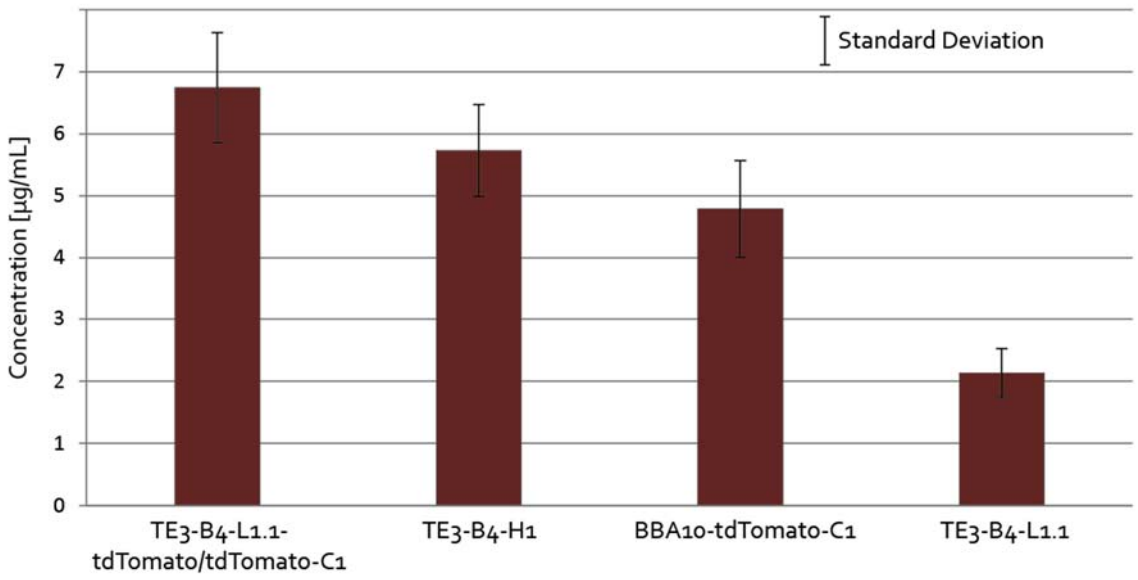

Figure 4-18: Protein concentrations obtained for cell extracts of tdTomato expressing cell lines with the Tecan MD 1000 fluorescent plate reader. Average protein concentrations of cell extracts obtained from triplicate batch cultures at 3 timepoints (24 h, 48 h and 72 h post-expansion) for different tdTomato expressing cell lines are shown. Error bars for the standard deviation are included (black bars). Data demonstrates that cell lines containing tdTomato in one exchange locus exhibit different level of expression depending on their chromosomal position (TE3-B4-H1, TE3-B4-L1.1 and BBA10-tdTomato). The binary producer cell line TE3-B4-L1.1-tdTomato/tdTomato-C1 which contains tdTomato in both exchange loci, as expected, shows the highest level of expression.

To determine if a difference in tdTomato expression can be observed between batches or harvesting timepoints, the obtained yields (Table A.2-2 in the appendix) were subjected to an analysis of variance (ANOVA) according to Section 3.9.2. ANOVA is a statistical method which enables the comparison between sample means and determine if they belong into the same overall group. ANOVA showed that the values obtained for parallel batch cultures and different harvesting timepoints belong to the same group (Table A.2-3 in appendix). This means, that there is no significant difference in expression between batches nor harvesting time points. Thus the reproducibility of tdTomato expression was demonstrated between triplicate batch cultures as well as their independence of the harvesting timepoint (for a determined cell number). This confirms the robust and reproducible expression properties of the tested stable cell lines. Moreover, these properties were not influenced by their growth phase.

To determine if the analysis of cell extracts obtained from a small number of cells ($3x10^6$ cells) will result in equivalent tdTomato yields as the analysis of purified tdTomato obtained from a larger number of cells ($2x10^8$ cells) both were compared. Purified tdTomato obtained from triplicate batch cultures of the same cell lines (Section 4.2.3), was analysed with the Tecan MD 1000 plate reader. The tdTomato calibration curve is available in the appendix (Figure A.2-2). Figure 4-19 compares the average yields (calculated for $1x10^9$ cells) of tdTomato obtained from cell extracts and purified tdTomato for each cell line including the SD for triplicate batch cultures. This confirms that the data obtained with the Tecan MD 1000 is consistent independent of the harvested cell number and therefore tdTomato concentration in the analysed sample as well as sample preparation (cell extract vs. purified protein). Particularly the similar expression level of the cell lines TE3-B4-H1 and BBA10-tdTomato-C1, as discussed above, are visualized in Figure 4-19. The specific expression properties for each cell line described in this section as well as other tdTomato expressing cell lines are also described in Section 4.2.4.

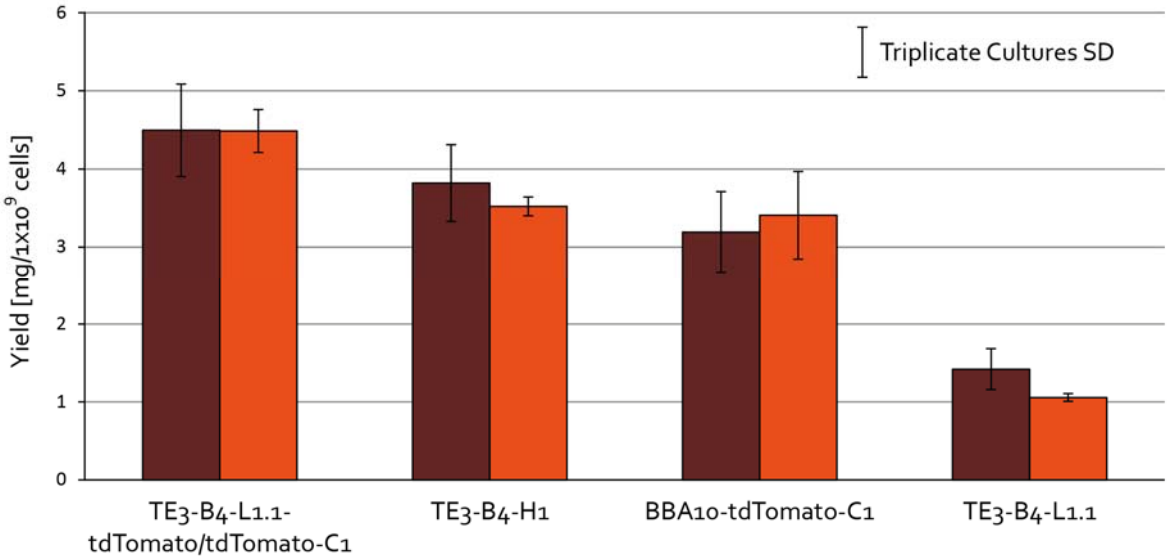

Figure 4-19: Comparison of protein yields obtained with the Tecan MD 1000 fluorescent plate reader for cell extracts of tdTomato expressing cell lines and purified tdTomato. Comparison of average protein yields for $1x10^9$ cells for triplicate batches of tdTomato expressing cell lines. Protein yields for tdTomato expression were either obtained through the measurement of cell extracts or purified tdTomato using the Tecan MD 1000 fluorescent plate reader. Error bars for the standard deviation between triplicate batch cultures (black bars) are included.

4.2.3 Quantification and comparison of tdTomato expressing RMCE master and producer cell lines after affinity chromatography

To quantify tdTomato expression the cell lines TE3-B4-H1, TE3-B4-L1.1, TE3-B4-L1.1-tdTomato/tdTomato-C1 and BBA10-tdTomato-C1 were cultivated in triplicate batch cultures. Cell extracts obtained from $2x10^8$ cells were purified using affinity chromatography (Ni-NTA). The spectrophotometrically obtained tdTomato yields for triplicate batch cultures are listed in Table 4-1. However, some unspecific background proteins co-purified with each sample raised the actual protein concentration un-proportionally for cell lines with lower expression of tdTomato as described in Section 4.2.5. The observed fragmentation of tdTomato caused by intramolecular nicking of tdTomato during SDS-PAGE (Figure 4-20) was previously described by Meyer, (2012). Full length tdTomato at 55 kDa as well as truncated fragments of tdTomato below 50 kDa and 37 kDa could be observed and identified as tdTomato fragments by MALDI-TOF. Native-PAGE (Figure 4-21) shows tdTomato in its mostly non-truncated state just one lower band was detected. Compared to SDS-PAGE, Native-PAGE demonstrates a better visualization of expression strength for each cell line due to the lack of fragmentation. Thus the cell lines TE3-B4-L1.1-tdTomato/tdTomato-C1 and TE3-B4-L1.1, which express the highest and lowest level of tdTomato, can be clearly differentiated from the remaining two cell lines. A detailed discussion and comparison of all cell lines is available in Section 4.2.5.

Table 4-1: Total yield from 2x10^8 cells of tdTomato expressing cell lines.

Cell Line Yield	Culture 1 [mg]	Culture 2 [mg]	Culture 3 [mg]	Mean [mg]
TE3-B4-H1	0.7	0.8	0.7	0.7 ± 0.1
TE3-B4-L1.1	0.5	0.5	0.4	0.5 ± 0.1
TE3-B4-L1.1-tdTomato/tdTomato-C1	1.1	0.9	0.9	1.0 ± 0.1
BBA10-tdTomato-C1	0.8	1.1	1.0	1.0 ± 0.1

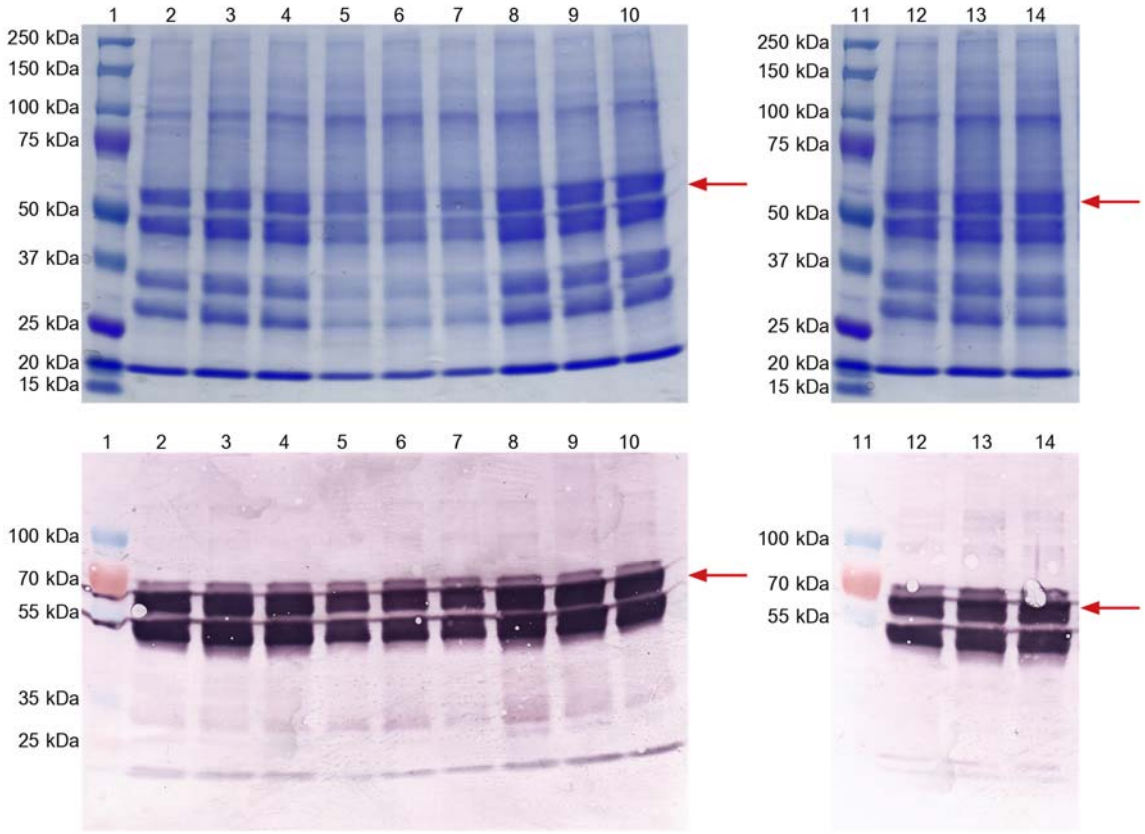

Lane	tdTomato (55.0 kDa)
1	Precision Plus Protein Dual Color (Bio-Rad) for SDS-PAGE or Page Ruler (Thermo Scientific) for Western
2	TE3-B4-H1 – Batch 1
3	TE3-B4-H1 – Batch 2
4	TE3-B4-H1 – Batch 3
5	TE3-B4-L1.1 – Batch 1
6	TE3-B4-L1.1 – Batch 2
7	TE3-B4-L1. 1 – Batch 3
8	TE3-B4-L1.1-tdTomato/tdTomato-C1 – Batch 1
9	TE3-B4-L1.1-tdTomato/tdTomato-C1 – Batch 2
10	TE3-B4-L1.1-tdTomato/tdTomato-C1 – Batch 3
11	Precision Plus Protein Dual Color (Bio-Rad) for SDS-PAGE or Page Ruler (Thermo Scientific) for Western
12	BBA10-tdTomato-C1 – Batch 1
13	BBA10-tdTomato-C1 – Batch 2
14	BBA10-tdTomato-C1 – Batch 3

Figure 4-20: 10 % SDS-PAGE and Western blot analysis of purified tdTomato. The tdTomato expressing cell lines TE3-B4-H1, TE3-B4-L1.1, TE3-B4-L1.1-tdTomato/tdTomato-C1 and BBA10-tdTomato-C1 were cultivated in triplicate batch cultures. Cell extracts obtained from 2x10^8 cells were used to purify tdTomato using Ni-NTA. SDS-PAGE and Western blot show tdTomato at 55 kDa and its truncated forms.

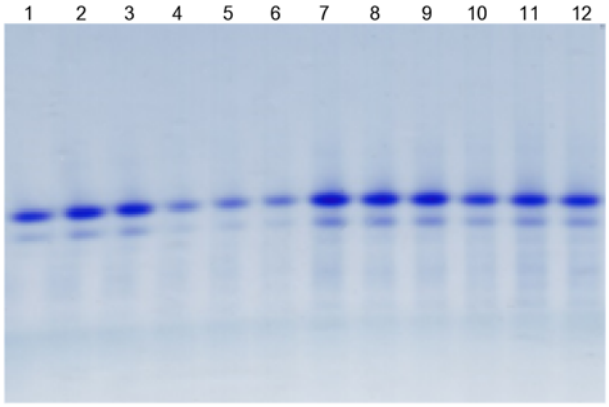

Lane	tdTomato (55.0 kDa)
1	TE3-B4-H1 – Batch 1
2	TE3-B4-H1 – Batch 2
3	TE3-B4-H1 – Batch 3
4	TE3-B4-L1.1 – Batch 1
5	TE3-B4-L1.1 – Batch 2
6	TE3-B4-L1. 1 – Batch 3
7	TE3-B4-L1.1-tdTomato/tdTomato-C1 – Batch 1
8	TE3-B4-L1.1-tdTomato/tdTomato-C1 – Batch 2
9	TE3-B4-L1.1-tdTomato/tdTomato-C1 – Batch 3
10	BBA10-tdTomato-C1 – Batch 1
11	BBA10-tdTomato-C1 – Batch 2
12	BBA10-tdTomato-C1 – Batch 3

Figure 4-21: 4 % - 16 % Native-PAGE of purified tdTomato. Native page shows purified tdTomato from Figure 4-20 in its mostly non-truncated form just one lower band was detected.

4.2.4 Flowcytometric analysis of tdTomato expressing RMCE master and producer cell lines

Flowcytometry was used to define the different level of tdTomato expression for the binary master cell lines TE3-B4-H1 and TE3-B4-L1.1 (Section 4.1.4) as well as the producer cell lines BBA10-tdTomato-C1, SMT_dneo2(24)-tdTomato-C1 and the binary producer cell lines TE3-B4-H1-tdTomato/tdTomato-C1 and TE3-B4-L1.1-tdTomato/tdTomato-C1 described below.

To generate binary producer cell lines expressing tdTomato in two chromosomal loci the binary master cell lines TE3-B4-H1 and TE3-B4-L1.1 were used. These binary master cell lines already express tdTomato in exchange locus 2 (P_{EF}-FRT_{13}-*tdTomato*-FRT_{14}-Δ*puro*). They were used to create the binary producer cell lines TE3-B4-H1-tdTomato/tdTomato-C1 (Johannes Spehr, HZI) and TE3-B4-L1.1-tdTomato/tdTomato-C1 respectively through the exchange of eGFP in locus 1 (P_{EF}-FRT_3-*eGFP*-FRT_{wt}-Δ*neo*) against tdTomato using RMCE. Successful integration of tdTomato into locus 1 was demonstrated via flowcytometry. The

introduction of a second copy of the tdTomato gene, and the consequent increase in tdTomato expression, could be detected through the rise in fluorescence levels (Figure 4-22). Likewise tdTomato was integrated into the master cell lines SWI3_26 and SMT_dneo(2)_24 to generate the producer cell lines BBA10-tdTomato-C1 as previously described in Section 4.1.2 and SMT_dneo(2)_24-tdTomato-C1 (Johannes Spehr, HZI) respectively (Figure 4-23).

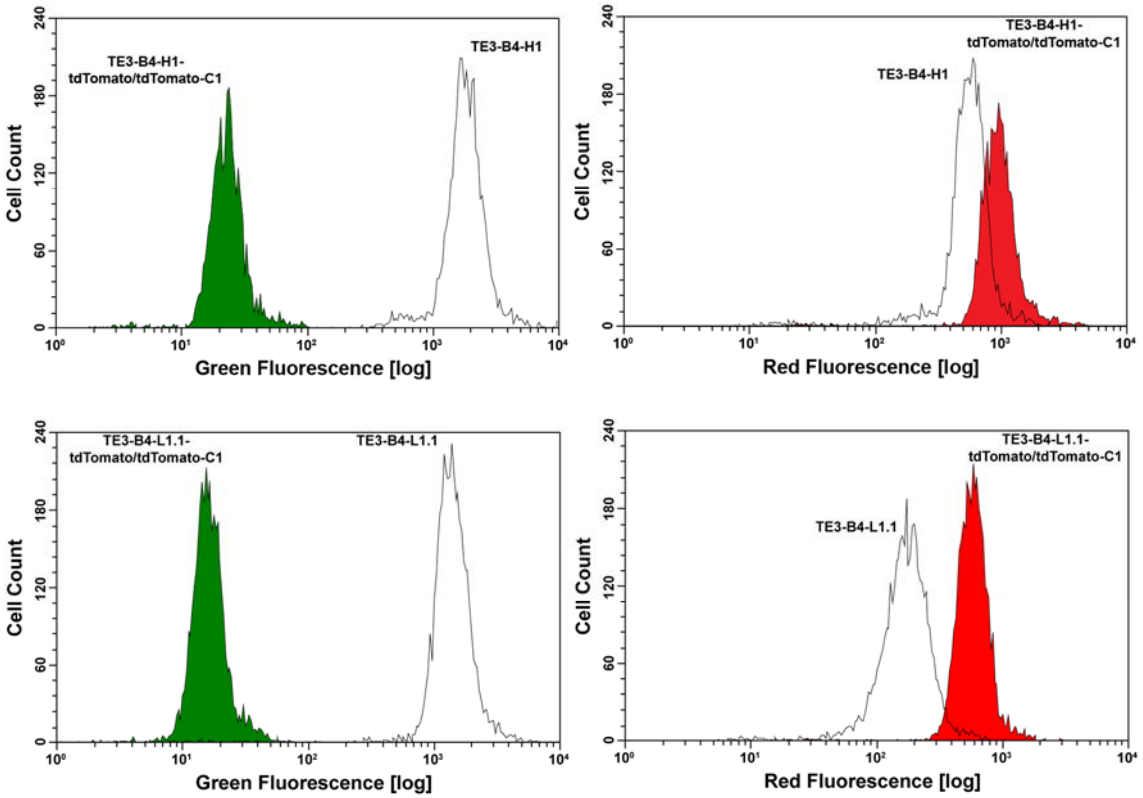

Figure 4-22: Flowcytometric analysis of binary RMCE master and producer cell lines expressing tdTomato: Histogram overlays obtained with the Guava easyCyte flowcytometer show the level of green fluorescence (left) and the level of red fluorescence (right) for binary master and producer cell line. **(Top)** Master cell line TE3-B4-H1 (black lines) and producer cell line TE3-B4-H1 tdTomato/tdTomato-C1 (solid green or red). **(Bottom)** Master cell line TE3-B4-L1.1 (black lines) and producer cell line TE3-B4-L1.1-tdTomato/tdTomato-C1 (solid green or red). Both producer cell lines were derived from their respective master cell lines through the exchange of eGFP against tdTomato in exchange locus 1 (P_{EF}-FRT_3-*eGFP*-FRT_{wt}-Δ*neo*) via RMCE. Data demonstrates the successful exchange of eGFP against tdTomato in locus 1.

The binary master cell lines TE3-B4-H1 and TE3-B4-L1.1 described in Section 4.1.4 contain only one exchange locus expressing tdTomato. Nonetheless, the integration of tdTomato at different chromosomal loci results in different expression level as shown previously (Section 4.1.4).

Histogram overlays of all tdTomato expressing cell lines are shown in Figure 4-23. This visualizes and demonstrates the different level of tdTomato expression for each cell line. Figure 4-24 shows a direct comparison of mean fluorescence for the binary producer cell

lines TE3-B4-H1-tdTomato/tdTomato-C1 and TE3-B4-L1.1-tdTomato/tdTomato-C1 that express tdTomato in both exchange loci in comparison to appropriate cell lines that express tdTomato in one of either locus alone. Numeric values are available in Table A.2-1 in the appendix. In summary this data demonstrates a cumulative effect in tdTomato expression for the binary RMCE system proportional to the expression capabilities of each locus if both exchange loci express tdTomato. Furthermore it was shown that the integration at a chromosomal location with high expression capabilities can have the same effect as the introduction of several copy numbers of a GOI. For example the binary producer cell line TE3-B4-L1.1-tdTomato/tdTomato-C1 shows similar level of tdTomato expression as the cell line TE3-B4-H1 that only expresses tdTomato in one exchange cassette. Likewise the effects of chromosomal positioning are demonstrated by the cell lines that express tdTomato in only one exchange cassette at different chromosomal loci (BBA10-tdTomato-C1, SMT_dneo(2)_24, TE3-B4-H1 and TE3-B4-L1.1).

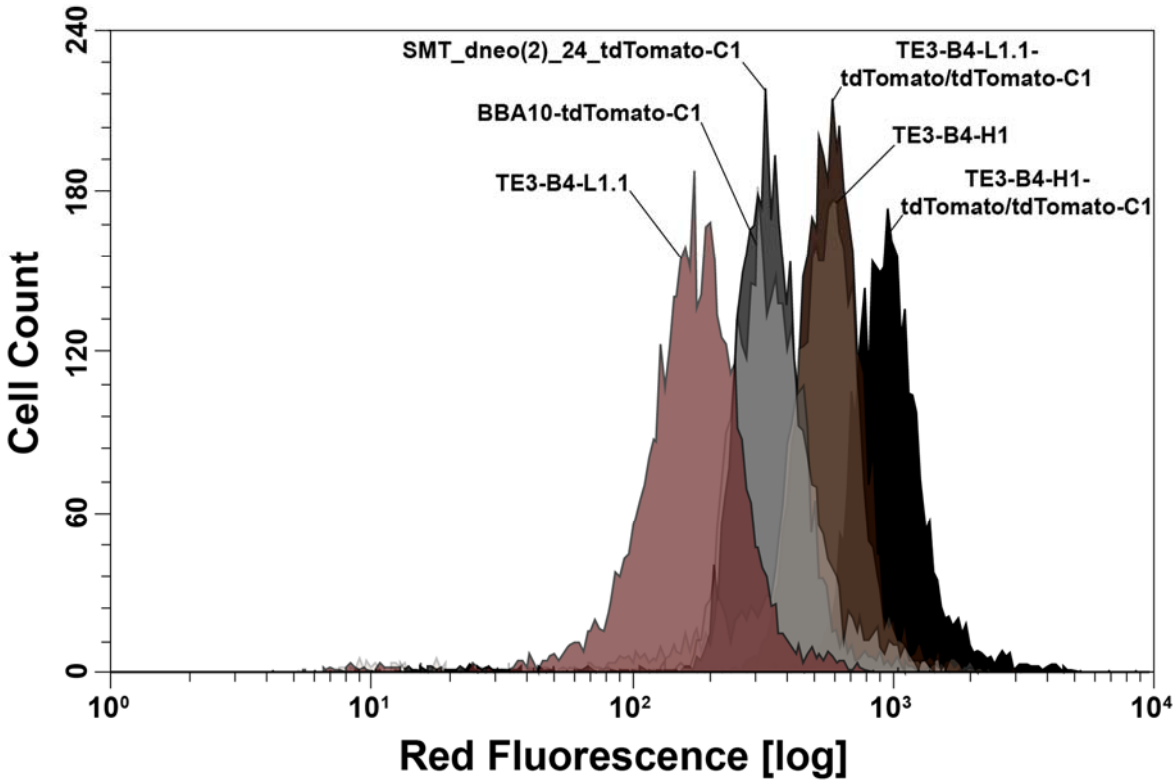

Figure 4-23: Flowcytometric analysis of all tdTomato expressing RMCE master and producer cell lines: Histogram overlay obtained with the Guava easyCyte flowcytometer shows the level of red fluorescence for the RMCE master cell lines TE3-B4-H1 (light brown) and TE3-B4-L1.1 (light red) as well as producer cell lines TE3-B4-H1-tdTomato/tdTomato-C1 (black) TE3-B4-L1.1-tdTomato/tdTomato-C1 (dark brown), SMT_dneo(2)_24-tdTomato-C1 (dark grey) and BBA10-tdTomato-C1 (light grey).

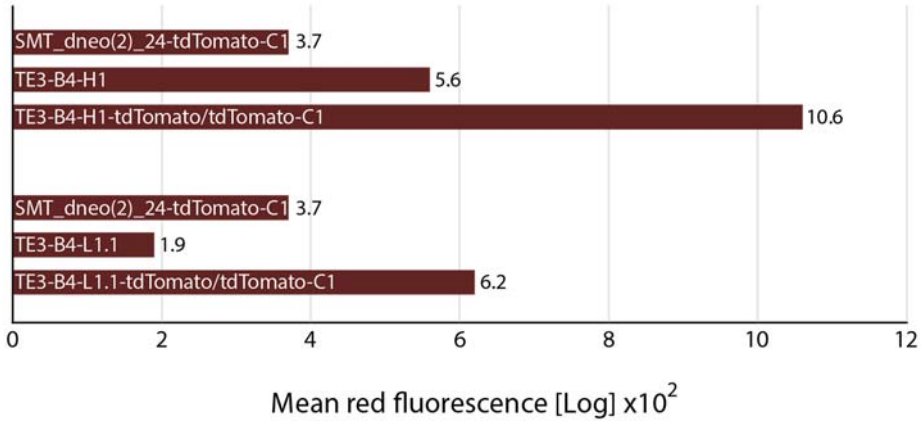

Figure 4-24: Mean red fluorescence of tdTomato expressing cell lines that express tdTomato at one or two chromosomal loci: (Top) Comparison of red fluorescence level in the binary producer cell line TE3-B4-H1-tdTomato/tdTomato-C1 which expresses tdTomato in both exchange cassettes, to the red fluorescence level of SMT_dneo(2)_24-tdTomato and TE3-B4-H1 that express tdTomato in only one exchange cassette that refer to locus 1 or locus 2 of the binary producer cell line respectively. **(Bottom)** Comparison of red fluorescence level in the binary producer cell line TE3-B4-L1.1-tdTomato/tdTomato-C1 which expresses tdTomato in both exchange cassettes, to the red fluorescence level of SMT_dneo(2)_24-tdTomato and TE3-B4-L1 that express tdTomato in only one exchange cassette that refer to locus 1 or locus 2 of the binary producer cell line respectively.

4.2.5 Summary and conclusion – evaluation of tdTomato expressing RMCE master and producer cell lines

Expression level of tdTomato expressing RMCE master and producer cell lines were evaluated in Sections 4.2.2 - 4.2.4 using several methods. Quantitative yield obtained from fluorometric quantification with the Tecan MD-1000 plate reader (Section 4.2.2) and protein purification (Section 4.2.3) are summarised in Table 4-2. As described previously in Section 4.2.3 some unspecifically bound protein was co-purified during Ni-NTA which raised the obtained protein yields unproportionally for cell lines with lower tdTomato expression (TE3-B4-L1.1 and BBA10-tdTomato-C1) when measured using a spectrophotometer (NanoDrop).

Table 4-2: Summary table for tdTomato expression data.

Cell Line	Yield [mg/1x10^9 cells] Cell extract Tecan MD 1000	Yield [mg/1x10^9 cells] Purified tdTomato Tecan MD 1000	Yield [mg/1x10^9 cells] Purified protein NanoDrop
TE3-B4-H1	3.8	3.5	3.6
TE3-B4-L1.1	1.4	1.1	2.4
TE3-B4-L1.1-tdTomato/tdTomato-C1	4.5	4.5	4.8
BBA10-tdTomato-C1	3.2	3.4	4.9

In summary, tdTomato expressing cell lines that comprise tdTomato in only one but distinct exchange locus (TE3-B4-L1.1, TE3-B4-H1, SMT_dneo(2)_24-tdTomato-C1 and BBA10-tdTomato-C1) showed locus specific levels of tdTomato expression as described in

Sections 4.2.2 - 4.2.4. The binary producer cell lines TE3-B4-H1-tdTomato/tdTomato-C1 and TE3-B4-L1.1-tdTomato/tdTomato-C1 that express tdTomato in two genomic loci showed cumulative level of expression which were proportional to the expression capabilities of each locus. This demonstrates that targeted integration into pre-characterised genomic loci in a binary RMCE system can be used to obtain stable producer cell lines with predictable expression properties. The use of chromosomal loci with high expression capabilities in both loci will be desirable for most targets. However, the use of binary RMCE cell lines that show different expression capabilities for each locus may proof useful for the co-expression of proteins that are required in a varying proportions. Monoclonal antibodies for example consist of heavy and light chain subunits in an equimolar ratio. However, it was show that an overproduction of the light chain improves overall productivity (Schlatter *et al.*, 2005). Even the co-expression of accessory molecules which are required in only small quantities could be expressed in such a cell line to not overload the transcription and translation machinery.

4.3 mGRP94 and mPRAT4A

4.3.1 Cloning of mPRAT4A and mGRP94 into pFlpBtM-II_F13/F14 vector

Difficult to express protein targets such as TLRs can serve as a formidable challenge. The stable co-expression of accessory molecules is anticipated to improve their expression. To generate stable binary CHO Lec3.2.8.1 cell lines that co-express Toll–like receptors with their ER chaperones mPRAT4A or mGRP94, these chaperones were cloned into the exchange vector pFlpBtM-II_F13/F14 made in Section 4.1.6. The commercially available plasmids pUNO1-mPRAT4A and pUNO1-mGRP94 (InvivoGen) were used to amplify full length murine PRAT4A and GRP94 constructs with N- and C-terminal FLAG-tags to test variances in expression using HEK293-6E before the stable integration into binary RMCE master cell lines (Section 4.3.2). Restriction sites *Nco*I and *Mlu*I were introduced for cloning of mPRAT4A constructs whereas *Cla*I and *Mlu*I sites were introduced for cloning of mGRP94 constructs as mGRP94 already contains internal *Nco*I restriction sites. For the ligation of mPRAT4A constructs, the pFlpBtM-II_F13/F14 vector was digested with *Nco*I and *Mlu*I restriction endonucleases. This resulted in the removal of the IgG secretion signal sequence, which was replaced by the native secretion signal sequence of mPRAT4A and the removal of the internal His- and Twin-Strep-tags, replacing those with a FLAG-tag. For the ligation of mGRP94 constructs, the pFlpBtM-II_F13/F14 vector was digested with *Bst*BI and *Mlu*I restriction endonucleases. As before this resulted in the removal of the IgG secretion signal sequence, which was replaced by the native secretion signal sequence of mGRP94 and the removal of the internal His- and Twin-Strep-tags, replacing those with a FLAG-tag. The Shine-Dalgarno sequence which was also removed due to the use of the *Bst*BI site needed to be replaced with the mGRP94 PCR fragments. The ligation of mGRP94 PCR fragments with the vector backbone resulted in the destruction of the compatible *Bst*BI/*Cla*I restriction sites. Cloning steps are described in Figure 4-25 and Figure 4-26.

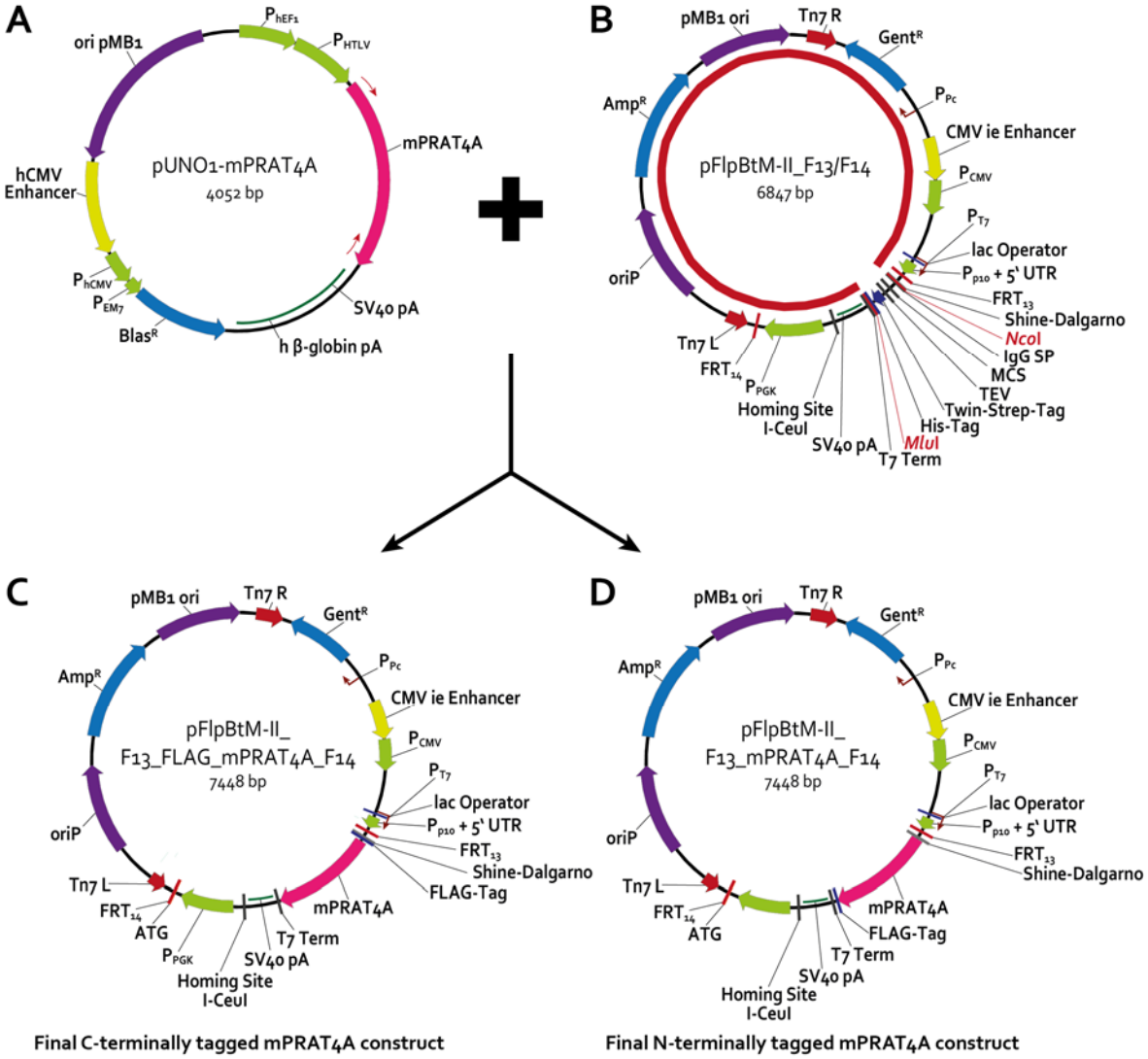

Figure 4-25: Cloning of C- and N-terminally FLAG-tagged mPRAT4A constructs. (A) PCR fragments for N- and C-terminally tagged mPRAT4A constructs were amplified using the commercial vector pUNO1-mPRAT4A (InvivoGen) (red arrows). **(B)** A pFlpBtM-II vector backbone (red line) was obtained through digestion with *Nco*I and *Mlu*I restriction endonucleases, thus removing the IgG secretion signal sequence and the internal His- and Twin-Strep-tag. **(C)** The ligation with the digested (*Nco*I and *Mlu*I) mPRTA4A PCR products resulted in the final exchange vectors for the N- terminally FLAG-tagged and **(D)** C-terminally FLAG-tagged mPRAT4A constructs.

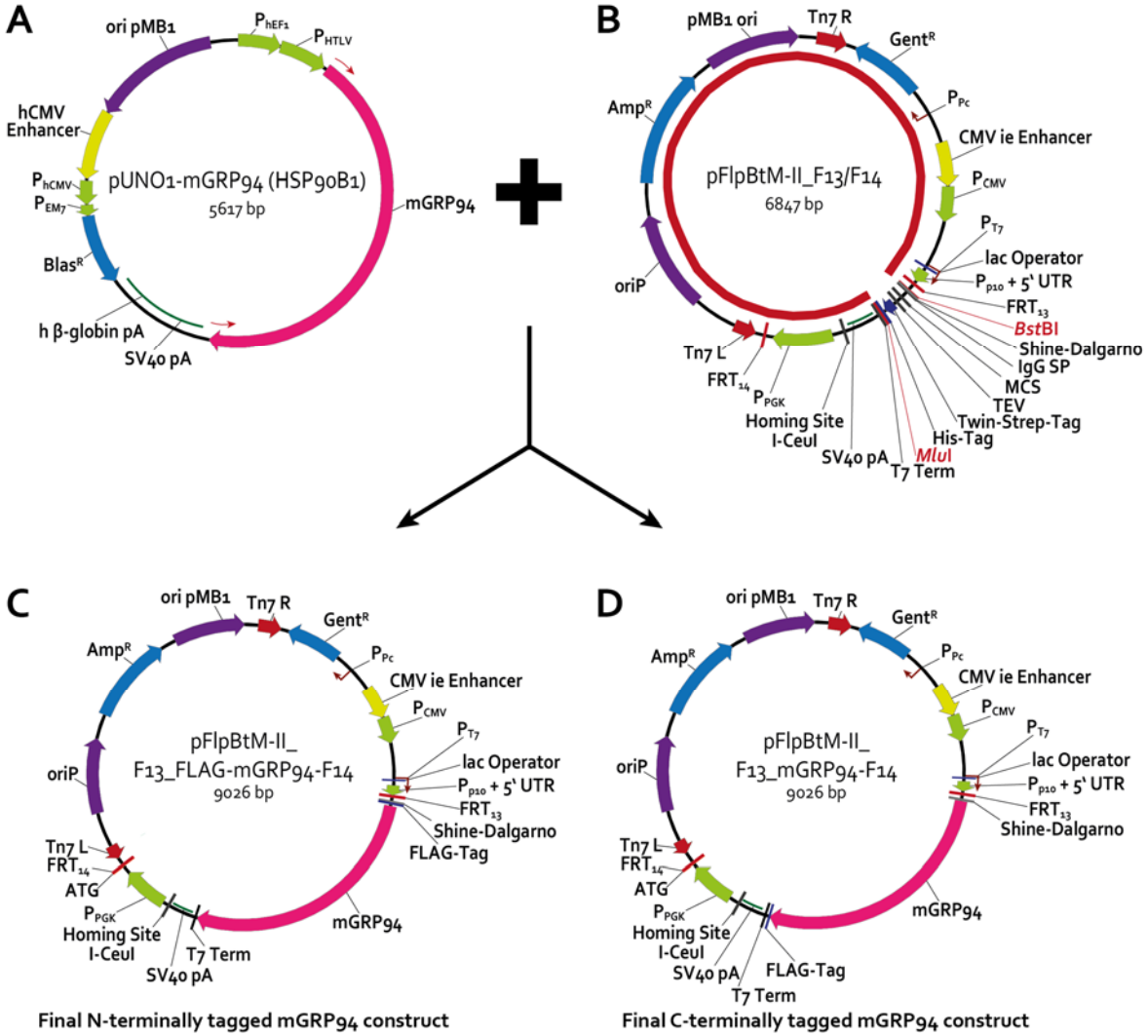

Figure 4-26: Cloning of C- and N-terminally FLAG-tagged mGRP94 constructs. (A) PCR fragments for N- and C-terminally tagged mGRP94 constructs were amplified using the commercial vector pUNO1-mGRP94 (InvivoGen) (red arrows). **(B)** A pFlpBtM-II vector backbone was obtained (red line) through digestion with *Bst*BI and *Mlu*I restriction endonucleases, thus removing the Shine-Dalgarno sequence, IgG secretion signal sequence and the internal His- and Twin-Strep-tag. **(C)** The ligation with the digested (*Cla*I and *Mlu*I) mGRP94 PCR products, which reintroduce the Shine-Dalgarno sequence and destroy the *Bst*BI/*Cla*I restriction sites, resulted in the final exchange vectors for the N- terminally FLAG-tagged **(D)** and C-terminally FLAG-tagged mGRP94 constructs.

4.3.2 Test expression of mPRAT4A and mGRP94 in HEK293-6E

To determine if the position of the FLAG-tag has an influence on the expression level of mPRAT4A or mGRP94; constructs with N- and C-terminal FLAG-tags were designed (Section 4.3.1) and transiently expressed in HEK293-6E using 250 mL batch cultures. mPRAT4A and mGRP94, obtained from cell extracts, were purified with FLAG magnetic beads and expression analysed using SDS-PAGE and Western blot. This demonstrated that C-terminally tagged constructs show better expression level for both mPRAT4A and mGRP94 (Figure 4-27). However, it is possible that the N-terminal FLAG-tag which was locatated upstream of the signal peptide was removed together with the signal peptide after

cellular sorting in the secretion pathway (Alberts, 2008). In that case mPRAT4A and mGRP94 might have been expressed, but could not be purified due to the loss of the FLAG-tags. Consequently, mPRAT4A and mGRP94 constructs with C-terminal FLAG-tags were used for small scale (6 mL) co-expression with mTLR1 and ssmTLR2 in HEK293-6E. These results were not conclusive but seemed to indicated improvement in TLR2 expression level (data not shown). Thus C-terminally FLAG-tagged mPRAT4A and mGRP94 constructs were used for the stable co-expression with TLR ECD constructs in binary RMCE cell lines (Section 4.4).

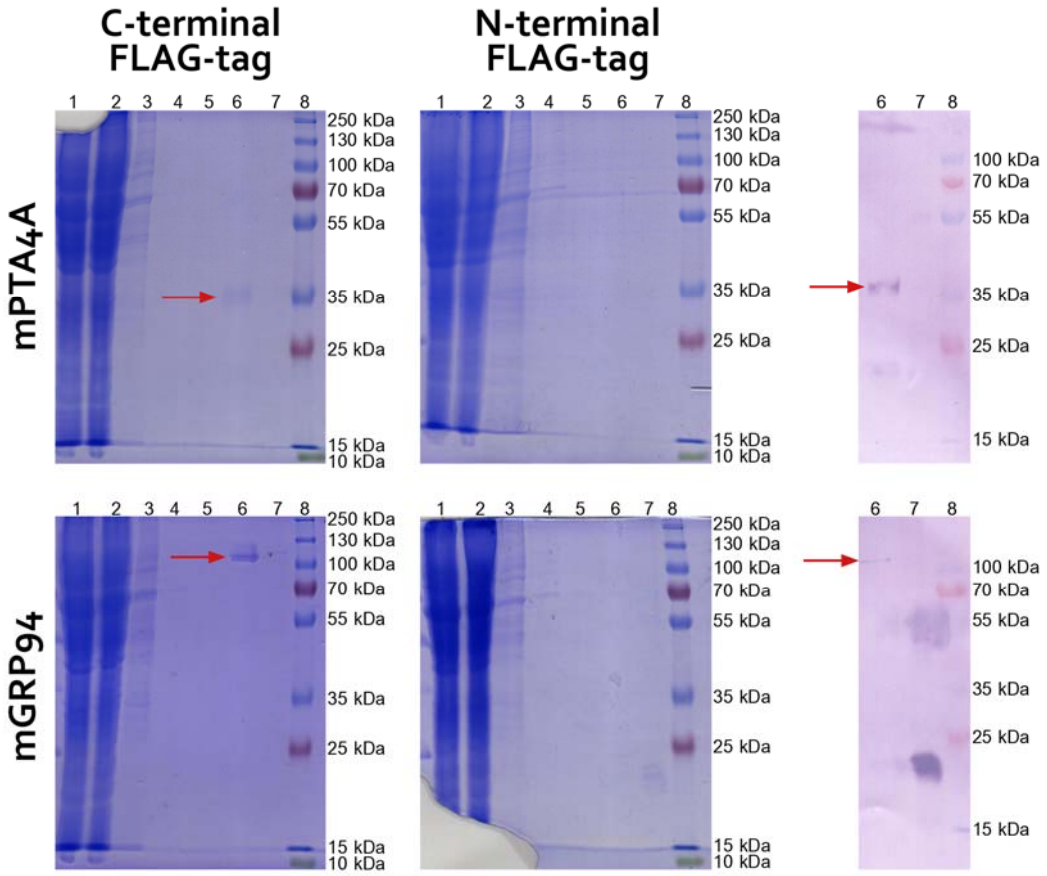

Lane	Top – mPRAT4A	Bottom – mGRP94
1	Cell extract	Cell Extract
2	Non-binding fraction	Non-binding fraction
3	Wash 1	Wash 1
4	Wash 2	Wash 2
5	Wash 3	Wash 3
6	Eluate – mPRAT4A (31.5 kDa)	Eluate – mGRP94 (93.5 kDa)
7	Regeneration	Regeneration
8	PageRuler Plus prestained [Thermo Scientific]	PageRuler Plus prestained [Thermo Scientific]

Figure 4-27: 12 % SDS-PAGE and Western blot analysis of C- and N-terminally FLAG-tagged mPRAT4A and mGRP94 constructs expressed transiently in HEK293-6E and purified with FLAG-magnetic beads. (Top) SDS-PAGE showing fractions of magnetic bead purification for C-terminally FLAG-tagged mPRAT4A (left) and N-terminally FLAG-tagged mPRAT4A (middle) with corresponding western blot (right). **(Bottom)** SDS-PAGE showing fractions of magnetic bead purification for C-terminally FLAG-tagged mGRP94 (left) and N-terminally FLAG-tagged mGRP94 (middle) with corresponding western blot (right). Please note that the two stronger signals on this blot are artefacts only.

4.3.3 Expression of mPRAT4A and mGRP94 in binary RMCE cell lines (CHO Lec3.2.8.1)

The first step for the generation of binary TLR/chaperone producer cell lines required the introduction of mPRAT4A and mGRP94 into the second exchange locus (P_{EF}-FRT_{13}-*tdTomato*-FRT_{14}-Δ*puro*) of the binary RMCE master cell line TE3-B4-H1 via RMCE. Previous efforts to introduce TLR and chaperones into both exchange loci simultaneously failed due to the low exchange rates realized by FLP recombinase. Consequently, the isolation of clones that successfully exchanged both cassettes and survived antibiotic selection against G418 and puromycin simultaneously could not be accomplished (data not shown). Figure 4-28 and Figure 4-29 show flowcytometric data for the binary producer cell lines TE3-B4-H1-eGFP/mPRAT4A-1.1 and TE3-B4-H1-eGFP/mGRP94-C1 compared to the RMCE master cell line TE3-B4-H1 from which they were derived. The slight shift within the green channel reflects a minor overlap of the upper detection limit of the green channel (555 nm) and the lower range of the tdTomato emission spectrum (Section 1.5.1). The successful exchange of tdTomato against mPRATT4A and mGRP94 is detected within the red channel.

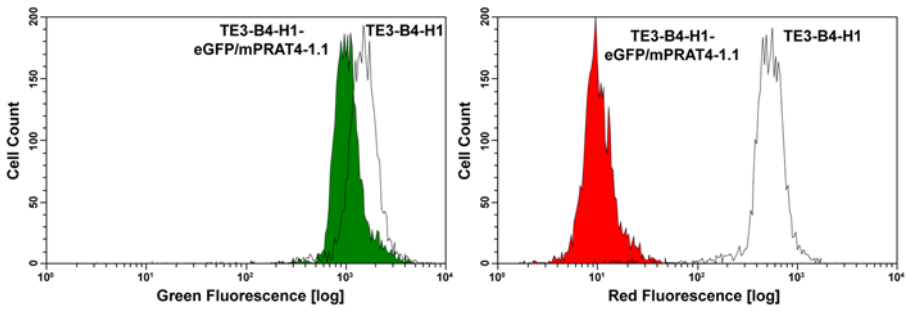

Figure 4-28: Flowcytometric analysis of TE3-B4-H1 master cell line and TE3-B4-H1-eGFP/mPRAT4A-1.1 producer cell line: Histogram overlays obtained with the Guava easyCyte flowcytometer show the level of green fluorescence (left) and the level of red fluorescence (right) of the binary RMCE master cell line TE3-B4-H1 (black line) before exchange of the second locus (P_{EF}-FRT_{13}-*tdTomato*-FRT_{14}-Δ*puro*) against mPRAT4A and the binary producer cell line TE3-B4-H1-eGFP/mPRAT4A-1.1 (green or red solid).

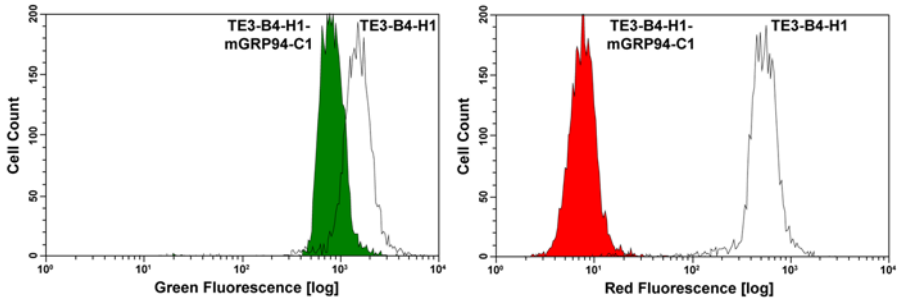

Figure 4-29: Flowcytometric analysis of TE3-B4-H1 master cell line and TE3-B4-H1-eGFP/mGRP94-C1 producer cell line: Histogram overlays obtained with the Guava easyCyte flowcytometer show the level of green fluorescence (left) and the level of red fluorescence (right) of the binary RMCE master cell line TE3-B4-H1 (black line) before exchange of the second locus (P_{EF}-FRT_{13}-*tdTomato*-FRT_{14}-Δ*puro*) against mGRP94 and the binary producer cell line TE3-B4-H1-eGFP/mGRp94-C1 (green or red solid).

To confirm the expression of mGRP94 and mPRAT4A, cell extracts were obtained from 1 L batch cultures of the producer cell lines TE3-B4-H1-ssmTLR2/mPRAT4A-C1 and TE3-B4-H1-ssmTLR2/mGRP94-C1 described in Section 4.4.2. Figure 4-30 shows SDS-PAGE and western blot analysis of concentrated mPRAT4A and mGRP94 eluates after one round of purification with Anti-FLAG® M2 affinity resin. While a strong background of unspecifically bound protein is still present, the expression of mPRAT4A and mGRP94 was confirmed by MALDI-TOF for the marked bands (red arrows). mPRAT4A, like tdTomato discussed in Section 4.2.3, seems to show some fragmentation under reducing conditions. mPRAT4A exhibits a strong band below the original 31.5 kDa band which can also be detected on Western blot analysis. In conclusion the expression of mGRP94 as well as mPRAT4A was confirmed. This result is valid for all generated binary producer cell lines co-expressing TLRs with chaperones in this work as these were all derived from the cell lines TE3-B4-H1-eGFP/mPRAT4A-1.1 or TE3-B4-H1-eGFP/mGRP94-C1.

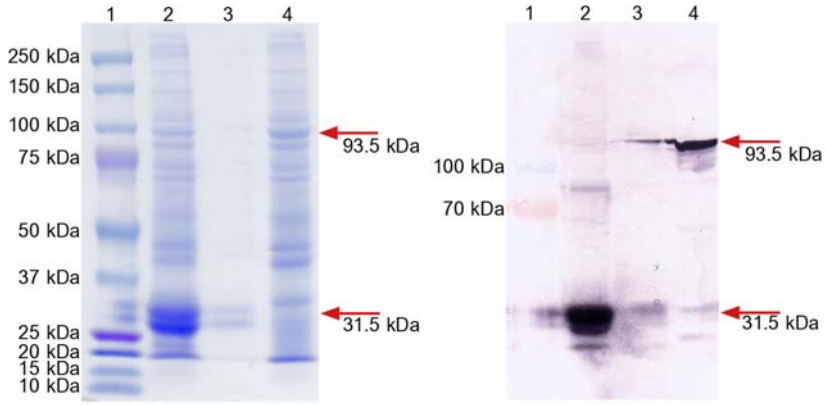

Lane	SDS-PAGE	Western blot
1	Precision Plus Protein Dual Color [BioRad]	PageRuler Plus prestained [Thermo Scientific]
2	Concentrated eluate – mPRAT4A (31.5 kDa)	Concentrated eluate – mPRAT4A (31.5 kDa)
3	-	-
4	Concentrated eluate – mGRP94 (93.5 kDa)	Concentrated eluate – mGRP94 (93.5 kDa)

Figure 4-30: 10 % SDS-PAGE and Western blot analysis of C-terminally FLAG-tagged mPRAT4A and mGRP94 purified with FLAG-affinity resin. Concentrated eluates of mPRAT4A and mGRP94 expressed stably in the producer cell lines TE3-B4-H1-mPRAT4A-1.1 and TE3-B4-H1-ssmTLR2/mGRP94-C1 respectively are shown with SDS-PAGE (left) and Western blot (right).

4.4 Toll-like receptors

4.4.1 Cloning of TLR constructs

TLR ECD and chimeric TLR-VLR ECD constructs are used in this work. They all encompass their own secretion signal sequence and comprise His-tags if cloned into the exchange vector pFlpBtM-I or Twin-Strep and His-tags separated by a protease cleavage site if cloned into pFlpBtM-II(beta). An overview of TLR ECD constructs used in this work is given in Figure 4-31.

Figure 4-31: TLR ECD constructs. TLR ECD (blue) or hybrid TLR ECD constructs with N-terminal VLR sequences (violet) were used in this work. Depending on the exchange vector they were introduced into, pFlpBtM-I or pFlpBtM-II(beta), they comprise a C-terminal His-tag (red) or His- and Twin-Strep-tag (green) separated by a TEV protease cleavage site (grey).

The vector pFlpBtM-ssmTLR2H8 (Figure 4-32) comprises a C-terminally His-tagged murine TLR2 ECD construct (amino acids 1-587) (Meyer *et al.*, 2013). It was used for transient expression tests in HEK293-6E and stable genomic integration into (binary) RMCE master cell lines SWI3_26, SMT_dneo(2)_24 and TE3-B4-H1 (Section 4.4.2).

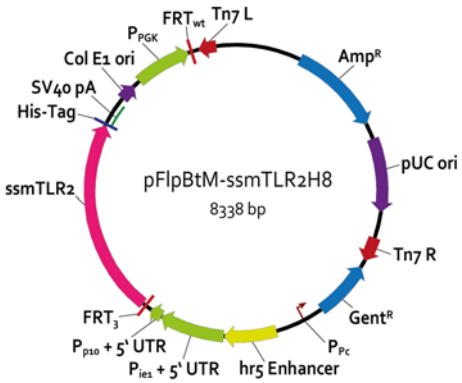

Figure 4-32: Vector pFlpBtM-ssmTLR2H8. Vector comprises an mTLR2 ECD construct (amino acids 1-587) (Meyer *et al.*, 2013).

Murine TLR1 constructs ranging from amino acids 1-408, 1-455 and 1-500 were previously reported to express solubly as chimera when fused C-terminally with a VLR fragment (amino acids 133-200) (Jin *et al.*, 2007). Therefore, mTLR1 ECD with these specific lengths

were amplifying from the vector pDUO_mTLR1_mTLR2 (InvivoGen) with the forward oligonucleotide TLR1_FWD_NcoI in combination with the reverse oligonucleotides TLR1_408_NheI_r, TLR1_455_NheI_r or TLR1_500_NheI_r. Restriction sites *Nco*I and *Nhe*I were introduced to enable the integration into a pFlpBtM-II(beta)-VLR-TEV-Strep-H8 backbone containing the VLR fragment which was obtained from vector pFlpBtM-IIbeta-sshTLR5-1-198-VLR-TEV-Strep-H8 through the removal of the hTLR5 insert with the same restriction endonucleases (Figure 4-33). After test expressions in HEK293-6E cells (Agarwal, 2012) construct mTLR1_1-455 was chosen for stable integration into the (binary) RMCE master cell lines SMT_dneo(2)_24 and TE3-B4-H1 as it showed the highest level of expression (Section 4.4.3).

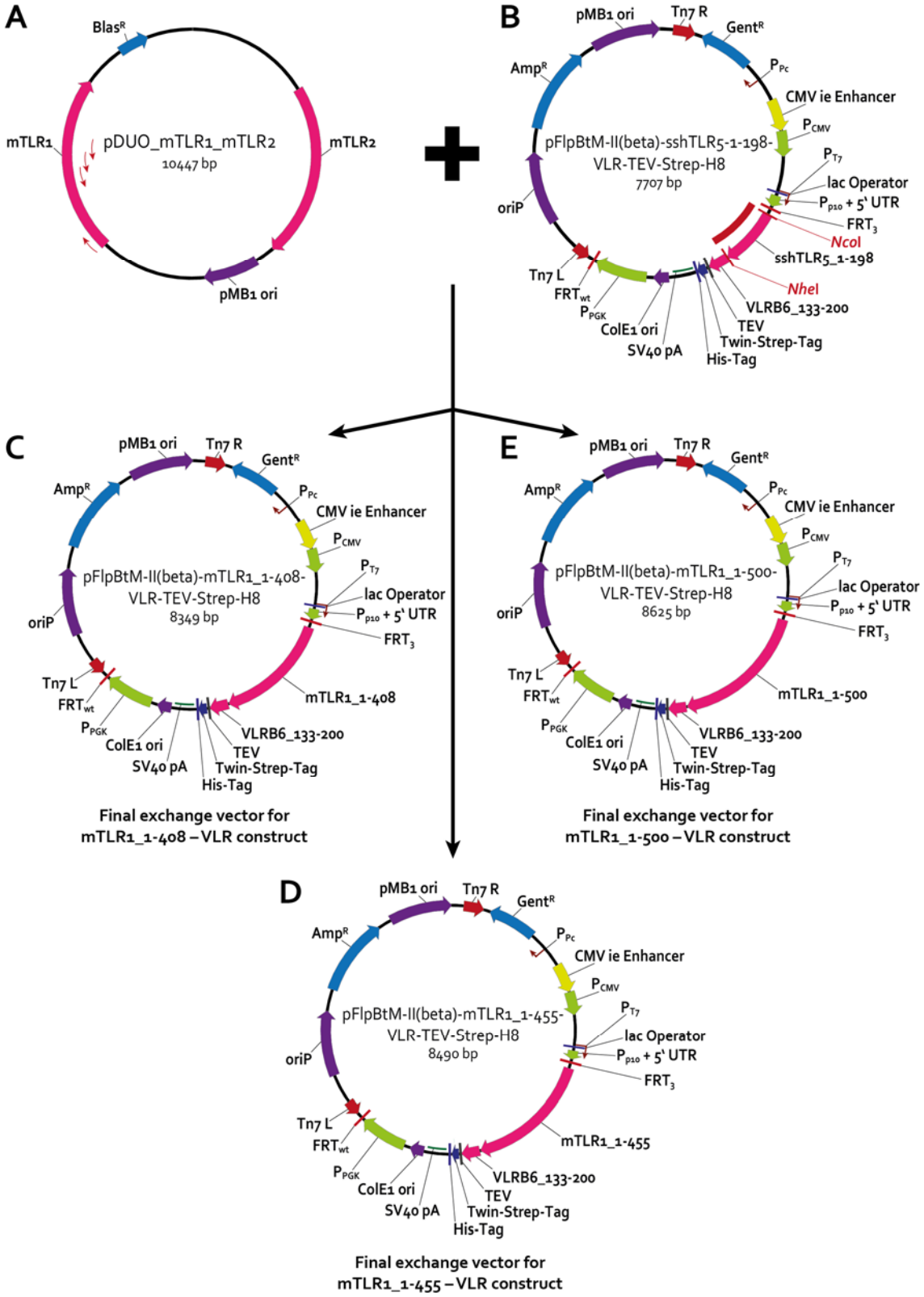

Figure 4-33: Cloning of mTLR1-VLR ECD constructs. (A) PCR fragments for mTLR1 ECD constructs with amino acids 1-408, 1-455 and 1-500 including *Nco*I and *Nhe*I restriction sites were amplified (red arrows) using the commercial vector pDUO_mTLR1_mTLR2 (InvivoGen). **(B)** A pFlpBtM-II(beta)-VLR-TEV-Strep-H8 vector backbone was obtained through removal of an sshTLR5 insert (red line) with *Nco*I and *Nhe*I restriction sites from vector pFlpBtM-II(beta)-sshTLR5-1-198-VLR-TEV-Strep-H8 (Steffen Meyer, HZI). **(C)** Ligation of the *Nco*I and *Nhe*I digested PCR fragments resulted in the final exchange vectors pFlpBtM-II(beta)-mTLR1_1-408-VLR-TEV-Strep-H8 **(D)** pFlpBtM-II(beta)-mTLR1_1-455-VLR-TEV-Strep-H8 and **(E)** pFlpBtM-II(beta)-mTLR1_1-500-VLR-TEV-Strep-H8.

A human TLR5 construct was prepared as follows; oligonucleotides TLR5_1-391NheRev and BamHI-Nco-For were used for the amplification of an hTLR5 ECD ranging from amino acids 1-391 introducing restriction sites for *Nco*I and *Nhe*I. The PCR fragment was inserted into a pFlpBtM-II(beta)-VLR-TEV-Strep-H8 backbone containing a VLR fragment which was obtained from vector pFlpBtM-II(beta)-sshTLR5-1-198-VLR-TEV-Strep-H8 through the removal of the hTLR5 insert with HF-*Nco*I and HF-*Nhe*I restriction endonucleases (Figure 4-34).

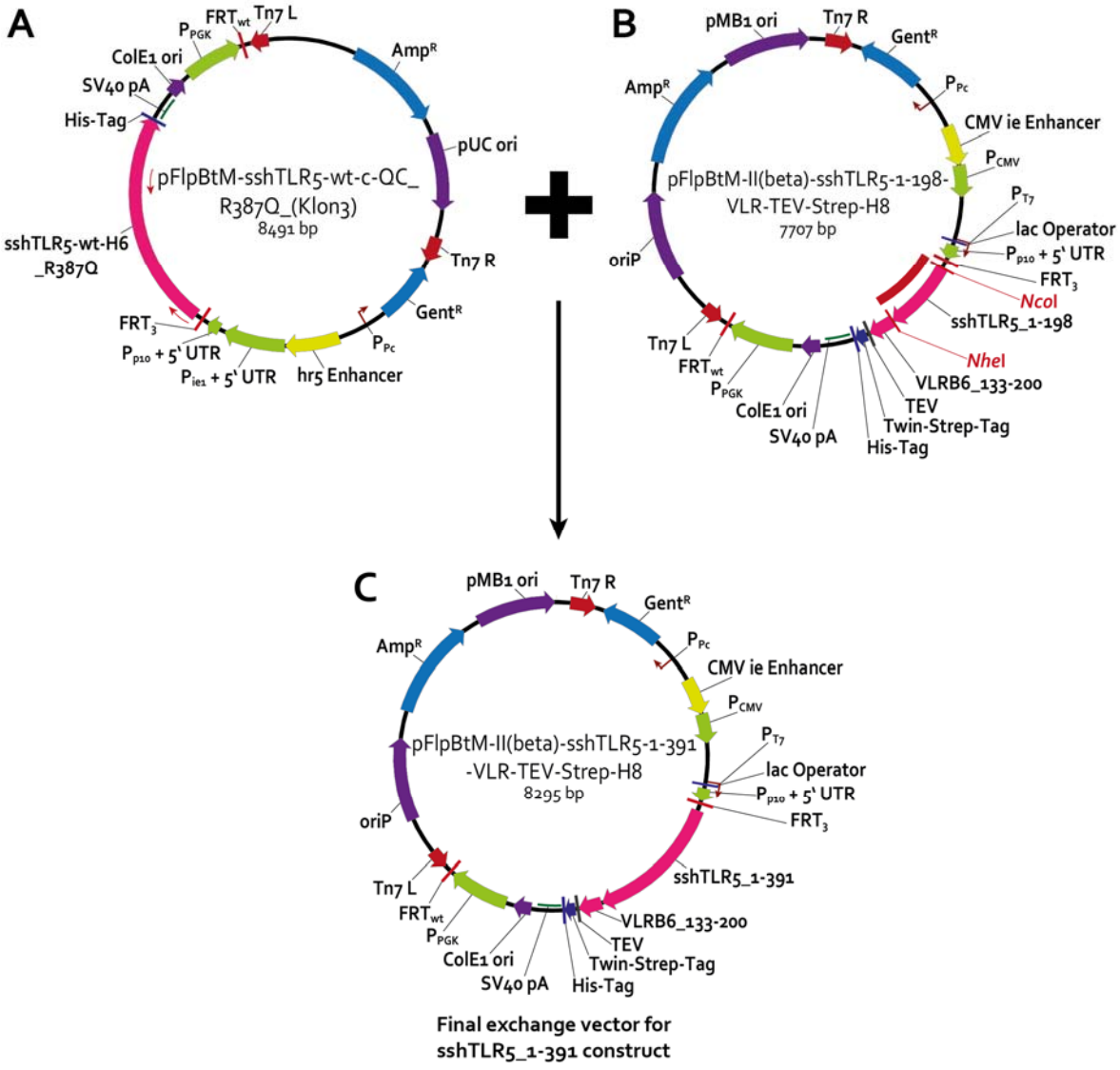

Figure 4-34: Cloning of the hTLR5-VLR ECD construct. (A) A PCR fragment for a hTLR5 ECD construct ranging from amino acids 1-391 including *Nco*I and *Nhe*I restriction sites was amplified (red arrows) using the vector pFlpBtM-sshTLR5-wt-c-QC_R387Q_(Klon3) (Steffen Meyer, HZI). **(B)** A pFlpBtM-II(beta)-VLR-TEV-Strep-H8 vector backbone was obtained through removal of an hTLR5 insert (red line) with *Nco*I and *Nhe*I restriction sites from vector pFlpBtM-II(beta)-sshTLR5-1-198-VLR-TEV-Strep-H8 (Steffen Meyer, HZI). **(C)** Ligation of the *Nco*I and *Nhe*I digested PCR fragment resulted in the final exchange vectors pFlpBtM-II(beta)-sshTLR5_1-391-VLR-TEV-STrEP-H8.

4.4.2 CHO Lec3.2.8.1 TLR2 producer cell lines

To determine if the co-expression of mTLR2 with molecular chaperones improves the expression of mTLR2, stable CHO Lec3.2.8.1 cell lines that produce mTLR2 with or without their molecular chaperones mPRAT4A or mGRP94 were generated as described below. Furthermore, it should be tested weather the solubly expressed mTLR2 shows a similar level of expression when integrated into the RMCE master cell lines SWI3_26 and SMT_dneo(2)_24 as was shown for the intracellular protein tdTomato (Section 4.2).

The mTLR2 ECD construct was introduced with the vector pFlpBtM-ssmTLR2H8 (Section 4.4.1) into the master cell lines SWI3_26 and SMT_dneo(2)_24 using RMCE. Both cell lines only comprise one exchange locus (P_{EF}-FRT_3-*eGFP*-FRT_{wt}-Δ*neo*) and were previously described in Section 4.1. Figure 4-35 shows the successful exchange of eGFP against mTLR2 using flowcytometry for the producer cell lines BBA10-TLR2-C1 and SMT_dneo(2)_24-ssmTLR2-C7. Likewise binary producer cell lines were generated through the introduction of mTLR2 into locus 1 (P_{EF}-FRT_3-*eGFP*-FRT_{wt}-Δ*neo*) of the cell lines TE3-B4-H1-mPRAT4A-C1.1 and TE3-B4-H1-mGRP94-C1 (Section 4.3.3) which already contain chaperones in exchange locus 2 (P_{EF}-FRT_{13}-*Chaperone*-FRT_{14}-Δ*puro*) as shown in Figure 4-36.

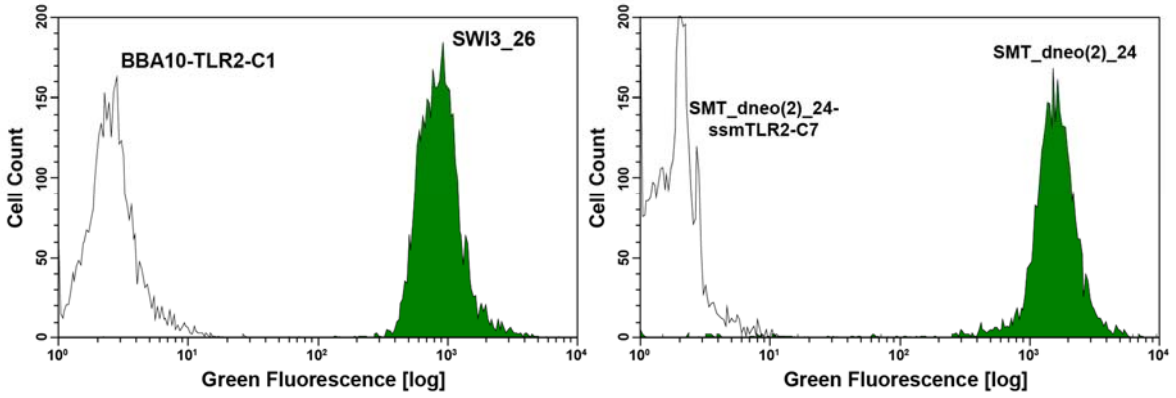

Figure 4-35: Generation of mTLR2 producer cell lines: (Left) Histogram overlays obtained with the Guava easyCyte flowcytometer show the level of green fluorescence of the RMCE master cell line SWI3_26 which contains eGFP (green solid) and the thereof derived producer cell line BBA10-TLR2-C1 (black line) after successful exchange of eGFP against mTLR2. **(Right)** Likewise the RMCE master cell line SMT_dneo(2)_24 (green solid) and the thereof derived producer cell lines SMT_dneo(2)_24-TLR2-C7 (black line) are shown.

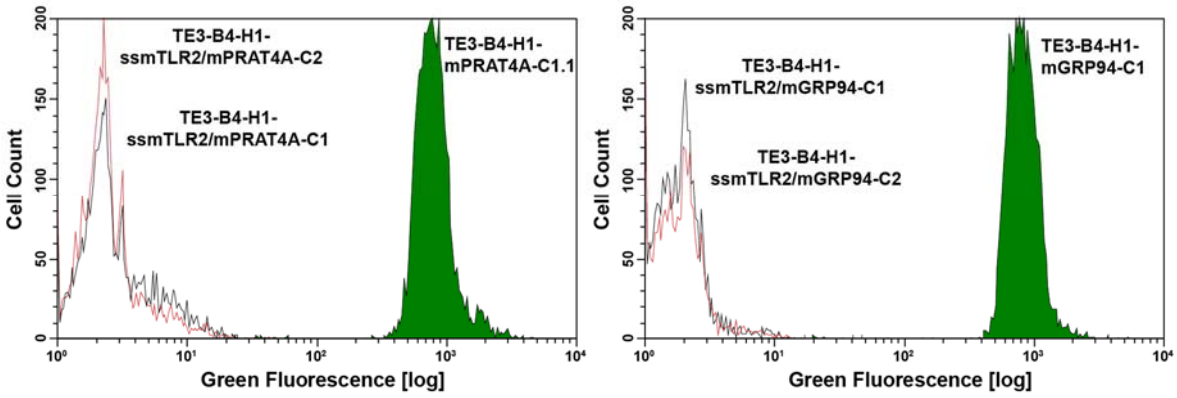

Figure 4-36: Generation of binary mTLR2 producer cell lines: Histogram overlays obtained with the Guava easyCyte flowcytometer show the level of green fluorescence of the binary cell lines TE3-B4-H1-eGFP/mPRAT4A-1.1 (left) and TE3-B4-H1-eGFP/mGRP94-C1 (right) which contain eGFP in locus 1 (solid green). The thereof derived producer cell lines TE3-B4-H1-ssmTLR2/mPRAT4A and TE3-B4-H1-ssmTLR2/mGRP94 are shown in the same gate as black line for clone 1 and red line for clone 2 after successful exchange of eGFP against mTLR2.

The expression of mTLR2 for one or two clones of each producer cell line was tested in 1 L - 1.5 L batch cultures in shake flasks. The cell line SMT_dneo(2)_24-ssmTLR2 was not tested in small scale batch culture due to time restrictions. Clones were either selected according to their flowcytometric profile alone (successful integration) or after screening of several clones using TCA precipitation of 1 mL culture supernatants as for BBA10-TLR2 and SMT_dneo(2)_24-ssmTLR2 clones in combination with Western blot analysis (Figure 4-37). It should be noted that one false positive clone was found for SMT_dneo(2)_24-ssmTLR2 (clone-1) which seems to have lost eGFP without successfully integrating mTLR2.

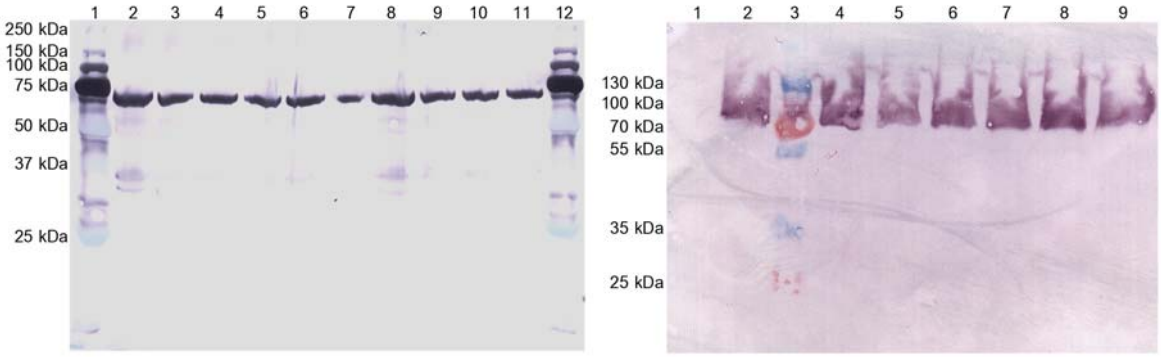

Lane	BBA10-TLR2 (67.2 kDa)	Lane	SMT_dneo(2)_24-ssmTLR2-C1 (67.2 kDa)
1	Precision Plus Protein All Blue (Bio-Rad)	1	SMT_dneo(2)_24-ssmTLR2-C1
2	BBA10-TLR2-C1	2	SMT_dneo(2)_24-ssmTLR2-C2
3	BBA10-TLR2-C2	3	PageRuler Plus prestained (Thermo Scientific)
4	BBA10-TLR2-C3	4	SMT_dneo(2)_24-ssmTLR2-C3
5	BBA10-TLR2-C4	5	SMT_dneo(2)_24-ssmTLR2-C4
6	BBA10-TLR2-C5	6	SMT_dneo(2)_24-ssmTLR2-C5
7	BBA10-TLR2-C6	7	SMT_dneo(2)_24-ssmTLR2-C6
8	BBA10-TLR2-C7	8	SMT_dneo(2)_24-ssmTLR2-C7
9	BBA10-TLR2-C8	9	SMT_dneo(2)_24-ssmTLR2-C8
10	BBA10-TLR2-C9	-	-
11	BBA10-TLR2-C10	-	-
12	Precision Plus Protein All Blue (Bio-Rad)	-	-

Figure 4-37: 12 % Western blot analysis of TCA precipitated mTLR2 expressed in BBA10-TLR2 and SMT_dneo(2)-24-ssmTLR2 cell clones. 10 clones of the SWI3_26 derived producer cell line BBA10-TLR2 and 8 clones of the SMT_dneo(2)_24 derived producer cell line SMT_dnoe(2)_24-ssmTLR2 were analysed for protein expression. One false positive clone was found for SMT_dnoe(2)_24-ssmTLR2 (clone-1).

Batch cultures of BBA10-ssmTLR2-C1 and BBA10-ssmTLR2-C7 in shaker flasks resulted in volumetric yields of 0.5 mg/L and 0.9 mg/L purified mTLR2 respectively. Figure 4-38 shows SDS-PAGE analysis of mTLR2 purified using one round of Ni-IMAC from these cell lines. mTLR2 that was concentrated more than 5x using Vivaspin columns shows some unspecific background. Volumetric yields of 0.9 ± 0.3 mg/L were obtained with large scale expressions in 40 L perfusion reactors for BBA10-TLR2-C1. Figure 4-39 shows purified mTLR2 obtained from a perfusion reactor run after purification with Ni-IMAC.

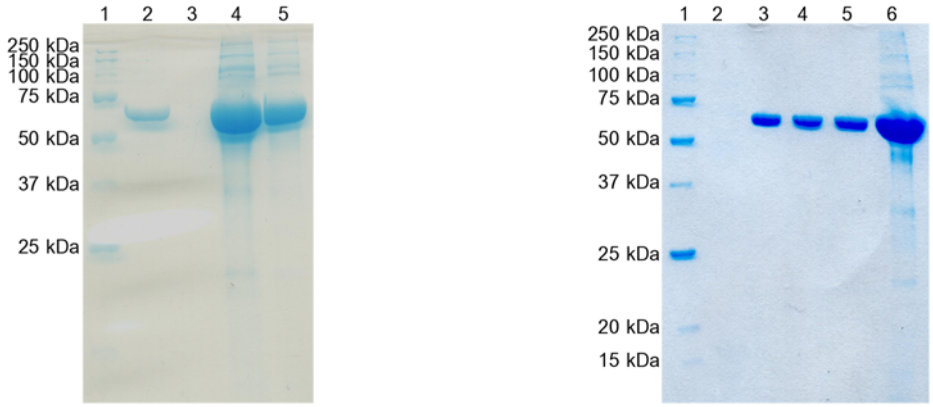

Lane	BBA10-TLR2-C1 (67.2 kDa)	Lane	BBA10-TLR2-C7 (67.2 kDa)
1	Precision Plus Protein unstained (Bio-Rad)	1	Precision Plus Protein unstained (Bio-Rad)
2	Purified mTLR2 (Ni-IMAC)	2	-
3	-	3	Purified mTLR2 (Ni-IMAC) – Run 1
4	10x concentrated mTLR2	4	Purified mTLR2 (Ni-IMAC) – Run 2
5	5x concentrated mTLR2	5	Purified mTLR2 (Ni-IMAC) – Run 1+2
-	-	6	7.65 x concentrated mTLR2

Figure 4-38: 12 % SDS-PAGE analysis of purified and concentrated mTLR2 expressed in batch cultures using cell lines BBA10-TLR2-C1 and BBA10-TLR2-C7. mTLR2 was produced in 1.25 L or 1.5 L batch cultures using the cell lines BBA10-TLR2-C1 and BBA10-TLR2-C7 respectively. SDS-PAGE shows ssmTLR2 purified via Ni-IMAC and concentrated mTLR2 for both cell lines. Note that BBA10-TLR2-C7 was purified in two separate runs and pooled afterwards. Volumetric yields of 0.5 mg/L and 0.9 mg/L were obtained for BBA10-TLR2-C1 and BBA10-TLR2-C7 respectively.

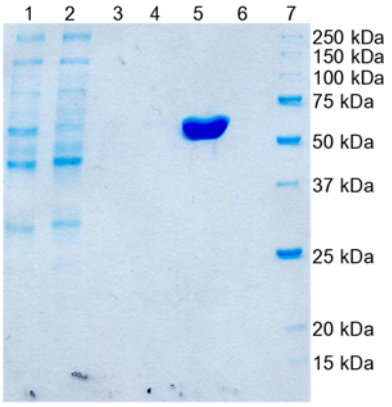

Lane	BBA10-TLR2-C1 (67.2 kDa)
1	Diafiltrated and concentrate culture supernatant
2	Non-binding fraction
3	Wash 1
4	Wash 2
5	Purified mTLR2 (Ni-IMAC)
6	-
7	Precision Plus Protein unstained (Bio-Rad)

Figure 4-39: 12 % SDS-PAGE analysis of purified mTLR2 expressed in a perfusion reactor using cell line BBA10-TLR2-C1. Example of mTLR2 that was produced in a perfusion reactor and purified using Ni-IMAC. Yields up to 0.9 ± 0.3 mg/L were reached in a 40 L scale.

However, it should be noted that the cell lines BBA10-ssmTLR2-C1 and BBA10-ssmTLR2-C7 were derived from the master cell line SWI3_26 (please see Figure 4-15 in Section 4.2 for an overview of master cell lines used in this work). The binary master cell

line used for the generation of mTLR2/mPRAT4A or mTLR2/mGRP94 producer cell lines on the contrary was derived from the master cell line SMT_dneo(2)_24. As described in Section 4.2, the cell lines BBA10-tdTomato-C1 and SMT_dneo(2)_24-tdTomato-C1 show similar expression yields for intracellular tdTomato. To determine if the yields of the solubly expressed mTLR2 are proportional for both cell lines as well, the cell line BBA10-ssmTLR2-C1 was compared to the cell line SMT_dneo(2)_24-ssmTLR2-C7. As described above the cell line BBA10-ssmTLR2-C1 expresses 0.9 ± 0.3 mg/L mTLR2 in bioreactor runs. Likewise the cell line SMT_dneo(2)_24-ssmTLR2-C7 was shown to express an average of 1.4 ± 0.1 mg/L mTLR2 in a bioreactor run as described below. Therefore it can be concluded that proteins, expressed intracellular or in soluble form, will exhibit a level of expression proportional to the expression capabilities of each exchange locus as described in Section 4.2.

Expression of mTLR2 in the binary cell line TE3-B4-H1-ssmTLR2/mGRP94-C1 as well as in the binary cell lines TE3-B4-H1-ssmTLR2/mPRAT4A-C1 and TE3-B4-H1-ssmTLR2/mPRAT4A-C2 was confirmed through expression in 1 L batch cultures in shaker flasks (Figure 4-40 and Figure 4-41). However one round of purification using Ni-IMAC was not sufficient to obtain volumetric yields. Large scale expressions in a 2.5 L bioreactors performed in batch mode were done by Nadine Konisch in duplicate for SMT_dneo(2)_24-ssmTLR2-C7 as well as for the binary cell lines TE3-B4-H1-ssmTLR2/mGRP94-C1 and SMT_dneo(2)_24-ssmTLR2/mPRAT4A-C1. Cell densities were adjusted to a similar level (between 3.8-6.0x10^6 cells/mL) to obtain comparable results. Subsequently, volumetric yields of mTLR2 expression were obtained for each cell line after purification with Ni-NTA. Figure A.2-3 - Figure A.2-5 in the appendix show examples for SDS-PAGE analysis of purified mTLR2 obtained from these reactor runs. Surprisingly the mTLR2 expression yields obtained for the cell line SMT_dneo(2)_24-ssmTLR2-C7 are the highest even though no chaperones were co-expressed. The co-expression of mPRAT4A or mGRP94 reduces the volumetric yields significantly as can be seen in Table 4-3.

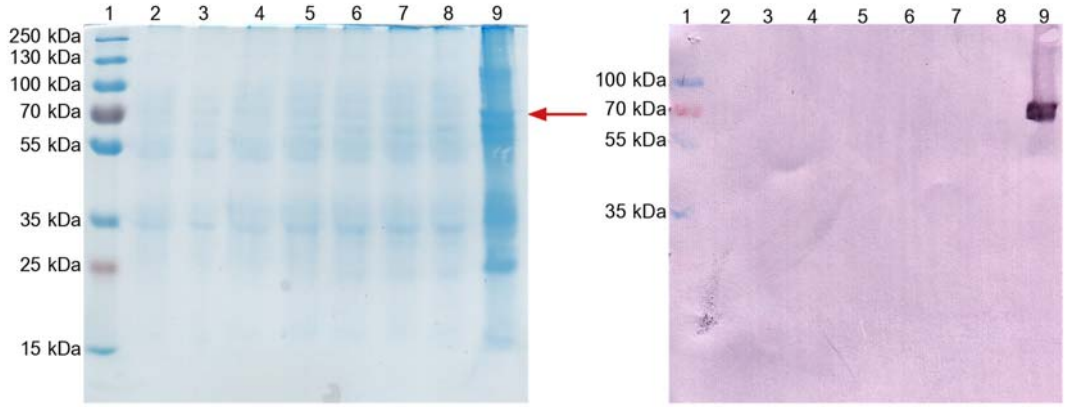

Lane	TE3-B4-H1-ssmTLR2/mGRP94-C1 (67.2 kDa)
1	PageRuler Plus prestained (Thermo Scientific)
2-8	Wash fractions
9	Eluate – mTLR2

Figure 4-40: 12 % SDS-PAGE and Western blot analysis of mTLR2 expressed in batch culture using the cell line TE3-B4-H1-ssmTLR2/mGRP94-C1. mTLR2 was produced in a 1 L batch culture using the cell line TE3-B4-H1-ssmTLR2/mGRP94-C1. Expression of mTLR2 was confirmed but no volumetric yields could be obtained for this cell line. SDS-PAGE and Western blot (α-His antibody) shows wash and eluate fractions after one round of purification (Ni-IMAC).

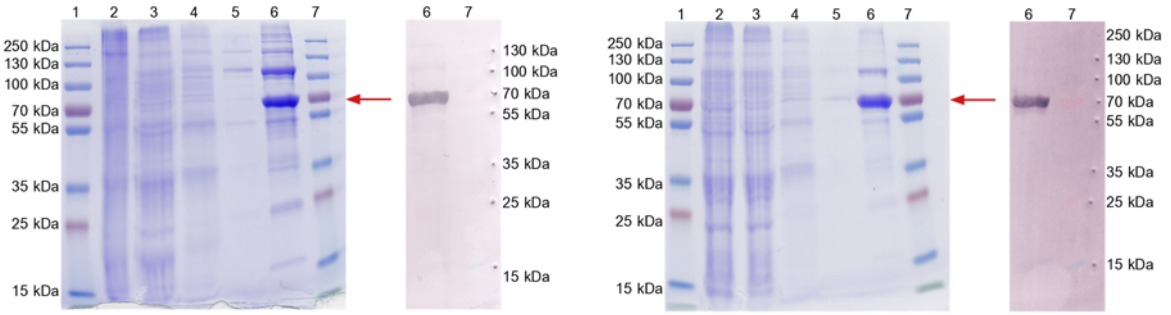

Lane	TE3-B4-H1-ssmTLR2/mPRAT4A-C1	Lane	TE3_B4-H1-ssmTLR2/mPRAT4A-C2
1	PageRuler Plus prestained (Thermo Scientific)	1	PageRuler Plus prestained (Thermo Scientific)
2	Diafiltrated/concentrated culture supernatant	2	Diafiltrated/concentrated culture supernatant
3	Non-binding fraction	3	Non-binding fraction
4	Wash 1	4	Wash 1
5	Wash 2	5	Wash 2
6	Eluate – mTLR2 (67.2 kDa)	6	Eluate – mTLR2 (67.2 kDa)
7	PageRuler Plus prestained (Thermo Scientific)	7	PageRuler Plus prestained (Thermo Scientific)

Figure 4-41: 12 % SDS-PAGE and Western blot analysis of mTLR2 expressed in batch cultures using the cell lines TE3-B4-H1-ssmTLR2/mPRAT4A-C1 and TE3-B4-H1-ssmTLR2/mPRAT4A-C2. mTLR2 was produced in 1 L batch cultures using the cell lines TE3-B4-H1-ssmTLR2/mPRAT4A-C1 and -C2. SDS-PAGE and Western blots (α-His antibody) show wash and eluate fractions after one round of purification with Ni-IMAC. Expression of mTLR2 was confirmed for both cell lines but no volumetric yields could be obtained as one round of purification was not sufficient.

Table 4-3: Comparison of yields obtained for the expression of ssmTLR2 and its co-expression with chaperons.

Cell Line	Run	Yield [mg/L]	Yield [mg/10^{10} cells]
SMT_dneo(2)_24-ssmTLR2-C7	1	1.5	2.3
SMT_dneo(2)_24-ssmTLR2-C7	2	1.2	2.5
TE3-B4-H1-ssmTLR2/mPRAT4A-C1	1	0.4	0.9
TE3-B4_H1-ssmTLR2/mPRAT4A-C1	2	0.5	1.0
TE3 B4 H1 ssmTLR2/mGRP94-C1	1	0.5	1.3
TE3 B4 H1 ssmTLR2/mGRP94-C1	2	0.7	1.4

4.4.3 CHO Lec3.2.8.1 TLR1 producer cell lines

To determine if the chaperone co-expression improves mTLR1 production stable CHO Lec3.2.8.1 cell lines that produce mTLR1 with or without their molecular chaperones mPRAT4A or mGRP94 were generated as described below.

The mTLR1 ECD construct ranging from amino acids 1-455 was introduced with the vector pFlpBtM-II(beta)-mTLR1_1-455-VLR-TEV-Strep-H8 (Section 4.4.1) into the master cell line SMT_dneo(2)_24 using RMCE. To evaluate the effects of chaperone co-expression on mTLR1 yields, mTLR1 was also introduced into locus 1 (P_{EF}-FRT_3-*eGFP*-FRT_{wt}-Δ*neo*) of the binary cell lines TE3-B4-H1-eGFP/mPRAT4A-1.1 and TE3-B4-H1-eGFP/mGRP94-C1 (Section 4.3.3). These cell lines already contain chaperones in exchange locus 2 (P_{EF}-FRT_{13}-*Chaperone*-FRT_{14}-Δ*puro*). Figure 4-42 shows the successful exchange of eGFP against mTLR1 using flowcytometry for two clones of the producer cell lines SMT_dneo(2)_24-mTLR1-455 as well as for the binary producer cell line TE3-B4-H1-mTLR1/mPRAT4A and for TE3-B4-H1-mTLR1/mGRP94-C1.

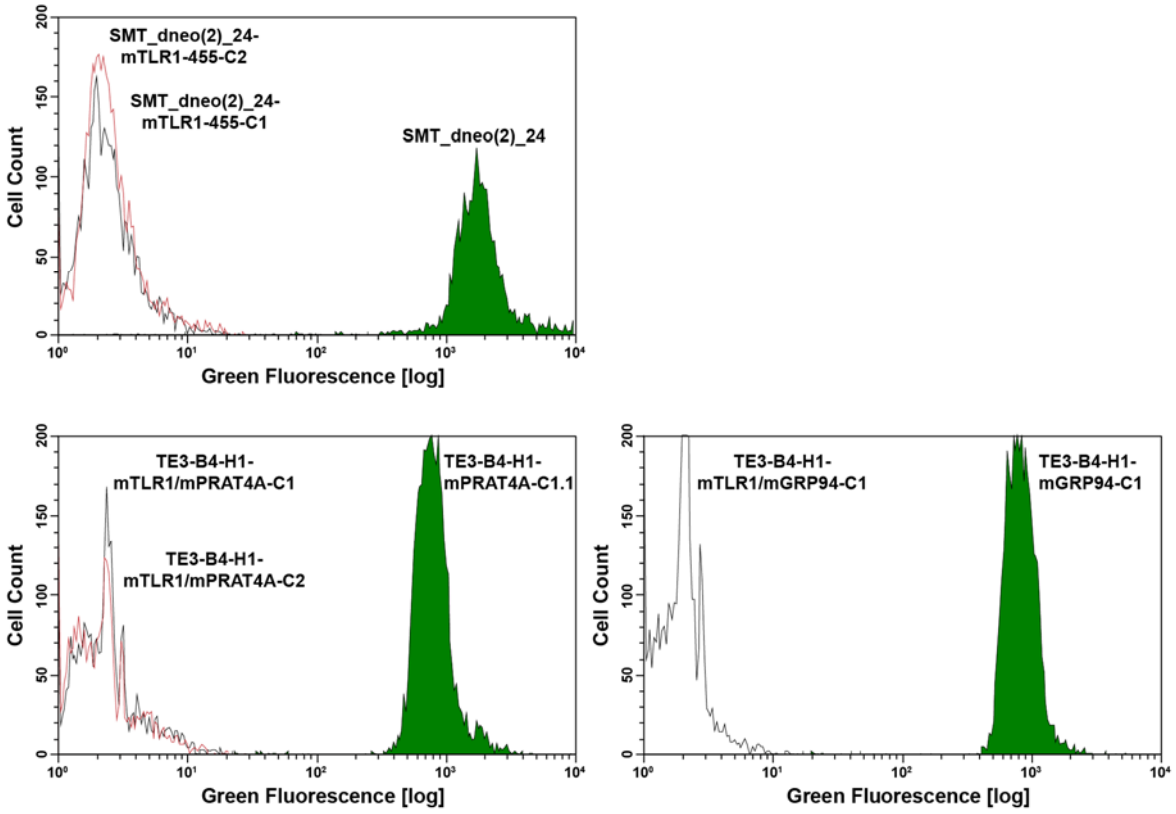

Figure 4-42: Generation of mTLR1 producer cell lines: Histogram overlays obtained with the Guava easyCyte flowcytometer show the level of green fluorescence of the RMCE master cell line SMT_dneo(2)_24 (top) as well as the binary cell lines TE3-B4-H1-eGFP/mPRAT4A-1.1 (bottom, left) and TE3-B4-H1-eGFP/mGRP94-C1 (bottom, right) which contain eGFP in locus 1 (solid green). The thereof derived producer cell lines SMT_dneo(2)_24-mTLR1-455, TE3-B4-H1-mTLR1/mPRAT4A and TE3-B4-H1-mTLR1/mGRP94-C1 are shown in the same gate as black line for clone 1 and red line for clone 2 after successful exchange of eGFP against mTLR1.

Expression of mTLR1 was confirmed in 1 L - 1.5 L batch cultures in shaker flasks for the cell lines SMT_dneo(2)_24-mTLR1-455-C1 and SMT_dneo(2)_24-mTLR1-455-C2 as well as the binary cell lines TE3-B4-H1-mTLR1/mPRAT4A-C1 and TE3-B4-H1-mTLR1/mPRAT4A-C2. The expression of mTLR1 was shown through SDS-PAGE and Western blot analysis of mTLR1 purifications obtained using either Ni-IMAC or Strep purification (Figure 4-43 and Figure 4-44). As can be seen one round of Strep purification is superior to one round of Ni-IMAC and thus the mTLR1 band can already be identified on SDS-PAGE (Figure 4-44). Purification with Ni-IMAC however exhibits a strong background. To specifically identify mTLR1 different antibodies were used to detect mTLR1 on western blot analysis. The anti-strep antibody however showed a high level of cross-interaction if a strong background was present. Antibodies raised against the His-tag and a TLR1 specific antibody gave the most accurate results. (Figure 4-43). However, due to the very low yields quantification was not possible. Expression was not yet confirmed for TE3-B4-H1-mTLR1/mGRP94-C1.

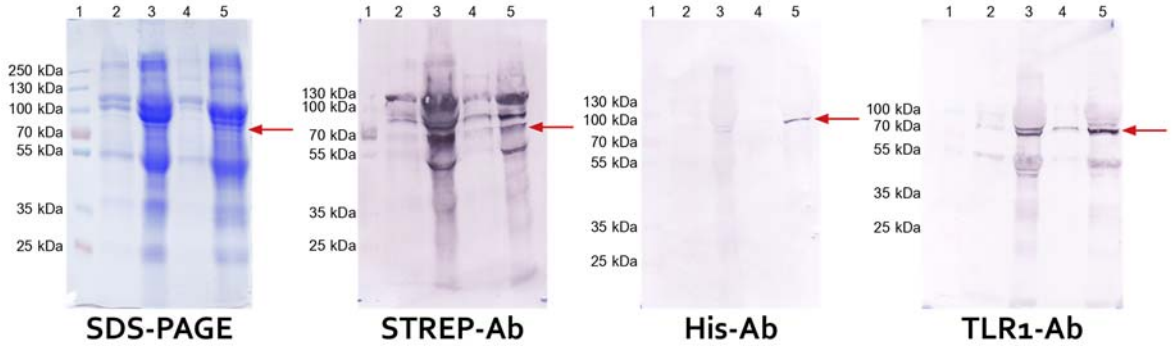

Lane	SMT_dneo(2)_24-mTLR1-C1 and -C2 (64.9 kDa)
1	PageRuler Plus prestained (Thermo Scientific)
2	Eluate (Ni-IMAC) – SMT_dneo(2)_24-mTLR1-455-C1
3	14.3x concentrated – SMT_dneo(2)_24-mTLR1-455-C1
4	Eluate (Ni-IMAC) – SMT_dneo(2)_24-mTLR1-455-C2
5	14.3x concentrated – SMT_dneo(2)_24-mTLR1-455-C2

Figure 4-43: 12 % SDS-PAGE and Western blot analysis of mTLR1 expressed in cell lines SMT_dneo(2)_24-mTLR1-C1 and SMT_dneo(2)_24-mTLR1-C2. mTLR1 was produced in 1.5 L and 1 L batch cultures using the cell lines SMT_dneo(2)_24-mTLR1-C1 and -C2 respectively. SDS-PAGE and Western blot shows mTLR1 after one round of purification (Ni-IMAC) and concentrated mTLR1 for both cell lines. Western blots were exposed to anti-Strep, anti-His or anti-TLR1 antibodies.

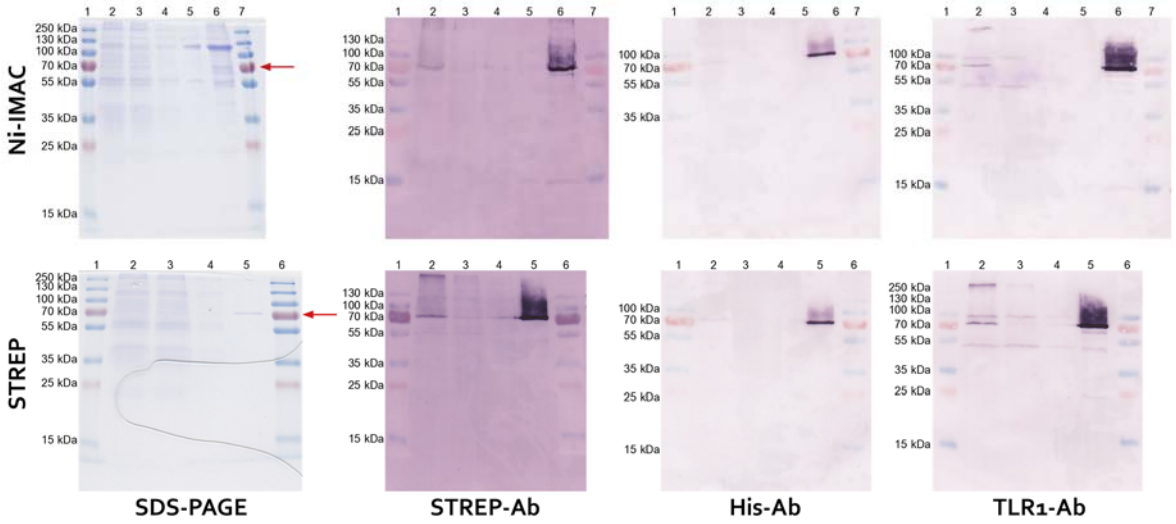

Lane	TE3-B4-H1-mTLR1/mPRAT4A-C1 (64.9 kDa)	TE3-B4-H1-mTLR1/mPRAT4A-C2 (64.9 kDa)
1	PageRuler Plus prestained (Thermo Scientific)	PageRuler Plus prestained (Thermo Scientific)
2	Non-binding fraction	Non-binding fraction
3	Wash 1	Wash
4	Wash 2	Eluate – mTLR1
5	Eluate – mTLR1	PageRuler Plus prestained
6	PageRuler Plus prestained	-

Figure 4-44: 12 % SDS-PAGE and Western blot analysis of purified TE3-B4-H1-mTLR1/mPRAT4A-C1 and TE3-B4-H1-mTLR1/mPRAT4A-C2. mTLR1 was produced in 1 L batch cultures using the cell lines TE3-B4-H1-mTLR1/mPRAT4A-C1 and -C2. SDS-PAGE and Western blots show fractions of mTLR1 purifications done using Ni-IMAC or Strep beads for cell lines TE3-B4-H1-mTLR1/mPRAT4A-C1 and -C2 respectively. Western blots were exposed to anti-Strep, anti-His or anti-TLR1 antibodies. Even though purified mTLR1 could be obtained with Strep purification the achieved yields were below the detection limit of the used photometric methods.

4.4.4 CHO Lec3.2.8.1 TLR5 producer cell lines

The hTLR5 ECD construct was introduced with the vector pFlpBtM-II(beta)-sshTLR5_1-391-VLR-TEV-STrEP-H8 (Section 4.4.1) into the master cell line SMT_dneo(2)_24 using RMCE. To evaluate the effects of chaperone co-expression hTLR5 was also integrated into locus 1 (P_{EF}-FRT_3-*eGFP*-FRT_{wt}-Δ*neo*) of the binary cell line TE3-B4-H1-eGFP/mPRAT4A-1.1 (Section 4.3.3). This cell line already contains mPRAT4A in exchange locus 2 (P_{EF}-FRT_{13}-*mRAT4A*-FRT_{14}-Δ*puro*). Figure 4-45 shows the successful exchange of eGFP against hTLR5 using flowcytometry for two clones of the producer cell lines SMT_dneo(2)_24-sshTLR5 and the binary producer cell line TE3-B4-H1-sshTLR5/mPRAT4A-C1.

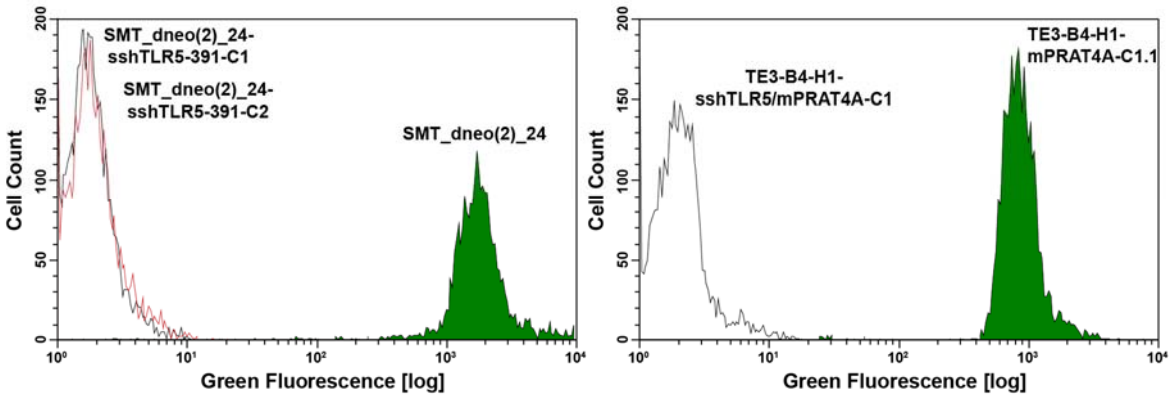

Figure 4-45: Generation of hTLR5 producer cell lines: (Left) Histogram overlays obtained with the Guava easyCyte flowcytometer show the level of green fluorescence of the RMCE master cell line SMT_dneo(2)_24 (green solid) and the thereof derived producer cell lines SMT_dneo(2)_24-mTLR1-455-C1 and -C2 (black and red lines respectively) after successful exchange of eGFP against hTLR5. **(Right)** Likewise the binary cell line TE3-B4-H1-eGFP/mPRAT4A-1.1 (green solid) and the thereof derived producer cell line TE3-B4-H1-sshTLR5/mPRAT4A-C1 (black line) are shown.

Expression of hTLR5 was tested in 1.5 L batch cultures for the cell lines SMT_dneo(2)_24-sshTLR5-C1 and SMT_dneo(2)_24-sshTLR5-C2 using culture flasks, followed by one round of Ni-IMAC (Figure 4-46). The binary cell line TE3-B4-H1-sshTLR5/mPRAT4A-C1 was expressed in a 1 L batch culture and subjected to one round of Strep purification (Figure 4-47). No quantitative yields could be obtained for the binary cell line TE3-B4-H1-sshTLR5/mPRAT4A-C1 as expression could only be detected using Western blot analysis. While expression of hTLR5 could be detected for the cell lines SMT_dneo(2)_24-sshTLR5-C1 and SMT_dneo(2)_24-sshTLR5-C2 using SDS-PAGE (Figure 4-46) quantification was not possible due the co-purification of unspecifically bound protein. However, volumetric yield could be obtained for the cell line SMT_dneo(2)_24-sshTLR5-C1 expressed in a 20 L perfusion reactor. Following two rounds of Ni-IMAC and one round of Strep purification a volumetric yield of 0.07 mg/L was

obtained. However, two bands on SDS-PAGE in the non-binding fraction (lane 2) might indicate that hTLR5 did not fully bind to the column (Figure 4-48). A stronger band at ~ 50 kDa and a weaker band right above it could fit the size of hTLR5 (57.5 kDa). If this is true the actual expression of hTLR5 would be higher than obtained from purification. Unfortunately no Western blot analysis nor MS-data is available for those two bands to confirm the identity of hTLR5. This suspicion was confirmed in a second perfusion reactor run performed in a 40 L scale with improved yields. Following one round of Ni-IMAC and one round of Strep purification volumetric a yield of 0.1 mg/L were obtained. No volumetric yields can be compared to determine if the co-expression of hTLR5 with mPRAT4A improved hTLR5 expression. However, as described for mTLR2 in Section 4.4.2, the co-expression of mPRAT4A seems to reduce hTLR5 yields. As described above hTLR5 co-expressed with mPRAT4A in batch culture can only be detected using Western blot analysis whereas hTLR5 expressed alone can also be detected using SDS-PAGE which leads to the conclusion that hTLR5 expression is negatively influenced.

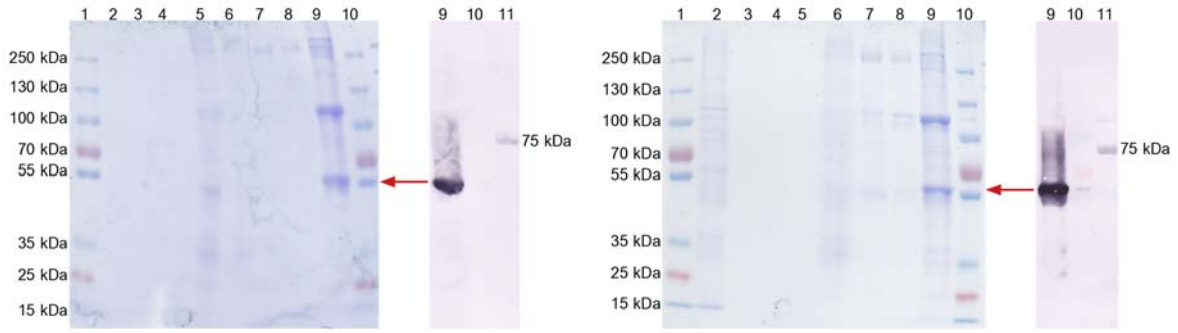

Lane	SMT_dneo(2)_24-sshTLR5-C1 (57.5 kDa)	SMT_dneo(2)_24-sshTLR5-C2 (57.5 kDa)
1	PageRuler Plus prestained	PageRuler Plus prestained
2	Culture supernatant	Culture supernatant
3	Filtrate of concentration	Filtrate of concentration
4	Filtrate of dialysis	Filtrate of dialysis
5	Concentrated and dialyzed sshTLR5	Concentrated and dialyzed sshTLR5
6	Non-binding fraction	Non-binding fraction
7	Wash 1	Wash 1
8	Wash 2	Wash 2
9	Eluate – hTLR5	Eluate – hTLR5
10	Fermentas PageRuler (Thermo Scientific)	Fermentas PageRuler (Thermo Scientific)
11	Precision Plus Protein Unstained (Bio-Rad)	Precision Plus Protein All Blue (Bio-Rad)

Figure 4-46: 10 % SDS-PAGE and Western blot analysis of purified SMT_dneo(2)_24-sshTLR5-C1 and SMT_dneo(2)_24-sshTLR5-C2. hTLR5 was produced in 1.5 L batch cultures using the cell lines SMT_dneo(2)_24-sshTLR5-C1 and -C2. SDS-PAGE and Western blots show fractions of sshTLR5 purifications done using Ni-IMAC. However, as one round of purification was not sufficient to obtain volumetric yields, these were estimated using ImageJ. The percentage of the hTLR5 band was calculated from the obtained histograms and used for the calculation of the estimated yields of SMT_dneo(2)_24-sshTLR5-C1 and SMT_dneo(2)_24-sshTLR5-C2 (0.11 mg/L and 0.17 mg/L respectively).

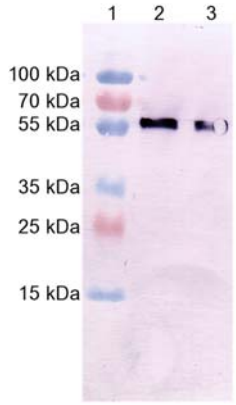

Lane	TE3-B4-H1-sshTLR5/mPRAT4A-C1 (57.5 kDa)
1	Fermentas PageRuler (Thermo Scientific)
2	Pooled eluate fractions of sshTLR5
3	2x concentrated Pooled eluate fractions of hTLR5

Figure 4-47: 10 % Western blot analysis of purified TE3-B4-H1-sshTLR5/mPRAT4A-C1. hTLR5 was produced in 1 L batch culture using the binary cell line TE3-B4-H1-sshTLR5/mPRAT4A-C1. Western blot analysis show the pooled eluate fractions of hTLR5 after Strep purification as well as 2x concentrated fraction of the same. However, volumetric yields were not high enough to be quantified or detected on SDS-PAGE.

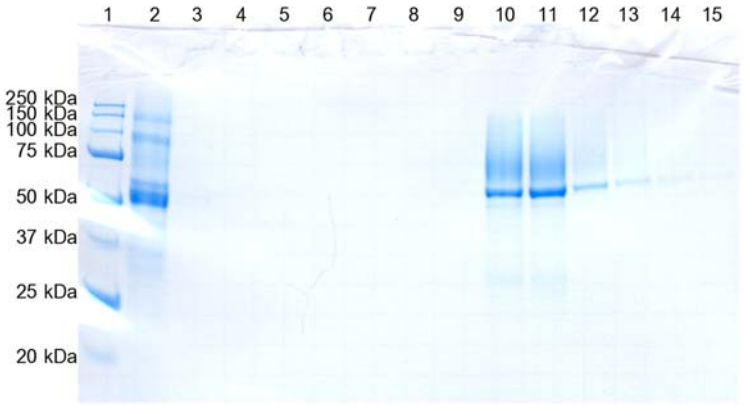

Lane	SMT_dneo(2)_24-sshTLR5-C1 (57.5 kDa)
1	Precision Plus Protein Unstained (Bio-Rad)
2	Non-binding fraction
3-9	Wash fractions
10-15	hTLR5 eluate fractions

Figure 4-48: 12 % SDS-PAGE of purified hTLR5 from expression in perfusion reactor using SMT_dneo(2)_24-sshTLR5-C1. hTLR5 that was produced in a 30 L perfusion reactor using the cell line SMT_dneo(2)_24-sshTLR5-C1 and purified using two rounds of Ni-IMAC and one round of Strep purification. Yield: 0.05 mg/L.

4.4.5 Summary – expression and co-expression of TLR ECDs and chaperones

Table 4-4 summarises the results obtained for the expression of the TLR ECD constructs mTLR1, mTLR2 and hTLR5 as well as their co-expression with the molecular chaperones mPRAT4A or mGRP94 as described in Section 4.4.2 – Section 4.4.4. The co-expression of

chaperones was not shown to improve the expression of TLRs. In the contrary, it was demonstrated that mTLR2 yields were reduced up to ~ 67 %. Most likely the yields of mTLR1 and hTLR5 were similarly impacted. A detailed discussion about the reasons that might have led to this result are available in Section 5.4.

Table 4-4: Summary table TLR (co)-expression

Cell Line	Locus 1	Locus 2	Yield mg/L Batch culture	Yield mg/L Bioreactor
BBA10-TLR2-C1	mTLR2	N/A	0.5	0.9 ± 0.3
BBA10-TLR2-C7	mTLR2	N/A	0.9	-
SMT_dneo(2)_24-ssmTLR2-C7	mTLR2	N/A	WB	1.4 ± 0.1
TE3-B4-H1-ssmTLR2/mPRAT4A-C1	mTLR2	mPRAT4A	SDS-PAGE/WB	0.5 ± 0.1
TE3-B4-H1-ssmTLR2/mPRAT4A-C2	mTLR2	mPRAT4A	SDS-PAGE/WB	-
TE3-B4-H1-ssmTLR2/mGRP94-C1	mTLR2	mGRP94	SDS-PAGE/WB	0.6 ± 0.1
SMT_dneo(2)_24-mTLR1-455-C1	mTLR1	N/A	SDS-PAGE/WB	-
SMT_dneo(2)_24-mTLR1-455-C2	mTLR1	N/A	SDS-PAGE/WB	-
TE3-B4-H1-mTLR1/mPRAT4A-C1	mTLR1	mPRAT4A	SDS-PAGE/WB	-
TE3-B4-H1-mTLR1/mPRAT4A-C2	mTLR1	mPRAT4A	SDS-PAGE/WB	-
TE3-B4-H1-mTLR1/mGRP94-C1	mTLR1	mGRP94	TBD	-
SMT_dneo(2)_24-sshTLR5-C1	hTLR5	N/A	SDS-PAGE	0.1
SMT_dneo(2)_24-sshTLR5-C1	hTLR5	N/A	SDS-PAGE	-
TE3-B4-H1-sshTLR5/mPRAT4A-C1	hTLR5	mPRAT4A	WB	-

5 Discussion

5.1 Stable cell line development

CHO cell lines are the most commonly used host for recombinant protein production in industrial applications (Datta *et al.*, 2013). Their well-established safety profile eases the approval of biopharmaceuticals with regulatory agencies and extensively optimized processes are already in place (Estes *et al.*, 2014). As a mammalian host PTMs are processed and can be modified to improve intrinsic properties such as plasma-half life, shield immunogenic epitopes or increase the uptake into target cells (Walsh *et al.*, 2006). The time invested into the generation and isolation of stable isogenic producer cell lines is compensated with the prospect to scale up protein production in a reproducible and robust manner using bioreactors.

Standard methods for stable cell line generation require the random integration of each target gene into the host genome. The identification of recombinant cells is based on the co-introduction of a selectable marker gene of choice. This marker can either result in the rescue or improvement of essential cellular processes as in the DHFR-system (Urlaub *et al.*, 1980) or the GS-system (Cockett *et al.*, 1990) or introduce entirely new properties into recombinant cells. For example, the introduction of a bacterial antibiotic marker will introduce resistance to a specific antibiotic (Southern *et al.*, 1982, Vara *et al.*, 1986) whereas the introduction of fluorescent marker genes will enable the identification of recombinant cells via flowcytometric methods which are preferably used for HTP approaches (Shi 2011). As random integration of a transgene into the host genome will result in unpredictable expression properties due to the site of integration (position-effect) and the number of transgene integrations, extensive screening is required to isolate isogenic high producer cell lines for each protein target (Wurm, 2004).

To simplify the generation of high producer cell lines the use of site specific recombinases for tag-and-target and tag-and-exchange strategies was introduced. Particularly Flp/*FRT* based methods are gaining popularity including: The Flp-in system (O'Gorman *et al.*, 1991, Invitrogen, 2010), the FLIRT system with its variations (Huang *et al.*, 1997, Kaufman *et al.*, 2008, Wilke *et al.*, 2010) and finally the RMCE system (Schlake *et al.*, 1994). While the generation of isogenic high producer master cell lines follows the same pattern as for

conventional cell line development, this initial effort to isolate a suitable master cell line with a tagged genomic locus enables the comparatively quick generation of high producer cell lines containing a GOI. Multiplexing approaches which employ the use of different sets of heterospecific *FRT* sites were proposed (Turan *et al.*, 2010).

Numerous examples wherein the co-expression of proteins favour the expression or function of a target gene are described in the literature. The use of one expression cassette (monocistronic or polycistronic) or several expression cassettes within one or more expression vectors can be used for the co-expression of protein subunits, ligands or accessory molecules. For example: (i) Improved cell-surface expression level were obtained for a G-protein-coupled receptor (GPCR), called olfactory receptor, when co-expressed with Hsc70t in HEK293 cells which was otherwise retained within the ER (Neuhaus *et al.*, 2006). (ii) The co-expression of farnesyltransferase heterodimer subunits in *Sf*9 improved functional activity of this enzyme (Chen *et al.*, 1993). (iii) Functional cytokine expression and *in vivo* half-life were improved in CHO cells for an IL-15 variant when combined with its receptor (Han *et al.*, 2011). Additional examples are reviewed elsewhere (Romier *et al.*, 2006, Kerrigan *et al.*, 2011). Expression systems which enable the co-expression of several protein targets through site specific recombination using the Cre/*loxP* system were established in *E.coli* (Acembl) (Bieniossek *et al.*, 2009) insect cells (MultiBac system) (Berger *et al.*, 2004, Fitzgerald *et al.*, 2007) and mammalian cells (MultiLabel) (Kriz *et al.*, 2010) and put to use for the co-expression of several multi-protein complexes (Bieniossek *et al.*, 2008).

In this work a binary Flp/*FRT* based RMCE system was set up in the glycosylation deficient CHO Lec3.2.8.1 cell line (Section 4.1). This binary system enables the co-expression of target genes at different pre-defined genomic loci. The generation and evaluation of this system is discussed in Section 5.2 and Section 5.3 respectively. The co-expression of TLR ECD constructs together with their chaperones mPRAT4A and mGRP94 are discussed in Section 5.4).

5.2 Generation of binary CHO Lec3.2.8.1 RMCE master and producer cell lines

Expression hosts capable of PTMs are favourable for protein expression and function of complex proteins. However heterogeneous glycosylation pattern do interfere in structural biology applications and thus the use of glycosylation inhibitors during protein expression

or the use of glycosylation deficient cell lines becomes necessary (Aricescu *et al.*, 2006, Nettleship *et al.*, 2010). CHO Lec3.2.8.1, a glycosylation deficient cell line which expresses a uniform $GlcNAc_2Man_5$ profile on the protein surface (Stanley, 1989), was used for the generation of the Flp/*FRT* based binary RMCE system described in this work.

It was desired to establish a cell line which enables the independent integration of two transgenes at different genomic loci. The co-expression of proteins with accessory molecules or the co-expression of multi-protein complexes might be beneficial for difficult to express targets. For this purpose binary RMCE cell lines containing the exchange cassettes P_{EF}-FRT_3-*eGFP*-FRT_{wt}-Δ*neo* and P_{EF}-FRT_{13}-*tdTomato*-FRT_{14}-Δ*puro* were generated (Section 4.1.4). Site specific recombination based on the Flp/*FRT* system was used to integrate transgenes at pre-defined chromosomal loci. The use of distinct sets of heterospecific *FRT* sites (FRT_3/FRT_{wt} and FRT_{13}/FRT_{14}) enabled the independent integration at either locus as described in Section 4.3 and Section 4.4.

The fluorescent marker gene *tdTomato* present in exchange locus 2 (P_{EF}-FRT_{13}-*tdTomato*-FRT_{14}-Δ*puro*) was used for the isolation of binary RMCE master cell lines after the genomic tagging of two different RMCE master cell lines that already contained locus 1 (P_{EF}-FRT_3-*eGFP*-FRT_{wt}-Δ*neo*) in their genome. As the cell sorter used for this work were not operated under sterile conditions drawbacks from frequent contaminations resulted in the delayed generation of the binary master cell lines. The attempt to control contaminations through the addition of antibiotics penicillin, streptomycin and gentamicin were of limited success as they seemed to have an adverse effect on the sorted cells most likely due to the cellular stress that resulted in low cell vitalities. Cells sorted without antibiotics however could be isolated as pools (≥22.000 positive cells derived from $1x10^7$ sorted cells) if not contaminated. Attempts to isolate single cells or a small pools of up to 100 cell in multi-well formats failed. When sorting small cell numbers of 1 cell/well or 10 cells/well these did not proliferate either due to the statistical probability of having a living cell in one well or due to the small cell number of surviving cells in each well. When sorting 100 cells/well however the prolonged time required for sorting into 96-well plates in an open system resulted in the contamination of virtually all wells. While the isolation of single cells via FACS would have been favourable to isolate truly isogenic master cell lines, the use of limiting dilution or the use of a second round of FACS yielded virtually isogenic cell lines as described in Section 4.1.4. It should be noted

that binary master cell line selection was based entirely on the level of fluorescence as selection criteria. No antibiotic selection pressure was used as this was shown to result in heterogeneous expression and epigenetic silencing of the isolated cells after removal of selective pressure (Liu *et al.*, 2006). Due to the problems confronted during FACS in this work the isolation of producer cell lines after RMCE was done using limiting dilution in combination with selective pressure. Even though the isolation of producer cell lines using limiting dilution can be time-consuming due to the varying amount of rounds required for the successful isolation of producer cell lines, the process was not slowed down due to contaminations and thus more predictable.

The integrity of both exchange loci was confirmed through genomic PCR (Section 4.1.5). The number of integration sites for locus 1 (P_{EF}-*FRT*$_3$-*eGFP*-*FRT*$_{wt}$-Δ*neo*) was previously determined by Wilke *et al.*, (2011) for the cell line SWI3_26 and by Sarah Maria Tokarski (HZI) for the cell line SMT_dneo(2)_24. Both cell lines comprise one exchange locus. To determine the number of integrated loci for the newly introduced locus 2 (P_{EF}-*FRT*$_{13}$-*tdTomato*-*FRT*$_{14}$-Δ*puro*) in the binary RMCE master cell lines Southern blots using digoxigenin (DIG)-labelling were done but yielded no results. Likewise no results using radioactive southern blots could yet be obtained. While this may leave doubts about the number of integration sites, the behaviour of the cell lines does not lead to the conclusion that more than one second locus was integrated. The exchange efficiency does not seem to be negatively influenced for locus 2. If more than one locus would be present within the binary RMCE cell lines it would be more difficult to obtain tdTomato negative clones as it would require the successful exchange in all integrated loci. Successful integration however is a rare event. As described in the next paragraph the simultaneous exchange of both exchange loci failed due to this very reason. If more than one second exchange locus would be present within the binary RMCE cell lines it would be very difficult to obtain tdTomato negative clones. Nonetheless, the number of integration sites still needs to be confirmed. An alternative or addition to Southern blot analysis would be whole genome sequencing of our binary RMCE master cell lines. This would not only confirm the number of integration loci but also the chromosomal integration site.

The generation of binary producer cell lines was performed through sequential integration into each exchange locus at one time. Attempts to exchange both loci simultaneously were not successful. Even though the RMCE reaction is driven through the molecular excess of

the used exchange plasmids as described by Seibler *et al.*, (1998) this does not necessary result in the exchange of both loci in the same cell. Although this event was observed microscopically in 100 mm cell culture dishes the isolation of these few cells was not possible. The application of selective pressure using both antibiotics (G418 and puromycin) to screen for double positive cells resulted in virtually total cell death of all present cells as the few that might have survived were not able to proliferate any further. A timeline for the generation of binary producer cell lines is shown in Figure 5-1. Each round of RMCE and producer cell line isolation takes 6-9 weeks thus at least 12-18 weeks are required for the generation of a binary producer cell line. This does not include expression analysis which would be required after each round of RMCE. Depending on the scale (40 mL – 1.5 L batch cultures) as well as the method of culture supernatant dialysis and concentration this will take another 1-3 weeks including sample purification and protein analysis. 3 months for the generation of a producer cell line with only one GOI is clearly an improvement to conventional cell line development which can take over 1 year (Wurm, 2004). The generation of a binary producer cell line with two GOIs does require approximately 6 months. While this is still an improvement the generation of binary producer cell lines would greatly benefit if optimized for FACS under sterile conditions as timelines could be cut significantly when double positive clones could be isolated in one step.

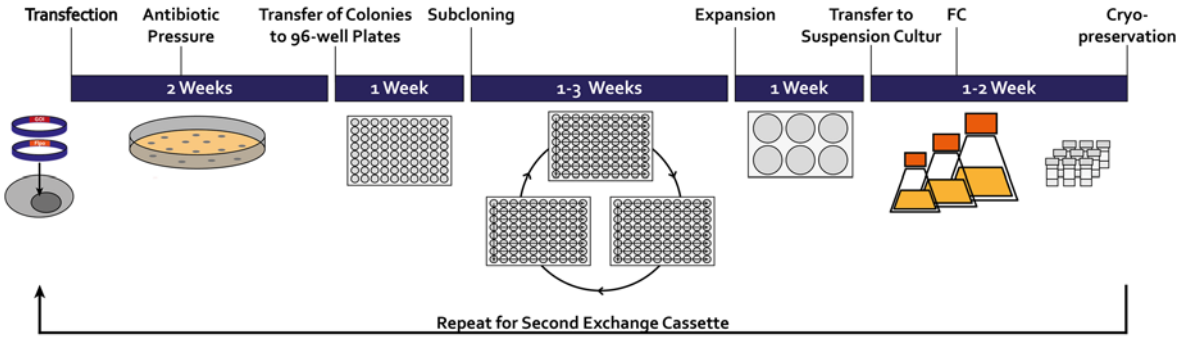

Figure 5-1: Timeline for the generation of binary producer cell lines using RMCE. After transfection of a binary master cell line with an exchange vector containing the first GOI and a helper vector containing Flippase the transfected cells are seeded to cell culture dishes after 1 day of incubation in 12-well suspension. Antibiotic pressure is applied 5 days after transfection. 2 weeks after transfection colonies can be picked from the cell culture dish and transferred to 96-well plates were they are permitted to grow for 1 week. The most promising clones are subjected to several rounds of limiting dilutions to obtain subclones of the desired producer cell line. This step can take up to 3 weeks and is the most labour intensive step. The isolated producer cell lines than are expanded gradually in different multi-well formats (1 week) before transfer into serum free suspension culture. Flowcytometric (FC) analysis is followed by expansion of the producer cell lines and cryopreservation. Analysis for protein expression (not shown) does take an additional 1-3 Weeks depending on the chosen format. To obtain a binary producer cell line this process needs to be repeated for the second GOI.

Furthermore it could be clearly observed that the selection stringency of locus 1 (P_{EF}-*FRT*$_3$-*eGFP*-*FRT*$_{wt}$-Δ*neo*) was significantly lower than that of locus 2

(P_{EF}-FRT_{13}-*tdTomato*-FRT_{14}-Δ*puro*) and thus required additional rounds of limiting dilution to obtain the desired producer cell lines. This can be attributed to the apparent resistance of CHO Lec3.2.8.1 cells towards G418 which require higher concentrations of antibiotic (2 mg/mL) compared to puromycin which only requires low concentrations (15 µg/mL). The more gradual decrease observed in cell viability when using G418 compared to the more sharp decrease in cell viability when using puromycin while estimating appropriate titres supports this observation in the obtained kill-curves (Figure 4-1). Thus future CHO Lec3.2.8.1 master cell lines should relinquish Δ*neo* as a selection trap and rather choose an alternative gene such as *hyg* which confers resistance towards hygromycin B and shows a similarly sharp decrease in cell viability as does puromycin in the obtained kill curve (Figure 4-1). However when producer cell line isolation could be optimized for FACS the leaky resistance against G418 would not present a challenge anymore as only GFP negative cells would be sorted.

RMCE compared to other Flp/*FRT* based integration methods bears the advantage that no additional prokaryotic elements are co-introduced with the GOI which might induce epigenetic silencing (Schlake *et al.*, 1994). The only prokaryotic elements introduced in the system are those present in the tagging vector. However, master cell lines are isolated according to their expression profile presented by the fluorescent marker in the integrated loci and observed over several weeks for uniform expression (Section 4.1.4). Thus it can be presumed that the site of exchange cassette integration was within the transcriptionally active euchromatin structure and that potential effects of epigenetic silencing can be disregarded for those loci. The system could be improved through the introduction of *cis*-regulatory elements such as S/MARs to oppose heterochromatin effects as it is occasionally done in conventional cell line development (Wurm, 2004). However instead of flanking the GOI which would unnecessarily increase the size of the insert and thus potentially reduce the integration efficiency of the RMCE reaction *cis*-regulatory elements could be designed to flank the entire exchange cassette before genomic tagging.

5.3 Evaluation of binary RMCE cell lines expressing tdTomato

To evaluate position and gene dose effects within the integrated exchange loci for several RMCE cell lines, the expression level of tdTomato which was transcribed in one or two loci within a given cell line was determined as described in Section 4.2. The obtained yields confirmed that the site of integration is directly correlated to the expression level of

tdTomato. Furthermore, the robustness of expression was shown when performed in triplicate which resulted in reproducible expression level for each cell line. The expression of tdTomato is dependent on the expression capabilities of each locus and shown to be cumulative. This allows the prediction of protein level if each locus express the same protein. In general, binary master cell lines with exchange loci integrated at genomic hot spots will be most desirable for difficult to express protein targets.

However, the use of master cell lines containing stable loci with varying expression capabilities may be of advantage for the co-expression of subunits that are required in different ratios for optimal expression such as light and heavy chains of antibodies (Schlatter *et al.*, 2005) or accessory molecules which are not required in abundance and therefore should not unnecessarily occupy the cellular transcription and translation machinery.

5.4 Expression of TLR ECD constructs

The information available about the expression of TLR ECD constructs is limited. Until today the production of TLRs still poses a formidable challenge. An overview regarding the current state for each TLR evaluated in this work (TLR2, TLR5 and TLR1) in position to the obtained outcomes is given in the following Sections.

5.4.1 Expression of TLR2 ECD

The expression of human and murine TLR2 ECD constructs fused to VLR fragments in High Five insect cells was reported by Jin *et al.*, (2007) and Kang *et al.*, (2009). While no specific yield for the human TLR2 ECD constructs were given a murine TLR2 ECD construct was reported to have an approximate volumetric yield of 100 µg/L by Kang *et al.*, (2009). Several TLR2 ECD hybrids fused with VLR fragments at their C- or N-terminus were screened for soluble expression (Jin *et al.*, 2007). The longest murine TLR2 ECD hybrid that was C-terminally fused at its last LRR sequence (LRR19) with the VLR fragment was successfully used for co-crystallisation with mTLR6 upon binding to the di-acylated lipopeptide Pam_2CSK_4 (Kang *et al.*, 2009). Likewise the longest human TLR2 ECD hybrid was co-crystallized with hTLR1 after binding to the tri-acylated lipopeptide ligand Pam_3CSK_4 (Jin *et al.*, 2007).

In this work a murine TLR2 construct that comprises the complete ECD including its own signal peptide, all LRR sequences and it natural LRRCT capping motive was utilized. RMCE based integration into several CHO Lec3.2.8.1 producer cell lines yielded soluble protein with volumetric yields of up to 0.9 mg/L in batch cultures and up to 1.5 mg/L when cultivated in a bioreactor (Section 4.4.2). Compared to the transient expression in insect cells used in the published literature (Jin *et al.*, 2007, Kang *et al.*, 2009) the production of mTLR2 was improved when expressed stably in CHO Lec3.2.8.1. This was further supported by previous experiments performed within our own group in which the full mTLR2 ECD construct was expressed in insect cells. While similar quantities of the mTLR2 ECD (up to 1 mg/L) were expressed these were only present in an insoluble form (Meyer, 2012) or showed strong batch to batch variations (personal communication Joop van den Heuvel, HZI). Likewise transient expression of mTLR2 in HEK293-6E cells yielded only insoluble protein (Meyer, 2012). In general higher protein yields can be obtained with transient expression systems due to the high copy-number of transgenes introduced into the transfected cells. However the extensive overexpression of a target protein may also cause problems if the protein-folding machinery is overloaded. This can cause protein aggregation that results in the retention of the improperly folded protein within intracellular compartments thus limiting the amount of soluble protein (Ishiyama *et al.*, 2010, Halff *et al.*, 2014). Clearly the stable expression of a single-copy mTLR2 ECD in CHO Lec3.2.8.1 is favourable to transient expression in BEVS or HEK293-6E when soluble protein is required. Knowing this, it would be worthwhile to evaluate the stable expression of a chimeric mTLR2-VLR construct in CHO Lec3.2.8.1 as this might positively influence volumetric yields. However the screening of constructs in transient HEK396-6E would still face the problem of protein aggregation if performed under standard conditions. The reduction of total protein expression as suggested by Halff *et al.*, (2014) through the transfection with smaller amounts of the express vector could improve the soluble expression of mTLR2 constructs in HEK293-6E. A different approach to improve the expression of the mTLR2 ECD was pursuit in this work. The co-expression of the mTLR2 ECD with the molecular chaperones mPRAT4A and mGRP94. To do so binary producer cell lines in CHO Lec3.2.8.1 that stably co-express the mTLR2 ECD and either mPRAT4A or mGRP94 were generated (Section 4.4.2). Expression of mPRAT4A and mGRP94 was confirmed after integration into locus 2 (P_{EF}-*FRT*$_{13}$-*tdTomato*-*FRT*$_{14}$-Δ*puro*) of the binary RMCE cell line TE3-B4-H1 (Section 4.3.3). Afterwards the mTLR2 ECD was integrated into

locus 1 (P_{EF}-FRT_3-*eGFP*-FRT_{wt}-Δ*neo*). The expression of mTLR2 in 2.5 L bioreactors yielded volumetric yield of 0.5 ± 0.1 mg/L and 0.6 ± 0.1 mg/L for the cell lines TE3-B4-H1-ssmTLR2/mPRAT4A-C1 and TE3-B4-H1-ssmTLR2/mGRP94-C1 respectively. Thus the expression of mTLR2 was clearly reduced when co-expressed with molecular chaperones. Reasons why the co-expression of TLR2 with mPRAT4A did not improve protein expression are discussed in Section 5.4.4.

5.4.2 Expression of TLR5 ECD

Yoon *et al.*, (2012) attempted to produce TLR5 ectodomains form several organisms including human, mouse, frog, trout and zebrafish in High Five insect cells. The full ECD construct of zebrafish TLR5 was the only one to express. However the obtained volumetric yields of secreted soluble protein remained clearly below 50 µg/L. To obtain sufficient quantities for structural analysis the creation of dsTLR5-VLR hybrids was pursued. Crystal structures could be solved for dsTLR5 ECDs with C-terminally fused VLR fragments at LRR12 and LRR14 but no specific yield were described. The same group further improved the expression of the non-hybrid dsTLR5 ECD through the addition of the flagellin FliC during production thus increasing the volumetric yield to 0.4 mg/L for the complex. This approach however could not be transferred to human TLR5. The expression of human TLR5 was aided through the generation of hTLR5-VLR hybrids. But only very short fragments could be expressed. The fusion of VLR fragments to the C-terminus at LRR4 or LRR6 yielded ~0.3 mg/L. The fusion of VLR fragments to both termini even yielded 0.8 mg/L when fused to LRR11 and LRR14. Likewise the expression of dsTLR5-VLR hybrids could be improved for truncated dsTLR5 domains if VLR fragments were fused at one or both termini reaching yields up to 3.8 mg/L (Hong *et al.*, 2012). However none of the short expressible hTLR5-VLR-hybrids was able to form a complex with FliC.

In this work a human TLR5-VLR hybrid was used. The hTLR5 ECD was fused at its C-terminus with a VLR fragment at LRR16 to ease expression. Upon stable integration into CHO Lec3.2.8.1 cells volumetric yields of 0.1 mg/L were achieved when cultivated in a perfusion reactor (Section 4.4.4). Comparable constructs, with C-terminal VLR-fusions at LLR14 and LRR17, tested by Hong *et al.*, (2012) in High Five insect cells did not yield any protein. As for the mTLR2 ECD discussed in Section 5.4.1 the over-expression of hTLR5 in insect cells appears to result in the intracellular accumulation of the protein as shown by Meyer, (2012) for several hTLR5 ECD constructs. The single-copy expression in stable

CHO Lec3.2.8.1 improves the soluble expression of hTLR5 compared to similar ECD constructs tested by Hong *et al.*, (2012) in BEVS. While a volumetric yield of 0.1 mg/L soluble hTLR5 in CHO Lec3.2.8.1 leaves space for improvement it is the largest solubly expressible hTLR5 ECD construct reported so far. To improve the expression of hTLR5 in CHO Lec3.2.8.1 a binary producer cell that co-expresses hTLR5 and mPRAT4A was generated (Section 4.4.4). Expression of hTLR5 was confirmed via Western blot but no volumetric yields could be obtained. The effects of chaperone co-expression are discussed in Section 5.4.4.

5.4.3 Expression of TLR1 ECD

A human TLR1 ECD C-terminally fused at LRR17 with a VLR fragment was previously expressed in High Five insect cells to obtain sufficient quantities for crystallization but no specific yields were given. Additional human and murine TLR1-VLR hybrids that can be solubly expressed in High Five were reported (Jin *et al.*, 2007). Three of these described soluble murine TLR1 constructs that were C-terminally fused at LRR14, LRR16 and LRR19 were screened in HEK293-6E by Agarwal, (2012) for this work. The mTLR1 construct fused C-terminally at LRR16 with a VLR fragment was the only one to show expression in HEK293-6E and was chosen for stable integration into CHO Lec3.2.8.1 via RMCE (Section 4.4.3). While mTLR1 was expressed solubly in CHO Lec3.2.8.1 no volumetric yields could be obtained due to its low expression level. To improve the expression of mTLR1 binary producer cell lines expressing mTLR1 with one chaperone, either mPRAT4A or mGRP94, were generated (Section 4.4.3). While the expression of mTLR1 in the binary producer cell line TE3-B4-H1-mTLR1/mGRP94-C1 could not yet be confirmed, the binary producer cell lines TE3-B4-H1-mTLR1/mPRAT4A-C1 and TE3-B4-H1-mTLR1/mPRAT4A-C2 do express mTLR1 but the volumetric yields are still too low for quantification. A more detailed discussion on the effects of chaperone co-expression can be found in Section 5.4.4. Like hTLR5 discussed in Section 5.4.2 mTLR1 shows a very low level of expression. Large scale cultivation in a perfusion reactor is likely to give quantifiable yields but will not reach those of hTLR5. The generation of mTLR1 ECD constructs N- and C-terminally fused to VLR fragments might improve expression as previously reported for dsTLR5 and hTLR5 by Hong *et al.*, (2012).

5.4.4 Co-expression of TLR ECDs with molecular chaperones

The importance of the ER resident chaperone GRP94 for conformational maturation and cell surface trafficking of TLR1, TLR2 and TLR5 was demonstrated by Randow *et al.*, (2001) and Yang *et al.*, (2006). Likewise the role of the ER resident chaperone PRAT4A for cell surface expression of TLR1, TLR2 and TLR5 was shown by Takahashi *et al.*, (2007) and Shibata *et al.*, (2012).

The binary RMCE system established during this work (Section 4.1) was used to generate several binary producer cell lines co-expressing one TLR ECD construct (mTLR1, mTLR2 or hTLR5) together with one molecular chaperone (mGRP94 or mPRAT4A) (Section 4.3 and Section 4.4). It was anticipated that the over-expression of the molecular chaperones will support the soluble expression of the TLR ECDs. However this could not be confirmed for any of the generated binary producer cell lines as described in Section 5.4.1–Section 5.4.3. In the contrary the expression level of mTLR2 were even reduced when co-expressed with molecular chaperones. On reason why the co-expression of mPRAT4A or mGRP94 did not improve TLR ECD expression could be that the overexpression of only one chaperone is not sufficient to significantly aid the expression of the tested TLR constructs. A publication by Liu *et al.*, (2010) demonstrated that at least TLR9, present in endosomal compartments, does require both PRAT4A and GRP94 for maturation. PRAT4A was shown to serves as co-chaperone of GRP94 in a tri-molecular complex with TLR9. It cannot be excluded that TLR1, TLR2 or TLR5 also require both chaperones in a 1:1 ratio for successful maturation. If only one chaperone is overexpressed this balance would not be given. A different reason, why the co-expression of mPRAT4A or mGRP94 negatively influenced TLR expression could be the design of the construct itself. Both chaperones were designed with a C-terminal FLAG-tag downstream of the ER retention signals KDEL or PDEL. These retention signals are required for the regulation of ER-retrieval of ER resident proteins from the Golgi apparatus. The ER-retention signals are recognized by KDEL-receptors and trafficked back to the ER (Alberts, 2008). If the C-terminal FLAG tag should impair recognition of the chaperones by the KDEL receptor these would not be shuttled back to the ER and gradually lost over time. If the molecular chaperones are lost from the ER they can no longer aid the TLR folding process. Furthermore, if improperly folded TLRs are still associated with the chaperones when they are lost from the ER they might be targeted for proteasomal degradation which would explain the reduced TLR yields. Thus the FLAG tag should be

located upstream before the KDEL or PDEL sequence or left out altogether. As the isolation and purification of mGRP94 and mPRAT4A are not necessarily required the FLAG tag could be omitted and target specific antibodies could be used to detect the overexpression of both using Western blot analysis. Moreover, the overexpression of mPRAT4A and mGRP94 might have occupied significant portions of the cellular transcription and transcription machinery or even imitated an unfolded protein responses (UPR) that might have resulted in the downregulation of cellular protein synthesis (Reid *et al.*, 2014). The integration of mPRAT4A and mGRP94 into a binary RMCE master cell line with an exchange locus that exhibits low expression capabilities might be favourable.

6 Outlook

A binary RMCE system in CHO Lec3.2.8.1 cells was established. Thus the stable integration of transgenes into predefined chromosomal loci via RMCE, based on the Flp/*FRT* system, enables the co-expression of different target proteins for structural biology applications. The binary RMCE system was shown to yield predictable expression pattern for each locus and therefore allows the reproducible production of recombinant proteins after the generation of stable producer cell lines. This system expands the Multi-Host system (Meyer *et al.*, 2013) developed in our group. The use of the binary RMCE system could be adapted for other mammalian cell lines including CHO-K1 or HEK293 when native glycosylation profiles are required. Likewise compatible RMCE as well as binary RMCE approaches could be established in insect and yeast platforms.

The use of targeted integration already reduces the time necessary for the isolation of stable high producer cell lines. However, isolation of master and producer cell lines would benefit immensely when adapted for FACS under sterile conditions. Limiting dilution, which was used for the clonal isolation of producer cell lines in this work, is cumbersome labour- and time-intensive. Therefore the reduction of limiting dilution steps would be favourable. Moreover, the number of cell lines that could be processed in parallel could be expanded as each cell line would require less attention from the operator. FACS based methods for the isolation of RMCE master and producer cell lines derived from CHO-K1 are used by the Rentschler Biotechnologie GmbH for the generation TurboCell™ lines. These cut their timelines by 50 % compared to random integration based cell line development (Rehberger *et al.*, 2013).

The expression properties of the TLR ECDs discussed in Section 5.4 showed intracellular accumulation in Insect and HEK293-6E cells (Meyer, 2012) whereas the soluble expression in CHO Lec3.2.8.1 cells was clearly improved. Recently Croset *et al.*, (2012) raised awareness that while there are only minor differences in glycosylation and glycoprotein isoform patter between different HEK cell lines (HEK293-EBNA and HEK293-6E were compared) major differences could be observed between HEK and CHO-S cells which might result in non-comparable results when switching from HEK to CHO systems. This may be a concern that should be addressed for the system used in this work. Currently HEK293-6E are used for transient screening to identify constructs that express solubly. Those constructs with the highest potential than are used for the generation of stable producer cell lines in

glycosylation mutant CHO Lec3.2.8.1. If differences in the glycoprotein isoform patter between HEK and CHO-S can be considered problematic (Croset *et al.*, 2012) this problem will reflect even more on glycosylation mutant CHO Lec3.2.8.1. Therefore the establishment of a transient CHO Lec3.2.8.1 platform might be of advantage when screening for solubly expressible constructs designated for stable integration in CHO Lec3.2.8.1. Examples for transient EBNA-1 based systems in CHO cell were described in the literature (Kunaparaju *et al.*, 2005, Goepfert *et al.*, 2010, Durocher *et al.*, 2011, Daramola *et al.*, 2014).

7 Bibliography

Agarwal, S. (2012). Transient Expression and Generation of Stable CHO-RMCE Production Cell Lines for Soluble Ectodomains of TLR Proteins, Fachhochschule Flensburg.

Agrawal, S., A. Agrawal, B. Doughty, A. Gerwitz, J. Blenis, T. Van Dyke and B. Pulendran (2003). Cutting edge: different Toll-like receptor agonists instruct dendritic cells to induce distinct Th responses via differential modulation of extracellular signal-regulated kinase-mitogen-activated protein kinase and c-Fos. *J Immunol* **171**(10): 4984-4989.

Akira, S. and K. Takeda (2004). Toll-like receptor signalling. *Nat Rev Immunol* **4**(7): 499-511.

Alberts, B. (2008). Molecular biology of the cell. New York, Garland Science.

Andersen-Nissen, E., K. D. Smith, R. Bonneau, R. K. Strong and A. Aderem (2007). A conserved surface on Toll-like receptor 5 recognizes bacterial flagellin. *The Journal of Experimental Medicine* **204**(2): 393-403.

Andersen-Nissen, E., K. D. Smith, K. L. Strobe, S. L. R. Barrett, B. T. Cookson, S. M. Logan and A. Aderem (2005). Evasion of Toll-like receptor 5 by flagellated bacteria. *Proceedings of the National Academy of Sciences of the United States of America* **102**(26): 9247-9252.

Andrews, B. J., G. A. Proteau, L. G. Beatty and P. D. Sadowski (1985). The FLP recombinase of the 2[mu] circle DNA of yeast: Interaction with its target sequences. *Cell* **40**(4): 795-803.

Angov, E., C. J. Hillier, R. L. Kincaid and J. A. Lyon (2008). Heterologous protein expression is enhanced by harmonizing the codon usage frequencies of the target gene with those of the expression host. *PLoS ONE* **3**(5): e2189.

Aricescu, A. R., W. Lu and E. Y. Jones (2006). A time- and cost-efficient system for high-level protein production in mammalian cells. *Acta Crystallogr D Biol Crystallogr* **62**(Pt 10): 1243-1250.

Aricescu, A. R. and R. J. Owens (2013). Expression of recombinant glycoproteins in mammalian cells: towards an integrative approach to structural biology. *Current Opinion in Structural Biology* **23**(3): 345-356.

Backliwal, G., M. Hildinger, S. Chenuet, S. Wulhfard, M. De Jesus and F. M. Wurm (2008). Rational vector design and multi-pathway modulation of HEK 293E cells yield recombinant antibody titers exceeding 1 g/l by transient transfection under serum-free conditions. *Nucleic Acids Research* **36**(15): e96.

Backliwal, G., M. Hildinger, V. Hasija and F. M. Wurm (2008). High-density transfection with HEK-293 cells allows doubling of transient titers and removes need for a priori DNA complex formation with PEI. *Biotechnology and Bioengineering* **99**(3): 721-727.

Backliwal, G., M. Hildinger, I. Kuettel, F. Delegrange, D. L. Hacker and F. M. Wurm (2008). Valproic acid: a viable alternative to sodium butyrate for enhancing protein expression in mammalian cell cultures. *Biotechnol Bioeng* **101**(1): 182-189.

Baldi, L., N. Muller, S. Picasso, R. Jacquet, P. Girard, H. P. Thanh, E. Derow and F. M. Wurm (2005). Transient gene expression in suspension HEK-293 cells: application to large-scale protein production. *Biotechnol Prog* **21**(1): 148-153.

Barton, G. M. and J. C. Kagan (2009). A cell biological view of Toll-like receptor function: regulation through compartmentalization. *Nat Rev Immunol* **9**(8): 535-542.

Baycin-Hizal, D., D. L. Tabb, R. Chaerkady, L. Chen, N. E. Lewis, H. Nagarajan, V. Sarkaria, A. Kumar, D. Wolozny, J. Colao, E. Jacobson, Y. Tian, R. N. O'Meally, S. S. Krag, R. N. Cole, B. O. Palsson, H. Zhang and M. Betenbaugh (2012). Proteomic analysis of Chinese hamster ovary cells. *J Proteome Res* **11**(11): 5265-5276.

Becker, J., C. Timmermann, T. Jakobi, O. Rupp, R. Szczepanowski, M. Hackl, A. Goesmann, A. Tauch, N. Borth, J. Grillari, A. Puhler, T. Noll and K. Brinkrolf (2011). Next-generation sequencing of the CHO cell transcriptome. *BMC Proceedings* **5**(Suppl 8): P6.

Bell, J. K., I. Botos, P. R. Hall, J. Askins, J. Shiloach, D. M. Segal and D. R. Davies (2005). The molecular structure of the Toll-like receptor 3 ligand-binding domain. *Proc Natl Acad Sci U S A* **102**(31): 10976-10980.

Berger, I., D. J. Fitzgerald and T. J. Richmond (2004). Baculovirus expression system for heterologous multiprotein complexes. *Nat Biotech* **22**(12): 1583-1587.

Bertani, G. (1951). Studies on lysogenesis. I. The mode of phage liberation by lysogenic Escherichia coli. *journal of Bacteriology* **62**: 293-300.

Bevis, B. J. and B. S. Glick (2002). Rapidly maturing variants of the Discosoma red fluorescent protein (DsRed). *Nat Biotech* **20**(1): 83-87.

Bieniossek, C., Y. Nie, D. Frey, N. Olieric, C. Schaffitzel, I. Collinson, C. Romier, P. Berger, T. J. Richmond, M. O. Steinmetz and I. Berger (2009). Automated unrestricted multigene recombineering for multiprotein complex production. *Nat Meth* **6**(6): 447-450.

Bieniossek, C., T. J. Richmond and I. Berger (2008). MultiBac: Multigene Baculovirus-Based Eukaryotic Protein Complex Production. *Current Protocols in Protein Science*.

Blasey, H. D. and V. Jäger (1991). Strategies to Increase the Efficiency of Membrane Aerated and Perfused Animal Cell Bioreactors by an Improved Medium Perfusion. Animal Cell Culture and Production of Biologicals. R. Sasaki and K. Ikura, Springer Netherlands**:** 61-73.

Buchholz, F., P.-O. Angrand and A. F. Stewart (1998). Improved properties of FLP recombinase evolved by cycling mutagenesis. *Nat Biotech* **16**(7): 657-662.

Butters, T. D., L. M. Sparks, K. Harlos, S. Ikemizu, D. I. Stuart, E. Y. Jones and S. J. Davis (1999). Effects of N-butyldeoxynojirimycin and the Lec3.2.8.1 mutant phenotype on N-glycan processing in Chinese hamster ovary cells: application to glycoprotein crystallization. *Protein Sci* **8**(8): 1696-1701.

Cai, Z., A. Sanchez, Z. Shi, T. Zhang, M. Liu and D. Zhang (2011). Activation of Toll-like Receptor 5 on Breast Cancer Cells by Flagellin Suppresses Cell Proliferation and Tumor Growth. *Cancer Research* **71**(7): 2466-2475.

Campbell, R. E., O. Tour, A. E. Palmer, P. A. Steinbach, G. S. Baird, D. A. Zacharias and R. Y. Tsien (2002). A monomeric red fluorescent protein. *Proc Natl Acad Sci U S A* **99**(12): 7877-7882.

Chalfie, M., Y. Tu, G. Euskirchen, W. W. Ward and D. C. Prasher (1994). Green fluorescent protein as a marker for gene expression. *Science* **263**(5148): 802-805.

Chang, V. T., M. Crispin, A. R. Aricescu, D. J. Harvey, J. E. Nettleship, J. A. Fennelly, C. Yu, K. S. Boles, E. J. Evans, D. I. Stuart, R. A. Dwek, E. Y. Jones, R. J. Owens and S. J. Davis (2007). Glycoprotein Structural Genomics: Solving the Glycosylation Problem. *Structure* **15**(3): 267-273.

Chaudhary, P. M., C. Ferguson, V. Nguyen, O. Nguyen, H. F. Massa, M. Eby, A. Jasmin, B. J. Trask, L. Hood and P. S. Nelson (1998). Cloning and Characterization of Two Toll/Interleukin-1 Receptor–Like Genes TIL3 and TIL4: Evidence for a Multi-Gene Receptor Family in Humans.

Chaudhary, S., J. E. Pak, F. Gruswitz, V. Sharma and R. M. Stroud (2012). Overexpressing human membrane proteins in stably transfected and clonal human embryonic kidney 293S cells. *Nat. Protocols* **7**(3): 453-466.

Chen, W. J., J. F. Moomaw, L. Overton, T. A. Kost and P. J. Casey (1993). High level expression of mammalian protein farnesyltransferase in a baculovirus system. The purified protein contains zinc. *J Biol Chem* **268**(13): 9675-9680.

Chen, Y. and P. A. Rice (2003). New insight into site-specific recombination from Flp recombinase-DNA structures. *Annu Rev Biophys Biomol Struct* **32**: 135-159.

Cheng, N., R. He, J. Tian, P. P. Ye and R. D. Ye (2008). Cutting edge: TLR2 is a functional receptor for acute-phase serum amyloid A. *J Immunol* **181**(1): 22-26.

Chiti, F. and C. M. Dobson (2006). Protein misfolding, functional amyloid, and human disease. *Annu Rev Biochem* **75**: 333-366.

Choe, J., M. S. Kelker and I. A. Wilson (2005). Crystal structure of human toll-like receptor 3 (TLR3) ectodomain. *Science* **309**(5734): 581-585.

Chudakov, D. M., M. V. Matz, S. Lukyanov and K. A. Lukyanov (2010). Fluorescent proteins and their applications in imaging living cells and tissues. *Physiol Rev* **90**(3): 1103-1163.

Cockett, M. I., C. R. Bebbington and G. T. Yarranton (1990). High level expression of tissue inhibitor of metalloproteinases in Chinese hamster ovary cells using glutamine synthetase gene amplification. *Biotechnology (N Y)* **8**(7): 662-667.

Cohen, S. N., A. C. Chang, H. W. Boyer and R. B. Helling (1973). Construction of biologically functional bacterial plasmids in vitro. *Proc Natl Acad Sci U S A* **70**(11): 3240-3244.

Cormack, B. P., R. H. Valdivia and S. Falkow (1996). FACS-optimized mutants of the green fluorescent protein (GFP). *Gene* **173**(1 Spec No): 33-38.

Croset, A., L. Delafosse, J. P. Gaudry, C. Arod, L. Glez, C. Losberger, D. Begue, A. Krstanovic, F. Robert, F. Vilbois, L. Chevalet and B. Antonsson (2012). Differences in the glycosylation of recombinant proteins expressed in HEK and CHO cells. *J Biotechnol* **161**(3): 336-348.

Daramola, O., J. Stevenson, G. Dean, D. Hatton, G. Pettman, W. Holmes and R. Field (2014). A high-yielding CHO transient system: Coexpression of genes encoding EBNA-1 and GS enhances transient protein expression. *Biotechnol Prog* **30**(1): 132-141.

Datta, P., R. J. Linhardt and S. T. Sharfstein (2013). An 'omics approach towards CHO cell engineering. *Biotechnology and Bioengineering* **110**(5): 1255-1271.

Davie, J. R. (2003). Inhibition of histone deacetylase activity by butyrate. *J Nutr* **133**(7 Suppl): 2485S-2493S.

Davies, A., A. Greene, E. Lullau and W. M. Abbott (2005). Optimisation and evaluation of a high-throughput mammalian protein expression system. *Protein Expr Purif* **42**(1): 111-121.

Dietmair, S., M. P. Hodson, L.-E. Quek, N. E. Timmins, P. Chrysanthopoulos, S. S. Jacob, P. Gray and L. K. Nielsen (2012). Metabolite profiling of CHO cells with different growth characteristics. *Biotechnology and Bioengineering* **109**(6): 1404-1414.

Dollins, D. E., J. J. Warren, R. M. Immormino and D. T. Gewirth (2007). Structures of GRP94-Nucleotide Complexes Reveal Mechanistic Differences between the hsp90 Chaperones. *Molecular Cell* **28**(1): 41-56.

Durocher, Y. and M. Loignon (2011). Process, Vectors and Engineered Cell Lines for Enhanced Large-Scale Transfection. **US 2011/0039339 A1**.

Durocher, Y., S. Perret and A. Kamen (2002). High-level and high-throughput recombinant protein production by transient transfection of suspension-growing human 293-EBNA1 cells. *Nucleic Acids Research* **30**(2): e9.

Elbein, A. D., R. Solf, P. R. Dorling and K. Vosbeck (1981). Swainsonine: An inhibitor of glycoprotein processing. *Proceedings of the National Academy of Sciences* **78**(12): 7393-7397.

Elbein, A. D., J. E. Tropea, M. Mitchell and G. P. Kaushal (1990). Kifunensine, a potent inhibitor of the glycoprotein processing mannosidase I. *Journal of Biological Chemistry* **265**(26): 15599-15605.

Estes, S. and M. Melville (2014). Mammalian cell line developments in speed and efficiency. *Adv Biochem Eng Biotechnol* **139**: 11-33.

Fernandes, F., J. Vidigal, M. M. Dias, K. L. Prather, A. S. Coroadinha, A. P. Teixeira and P. M. Alves (2012). Flipase-mediated cassette exchange in Sf9 insect cells for stable gene expression. *Biotechnol Bioeng* **109**(11): 2836-2844.

Fitzgerald, D. J., C. Schaffitzel, P. Berger, R. Wellinger, C. Bieniossek, Timothy J. Richmond and I. Berger (2007). Multiprotein Expression Strategy for Structural Biology of Eukaryotic Complexes. *Structure* **15**(3): 275-279.

Frank, S. A. (2004). Genetic predisposition to cancer [mdash] insights from population genetics. *Nat Rev Genet* **5**(10): 764-772.

Freeze, H. H. (2006). Genetic defects in the human glycome. *Nat Rev Genet* **7**(7): 537-551.

Fukushige, S. and B. Sauer (1992). Genomic targeting with a positive-selection lox integration vector allows highly reproducible gene expression in mammalian cells. *Proceedings of the National Academy of Sciences* **89**(17): 7905-7909.

Furrie, E., S. Macfarlane, G. Thomson, G. T. Macfarlane, Microbiology, T. T. Gut Biology Group and B. Tumour (2005). Toll-like receptors-2, -3 and -4 expression patterns on human colon and their regulation by mucosal-associated bacteria. *Immunology* **115**(4): 565-574.

Gaj, T., C. A. Gersbach and C. F. Barbas, 3rd (2013). ZFN, TALEN, and CRISPR/Cas-based methods for genome engineering. *Trends Biotechnol* **31**(7): 397-405.

Geisse, S. and M. Henke (2005). Large-scale transient transfection of mammalian cells: a newly emerging attractive option for recombinant protein production. *J Struct Funct Genomics* **6**(2-3): 165-170.

Ghosh, K. and G. D. Van Duyne (2002). Cre-loxP biochemistry. *Methods* **28**(3): 374-383.

Goeddel, D. V., D. G. Kleid, F. Bolivar, H. L. Heyneker, D. G. Yansura, R. Crea, T. Hirose, A. Kraszewski, K. Itakura and A. D. Riggs (1979). Expression in Escherichia coli of chemically synthesized genes for human insulin. *Proceedings of the National Academy of Sciences* **76**(1): 106-110.

Goepfert, U. and E. Kopetzki (2010). Protein Expression in Rodent Cells. **US 2010/0021965 A1**.

Gomord, V. and L. Faye (2004). Posttranslational modification of therapeutic proteins in plants. *Curr Opin Plant Biol* **7**(2): 171-181.

Graham, F. L., J. Smiley, W. C. Russell and R. Nairn (1977). Characteristics of a Human Cell Line Transformed by DNA from Human Adenovirus Type 5. *Journal of General Virology* **36**(1): 59-72.

Halff, E. F., M. Versteeg, T. H. Brondijk and E. G. Huizinga (2014). When less becomes more: optimization of protein expression in HEK293-EBNA1 cells using plasmid titration - a case study for NLRs. *Protein Expr Purif* **99**: 27-34.

Han, K. P., X. Zhu, B. Liu, E. Jeng, L. Kong, J. L. Yovandich, V. V. Vyas, W. D. Marcus, P. A. Chavaillaz, C. A. Romero, P. R. Rhode and H. C. Wong (2011). IL-15:IL-15 receptor alpha superagonist complex: high-level co-expression in recombinant mammalian cells, purification and characterization. *Cytokine* **56**(3): 804-810.

Hart, B. E. and R. I. Tapping (2012). Cell surface trafficking of TLR1 is differentially regulated by the ER chaperones PRAT4A and PRAT4B. *Journal of Biological Chemistry*.

Hayashi, F., K. D. Smith, A. Ozinsky, T. R. Hawn, E. C. Yi, D. R. Goodlett, J. K. Eng, S. Akira, D. M. Underhill and A. Aderem (2001). The innate immune response to bacterial flagellin is mediated by Toll-like receptor 5. *Nature* **410**(6832): 1099-1103.

He, R. L., J. Zhou, C. Z. Hanson, J. Chen, N. Cheng and R. D. Ye (2009). Serum amyloid A induces G-CSF expression and neutrophilia via Toll-like receptor 2. *Blood* **113**(2): 429-437.

Heim, R., D. C. Prasher and R. Y. Tsien (1994). Wavelength mutations and posttranslational autoxidation of green fluorescent protein. *Proc Natl Acad Sci U S A* **91**(26): 12501-12504.

Heim, R. and R. Y. Tsien (1996). Engineering green fluorescent protein for improved brightness, longer wavelengths and fluorescence resonance energy transfer. *Curr Biol* **6**(2): 178-182.

Hidmark, A., A. von Saint Paul and A. H. Dalpke (2012). Cutting edge: TLR13 is a receptor for bacterial RNA. *J Immunol* **189**(6): 2717-2721.

Hirano, N., T. Muroi, H. Takahashi and M. Haruki (2011). Site-specific recombinases as tools for heterologous gene integration. *Applied Microbiology and Biotechnology* **92**(2): 227-239.

Hong, M., S.-i. Yoon and I. A. Wilson (2012). Recombinant expression of TLR5 proteins by ligand supplementation and a leucine-rich repeat hybrid technique. *Biochemical and Biophysical Research Communications* **427**(1): 119-124.

Huang, L. C., E. A. Wood and M. M. Cox (1997). Convenient and reversible site-specific targeting of exogenous DNA into a bacterial chromosome by use of the FLP recombinase: the FLIRT system. *J Bacteriol* **179**(19): 6076-6083.

Hudson, P. J. and C. Souriau (2003). Engineered antibodies. *Nat Med* **9**(1): 129-134.

Invitrogen (2010). Flp-In™ System For Generating Stable Mammalian Expression Cell Lines by Flp Recombinase -Mediated Integration. (Version E).

InvivoGen (2014). "Low-CpG Pac." Retrieved 08.09.2014, from http://www.invivogen.com/pmod2-puro.

Ishii, K. J., C. Coban and S. Akira (2005). Manifold mechanisms of Toll-like receptor-ligand recognition. *J Clin Immunol* **25**(6): 511-521.

Ishiyama, S. and M. Ikeda (2010). High-level expression and improved folding of proteins by using the vp39 late promoter enhanced with homologous DNA regions. *Biotechnol Lett* **32**(11): 1637-1647.

Ivics, Z. and Z. Izsvák (2010). The expanding universe of transposon technologies for gene and cell engineering. *Mobile DNA* **1**(1): 1-15.

Jacchieri, S. G., R. Torquato and R. R. Brentani (2003). Structural study of binding of flagellin by Toll-like receptor 5. *J Bacteriol* **185**(14): 4243-4247.

Jana, M., C. A. Palencia and K. Pahan (2008). Fibrillar amyloid-beta peptides activate microglia via TLR2: implications for Alzheimer's disease. *J Immunol* **181**(10): 7254-7262.

Jin, M. S., S. E. Kim, J. Y. Heo, M. E. Lee, H. M. Kim, S.-G. Paik, H. Lee and J.-O. Lee (2007). Crystal Structure of the TLR1-TLR2 Heterodimer Induced by Binding of a Tri-Acylated Lipopeptide. *Cell* **130**(6): 1071-1082.

Jin, M. S. and J. O. Lee (2008). Application of hybrid LRR technique to protein crystallization. *BMB Rep* **41**(5): 353-357.

Jin, M. S. and J. O. Lee (2008). Structures of the toll-like receptor family and its ligand complexes. *Immunity* **29**(2): 182-191.

Johnson, J. L., M. B. Jones, S. O. Ryan and B. A. Cobb (2013). The regulatory power of glycans and their binding partners in immunity. *Trends in Immunology* **34**(6): 290-298.

Kang, J. Y., X. Nan, M. S. Jin, S.-J. Youn, Y. H. Ryu, S. Mah, S. H. Han, H. Lee, S.-G. Paik and J.-O. Lee (2009). Recognition of Lipopeptide Patterns by Toll-like Receptor 2-Toll-like Receptor 6 Heterodimer. *Immunity* **31**(6): 873-884.

Kao, F. T. and T. T. Puck (1968). Genetics of somatic mammalian cells, VII. Induction and isolation of nutritional mutants in Chinese hamster cells. *Proc Natl Acad Sci U S A* **60**(4): 1275-1281.

Kasamatsu, J., Y. Sutoh, K. Fugo, N. Otsuka, K. Iwabuchi and M. Kasahara (2010). Identification of a third variable lymphocyte receptor in the lamprey. *Proceedings of the National Academy of Sciences* **107**(32): 14304-14308.

Kaufman, R. J., L. C. Wasley, A. J. Spiliotes, S. D. Gossels, S. A. Latt, G. R. Larsen and R. M. Kay (1985). Coamplification and coexpression of human tissue-type plasminogen activator and murine dihydrofolate reductase sequences in Chinese hamster ovary cells. *Mol Cell Biol* **5**(7): 1750-1759.

Kaufman, W. L., I. Kocman, V. Agrawal, H.-P. Rahn, D. Besser and M. Gossen (2008). Homogeneity and persistence of transgene expression by omitting antibiotic selection in cell line isolation. *Nucleic Acids Research* **36**(17): e111.

Kazantsev, A. G. and L. M. Thompson (2008). Therapeutic application of histone deacetylase inhibitors for central nervous system disorders. *Nat Rev Drug Discov* **7**(10): 854-868.

Keestra, A. M., M. R. de Zoete, R. A. M. H. van Aubel and J. P. M. van Putten (2008). Functional characterization of chicken TLR5 reveals species-specific recognition of flagellin. *Molecular Immunology* **45**(5): 1298-1307.

Kendrew, J. C., G. Bodo, H. M. Dintzis, R. G. Parrish, H. Wyckoff and D. C. Phillips (1958). A three-dimensional model of the myoglobin molecule obtained by x-ray analysis. *Nature* **181**(4610): 662-666.

Kerrigan, J. J., Q. Xie, R. S. Ames and Q. Lu (2011). Production of protein complexes via co-expression. *Protein Expression and Purification* **75**(1): 1-14.

Kim, H. M., S. C. Oh, K. J. Lim, J. Kasamatsu, J. Y. Heo, B. S. Park, H. Lee, O. J. Yoo, M. Kasahara and J. O. Lee (2007). Structural diversity of the hagfish variable lymphocyte receptors. *J Biol Chem* **282**(9): 6726-6732.

Kim, H. M., B. S. Park, J.-I. Kim, S. E. Kim, J. Lee, S. C. Oh, P. Enkhbayar, N. Matsushima, H. Lee, O. J. Yoo and J.-O. Lee (2007). Crystal Structure of the TLR4-MD-2 Complex with Bound Endotoxin Antagonist Eritoran. *Cell* **130**(5): 906-917.

Kim, N. S., S. J. Kim and G. M. Lee (1998). Clonal variability within dihydrofolate reductase-mediated gene amplified Chinese hamster ovary cells: stability in the absence of selective pressure. *Biotechnol Bioeng* **60**(6): 679-688.

Kiyokawa, T., S. Akashi-Takamura, T. Shibata, F. Matsumoto, C. Nishitani, Y. Kuroki, Y. Seto and K. Miyake (2008). A single base mutation in the PRAT4A gene reveals differential interaction of PRAT4A with Toll-like receptors. *International Immunology* **20**(11): 1407-1415.

Kokatla, H. P., D. Sil, H. Tanji, U. Ohto, S. S. Malladi, L. M. Fox, T. Shimizu and S. A. David (2014). Structure-based design of novel human Toll-like receptor 8 agonists. *ChemMedChem* **9**(4): 719-723.

Konno, K., Y. Wakabayashi, S. Akashi-Takamura, T. Ishii, M. Kobayashi, K. Takahashi, Y. Kusumoto, S.-i. Saitoh, Y. Yoshizawa and K. Miyake (2006). A molecule that is associated with Toll-like receptor 4 and regulates its cell surface expression. *Biochemical and Biophysical Research Communications* **339**(4): 1076-1082.

Kranz, A., J. Fu, K. Duerschke, S. Weidlich, R. Naumann, A. F. Stewart and K. Anastassiadis (2010). An improved Flp deleter mouse in C57Bl/6 based on Flpo recombinase. *genesis* **48**(8): 512-520.

Kriz, A., K. Schmid, N. Baumgartner, U. Ziegler, I. Berger, K. Ballmer-Hofer and P. Berger (2010). A plasmid-based multigene expression system for mammalian cells. *Nat Commun* **1**(8): 120.

Kunaparaju, R., M. Liao and N.-A. Sunstrom (2005). Epi-CHO, an episomal expression system for recombinant protein production in CHO cells. *Biotechnology and Bioengineering* **91**(6): 670-677.

Kyhse-Andersen, J. (1984). Electroblotting of multiple gels: a simple apparatus without buffer tank for rapid transfer of proteins from polyacrylamide to nitrocellulose. *J Biochem Biophys Methods* **10**(3-4): 203-209.

Laemmli, U. K., F. Beguin and G. Gujer-Kellenberger (1970). A factor preventing the major head protein of bacteriophage T4 from random aggregation. *J Mol Biol* **47**(1): 69-85.

Lauth, M., F. Spreafico, K. Dethleffsen and M. Meyer (2002). Stable and efficient cassette exchange under non-selectable conditions by combined use of two site-specific recombinases. *Nucleic Acids Res* **30**(21): e115.

Lebkowski, J. S., S. Clancy and M. P. Calos (1985). Simian virus 40 replication in adenovirus-transformed human cells antagonizes gene expression. *Nature* **317**(6033): 169-171.

Lee, J. E., M. L. Fusco and E. O. Saphire (2009). An efficient platform for screening expression and crystallization of glycoproteins produced in human cells. *Nat Protoc* **4**(4): 592-604.

Lehmann, J., G. W. Piehl and R. Schulz (1987). Bubble free cell culture aeration with porous moving membranes. *Dev Biol Stand* **66**: 227-240.

Letran, S. E., S.-J. Lee, S. M. Atif, S. Uematsu, S. Akira and S. J. McSorley (2011). TLR5 functions as an endocytic receptor to enhance flagellin-specific adaptive immunity. *European Journal of Immunology* **41**(1): 29-38.

Lewis, N. E., X. Liu, Y. Li, H. Nagarajan, G. Yerganian, E. O'Brien, A. Bordbar, A. M. Roth, J. Rosenbloom, C. Bian, M. Xie, W. Chen, N. Li, D. Baycin-Hizal, H. Latif, J. Forster, M. J. Betenbaugh, I. Famili, X. Xu, J. Wang and B. O. Palsson (2013). Genomic landscapes of Chinese hamster ovary cell lines as revealed by the Cricetulus griseus draft genome. *Nat Biotech* **31**(8): 759-765.

Li, Z., I. P. Michael, D. Zhou, A. Nagy and J. M. Rini (2013). Simple piggyBac transposon-based mammalian cell expression system for inducible protein production. *Proc Natl Acad Sci U S A* **110**(13): 5004-5009.

Liew, F. Y., D. Xu, E. K. Brint and L. A. J. O'Neill (2005). Negative regulation of Toll-like receptor-mediated immune responses. *Nat Rev Immunol* **5**(6): 446-458.

Liu, B., Y. Yang, Z. Qiu, M. Staron, F. Hong, Y. Li, S. Wu, Y. Li, B. Hao, R. Bona, D. Han and Z. Li (2010). Folding of Toll-like receptors by the HSP90 paralogue gp96 requires a substrate-specific cochaperone. *Nat Commun* **1**: 79.

Liu, L., I. Botos, Y. Wang, J. N. Leonard, J. Shiloach, D. M. Segal and D. R. Davies (2008). Structural basis of toll-like receptor 3 signaling with double-stranded RNA. *Science* **320**(5874): 379-381.

Liu, S., Y. Liu, W. Hao, L. Wolf, A. J. Kiliaan, B. Penke, C. E. Rube, J. Walter, M. T. Heneka, T. Hartmann, M. D. Menger and K. Fassbender (2012). TLR2 is a primary receptor for Alzheimer's amyloid beta peptide to trigger neuroinflammatory activation. *J Immunol* **188**(3): 1098-1107.

Liu, W., Y. Xiong and M. Gossen (2006). Stability and homogeneity of transgene expression in isogenic cells. *Journal of Molecular Medicine* **84**(1): 57-64.

Luo, J., G. Obmolova, T. J. Malia, S.-J. Wu, K. E. Duffy, J. D. Marion, J. K. Bell, P. Ge, Z. H. Zhou, A. Teplyakov, Y. Zhao, R. J. Lamb, J. L. Jordan, L. R. San Mateo, R. W. Sweet and G. L. Gilliland (2012). Lateral Clustering of TLR3:dsRNA Signaling Units Revealed by TLR3ecd:3Fabs Quaternary Structure. *Journal of Molecular Biology* **421**(1): 112-124.

Malhotra, A. (2009). Chapter 16 Tagging for Protein Expression. Methods Enzymol. R. B. Richard and P. D. Murray, Academic Press. **Volume 463:** 239-258.

Mancia, F., S. D. Patel, M. W. Rajala, P. E. Scherer, A. Nemes, I. Schieren, W. A. Hendrickson and L. Shapiro (2004). Optimization of Protein Production in Mammalian Cells with a Coexpressed Fluorescent Marker. *Structure* **12**(8): 1355-1360.

Matz, M. V., A. F. Fradkov, Y. A. Labas, A. P. Savitsky, A. G. Zaraisky, M. L. Markelov and S. A. Lukyanov (1999). Fluorescent proteins from nonbioluminescent Anthozoa species. *Nat Biotechnol* **17**(10): 969-973.

Mayrhofer, P., B. Kratzer, W. Sommeregger, W. Steinfellner, D. Reinhart, A. Mader, S. Turan, J. Qiao, J. Bode and R. Kunert (2014). Accurate comparison of antibody expression levels by reproducible transgene targeting in engineered recombination-competent CHO cells. *Appl Microbiol Biotechnol*.

McLeod, M., S. Craft and J. R. Broach (1986). Identification of the crossover site during FLP-mediated recombination in the Saccharomyces cerevisiae plasmid 2 microns circle. *Molecular and Cellular Biology* **6**(10): 3357-3367.

Meissner, P., H. Pick, A. Kulangara, P. Chatellard, K. Friedrich and F. M. Wurm (2001). Transient gene expression: Recombinant protein production with suspension-adapted HEK293-EBNA cells. *Biotechnology and Bioengineering* **75**(2): 197-203.

Metcalfe, H. J., R. M. La Ragione, D. G. E. Smith and D. Werling (2014). Functional characterisation of bovine TLR5 indicates species-specific recognition of flagellin. *Veterinary Immunology and Immunopathology* **157**(3–4): 197-205.

Meyer, S. (2012). Development of an integrated expression platform for protein production in eukaryotic hosts, Technischen Universität Carolo-Wilhelmina zu Braunschweig.

Meyer, S., C. Lorenz, B. Baser, M. Wördehoff, V. Jäger and J. van den Heuvel (2013). Multi-Host Expression System for Recombinant Production of Challenging Proteins. *PLoS ONE* **8**(7): e68674.

Miller, L. S., O. E. Sørensen, P. T. Liu, H. R. Jalian, D. Eshtiaghpour, B. E. Behmanesh, W. Chung, T. D. Starner, J. Kim, P. A. Sieling, T. Ganz and R. L. Modlin (2005). TGF-α Regulates TLR Expression and Function on Epidermal Keratinocytes. *The Journal of Immunology* **174**(10): 6137-6143.

Mizel, S. B., A. P. West and R. R. Hantgan (2003). Identification of a sequence in human toll-like receptor 5 required for the binding of Gram-negative flagellin. *J Biol Chem* **278**(26): 23624-23629.

Muirhead, H. and M. F. Perutz (1963). STRUCTURE OF HAEMOGLOBIN. A THREE-DIMENSIONAL FOURIER SYNTHESIS OF REDUCED HUMAN HAEMOGLOBIN AT 5-5 A RESOLUTION. *Nature* **199**: 633-638.

Muzio, M., D. Bosisio, N. Polentarutti, G. D'amico, A. Stoppacciaro, R. Mancinelli, C. van't Veer, G. Penton-Rol, L. P. Ruco, P. Allavena and A. Mantovani (2000). Differential Expression and Regulation of Toll-Like Receptors (TLR) in Human Leukocytes: Selective Expression of TLR3 in Dendritic Cells. *The Journal of Immunology* **164**(11): 5998-6004.

Nehlsen, K., R. Schucht, L. da Gama-Norton, W. Kromer, A. Baer, A. Cayli, H. Hauser and D. Wirth (2009). Recombinant protein expression by targeting pre-selected chromosomal loci. *BMC Biotechnol* **9**(1): 100.

Nettleship, J. E., R. Assenberg, J. M. Diprose, N. Rahman-Huq and R. J. Owens (2010). Recent advances in the production of proteins in insect and mammalian cells for structural biology. *Journal of Structural Biology* **172**(1): 55-65.

Neuhaus, E. M., A. Mashukova, W. Zhang, J. Barbour and H. Hatt (2006). A specific heat shock protein enhances the expression of mammalian olfactory receptor proteins. *Chem Senses* **31**(5): 445-452.

Nomura, N., N. Miyajima, T. Sazuka, A. Tanaka, Y. Kawarabayasi, S. Sato, T. Nagase, N. Seki, K.-i. Ishikawa and S. Tabata (1994). Prediction of the Coding Sequences of Unidentified Human Genes. I. The Coding Sequences of 40 New Genes (KIAA0001-KIAA0040) Deduced by Analysis of Randomly Sampled cDNA Clones from Human Immature Myeloid Cell Line KG-1. *DNA Research* **1**(1): 27-35.

North, S. J., H. H. Huang, S. Sundaram, J. Jang-Lee, A. T. Etienne, A. Trollope, S. Chalabi, A. Dell, P. Stanley and S. M. Haslam (2010). Glycomics profiling of Chinese hamster ovary cell glycosylation mutants reveals N-glycans of a novel size and complexity. *J Biol Chem* **285**(8): 5759-5775.

O'Gorman, S., D. Fox and G. Wahl (1991). Recombinase-mediated gene activation and site-specific integration in mammalian cells. *Science* **251**(4999): 1351-1355.

O'Neill, L. A. J. and A. G. Bowie (2007). The family of five: TIR-domain-containing adaptors in Toll-like receptor signalling. *Nat Rev Immunol* **7**(5): 353-364.

Ohto, U., K. Fukase, K. Miyake and T. Shimizu (2012). Structural basis of species-specific endotoxin sensing by innate immune receptor TLR4/MD-2. *Proc Natl Acad Sci U S A* **109**(19): 7421-7426.

Ohto, U., N. Yamakawa, S. Akashi-Takamura, K. Miyake and T. Shimizu (2012). Structural Analyses of Human Toll-like Receptor 4 Polymorphisms D299G and T399I. *Journal of Biological Chemistry* **287**(48): 40611-40617.

Oppong, G. O., G. J. Rapsinski, T. N. Newman, J. H. Nishimori, S. G. Biesecker and C. Tukel (2013). Epithelial cells augment barrier function via activation of the Toll-like receptor 2/phosphatidylinositol 3-kinase pathway upon recognition of Salmonella enterica serovar Typhimurium curli fibrils in the gut. *Infect Immun* **81**(2): 478-486.

Oumard, A., J. Qiao, T. Jostock, J. Li and J. Bode (2006). Recommended Method for Chromosome Exploitation: RMCE-based Cassette-exchange Systems in Animal Cell Biotechnology. *Cytotechnology* **50**(1): 93-108.

Pancer, Z., C. T. Amemiya, G. R. Ehrhardt, J. Ceitlin, G. L. Gartland and M. D. Cooper (2004). Somatic diversification of variable lymphocyte receptors in the agnathan sea lamprey. *Nature* **430**(6996): 174-180.

Pancer, Z., N. R. Saha, J. Kasamatsu, T. Suzuki, C. T. Amemiya, M. Kasahara and M. D. Cooper (2005). Variable lymphocyte receptors in hagfish. *Proceedings of the National Academy of Sciences of the United States of America* **102**(26): 9224-9229.

Park, B. S., D. H. Song, H. M. Kim, B. S. Choi, H. Lee and J. O. Lee (2009). The structural basis of lipopolysaccharide recognition by the TLR4-MD-2 complex. *Nature* **458**(7242): 1191-1195.

Pegu, A., S. Qin, B. A. Fallert Junecko, R. E. Nisato, M. S. Pepper and T. A. Reinhart (2008). Human Lymphatic Endothelial Cells Express Multiple Functional TLRs. *The Journal of Immunology* **180**(5): 3399-3405.

Pilbrough, W., T. P. Munro and P. Gray (2009). Intraclonal protein expression heterogeneity in recombinant CHO cells. *PLoS ONE* **4**(12): e8432.

Prasher, D. C., V. K. Eckenrode, W. W. Ward, F. G. Prendergast and M. J. Cormier (1992). Primary structure of the Aequorea victoria green-fluorescent protein. *Gene* **111**(2): 229-233.

Puck, T. T., S. J. Cieciura and A. Robinson (1958). Genetics of somatic mammalian cells. III. Long-term cultivation of euploid cells from human and animal subjects. *J Exp Med* **108**(6): 945-956.

Qiao, J., A. Oumard, W. Wegloehner and J. Bode (2009). Novel Tag-and-Exchange (RMCE) Strategies Generate Master Cell Clones with Predictable and Stable Transgene Expression Properties. *Journal of Molecular Biology* **390**(4): 579-594.

Raetz, M., A. Kibardin, C. R. Sturge, R. Pifer, H. Li, E. Burstein, K. Ozato, S. Larin and F. Yarovinsky (2013). Cooperation of TLR12 and TLR11 in the IRF8-dependent IL-12 response to Toxoplasma gondii profilin. *J Immunol* **191**(9): 4818-4827.

Randow, F. and B. Seed (2001). Endoplasmic reticulum chaperone gp96 is required for innate immunity but not cell viability. *Nat Cell Biol* **3**(10): 891-896.

Rapsinski, G. J., T. N. Newman, G. O. Oppong, J. P. van Putten and C. Tukel (2013). CD14 protein acts as an adaptor molecule for the immune recognition of Salmonella curli fibers. *J Biol Chem* **288**(20): 14178-14188.

Raymond, C. S. and P. Soriano (2007). High-Efficiency FLP and ΦC31 Site-Specific Recombination in Mammalian Cells. *PLoS ONE* **2**(1): e162.

Reed-Geaghan, E. G., J. C. Savage, A. G. Hise and G. E. Landreth (2009). CD14 and toll-like receptors 2 and 4 are required for fibrillar A{beta}-stimulated microglial activation. *J Neurosci* **29**(38): 11982-11992.

Reeves, P. J., N. Callewaert, R. Contreras and H. G. Khorana (2002). Structure and function in rhodopsin: High-level expression of rhodopsin with restricted and homogeneous N-glycosylation by a tetracycline-inducible N-acetylglucosaminyltransferase I-negative HEK293S stable mammalian cell line. *Proceedings of the National Academy of Sciences of the United States of America* **99**(21): 13419-13424.

Rehberger, B., C. Wodarczyk, B. Reichenbacher, J. Kohler, R. Weber and D. Muller (2013). Accelerating stable recombinant cell line development by targeted integration. *BMC Proceedings* **7**(Suppl 6): P111.

Reid, David W., Q. Chen, Angeline S. L. Tay, S. Shenolikar and Christopher V. Nicchitta (2014). The Unfolded Protein Response Triggers Selective mRNA Release from the Endoplasmic Reticulum. *Cell* **158**(6): 1362-1374.

Rock, F. L., G. Hardiman, J. C. Timans, R. A. Kastelein and J. F. Bazan (1998). A family of human receptors structurally related to Drosophila Toll. *Proc Natl Acad Sci U S A* **95**(2): 588-593.

Romier, C., M. Ben Jelloul, S. Albeck, G. Buchwald, D. Busso, P. H. Celie, E. Christodoulou, V. De Marco, S. van Gerwen, P. Knipscheer, J. H. Lebbink, V. Notenboom, A. Poterszman, N. Rochel, S. X. Cohen, T. Unger, J. L. Sussman, D. Moras, T. K. Sixma and A. Perrakis (2006). Co-expression of protein complexes in prokaryotic and eukaryotic hosts: experimental procedures, database tracking and case studies. *Acta Crystallogr D Biol Crystallogr* **62**(Pt 10): 1232-1242.

Sambrook, J. and D. W. Russell (2001). Molecular Cloning: A Laboratory Manual, Cold Spring Harbor Laboratory Press.

Sander, J. D. and J. K. Joung (2014). CRISPR-Cas systems for editing, regulating and targeting genomes. *Nat Biotech* **32**(4): 347-355.

Sanger, F. (1949). The terminal peptides of insulin. *Biochem J* **45**(5): 563-574.

Schlaeger, E.-J. and K. Christensen (1999). Transient gene expression in mammalian cells grown in serum-free suspension culture. *Cytotechnology* **30**(1-3): 71-83.

Schlake, T. and J. Bode (1994). Use of Mutant FLP TRecognition Target (FRT) Sites for the Exchange of Expression Cassettes at Defined Chromosomal Loci. *Biochemistry* **33**(43): 12746-12751.

Schlatter, S., S. H. Stansfield, D. M. Dinnis, A. J. Racher, J. R. Birch and D. C. James (2005). On the optimal ratio of heavy to light chain genes for efficient recombinant antibody production by CHO cells. *Biotechnol Prog* **21**(1): 122-133.

Schnütgen, F., S. De-Zolt, P. Van Sloun, M. Hollatz, T. Floss, J. Hansen, J. Altschmied, C. Seisenberger, N. B. Ghyselinck, P. Ruiz, P. Chambon, W. Wurst and H. von Melchner (2005). Genomewide production of multipurpose alleles for the functional analysis of the mouse genome. *Proceedings of the National Academy of Sciences of the United States of America* **102**(20): 7221-7226.

Schnütgen, F., N. Doerflinger, C. Calleja, O. Wendling, P. Chambon and N. B. Ghyselinck (2003). A directional strategy for monitoring Cre-mediated recombination at the cellular level in the mouse. *Nat Biotechnol* **21**(5): 562-565.

Seibler, J., D. Schubeler, S. Fiering, M. Groudine and J. Bode (1998). DNA cassette exchange in ES cells mediated by Flp recombinase: an efficient strategy for repeated modification of tagged loci by marker-free constructs. *Biochemistry* **37**(18): 6229-6234.

Shaner, N. C., R. E. Campbell, P. A. Steinbach, B. N. Giepmans, A. E. Palmer and R. Y. Tsien (2004). Improved monomeric red, orange and yellow fluorescent proteins derived from Discosoma sp. red fluorescent protein. *Nat Biotechnol* **22**(12): 1567-1572.

Shi, S., R. G. Condon, L. Deng, J. Saunders, F. Hung, Y. S. Tsao and Z. Liu (2011). A high-throughput automated platform for the development of manufacturing cell lines for protein therapeutics. *J Vis Exp*(55).

Shibata, T., N. Takemura, Y. Motoi, Y. Goto, T. Karuppuchamy, K. Izawa, X. Li, S. Akashi-Takamura, N. Tanimura, J. Kunisawa, H. Kiyono, S. Akira, T. Kitamura, J. Kitaura, S. Uematsu and K. Miyake (2012). PRAT4A-dependent expression of cell surface TLR5 on neutrophils, classical monocytes and dendritic cells. *International Immunology* **24**(10): 613-623.

Shimomura, O., F. H. Johnson and Y. Saiga (1962). Extraction, purification and properties of aequorin, a bioluminescent protein from the luminous hydromedusan, Aequorea. *J Cell Comp Physiol* **59**: 223-239.

Smith, K. D., E. Andersen-Nissen, F. Hayashi, K. Strobe, M. A. Bergman, S. L. Barrett, B. T. Cookson and A. Aderem (2003). Toll-like receptor 5 recognizes a conserved site on flagellin required for protofilament formation and bacterial motility. *Nat Immunol* **4**(12): 1247-1253.

Southern, P. J. and P. Berg (1982). Transformation of mammalian cells to antibiotic resistance with a bacterial gene under control of the SV40 early region promoter. *J Mol Appl Genet* **1**(4): 327-341.

Stanley, P. (1989). Chinese hamster ovary cell mutants with multiple glycosylation defects for production of glycoproteins with minimal carbohydrate heterogeneity. *Molecular and Cellular Biology* **9**(2): 377-383.

Taguchi, T., J. L. Mitcham, S. K. Dower, J. E. Sims and J. R. Testa (1996). Chromosomal Localization ofTIL,a Gene Encoding a Protein Related to theDrosophilaTransmembrane Receptor Toll, to Human Chromosome 4p14. *Genomics* **32**(3): 486-488.

Takahashi, K., T. Shibata, S. Akashi-Takamura, T. Kiyokawa, Y. Wakabayashi, N. Tanimura, T. Kobayashi, F. Matsumoto, R. Fukui, T. Kouro, Y. Nagai, K. Takatsu, S.-i. Saitoh and K. Miyake (2007). A protein associated with Toll-like receptor (TLR) 4 (PRAT4A) is required for TLR-dependent immune responses. *The Journal of Experimental Medicine* **204**(12): 2963-2976.

Tang, D., R. Kang, C. B. Coyne, H. J. Zeh and M. T. Lotze (2012). PAMPs and DAMPs: signal 0s that spur autophagy and immunity. *Immunological Reviews* **249**(1): 158-175.

Tanji, H., U. Ohto, T. Shibata, K. Miyake and T. Shimizu (2013). Structural reorganization of the Toll-like receptor 8 dimer induced by agonistic ligands. *Science* **339**(6126): 1426-1429.

Tep, S., M. Hincapie and W. S. Hancock (2012). The characterization and quantitation of glycomic changes in CHO cells during a bioreactor campaign. *Biotechnology and Bioengineering* **109**(12): 3007-3017.

Trinchieri, G. and A. Sher (2007). Cooperation of Toll-like receptor signals in innate immune defence. *Nat Rev Immunol* **7**(3): 179-190.

Tükel, Ç., J. H. Nishimori, R. P. Wilson, M. G. Winter, A. M. Keestra, J. P. M. Van Putten and A. J. Bäumler (2010). Toll-like receptors 1 and 2 cooperatively mediate immune

responses to curli, a common amyloid from enterobacterial biofilms. *Cellular Microbiology* **12**(10): 1495-1505.

Tükel, C., M. Raffatellu, A. D. Humphries, R. P. Wilson, H. L. Andrews-Polymenis, T. Gull, J. F. Figueiredo, M. H. Wong, K. S. Michelsen, M. Akcelik, L. G. Adams and A. J. Baumler (2005). CsgA is a pathogen-associated molecular pattern of Salmonella enterica serotype Typhimurium that is recognized by Toll-like receptor 2. *Mol Microbiol* **58**(1): 289-304.

Tükel, Ç., R. P. Wilson, J. H. Nishimori, M. Pezeshki, B. A. Chromy and A. J. Bäumler (2009). Responses to Amyloids of Microbial and Host Origin Are Mediated through Toll-like Receptor 2. *Cell Host & Microbe* **6**(1): 45-53.

Turan, S. and J. Bode (2011). Site-specific recombinases: from tag-and-target- to tag-and-exchange-based genomic modifications. *The FASEB Journal* **25**(12): 4088-4107.

Turan, S., M. Galla, E. Ernst, J. Qiao, C. Voelkel, B. Schiedlmeier, C. Zehe and J. Bode (2011). Recombinase-Mediated Cassette Exchange (RMCE): Traditional Concepts and Current Challenges. *Journal of Molecular Biology* **407**(2): 193-221.

Turan, S., J. Kuehle, A. Schambach, C. Baum and J. Bode (2010). Multiplexing RMCE: Versatile Extensions of the Flp-Recombinase-Mediated Cassette-Exchange Technology. *Journal of Molecular Biology* **402**(1): 52-69.

Udan, M. L., D. Ajit, N. R. Crouse and M. R. Nichols (2008). Toll-like receptors 2 and 4 mediate Abeta(1-42) activation of the innate immune response in a human monocytic cell line. *J Neurochem* **104**(2): 524-533.

Urlaub, G. and L. A. Chasin (1980). Isolation of Chinese hamster cell mutants deficient in dihydrofolate reductase activity. *Proc Natl Acad Sci U S A* **77**(7): 4216-4220.

Vara, J. A., A. Portela, J. Ortìn and A. Jimènez (1986). Expression in mammalian cells of a gene from Streptomyces alboniger conferring puromycin resistance. *Nucleic Acids Research* **14**(11): 4617-4624.

Villaverde, A. and M. M. Carrio (2003). Protein aggregation in recombinant bacteria: biological role of inclusion bodies. *Biotechnol Lett* **25**(17): 1385-1395.

Wakabayashi, Y., M. Kobayashi, S. Akashi-Takamura, N. Tanimura, K. Konno, K. Takahashi, T. Ishii, T. Mizutani, H. Iba, T. Kouro, S. Takaki, K. Takatsu, Y. Oda, Y. Ishihama, S.-i. Saitoh and K. Miyake (2006). A Protein Associated with Toll-Like Receptor 4 (PRAT4A) Regulates Cell Surface Expression of TLR4. *The Journal of Immunology* **177**(3): 1772-1779.

Waldner, C., O. Rempel, F. Schutte, M. Yanik, N. Solomentsew and G. U. Ryffel (2011). Double conditional human embryonic kidney cell line based on FLP and PhiC31 mediated transgene integration. *BMC Res Notes* **4**: 420.

Walsh, G. and R. Jefferis (2006). Post-translational modifications in the context of therapeutic proteins. *Nat Biotech* **24**(10): 1241-1252.

Weatherall, D. J. (2004). Thalassaemia: the long road from bedside to genome. *Nat Rev Genet* **5**(8): 625-631.

Wilke, S., L. Groebe, V. Maffenbeier, V. Jäger, M. Gossen and e. al. (2011). Streamlining Homogeneous Glycoprotein Production for Biophysical and Structural Applications by Targeted Cell Line Development. *PLoS ONE* **6**(12): e27829. doi:27810.21371/journal.pone.0027829.

Wilke, S., J. Krausze, M. Gossen, L. Groebe, V. Jäger, E. Gherardi, J. van den Heuvel and K. Büssow (2010). Glycoprotein production for structure analysis with stable, glycosylation mutant CHO cell lines established by fluorescence-activated cell sorting. *Protein Science* **19**(6): 1264-1271.

Wu, S., F. Hong, D. Gewirth, B. Guo, B. Liu and Z. Li (2012). The Molecular Chaperone gp96/GRP94 Interacts with Toll-like Receptors and Integrins via Its C-terminal Hydrophobic Domain. *Journal of Biological Chemistry* **287**(9): 6735-6742.

Wurm, F. M. (2004). Production of recombinant protein therapeutics in cultivated mammalian cells. *Nat Biotech* **22**(11): 1393-1398.

Wurm, F. M. and D. Hacker (2011). First CHO genome. *Nat Biotechnol* **29**(8): 718-720.

Xu, X., H. Nagarajan, N. E. Lewis, S. Pan, Z. Cai, X. Liu, W. Chen, M. Xie, W. Wang, S. Hammond, M. R. Andersen, N. Neff, B. Passarelli, W. Koh, H. C. Fan, J. Wang, Y. Gui, K. H. Lee, M. J. Betenbaugh, S. R. Quake, I. Famili, B. O. Palsson and J. Wang (2011). The genomic sequence of the Chinese hamster ovary (CHO)-K1 cell line. *Nat Biotech* **29**(8): 735-741.

Yang, Y., B. Liu, J. Dai, P. K. Srivastava, D. J. Zammit, L. Lefrançois and Z. Li (2006). Heat Shock Protein gp96 Is a Master Chaperone for Toll-like Receptors and Is Important in the Innate Function of Macrophages. *Immunity* **26**(2): 215-226.

Yates, J. L., S. M. Camiolo and J. M. Bashaw (2000). The minimal replicator of Epstein-Barr virus oriP. *J Virol* **74**(10): 4512-4522.

Yoon, S.-i., O. Kurnasov, V. Natarajan, M. Hong, A. V. Gudkov, A. L. Osterman and I. A. Wilson (2012). Structural Basis of TLR5-Flagellin Recognition and Signaling. *Science* **335**(6070): 859-864.

Young, J. M., C. Cheadle, J. S. Foulke Jr, W. N. Drohan and N. Sarver (1988). Utilization of an Epstein-Barr virus replicon as a eukaryotic expression vector. *Gene* **62**(2): 171-185.

Zhao, Y., B. Bishop, J. E. Clay, W. Lu, M. Jones, S. Daenke, C. Siebold, D. I. Stuart, E. Y. Jones and A. R. Aricescu (2011). Automation of large scale transient protein expression in mammalian cells. *J Struct Biol* **175**(2): 209-215.

Zhu, X.-D. and P. D. Sadowski (1995). Cleavage-dependent Ligation by the FLP Recombinase. *Journal of Biological Chemistry* **270**(39): 23044-23054.

Appendix

A.1 Materials and Methods

Table A.1-1: Instruments

Instrument	Model	Company
Autoclave	Infection Control	Belimed
Biochemical Analyser	2700 Select	YSI
Biochemical Analyser	Gallery	Thermo Scientific
Blot chamber	Trans-blot® Turbo Transfer System	Bio-Rad
Blot chamber	Trans-Blot SH semi-dry transfer cell	Bio-Rad
Cell Counter	CASY cell counter	Innovatis
Centrifuge	Biofuge pico	Heraeus
Centrifuge	Heraeus Fresco 17	Thermo Scientific
Centrifuge	Heraeus Megafuge 40R Rotor 75003607	Thermo Scientific
Centrifuge	Multifuge 1 S-R Rotor 750020000	Heraeus Sorvall
Centrifuge	Multifuge 3 S-R Rotor 75006435	Heraeus Sorvall Heraeus
Centrifuge	RC 12BP Rotor H-12000	Sorvall/ Thermo Scientific
Centrifuge	Sorvall RC 6	Thermo Scientific
Centrifuge	Sorvall RC 6+ Rotors: FibreLite® F10-4x1000Lex FiberLite® F12-6x500 Lex FibreLite® F13-14x50y FibreLite® F14-6x250y FibreLite® F18x 12x50 SLA-1500 SLA-3000 F95-4x100y	Thermo Scientific Thermo Scientific Thermo Scientific Thermo Scientific Thermo Scientific Thermo Scientific Sorvall Sorvall PTI
Centrifuge	Avanti™ J-20 XP J-Lite® JLA-16.250 J-Lite® JA-25.50	Beckmann Coulter
Chromatography system	ÄKTAFPLC (UPC-900, P-920)	Amersham pharmacia biotech
Chromatography system	ÄKTApilot	GE
Chromatography system	Profinia™ Protein Purification System	Bio-Rad
Cleanbench	Heraeus – Hera safe KS-12	Thermo Electron Corporation
Cleanbench	Heraeus – Hera safe KS-15	Thermo Electron Corporation
Cleanbench	Hera safe KSP	Thermo Scientific
Cleanbench	Maxisafe 2020	Thermo Scientific
Controller	Biomodul 40B controller	VarioMag
Controller	Infors HT X-controller	Infors HT
Cryotank	K Series Cryostorage System	Taylor-Wharton
Dishwasher	G7836 CD	Miele professional

Documentation System	Molecular imaging system, GelLogic 212 imaging system, 254 nm	Carestream/Kodak
Electrophoresis chamber	Criterion cell	Bio-Rad
Electrophoresis chamber	Mini Protean II 2-D-cell	Bio-Rad
Electrophoresis chamber	Mini Protean 3 cell	Bio-Rad
Electrophoresis chamber	Mini Protean tetra cell	Bio-Rad
Electrophoresis chamber	Sub Cell GT Mini Sub Cell GT Wide Mini Sub Cell GT	Bio-Rad
Electroporation	Capacity extender	Bio-Rad
	Pulse controller	Bio-Rad
	Gene Pulser	BioRad
FACS sorter	MoFlo XDP	Beckman Coulter
	Aria-II	Becton Dickinson
	Vantage SE	Becton Dickinson
Filtration system	KrosFlow Research II I TFF Hollow fiber filter modules MidiKros 30kDa Cat# D04-E030-05-N MidiKros 10kDa Cat# D04-E010-05-N	Spectrumlabs.com
Filtration system	ProFlux® M12 tangential flow filtration system	Millipore
Filtration system	VivaFlow 200 Cat# VF20P0, 10.000 PES	Vivascience
Flowcytometer	Guava EasyCyte, 488 nm diode laser, fluorescence detectors 583/26 nm (yellow), 680/30 nm (red) and 525/30 nm (green)	Merck
Fluorescence microscope	Axiovert 100 (Imaging Software NIS-Elements F3.0) Filter set 44 (BP 530/50) Filter set 25 (TBP 460 + 530 + 625) Filter set 9 (LP 515) Filter set 43 (BP 605/70)	Zeiss
Fluorescence microscope	Evos GFP LED Cube AMEP-4651 (Em: 510/42 nm) RFP LED Cube AMEP-4652 (Em: 593/40 nm) Tx-RFP LED Cube AMEP-46 (Em 624/40 nm)	AMG
Fluorescence plate reader	Infinite® MD 1000	Tecan
Hood	Labcontrol	Hesco
Ice machine	Sno 095294	Ziegra
Incubator	Climo-Shaker ISF1-XC	Kuhner Shaker X
Incubator	Forma Reach-In CO_2 Incubator	Thermo Electron Corporation
Incubator	Function line CO_2 Incubator BB15	Thermo Electron Corporation
Incubator	Function line CO_2 Incubator BB16	Thermo Electron Corporation
Incubator	HT Infors Minitron Shaking Incubator	Infors
Incubator	HT Infors Multitron	Infors
Label printer	Laboratory labelling system Label: Hi-Perf Lab Polyester XSL-86-461	Labxpert
Laminator	Vacpull	Petra electronics
Light microscope	BA200	Motic
Light microscope	CKX41	Olympus
Light microscope	1T, 47 3011-9901 and Invertoscope ID 02	Zeiss
Light table	Color-control 5000	Biotech-Fischer

Luminometer	LAS 3000	FujiFilm
Magnetic stirrer	Electronicrührer Biosystem, Biosystem B, Mobil 60 and Monotherm	VarioMag
Magnetic stirrer	VarioMag Mono	Thermo Scientific
Magnetic stirrer	KMO2 basic, RCT basic and Colour squid	IKA
Magnetic stirrer	RMH	Gerhard
Magnetic stirrer	MR 2000	Heidolph
Microbioreactor system	BioLector® Basic	m2p labs
Microwave	M1712N	Samsung
Microwave	R-7280 and R-963	Sharp
Nucleofector	Amaxa	Lonza
pH meter	Five easy and Seven multi	Mettler Toledo
pH meter	WIW series pH 720	inoLab
Power supply	PowerPac basic, HC, universal, 300	Bio-Rad
Roller Mixer	SRT 6D	Stuart
Rotator	Disk rotator	Sauer
Scale	A200S	Sartorius analytic
Scale	Combics 3, L22 and BP 3100S	Sartorius
Scale	G4200-2 NM and EG 4200-2NM	Kern
Scale	XB 6200D	Precisa
Scale	WT12	Biometra
Scanner	Canon Scan LiDE 700F	Canon
Shaker	Duomax 2030	Heidolph
Shaker	K15-500	Incutec
Shaker	Lab-Shaker ES4x	Kühner
Shaker	Nutatig Mixer	VWR International
Spectrophotometer	Biowave CO8000 cell density meter	WPA
Spectrophotometer	GeneRay	Biometra
Spectrophotometer	NanoDrop ND-1000 and 2000	Thermo Scientific
Thermocycler	T3000	Biometra
Thermocycler	T personal 48	Biometra
Thermocycler	T professional gradient thermocycler	Biometra
Thermomixer	Thermomixer comfort and compact	Eppendorf
Tube pump	501 U, 503, 505 Du and 520 Du	Watson Marlow
Tube pump	Masterflex L/S economy drive	Cole Parmer
Tube pump	Masterflex L/S digital standard drive	Cole Parmer
Tube pump	P-1	GE
UV-table	Science imaging, 312 nm	INTAS
Vacuum pump	2522c-02	Welch
Vacuum pump	BVC professional	Vacubrand
Vacuum pump	Laborport	KNF Lab
Vortex	Vortex Genie 2	Bender & Hobein AG
Vortex	Vortex Genie 2	Scientific Industries
Vortex	Reax top	Heidolph
Vortex	MS1 Minishaker and MS2 Minishaker	IKA
Waterbath	Ecoline Staredition 003	Lauda
Waterbath	Ecoline 006	Lauda

Waterbath	M3	mgwland
Water purification system	membraPure	membraPure
Water purification system	MilliQ advantage A10	Millipore

Table A.1-2: Cell culture consumables and flasks

Instrument	Model	Cat#	Company
Cell culture cish	100 mm x 20 mm style, polystyrene, non-pyrogenic, sterile	430293	Corning
Tissue culture flat tubes	10 cm^2	91253	TPP
96-well plate	untreated, straight w/Lid	260860	Nunc / Thermo Scientific
96-well plate	Treated	353075	BD Falcon
48-well plate	Tissue culture plate, flat bottom with low evaporation lid, polystyrene, non-pyrogenic, treated by vacuum gas plasma	353078	BD Falcon
24-well plate	Tissue culture plate, flat bottom with low evaporation lid, polystyrene, non-pyrogenic, treated by vacuum gas plasma	353047	BD Falcon
12-well plate	Non-tissue culture treated plate, flat bottom with low evaporation lid, polystyrene	351143	BD Falcon
12-well plate	Tissue culture plate, flat bottom with low evaporation lid, polystyrene, non-pyrogenic, treated by vacuum gas plasma	353043	BD Falcon
6-well plate	Tissue culture plate, flat bottom with low evaporation lid, polystyrene, non-pyrogenic, treated by vacuum gas plasma	353046	BD Falcon
Shake flask (125 mL)	Polycarbonate Erlenmeyer flask with 0.2µm vent cap (culture volume 20-50 mL)	431143	Corning
Shake flask (125 mL)	Flat base polycarbonate Erlenmeyer flask (culture volume 20-50 mL)	355117	BD Falcon
Shake flask (500 mL)	Polycarbonate Erlenmeyer flask with 0.2µm vent cap (culture volume 100-200 mL)	431145	Corning
Shake flask (500 mL)	Flat base polycarbonate Erlenmeyer flask (culture volume 100-200 mL)	355125	BD Falcon
Shake flask (1 L)	Polycarbonate Erlenmeyer flask with 0.2µm vent cap (culture volume 200-300 mL)	431147	Corning
Shake flask (1 L)	Flat base polycarbonate Erlenmeyer flask (culture volume 200-300 mL)	355129	BD Falcon
Shake flask (2 L)	Flat base polycarbonate Erlenmeyer flask (culture volume 300-500 mL)	355133	BD Falcon
Shake flask (3 L)	Polycarbonate Erlenmeyer (Fernbach design) flask with vent cap (culture volume 1 L-1.5 L)	431252	Corning
Cryogenic vials	Nalgene® cryoware cryogenic vials (2 mL)	5000-0020	Thermo Scientific/ Nalgene
Cryogenic vials	CryoTube™ Vials	375418	Thermo Scientific/ Nunc
Freezing container	Nalgene™ cryo 1 °C freezing container	5100-0001	Nalgene

A.2 Results

Table A.2-1: Flowcytometric data for tdTomato expressing master and producer cell lines.

Cell Line	Red positive cells	Geometric mean [x10²]	Mean [x10²]	Median [x10²]
BBA10-tdTomato-C1	99 %	3.6	3.9	3.5
SMT_dneo(2)_24-tdTomato-C1	99 %	3.5	3.7	3.4
TE3-B4-H1	98 %	5.0	5.6	5.5
TE3-B4-H1-tdTomato/tdTomato-C1	99 %	9.9	10.6	9.7
TE3-B4-L1.1	98 %	1.8	1.9	1.8
TE3-B4-L1.1-tdTomato/tdTomato-C1	99 %	6.0	6.2	5.8

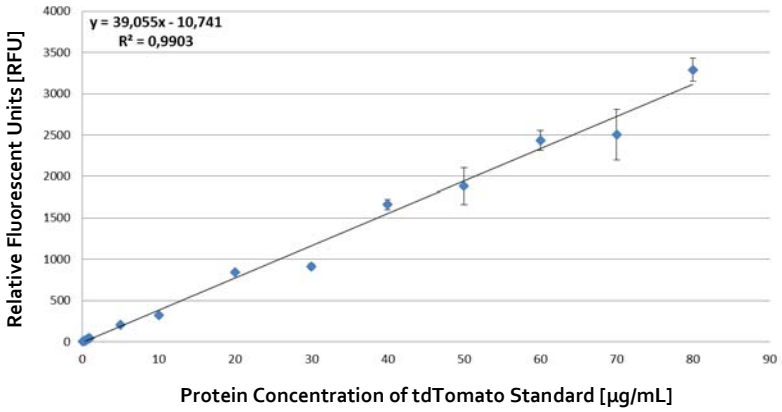

Figure A.2-1: Calibration curve for tdTomato standard used for the analysis of cell extracts: This tdTomato calibration curve was used to analyse cell extracts obtained from tdTomato expressing cell lines. The tdTomato standard was diluted in cell extract not expressing tdTomato to assure the correct background. Standard deviations of measured RFU are shown as vertical marker.

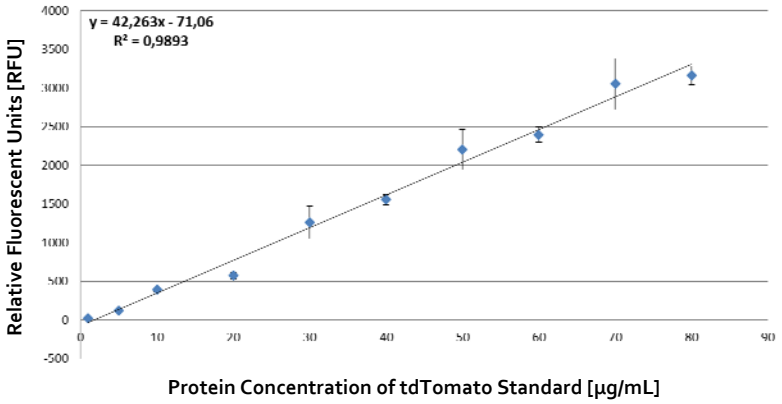

Figure A.2-2: Calibration curve for tdTomato standard used for the analysis of purified tdTomato: This tdTomato calibration curve was used to analyse purified tdTomato obtained from tdTomato expressing cell lines. The tdTomato standard was diluted in buffer present in purified tdTomato to assure the correct background. Standard deviations of measured RFU are shown as vertical marker.

Table A.2-2: Yields obtained using cell extracts from tdTomato expressing cell lines at different timepoints using the Tecan MD 1000 plate reader.

TE3-B4-H1	**Timepoint 1 Yield [µg/mL]**	**Timepoint 2 Yield [µg/mL]**	**Timepoint 3 Yield [µg/mL]**
Culture 1	5.60	6.56	4.85
Culture 2	6.69	4.74	6.81
Culture 3	5.25	5.57	5.52
TE3-B4-L1.1	**Timepoint 1 Yield [µg/mL]**	**Timepoint 2 Yield [µg/mL]**	**Timepoint 3 Yield [µg/mL]**
Culture 1	2.43	1.44	2.20
Culture 2	2.01	1.94	1.96
Culture 3	2.91	1.88	2.41
TE3-B4-L1.1-tdTomato/tdTomato-C1	**Timepoint 1 Yield [µg/mL]**	**Timepoint 2 Yield [µg/mL]**	**Timepoint 3 Yield [µg/mL]**
Culture 1	5.99	5.61	8.04
Culture 2	7.44	5.47	7.75
Culture 3	7.28	6.36	6.76
BBA10-tdTomato-C1	**Timepoint 1 Yield [µg/mL]**	**Timepoint 2 Yield [µg/mL]**	**Timepoint 3 Yield [µg/mL]**
Culture 1	5.91	3.70	4.82
Culture 2	5.46	3.65	4.97
Culture 3	4.52	4.33	5.75

Table A.2-3: ANOVA analysis of tdTomato yields for triplicate batch cultures at 3 timepoints.

TE3-B4-H1	**F**	**P-value**	**F_{crit}**
Cultures	0.04	0.97	6.94
Timepoints	0.30	0.76	6.94
TE3-B4-L1.1	**F**	**P-value**	**F_{crit}**
Cultures	4.58	0.09	6.94
Timepoints	2.02	0.25	6.94
TE3-B4-L1.1-tdTomato/tdTomato-C1	**F**	**P-value**	**F_{crit}**
Cultures	3.67	0.12	6.94
Timepoints	0.15	0.86	6.94
BBA10-tdTomato-C1	**F**	**P-value**	**F_{crit}**
Cultures	4.16	0.12	6.94
Timepoints	0.05	0.95	6.94

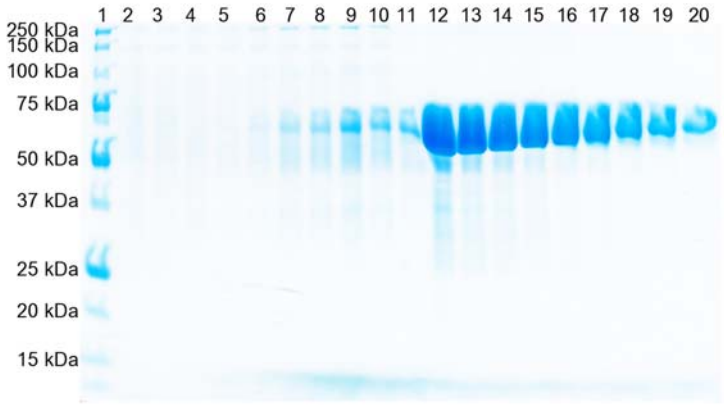

Lane	SMT_dneo(2)_24-ssmTLR2-C7
1	Precision Plus unstained (BioRad)
2	Permeate of dialysis
3	Filtrate of dialysis
4	Flowthrough
5-10	Wash fractions
11-20	Eluate fractions – mTLR2 (67.2 kDa)

Figure A.2-3: 12 % SDS-PAGE analysis of purified mTLR2 from expression in perfusion reactor using the cell line SMT_dneo(2)_24-ssmTLR2-C7. ssmTLR2 was produced in duplicate in 5 L perfusion reactors and purified using Ni-NTA. Yields up to 1.5 mg/L were obtained. SDS-PAGE shows fractions of one reactor run after purification.

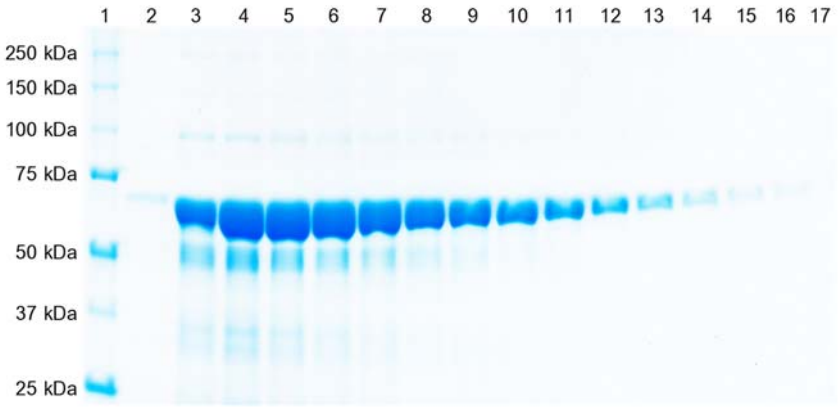

Lane	SMT_dneo(2)_24-ssmTLR2/mPRAT4A-C1
1	Precision Plus unstained (BioRad)
2-17	Eluate fractions – mTLR2 (67.2 kDa)

Figure A.2-4: 12 % SDS-PAGE analysis of purified mTLR2 from expression in perfusion reactor using the cell line SMT_dneo(2)_24 ssmTLR2/mPRAT4A-C1. mTLR2 was produced in duplicate in 5 L perfusion reactors and purified using Ni-NTA. Yields up to 0.5 mg/L were obtained. Thus the co-expression of mPRAT4A reduces mTLR2 yields. SDS-PAGE shows fractions of one reactor run after purification.

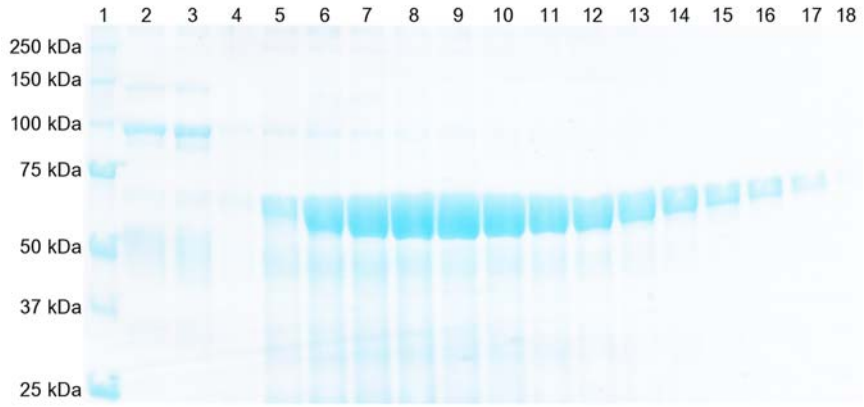

Lane	TE3-B4-H1-ssmTLR2/mGRP94-C1
1	Precision Plus unstained (BioRad)
2-3	Wash fractions
4-18	Eluate fractions – mTLR2 (67.2 kDa)

Figure A.2-5: 12 % SDS-PAGE analysis of purified mTLR2 from expression in perfusion reactor using the cell line TE3-B4-H1-ssmTLR2/mGRP94-C1. mTLR2 was produced in duplicate in 5 L perfusion reactors and purified using Ni-NTA. Yields up to 0.7 mg/L were obtained. Thus the co-expression of mGRP94 reduces mTLR2 yields. SDS-PAGE shows fractions of one reactor run after purification.

A.3 Protein Information

Table A.1-3: Protein information

Protein	Size	Length	A280 correction	Emission/Excitation
tdTomato	55.0 kDa	482 aa	0.79 mg/mL	554 nm/ 581 nm
eGFP (gb ADD98904.1)	28.0 kDa	248 aa	1.40 mg/mL	488 nm/ 507 nm
ssmTLR2_1-587 (UniProt Q9QUN7)	67.2 kDa	594 aa	1.28 mg/mL	-
sshTLR5 _1-391 (UniProt O60602)	57.5 kDa	511 aa	0.94 mg/mL	-
ssmTLR1_1-408 (UniProt Q9EPQ1)	59.8 kDa	529 aa	1.06 mg/mL	-
ssmTLR1_1-455 (UniProt Q9EPQ1)	64.9 kDa	576 aa	1.02 mg/mL	-
ssmTLR1_1-500 (UniProt Q9EPQ1)	69.7 kDa	621 aa	1.09 mg/mL	-
mPRAT4A (UniProt Q9DAU1)	31.5 kDa	284 aa	0.97 mg/mL	-
mGRP94 (UniProt P08113)	93.5 kDa	810 aa	1.12 mg/mL	-

Table A.1-4: Protein sequences (Signal-peptide, VLR sequence, ER-retention signal, Affinity-Tag)

tdTomato
MVSKGEEVIKEFMRFKVRMEGSMNGHEFEIEGEGEGRPYEGTQTAKLKVTKGGPLPFAWDILSPQFMYGSKAYVKHPAD IPDYKKLSFPEGFKWERVMNFEDGGLVTVTQDSSLQDGTLIYKVKMRGTNFPPDGPVMQKKTMGWEASTERLYPRDGV LKGEIHQALKLKDGGHYLVEFKTIYMAKKPVQLPGYYYVDTKLDITSHNEDYTIVEQYERSEGRHHLFLGHGTGSTGSGSS GTASSEDNNMAVIKEFMRFKVRMEGSMNGHEFEIEGEGEGRPYEGTQTAKLKVTKGGPLPFAWDILSPQFMYGSKAYV KHPADIPDYKKLSFPEGFKWERVMNFEDGGLVTVTQDSSLQDGTLIYKVKMRGTNFPPDGPVMQKKTMGWEASTERLY PRDGVLKGEIHQALKLKDGGHYLVEFKTIYMAKKPVQLPGYYYVDTKLDITSHNEDYTIVEQYERSEGRHHLFLYGMDEL YKHHHHHH
eGFP
MVSKGEELFTGVVPILVELDGDVNGHKFSVSGEGEGDATYGKLTLKFICTTGKLPVPWPTLVTTLTYGVQCFSRYPDHMK QHDFFKSAMPEGYVQERTIFFKDDGNYKTRAEVKFEGDTLVNRIELKGIDFKEDGNILGHKLEYNYNSHNVYIMADKQKN GIKVNFKIRHNIEDGSVQLADHYQQNTPIGDGPVLLPDNHYLSTQSALSKDPNEKRDHMVLLEFVTAAGITLGMDELYKS GRTQIHRI

mTLR2_1-587

MLRALWLFWILVAITVLFSKRCSAQESLSCDASGVCDGRSRSFTSIPSGLTAAMKSLDLSFNKITYIGHGDLRACANLQV
LILKSSRINTIEGDAFYSLGSLEHLDLSDNHLSSLSSSWFGPLSSLKYLNLMGNPYQTLGVTSLFPNLTNLQTLRIGNVETF
SEIRRIDFAGLTSLNELEIKALSLRNYQSQSLKSIRDIHHLTLHLSESAFLLEIFADILSSVRYLELRDTNLARFQFSPLPVDEV
SSPMKKLAFRGSVLTDESFNELLKLLRYILELSEVEFDDCTLNGLGDFNPSESDVVSELGKVETVTIRRLHIPQFYLFYDLST
VYSLLEKVKRITVENSKVFLVPCSFSQHLKSLEFLDLSENLMVEEYLKNSACKGAWPSLQTLVLSQNHLRSMQKTGEILLT
LKNLTSLDISRNTFHPMPDSCQWPEKMRFLNLSSTGIRVVKTCIPQTLEVLDVSNNNLDSFSLFLPRLQELYISRNKLKTLP
DASLFPVLLVMKIRENAVSTFSKDQLGSFPKLETLEAGDNHFVCSCELLSFTMETPALAQILVDWPDSYLCDSPPRLHGH
RLQDARPSVLECHQ**HHHHHHHH**

hTLR5 _1-391

MGDHLDLLLGVVLMAGPVFGIPSCSFDGRIAFYRFCNLTQVPQVLNTTERLLLSFNYIRTVTASSFPFLEQLQLLELGSQY
TPLTIDKEAFRNLPNLRILDLGSSKIYFLHPDAFQGLFHLFELRLYFCGLSDAVLKDGYFRNLKALTRLDLSKNQIRSLYLHP
SFGKLNSLKSIDFSSNQIFLVCEHELEPLQGKTLSFFSLAANSLYSRVSVDWGKCMNPFRNMVLEILDVSGNGWTVDITG
NFSNAISKSQAFSLILAHHIMGAGFGFHNIKDPDQNTFAGLARSSVRHLDLSHGFVFSLNSRVFETLKDLKVLNLAYNKIN
KIADEAFYGLDNLQVLNLSYNLLGELYSSNFYGLPKVAYIDLQKNHIAIIQDQTFKFLEKLQTLDLAS**NQLKSVPDGIFDR**
LTSLQKIWLHTNPWDCSCPRIDYLSRWLNKNSQKEQGSAKCSGSGKPVRSIICPTSRENLYFQGGSA**WSHPQFEKGG**
GSGGGSGGSAWSHPQFEKGS**HHHHHHHH**

mTLR1_1-408

MGTKPNSLIFYCIIVLGLTLMKIQLSEKCELIIKRPNANLTRVPKDLPLQTTTLDLSQNNISELQTSDILSLSKLRVLIMSYNR
LQYLNISVFKFNTELEYLDLSHNELKVILCHPTVSLKHLDLSFNAFDALPICKEFGNMSQLQFLGLSGSRVQSSSVQLIAHL
NISKVLLVLGDAYGEKEDPESLRHVSTETLHIVFPSKREFRFLLDVSVSTTIGLELSNIKCVLEDQGCSYFLRALSKLGKNLK
LSNLTLNNVETTWNSFINILQIVWHTPVKYFSISNVKLQGQLAFRMFNYSDTSLKALSIHQVVTDVFSFPQSYIYSIFANMN
IQNFTMSGTHMVHMLCPSQVSPFLHVDFTDNLLTDMVFKDCRNLVRLKTLSLQKNQLKNLENIILTSAKMTSLQKLDIAS
NQLKSVPDGIFDRLTSLQKIWLHTNPWDCSCPRIDYLSRWLNKNSQKEQGSAKCSGSGKPVRSIICPTSRENLYFQG
GSA**WSHPQFEKGGGSGGGSGGSAWSHPQFE**KGS**HHHHHHHH**

mTLR1_1-455

MGTKPNSLIFYCIIVLGLTLMKIQLSEKCELIIKRPNANLTRVPKDLPLQTTTLDLSQNNISELQTSDILSLSKLRVLIMSYNR
LQYLNISVFKFNTELEYLDLSHNELKVILCHPTVSLKHLDLSFNAFDALPICKEFGNMSQLQFLGLSGSRVQSSSVQLIAHL
NISKVLLVLGDAYGEKEDPESLRHVSTETLHIVFPSKREFRFLLDVSVSTTIGLELSNIKCVLEDQGCSYFLRALSKLGKNLK
LSNLTLNNVETTWNSFINILQIVWHTPVKYFSISNVKLQGQLAFRMFNYSDTSLKALSIHQVVTDVFSFPQSYIYSIFANMN
IQNFTMSGTHMVHMLCPSQVSPFLHVDFTDNLLTDMVFKDCRNLVRLKTLSLQKNQLKNLENIILTSAKMTSLQKLDISQ
NSLRYSDGGIPCAWTQSLLVLNLSSNMLTGSVFRCLPPKVKVLDLAS**NQLKSVPDGIFDRLTSLQKIWLHTNPWDCSC**
PRIDYLSRWLNKNSQKEQGSAKCSGSGKPVRSIICPTSRENLYFQGGSA**WSHPQFEKGGGSGGGSGGSAWSHPQFE**
KGS**HHHHHHHH**

ssmTLR1_1-500

MGTKPNSLIFYCIIVLGLTLMKIQLSEKCELIIKRPNANLTRVPKDLPLQTTTLDLSQNNISELQTSDILSLSKLRVLIMSYNR
LQYLNISVFKFNTELEYLDLSHNELKVILCHPTVSLKHLDLSFNAFDALPICKEFGNMSQLQFLGLSGSRVQSSSVQLIAHL
NISKVLLVLGDAYGEKEDPESLRHVSTETLHIVFPSKREFRFLLDVSVSTTIGLELSNIKCVLEDQGCSYFLRALSKLGKNLK
LSNLTLNNVETTWNSFINILQIVWHTPVKYFSISNVKLQGQLAFRMFNYSDTSLKALSIHQVVTDVFSFPQSYIYSIFANMN
IQNFTMSGTHMVHMLCPSQVSPFLHVDFTDNLLTDMVFKDCRNLVRLKTLSLQKNQLKNLENIILTSAKMTSLQKLDISQ
NSLRYSDGGIPCAWTQSLLVLNLSSNMLTGSVFRCLPPKVKVLDLHNNRIMSIPKDVTHLQALQELNVASNSLTDLPGCG
AFSSLSVLVIAS**NQLKSVPDGIFDRLTSLQKIWLHTNPWDCSCPRIDYLSRWLNKNSQKEQGSAKCSGSGKPVRSIICP**
TSRENLYFQGGSA**WSHPQFEKGGGSGGGSGGSAWSHPQFEK**GS**HHHHHHHH**

mPRAT4A (UniProt accession Q9DAU1)

C-terminal FLAG-tag

MESMSELAPRCLLFPLLLLLPLLLLPAPKLGPSPAGAEETDWVRLPSKCEVCKYVAVELKSAFEETGKTKEVIDTGYGILD
GKGSGVKYTKSDLRLIEVTETICKRLLDYSLHKERTGSNRFAKGMSETFETLHNLVHKGVKVVMDIPYELWNETSAEVAD
LKKQCDVLVEEFEEVIEDWYRNHQEEDLTEFLCANHVLKGKDTSCLAERWSGKKGDIASLGGKKSKKKRSGVKGSSSGS
SKQRKELGGLGEDANAEEEEGVQKASPLPHSP**PDEL****DYKDDDDK**

N-terminal FLAG-tag

MDYKDDDDKESMSELAPRCLLFPLLLLLPLLLLPAPKLGPSPAGAEETDWVRLPSKCEVCKYVAVELKSAFEETGKTKE
VIDTGYGILDGKGSGVKYTKSDLRLIEVTETICKRLLDYSLHKERTGSNRFAKGMSETFETLHNLVHKGVKVVMDIPYELW

NETSAEVADLKKQCDVLVEEFEEVIEDWYRNHQEEDLTEFLCANHVLKGKDTSCLAERWSGKKGDIASLGGKKSKKKRS
GVKGSSSGSSKQRKELGGLGEDANAEEEEGVQKASPLPHSP**PDEL**

mGRP94

C-terminal FLAG-tag

MRVLWVLGLCCVLLTFGFVRADDEVDVDGTVEEDLGKSREGSRTDDEVVQREEEAIQLDGLNASQIRELREKSEKFAFQ
AEVNRMMKLIINSLYKNKEIFLRELISNASDALDKIRLISLTDENALAGNEELTVKIKCDKEKNLLHVTDTGVGMTREELVK
NLGTIAKSGTSEFLNKMTEAQEDGQSTSELIGQFGVGFYSAFLVADKVIVTSKHNNDTQHIWESDSNEFSVIADPRGNTL
GRGTTITLVLKEEASDYLELDTIKNLVRKYSQFINFPIYVWSSKTETVEEPLEEDEAAKEEKEESDDEAAVEEEEEEKKPKTK
KVEKTVWDWELMNDIKPIWQRPSKEVEEDEYKAFYKSFSKESDDPMAYIHFTAEGEVTFKSILFVPTSAPRGLFDEYGSKK
SDYIKLYVRRVFITDDFHDMMPKYLNFVKGVVDSDDLPLNVSRETLQQHKLLKVIRKKLVRKTLDMIKKIADEKYNDTFW
KEFGTNIKLGVIEDHSNRTRLAKLLRFQSSHHSTDITSLDQYVERMKEKQDKIYFMAGSSRKEAESSPFVERLLKKGYEVIY
LTEPVDEYCIQALPEFDGKRFQNVAKEGVKFDESEKTKESREATEKEFEPLLNWMKDKALKDKIEKAVVSQRLTESPCAL
VASQYGWSGNMERIMKAQAYQTGKDISTNYYASQKKTFEINPRHPLIRDMLRRIKEDEDDKTVMDLAVVLFETATLRSG
YLLPDTKAYGDRIERMLRLSLNIDPEAQVEEEPEEEPEDTSEDAEDSEQDEGEEMDAGTEEEEEETEKESTE**KDELDYKD
DDDK**

N-terminal FLAG-tag

MDYKDDDDKRVLWVLGLCCVLLTFGFVRADDEVDVDGTVEEDLGKSREGSRTDDEVVQREEEAIQLDGLNASQIRELR
EKSEKFAFQAEVNRMMKLIINSLYKNKEIFLRELISNASDALDKIRLISLTDENALAGNEELTVKIKCDKEKNLLHVTDTGVG
MTREELVKNLGTIAKSGTSEFLNKMTEAQEDGQSTSELIGQFGVGFYSAFLVADKVIVTSKHNNDTQHIWESDSNEFSVI
ADPRGNTLGRGTTITLVLKEEASDYLELDTIKNLVRKYSQFINFPIYVWSSKTETVEEPLEEDEAAKEEKEESDDEAAVEEE
EEEKKPKTKKVEKTVWDWELMNDIKPIWQRPSKEVEEDEYKAFYKSFSKESDDPMAYIHFTAEGEVTFKSILFVPTSAPRG
LFDEYGSKKSDYIKLYVRRVFITDDFHDMMPKYLNFVKGVVDSDDLPLNVSRETLQQHKLLKVIRKKLVRKTLDMIKKIAD
EKYNDTFWKEFGTNIKLGVIEDHSNRTRLAKLLRFQSSHHSTDITSLDQYVERMKEKQDKIYFMAGSSRKEAESSPFVERL
LKKGYEVIYLTEPVDEYCIQALPEFDGKRFQNVAKEGVKFDESEKTKESREATEKEFEPLLNWMKDKALKDKIEKAVVSQR
LTESPCALVASQYGWSGNMERIMKAQAYQTGKDISTNYYASQKKTFEINPRHPLIRDMLRRIKEDEDDKTVMDLAVVLFE
TATLRSGYLLPDTKAYGDRIERMLRLSLNIDPEAQVEEEPEEEPEDTSEDAEDSEQDEGEEMDAGTEEEEEETEKESTE**KD
EL**

Acknowledgments

I would like to thank Dr. Joop van den Heuvel for giving me the opportunity to work on this PhD project as well as his constant support and feedback. Furthermore, I would like to thank the board of examiners Prof. Wulf Blankenfeldt, Prof. Stefan Dübel and Prof. Michael Hust for taking the time and afford to support my doctorate. Moreover, I would like to thank Prof. Christane Ritter and Prof. Melanie Brinkmann for their support and feedback during my thesis committees.

For the technical support in the laboratory I would like to thank our technicians. Daniela Gebauer for her support in protein purification and advice in all areas of laboratory live. Nadine Konisch for fermentation and the introduction into the cell culture laboratory. Sarah Maria Tokarski for the introduction into RMCE and Anke Samuels for her support in cell culture. She is probably relived that she does not need to count a single cell for me ever again.

I would like to thank Dr. Johannes Spehr, Dr. Sonja Wilke and Maren Bleckmann for reading my dissertation and giving me valuable feedback. For the introduction into Adobe illustrator I would like to thank Dr. Johannes Spehr. Likewise I would like to thank Dr. Jörn Krause for the crash course in pyMol. Furthermore, I would like to thank my master and bachelor students Shiwani Agarwal and Tabea Ellebracht for their good work and enthusiasm. Moreover, I would like to thank Dr. Lothar Gröbe and Maria Höxter for cell sorting.

All members of the research groups RPEX, SBAU and SFPR; I would like to thank for their advice, support and the supply with laboratory reagents. They made my time at the HZI enjoyable inside as well as outside of the laboratory.

Particularly I would like to thank Christian Schinkowski for rescuing my data and me from heart failure.

This work was supported by the Helmholtz Protein Sample Production Facility and by Instruct, part of the European Strategy Forum on Research Infrastructures (ESFRI). The research leading to these results also received funding from the European Community's Seventh Framework Programme (FP7/2007-2013) for the ComplexInc Project under grant agreement N° 270089

Curriculum Vitae

Education

2010-Present	**PhD Student** **Helmholtz Centre for Infection Research, Brunswick (Germany)** **RG Recombinant Protein Expression (RPEX)** Group Leader: Dr. Joop van den Heuvel "New Strategies to Improve the Expression of Recombinant Mammalian Proteins in Engineered Animal Cell Lines"
2008-2009	**Biotechnology, MSc, Distinction** **Oxford Brookes University, Oxford (UK)** Master Thesis **University of Oxford, Division of Structural Biology (STRUBI), Oxford (UK)** Group Leader: Dr. Radu Aricescu "Expression of GABAB Receptor Subunits for Structural Analysis"
2006-2007	**Industrial Placement** **LONZA Biologics Plc., Dept. Assay Development, Slough (UK)** Group Leader: Dr. Kym Baker, Supervisor: Dr. Jeffery Gerard "Technical Development - Evaluation iCE 280 Analyser "
2004-2008	**Biotechnology, BSc Hons., Upper Second Class** **Oxford Brookes University, Oxford (UK)**
2004	**English for University Studies (EUS)** **Oxford Brookes University, Oxford (UK)**
2002-2004	**Chemistry** **Technische Universität München, Munich (Germany)**
1994-2002	**A-Levels, Zeugnis der Allgemeinen Hochschulreife** **Clemens-Brentano-Europaschule, Lollar (Germany)**

Awards

6–8 Mar 2013	**1st poster prize at RPP7 – Laupheim , 7th Conference on Recombinant Protein Production, Laupheim, Germany (Poster)**

Conference Contributions

6–8 Mar 2013	**RPP7 – Laupheim , 7th Conference on Recombinant Protein Production, Laupheim, Germany (Poster)**
4–8 Nov 2013	**PEGS Europe 2013: Protein & Antibody Engineering Summit, Lisbon, Portugal (Poster)**

Publications

Meyer, S., C. Lorenz, **B. Baser**, M. Wördehoff, V. Jäger and J. van den Heuvel (2013). Multi-Host Expression System for Recombinant Production of Challenging Proteins. PLoS ONE 8(7): e68674.